Identification and Characterization of Protein Phosphatase 4 Regulatory Subunit 1 (PP4R1) as a Suppressor of NF-κB in T Lymphocytes and T Cell Lymphomas

DISSERTATION

submitted to the
Faculty of Biosciences
of the Ruperto-Carola University of Heidelberg, Germany
for the degree of Doctor *rerum naturalium*

presented by
Dipl. Biochem. Markus Brechmann
born in Bielefeld, Germany

Oral-examination: September 10th, 2010

Identification and Characterization of Protein Phosphatase 4 Regulatory Subunit 1 (PP4R1) as a Suppressor of NF-κB in T Lymphocytes and T Cell Lymphomas

Referees: PD Dr. Philipp Beckhove
German Cancer Research Center, Heidelberg

Prof. Dr. Peter H. Krammer
German Cancer Research Center, Heidelberg

This thesis is based on research conducted in the Division of Immunogenetics at the German Cancer Research Center (DKFZ), under supervision of Prof. Dr. Peter H. Krammer and direct supervision of PD Dr. Rüdiger Arnold in the period from October 2006 to June 2010.

„Chance favours the prepared mind.“

LOUIS PASTEUR

Danksagung

Denen, die mich in den zurückliegenden dreieinhalb Jahren während meiner Doktorarbeit unterstützt und begleitet haben, möchte ich meinen großen Dank aussprechen.

Zunächst möchte ich mich bei Prof. Dr. Peter H. Krammer für seine Unterstützung und stete Diskussionsbereitschaft bedanken. Peter hat mir in seiner Abteilung nicht nur exzellente Arbeitsbedingungen zur Verfügung gestellt. Insbesondere verkörpert er eine Kultur sowohl (selbst)kritischer als auch auch kreativer Wissenschaft, welche mein eigenes wissenschaftliches Denken maßgeblich geprägt hat und auch in Zukunft weiter fortwirken wird.

Herrn PD Dr. Philipp Beckhove danke ich für die Betreuung dieser Arbeit als Erstgutachter. Ferner möchte ich mich bei Prof. Dr. Felix Wieland, Prof. Dr. Martin Müller und Prof. Dr. Carsten Watzl für die Betreuung meiner Promotion bedanken.

Insbesondere gilt ein großes DANKE PD Dr. Rüdiger Arnold, meinem direkten Mentor und Betreuer. Seine Lebendigkeit, sein Optimismus und sein unbeirrter Glaube an mich haben mir durch so manche Talsohle geholfen. Die ungezwungene und freundschaftliche Zusammenarbeit mit Dir hat mir sehr viel Freude bereitet!

Darüber hinaus gilt mein großer Dank Thomas Mock, mit dem ich in den letzten zwei Jahren nicht nur wissenschaftlich hervorragend zusammengearbeitet habe. Es ist nicht selbstverständlich, derart vertrauensvoll und konstruktiv ein gemeinsames wissenschaftliches Team zu bilden.

Auch möchte ich mich vor allem bei Dorothee Nickles wie auch Felice Frey für die sehr fruchtbare und schöne Zusammenarbeit bedanken. Doro, Du hast einen sicherlich sehr grundlegenden Anteil an dieser Arbeit! In diesem Zusammenhang danke ich auch Prof. Dr. Michael Boutros für die exzellente Kooperation.

Ein großer Dank gilt vielen jetzigen und ehemaligen Mitgliedern der Abteilung Immungenetik für Ihre Unterstützung in wissenschaftlichen Fragen, ihren Zuspruch und natürlich für so manchen lebenswerten Moment jenseits der Laborbank! Insbesondere danke ich Dirk Brenner, Julia Hoffmann, Michael Kiessling, Björn Linke, Mareike Becker,

Wolfgang Müller und Marco Giasi, die mich durch diese sehr intensive Zeit begleitet haben. Danke für die gemeinsame Zeit innerhalb und außerhalb des Labors!

Darüber hinaus danke ich Rüdiger Arnold, Thomas Mock, Michael Kiessling, Karsten Gülow und Gernot Polier für das Korrekturlesen dieser Arbeit.

Daniel Dependahl und Boris Ullrich danke ich ganz besonders für unsere langjährige Freundschaft.

Bei Eva-Maria Weiss bedanke ich mich für die sehr schöne Zeit auf der letzten Strecke dieser Arbeit!

Bei meiner Schwester bedanke ich mich für ein jederzeit offenes Ohr und Deine großartige Unterstützung in so manchen Lebensfragen während der zurückliegenden Zeit in Heidelberg. Schön, dass es Schwestern wie Dich gibt!

Der größte Dank gilt meinen Eltern, die mich jederzeit bedingungslos unterstützt haben. Ich danke Euch aus ganzem Herzen für Euer Verständnis, Euer Interesse und Eure Rücksichtnahme. Ohne Euch wäre das alles nicht möglich gewesen. Ihr bedeutet mir viel.

Summary

The transcription factor nuclear factor-kappaB (NF-κB) plays a key role in the immune system by controlling lymphocyte survival and activation. Conversely, aberrant NF-κB activity has been implicated in several lymphoid malignancies and contributes to a variety of autoimmune disorders.

While multiple kinases and phosphorylated target proteins that induce NF-κB activity have been identified, the molecular machinery involved in the termination of antigen receptor-mediated NF-κB activation is only partially understood. Since signal transduction from activated receptors to NF-κB largely relies on phosphorylation events, phosphatases are expected to play a major role in the modulation and termination of NF-κB activity.

Therefore, the current study aimed at systematically defining phosphatases that are involved in T cell receptor (TCR)-induced NF-κB signaling. To this end, an RNA interference (RNAi) genetic screen has been adopted based on a novel NF-κB-dependent reporter system. Using this approach, several NF-κB-modulating phosphatases were identified among which the protein phosphatase 4 regulatory subunit 1 (PP4R1) was confirmed as a central negative regulator of NF-κB activity in T lymphocytes. PP4R1 expression is strongly upregulated in primary human T lymphocytes upon activation. PP4R1 specifically binds to the inhibitor of NF-κB kinase α (IKKα) and the catalytic subunit PP4c, thereby directing PP4c phosphatase activity to dephosphorylate and inactivate the IKK complex. Accordingly, PP4R1 silencing causes sustained and increased IKK activity and T cell hyperactivation as reflected by enhanced induction of NF-κB target genes and secretion of cytokines. Conversely, PP4R1 overexpression significantly impairs NF-κB activation upon TCR stimulation, but does not affect AP-1 signaling. Furthermore, PP4R1 was found to be downregulated in a subset of malignant T lymphocytes derived from patients with Sézary syndrome, a severe form of cutaneous T cell lymphoma (CTCL). PP4R1 deficiency causes constitutive IKK/NF-κB signaling and is required for survival of NF-κB-addicted CTCL cells.

In summary, the present work identified PP4R1 as a central gatekeeper of IKK activity and as a suppressor of T cell activation and lymphoma survival. These findings expand our current knowledge of NF-κB signal transduction and contribute to a more precise molecular understanding of NF-κB regulation in health and disease.

Zusammenfassung

Der Transkriptionsfaktor *nuclear factor-kappaB* (NF-κB) nimmt eine zentrale Stellung im Immunsystem ein. Physiologische NF-κB Aktivität ist essentiell für das Überleben und die Aktivierung von Lymphozyten. Hingegen ist aberrante NF-κB Signalgebung mit verschiedenen hämatologischen Neoplasien und Autoimmunerkrankungen assoziiert.

Die T Zell-Rezeptor (TZR)-induzierte NF-κB Signalkaskade involviert eine Vielzahl von Kinasen und phosphorylierter Effektormoleküle. Im Gegensatz hierzu sind die molekularen Mechanismen, die der negativen Regulation des NF-κB Signalweges zugrunde liegen, nur zum Teil verstanden. Da Phosphorylierungsreaktionen ein zentrales Merkmal der Rezeptor-induzierten NF-κB Aktivierung darstellen, werden Phosphatasen als wichtige Modulatoren von NF-κB Aktivität vermutet.

Ziel der vorliegenden Studie war es daher, die Funktion einzelner Phosphatasen im TZR-induzierten NF-κB Signalweg systematisch zu adressieren. Hierfür wurde ein RNA Interferenz (RNAi) Screen durchgeführt auf Grundlage eines neu entwickelten NF-κB-spezifischen Reporter-Systems. Unter verschiedenen NF-κB-modulierenden Phosphatasen wurde die *protein phosphatase 4 regulatory subunit 1* (PP4R1) als ein zentraler negativer Regulator der NF-κB Aktivierung in T Lymphozyten identifiziert. Die PP4R1 Expression wird in aktivierten humanen T Lymphozyten stark induziert. PP4R1 fungiert als ein Adapter zwischen der *inhibitor of NF-κB kinase* α (IKKα) und der katalytischen PP4 Untereinheit PP4c und reguliert somit PP4 Phosphatase Aktivität zur spezifischen Dephosphorylierung und Inaktivierung des IKK Komplexes. Die RNAi-vermittelte Suppression der PP4R1 Expression verursacht eine erhöhte und prolongierte IKK Aktivität und eine verstärkte Induktion und Sekretion NF-κB-abhängiger Gene bzw. Zytokine. Umgekehrt führt die Überexpression von PP4R1 zu einer spezifischen Blockade des NF-κB Signalweges nach TZR Stimulation. In malignen T Lymphozyten von Patienten mit dem Sézary Syndrom, einer aggressiven und leukemischen Variante des Kutanen T Zell Lymphoms (*engl.: cutaneous T cell lymphoma*, CTCL) ist die PP4R1 Expression deutlich erniedrigt. Die Defizienz von PP4R1 resultiert in konstitutiver IKK/NF-κB Signalgebung und ist verantwortlich für das Überleben NF-κB-abhängiger CTCL-Zellen.

In dieser Arbeit konnte PP4R1 als ein neuer zentraler Regulator des NF-κB Signalweges und als ein Suppressor von T Zell-Aktivierung und T Zell-Lymphomen identifiziert werden. Dies erweitert unser molekulares Verständnis des NF-κB Signalweges und seiner Regulation unter physiologischen und pathophysiologischen Bedingungen.

Table of contents

1 Introduction

1.1 The immune system

Metazoan organisms are exposed throughout their whole life span to a wide variety of infectious microbial pathogens. In order to counteract this permanent menace the immune system has evolved as a highly efficient humoral and cellular network capable of microbial recognition and elimination. In vertebrates two general branches of immunity can be distinguished: innate and adaptive (acquired) immunity. The main distinction between these two immunological components lies in the receptor systems and signaling pathways used for antigen sensing and subsequent induction of effector responses. Both systems do not act independently of each other, but are functionally interconnected. Although still being partially enigmatic, the capability to discriminate between “self” and “nonself” has emerged as a fundamental paradigm of immunity (Janeway, Jr., 1992; Matzinger, 2002).

1.1.1 Innate immunity

The innate immune system is an evolutionarily ancient form of the host defence present in most multicellular organisms. The innate immune response is rapidly initiated in the early phase of an infection, provides the first line of host defence, and controls and precedes the initiation of the primary adaptive response. Cellular constituents of this type of immunity are dendritic cells (DCs), granulocytes, mast cells, neutrophils, monocytes, macrophages and natural killer cells (NK cells). In addition, humoral components of innate immunity comprise the complement system, acute phase proteins, as well as different enzymes, cytokines (*e.g.* interferons), and lysozymes.

A hallmark of innate immunity is the use of a restricted number of germline-encoded receptors – so-called pattern recognition receptors (PRRs) – that act as sensors of conserved and constitutive microbial structures, known as pathogen-associated molecular patterns (PAMPs). Since these molecular signatures are unique to microorganisms of a given class the innate immune recognition system is able to efficiently detect both the presence and the nature of infectious agents (Fearon and Locksley, 1996; Medzhitov, 2001; Medzhitov and Janeway, Jr., 2002). Multiple and distinct PRRs have been identified that can be broadly categorized into secreted, transmembrane, and cytosolic receptor families. The major effector functions of PRRs comprise opsonization, activation of complement and coagulation cascades, phagocytosis, and triggering of proinflammatory signaling pathways (Iwasaki and Medzhitov, 2010).

1.1.2 Adaptive immunity

The adaptive immune response is organized around two classes of specialized cells: B lymphocytes (B referring to the avian bursa of Fabricius) and T lymphocytes (T referring to thymus). Both types of lymphocytes originate from haematopoietic stem cells within the bone marrow. A small fraction of these cells further develops into lymphoid precursor cells that finally give rise to mature B and T lymphocytes. Whereas B lymphocytes mature in the bone marrow and spleen, T cell progenitors migrate into the thymus to ultimately differentiate into mature T lymphocytes (Shortman et al., 1990).

The clonal selection of antigen-specific lymphocytes is the basis of adaptive immunity (Burnet, 1959; Litman et al., 1993). Since each lymphocyte is endowed with a single kind of receptor of potentially unique specificity – the B and T cell antigen receptor, respectively (BCR and TCR) – the repertoire of antigen receptors in the entire population of lymphocytes is extremely large and diverse, capable of recognizing virtually any antigen (Medzhitov and Janeway, 2000). In contrast to the relatively small number of PRRs of innate immunity, the high diversity of antigen-specific receptors is generated randomly by somatic receptor gene rearrangements during lymphopoesis (Tonegawa, 1993; Jung and Alt, 2004). Early in ontogenesis encountering of (auto-)antigens induces negative selection by programmed cell death (apoptosis), thus ensuring self-tolerance (Rathmell and Thompson, 2002; Starr et al., 2003). By contrast, binding of specific antigen by clonotypic receptors on mature lymphocytes triggers clonal expansion and differentiation into effector cells. B lymphocytes either differentiate into plasma cells or germinal center (GC) B cells to secrete antigen-specific antibodies and thereby constitute the humoral branch of adaptive immunity (Rajewsky, 1996). Similarly, T lymphocytes are able to differentiate into various T cell effector subsets such as $CD8^+$ cytotoxic T cells or $CD4^+$ T helper cells, including Th1, Th2 and Th17 T cells (Locksley, 2009). Subsets of B and T cells that have encountered antigen persist within the organism over a long time and provide rapid and specific protection against reinfection, a process referred to as immunological memory (Ahmed and Gray, 1996). The plasticity of the adaptive antigen receptor repertoire and the ability to establish a long lasting antigen-specific memory represent major distinctions from the rather static immune recognition systems employed by innate immunity.

1.1.3 Cross talk between innate and adaptive immunity: initiation of an acquired immune response

Since antigen receptors are generated *de novo* during lymphocyte ontogenesis they lack the intrinsic capability to discriminate between antigens derived from “infectious-nonself” and “noninfectious-self”. Therefore, the immune system has evolved as multi-layered control system in order to mount a specific immune response against microbial invaders while exercising tolerance to auto-antigens. At a first level in T development self-reactive thymocytes are clonally deleted (central tolerance). A second level of control in the periphery (peripheral tolerance) involves the requirement of proper (co-)stimulation of antigen-specific T lymphocytes by specialized antigen presenting cells (APCs) to undergo full activation, proliferation and differentiation (Janeway, Jr., 1989; Medzhitov and Janeway, Jr., 1999; Medzhitov and Janeway, Jr., 1999). APCs include B cells, macrophages and in particular DCs (Inaba et al., 1990). Foreign antigens that are physically associated with PAMPs are recognized and internalized by APCs, enzymatically processed and the resulting microbial peptide fragments are bound to major histocompatibility complex (MHC) molecules and presented on the cell surface (Inaba et al., 1990; Trombetta and Mellman, 2005). Activation of an antigen-specific T cell occurs *via* specific binding of the clonal TCR to the complex composed of “nonself” peptide (p) and “self” MHC (pMHC) (Hennecke and Wiley, 2001). Whereas $CD8^+$ T cells bind to MHC class I molecules loaded with peptides of cytosolic origin, $CD4^+$ T cells bind to complexes of MHC class II molecules and peptides of extracellular origin that have been internalized by phagocytosis or macropinocytosis (Rudolph et al., 2006). However, there is cross talk between the cell-intrinsic MHC class I and the cell-extrinsic MHC class II pathways *via* mechanisms including autophagy and cross-presentation (Iwasaki and Medzhitov, 2010). Importantly, binding of the TCR to pMHC alone is not sufficient to induce T cell activation, but has to be complemented by two auxiliary signals. (i) For a naïve T lymphocyte to get programmed into a differentiated effector cell a co-stimulating signal is required that has to be delivered by the same pMHC-presenting APC. Among the co-stimulating receptors on T cells that mediate this signal CD28 is the most important member. Its natural ligands are B7 family members (CD80 and CD86) expressed on mature APCs (Greenwald et al., 2005). (ii) T cell activation depends on the presence of interleukin 2 (IL-2), a T cell growth factor that binds to IL-2 receptors on the T cell surface (Mak, 2007). In contrast, TCR triggering in the absence of co-stimulation results in a long-lived state of functional unresponsiveness, termed anergy (Ohashi, 2002; Fathman and Lineberry, 2007).

The interactions between T cells and DCs take place within the secondary lymphoid organs. Activated DCs that have encountered foreign antigen express high levels of MHC and co-stimulatory molecules and start migrating into the draining lymph nodes. Here, naïve antigen specifc T cells are primed by mature DCs and subsequently undergo clonal expansion. The upregulated expression of co-stimulating molecules requires the maturation of DCs which is in turn dependent on the activation of PRRs. The physical association between antigenic peptides presented by MHC molecules and PAMPs provides a functional link between innate and adaptive immunity and ensures that the adaptive immune response is selectively directed against infectious pathogens, but not against self-antigens (Medzhitov and Janeway, Jr., 2002).

1.2 Signal transduction from the T cell antigen receptor (TCR)

The adaptive immune response is based on an intricate network of cellular interactions. Accordingly, the outcome of an individual cellular response is determined by the reception and transduction of extracellular signals through antigen receptors and regulatory co-receptors followed by signal amplification, integration and processing involving a series of complex intracellular signaling circuits. In the following sections the molecular mechanisms underlying initiation, propagation and regulation of TCR-mediated signal transduction will be discussed in detail.

1.2.1 Structure and composition of the TCR

The TCR, together with the BCR and certain types of Fc receptors, belongs to the family of multichain immune recognition receptors. In contrast to receptor protein tyrosine kinases (*e.g.* epidermal growth factor receptor, EGFR) ligand binding and signaling subunits are located on different polypeptide chains, and immunoreceptors lack intrinsic catalytic activity. The TCR consists of clonotypic α and β subunits mediating ligand recognition and binding, and a number of non-polymorphic signal transducing units including the the γ, δ, ε and ζ chains of the CD3 complex (Samelson, 2002). A minority of T cells of about 5% express a TCR composed of a TCRγ and a TCRδ chain.

The exact stoichiometry of the TCR/CD3 complex has been a long-standing controversy in immunology. It is now assumed that the CD3 complex is composed of a CD3γ-CD3ε heterodimer, a CD3δ-CD3ε heterodimer and a ζ-homodimer that are non-covalently associated with the TCR. However, it is still elusive whether one or two single $\alpha\beta$ TCR

heterodimers form part of one TCR/CD3 complex (Exley et al., 1995; Fernandez-Miguel et al., 1999; Davis, 2002; Smith-Garvin et al., 2009).

The CD3 complex forms the invariant signal transducing subunit of the TCR complex. Unlike the TCR polypeptides CD3 proteins have long cytosolic tails containing conserved peptide motifs, designated immunoreceptor tyrosine-based activation motifs (ITAMs), that are also found in the signaling components of the BCR and some types of Fc receptors. The ITAM is characterized by the consensus amino acid sequence $D/Ex_7D/ExxYxxI/Lx_7YxxI/L$ (in single-letter code for amino acids, x may be any residue) (Reth, 1989; Cambier, 1995). Whereas each ζ chain contains three copies of one ITAM, the CD3 γ, δ and ε proteins each harbour on ITAM sequence in their intracytoplasmic domains resulting in ten ITAM sequences per CD3 complex (Pitcher and van Oers, 2003). Using transmembrane chimeras it could be demonstrated that the ITAM is the minimally functional motif required for coupling of the TCR and other immunoreceptors to the intracellular signaling apparatus (Irving and Weiss, 1991; Letourneur and Klausner, 1992; Romeo et al., 1992; Flaswinkel and Reth, 1994). Whether multiple ITAM motifs of the CD3 complex serve redundant or specific functions remains elusive, though (Pitcher and van Oers, 2003). The functional and physical association of the TCR with the CD3 complex is further demonstrated by the fact that there is an obligatory co-expression of both entities on the T cell surface (Weiss and Stobo, 1984).

1.2.2 Assembly and activation of the TCR proximal signalosome

Engagement of TCR by cognate pMHC or agonistic antibodies is thought to induce conformational changes within the TCR as well as receptor oligomerization (Smith-Garvin et al., 2009), which is accompanied and/or followed by the transient translocation of activated TCR/CD3 complexes into particular compartments of the plasma membrane, known as glycosphingolipid-enriched microdomains (GEMs) or lipid-rafts (Xavier and Seed, 1999; Janes et al., 1999). One of the earliest events detectable upon triggering of the TCR and its co-receptors (CD4 or CD8) includes the activation of Src family protein tyrosine kinases (SFKs). All SFK family members share a common molecular architecture composed of highly homologous regions denoted by Src homology domains 1-4 (SH1-SH4). The SH1 domain confers kinase activity, the SH2 and SH3 domains recognize and bind to phospho-tyrosine motifs and proline-rich regions, respectively, and the SH4 domain mediates fatty acid modifications. In T lymphocytes the SFK family members Lck and Fyn are expressed (Kiefer et al., 2002).

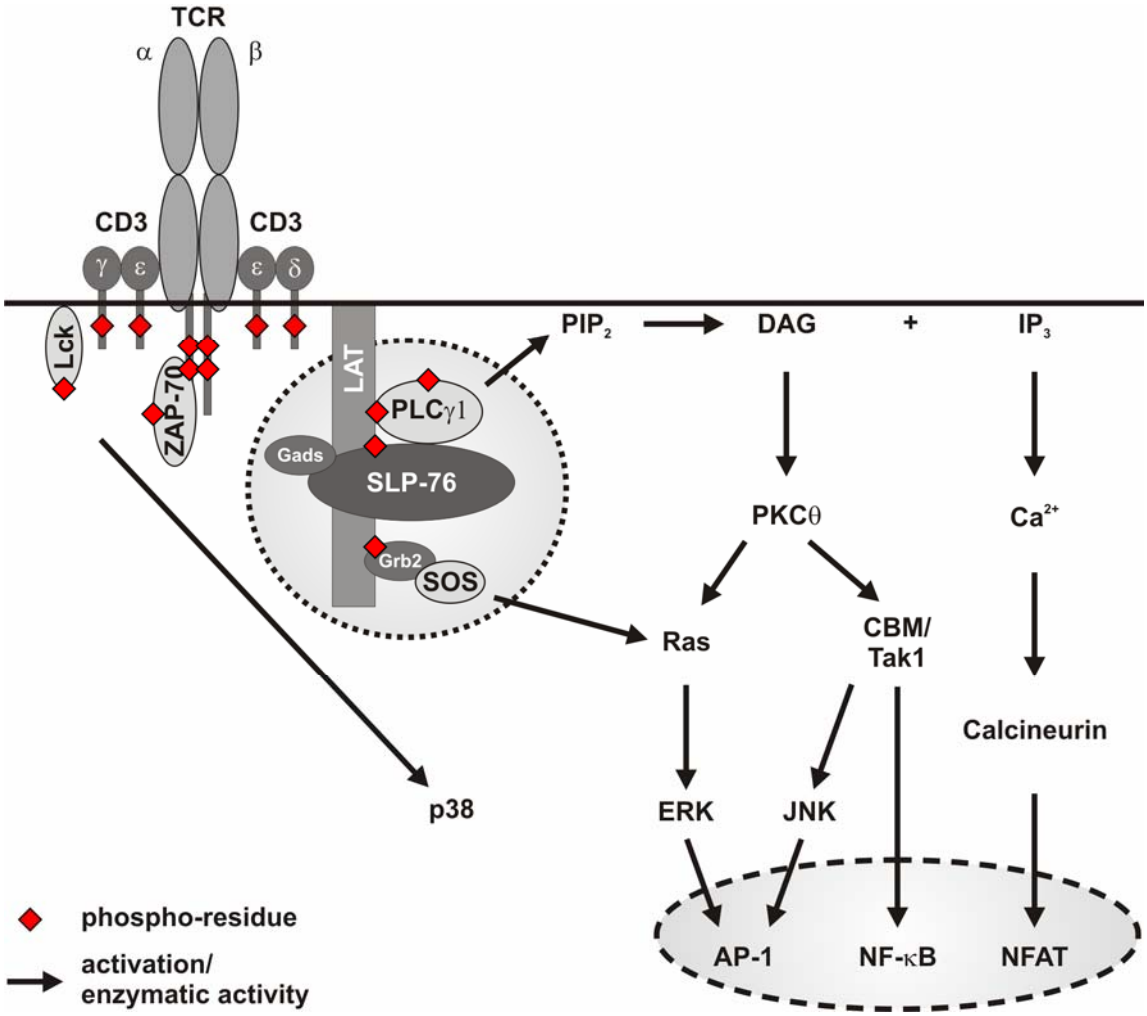

Figure 1.1 | TCR proximal signaling events. Engagement of the TCR and its co-receptors by cognate ligand leads to TCR/CD3 aggregation followed by recruitment and activation of Src and Syk family PTKs, such as Lck and ZAP-70, respectively. Activated ITAM-bound ZAP-70 phosphorylates the adapter proteins LAT and SLP-76. In turn, SLP-76 interacts with phospho-LAT *via* Gads leading to the assembly of a membrane and TCR proximal core signalosome containing several effector enzymes (grey circle). Recruitment of PLCγ1 to the trimeric LAT-Gads-SLP-76 scaffold facilitates its phosphorylation and activation by PTKs and increases access to its substrate, the membrane phosphatidylinositol PtdIns(4,5)P_2. Activated PLCγ1 then catalyzes phospho-inositide breakdown giving rise to the second messengers DAG and IP_3. TCR-induced IP_3 production triggers intracellular Ca^{2+} mobilization and ultimately results in activation of the transcription factor NFAT. TCR-induced generation of DAG leads to PKCθ activation which in turn triggers several downstream pathways, such as the ERK or NF-κB pathway. In addition to its activation by PKCθ, Ras activity relies on the GEF SOS that is recruited in a phosphorylation-dependent manner to the TCR proximal core signalosome *via* the adapter Grb2. Activation of the MAPKs ERK and JNK through upstream phosphorylation cascades culminates in AP-1 activity. Activation of the MAPK p38 involves the PTKs Lck and ZAP-70 and proceeds *via* a PKCθ-independent mechanism.

TCR-induced activation of SFKs constitutes a first wave of protein tyrosine kinase (PTK) activation. Activated SFKs that are intracellularly associated with the TCR co-receptors CD4 and CD8 subsequently phosphorylate ITAMs within the cytoplasmatic tails of the TCR-associated CD3 complex (Weiss and Littman, 1994). In turn, doubly phosphorylated ITAMs (ppITAMs) provide spatially defined docking sites for a second class of PTKs, the spleen tyrosine kinase (Syk) PTKs (Latour and Veillette, 2001). Among the Syk PTK family members Syk itself is most prominently found in B cells, whereas its homologue, the ζ chain-associated kinase of 70 kDa (ZAP-70), is predominantly expressed throughout the whole T cell compartment (Chan et al., 1994). Binding of the tandemly-arranged SH2 domains to a ppITAM recruits ZAP-70 to the activated TCR allowing for its phosphorylation and activation by SFKs (Wange and Samelson, 1996). Among the most important immediately downstream targets of ZAP-70 are the transmembrane adapter protein linker of activated T cells (LAT) (Zhang et al., 1998a) and the cytosolic adapter protein SH2 domain-containing leukocyte phosphoprotein of 76 kDa (SLP-76) (Bubeck et al., 1996). The indispensable role of these two adapter proteins in TCR signaling is documented by *in vitro* and *in vivo* studies showing that loss of either LAT or SLP-76 nearly completely abrogates TCR-induced signal transmission and T cell activation (Zhang et al., 1999; Yablonski et al., 1998; Clements et al., 1998). By virtue of palmitoylation LAT is constitutively raft-resident (Zhang et al., 1998b), and tyrosine phosphorylation creates docking sites for the adapter protein Grb2-related adaptor downstream of Shc (Gads) (Wonerow and Watson, 2001). Gads constitutively interacts *via* its SH3 domain with SLP-76, and, consequently, binding of Gads to phospho-LAT relocalizes SLP-76 to the activated TCR (Liu et al., 1999). Formation of the membrane proximal trimeric LAT-Gads-SLP-76 complex serves as a backbone for the nucleation of a multimolecular signalosome that contains several effector proteins, such as phospholipase Cγ1 (PLCγ1), the guanine-nucleotide-exchange factor (GEF) Vav1, the adapter non-catalytic region of tyrosine kinase (Nck), the tyrosine kinase IL-2 inducible Tec kinase (Itk), the adhesion- and degranulation-promoting adapter protein (ADAP), Lck as well as the haematopoietic progenitor kinase 1 (HPK1) (Leo and Schraven, 2001; Koretzky et al., 2006). This core signaling complex, also termed the Ca^{2+} signalosome, collects and integrates signals from the activated TCR and co-receptors in a regulated spatiotemporal manner to allow for the initiation of diverging downstream signaling cascades, including Ca^{2+} and diacylglycerol (DAG)-induced responses as well as cytoskeletal rearrangements and integrin signaling (Smith-Garvin et al., 2009).

1.2.3 Activation of PLCγ1

PLCγ1 is a central TCR proximal effector molecule. Upon TCR engagement PLCγ1 is recruited to the trimeric LAT-Gads-SLP-76 complex *via* binding of its SH2 domain to phospho-LAT (Zhang et al., 2000). Membrane relocalization is further promoted and stabilized by binding of its PLCγ1 pleckstrin homology (PH) domain to specific membrane phosphoinositides (Kiefer et al., 2002). Activation of PLCγ1 requires dual phosphorylation by Itk and ZAP-70 (Liu et al., 1998a). Additionally, complete phospholipase activity of PLCγ1 seems to require its constitutive association with the proline-rich domain of SLP-76 (Yablonski et al., 2001). Enzymatically active membrane-associated PLCγ1 then catalyses hydrolysis of the membrane lipid phosphatidylinositol 4,5-bisphosphate (PtdIns(4,5)P_2) giving rise to the second messengers inositol 1,4,5-trisphosphate (IP_3) and DAG. Generation of these two second messengers leads to the amplification of the TCR signal and serves as a bifurcation point to induce separate signaling cascades.

1.2.4 TCR-induced Ca^{2+} signaling

The mobilization of intracellular and extracellular calcium ions (Ca^{2+}) into the cytoplasm occurs in two steps. (i) PLCγ1-generated IP_3 is highly diffusible and binds to tetrameric Ca^{2+} permeable ion channel receptors (IP_3R) located within the endoplasmic reticulum (ER) membrane. This leads to the depletion of ER Ca^{2+} stores into the cytoplasm. (ii) The transient mobilization of intracellular Ca^{2+} in turn stimulates opening of Ca^{2+} release activated channels (CRACs) in the plasma membrane, a process referred to as store-operated Ca^{2+} entry (SOCE). Thereby, the sustained Ca^{2+} influx from the extracellular space leads to a stabilization of the intracellular Ca^{2+} signal (Oh-Hora and Rao, 2008). Elevated Ca^{2+} levels mediate the activation of the Ca^{2+}/calmodulin-dependent phosphatase calcineurin which results in the dephosphorylation and activation of members of the nuclear factor of activated T cells (NFAT) family. In their inactive phosphorylated state NFAT transcription factors reside in the cytosol. Calcineurin-mediated dephosphorylation of several phospho-sites leads to the translocation of the NFAT/calcineurin complex into the nucleus. This ultimately results into the initiation of various transcriptional programs dependent on the coaction of other transcription factors and the context of the TCR signal. Finally, decreasing cytosolic Ca^{2+} levels cause rapid dissociation of NFAT/calcineurin complexes and export of its components into the cytoplasm (Serfling et al., 2000).

1.2.5 Activation of DAG-dependent pathways

The TCR-induced generation of the membrane-integral second messenger DAG induces activation of two major pathways: the PKCθ-dependent pathway and the Ras-MAPK pathway. PKCθ-induced signaling is crucial for NF-κB activation in T lymphocytes and, therefore, will be discussed in section 1.3.5.

MAPKs are evolutionarily conserved enzymes that regulate important cellular processes like proliferation and apoptosis (Tibbles and Woodgett, 1999). MAPK are categorized into at least three classes of enzymes: the extracellular signal-regulated kinases 1 and 2 (ERK1/2), the c-Jun N-terminal kinases (JNKs), and the MAPK p38 (see section 1.2.6). MAPKs are activated by dual phosphorylation of threonine and tyrosine residues. Phosphorylation of MAPKs is part of a hierachical phosphorylation cascade involving upstream MAPK kinases (MAPKKs) and MAPKK kinases (MAPKKKs) (Dong et al., 2002). In T cells the Ras-MAPK pathway has been shown to play a crucial role in the initiation of proliferation and differentiation programs (Rincon, 2001). (Ras is a plasma membrane-associated guanine nucleotide-binding protein that acts upstream of the serine-threonine kinase Raf-1. Raf-1 acts as a MAPKKKs and activation of Raf-1 by Ras induces a mitogen-associated protein kinase (MAPK) activation cascade that ultimately results in the phosphorylation and activation of the MAPKs ERK1 and ERK2. ERK kinase activity leads to the activation of the transcription factor Elk1 that, in turn, drives the expression of the transcription factor c-Fos and thereby contributes to the activation of the activator protein-1 (AP-1) (c-Jun/c-Fos) transcription factor complex (Smith-Garvin et al., 2009).

Ras is only active in its GTP-bound conformation. Its activation is induced by the action of GEFs and counteracted by GTPase-activating proteins (GAPs). Two distinct GEFs, the GEF son of sevenless (SOS) and the Ras guanyl nucleotide-releasing protein (RasGRP), have been described to catalyze Ras activation in T lymphocytes (Ebinu et al., 2000; Egan et al., 1993). SOS is recruited *via* its constitutive interaction with the adapter growth factor receptor-bound protein 2 (Grb2) to phospho-LAT upon TCR stimulation. Subsequently, membrane-proximal SOS catalyzes the GDP-GTP exchange of Ras thereby leading to Ras activation (Egan et al., 1993). Additionally, RasGRP is recruited to the plasma membrane by virtue of its DAG-binding domain und undergoes phosphorylation and activation by PKCθ (Ebinu et al., 1998; Roose et al., 2005). Apparently, these two modes of Ras activation serve distinct and non-redundant functions in MAPK signaling since RasGRP seems to be more important in the initial phase of Ras activation and SOS cannot compensate for RasGRP deficiency (Dower et al., 2000).

1.2.6 TCR-induced JNK and p38 activation

Besides activation of the ERK kinases TCR ligation also triggers the activation of another group of MAPKs, the stress-activated protein kinases (SAPKs) including members of the JNK and p38 MAPK families.

(i) TCR-induced JNK activation

Three members of the JNK family (JNK1-3) have been identified. Whereas expression of JNK3 is predominantly confined to non-lymphoid tissues, both JNK1 and JNK2 are ubiquitously expressed. However, in resting lymphocytes levels of JNK1/2 are very low and their expression is induced upon antigen receptor stimulation. JNK1/2 each exist in four distinct isoforms although the relative importance of the individual isoforms for overall JNK activity remains unclear (Rincon and Davis, 2009). A major substrate of active JNK kinases is the transcription factor c-Jun. Upon phosphorylation on serine 63 and serine 73 c-Jun gains increased transcriptional activity and heterodimerizes with the c-Fos protein to form the active AP-1 transcriptional complex (Davis, 2000).

JNKs themselves are activated by dual phosphorylation on threonine 183 and tyrosine 185 in their T loop by MAPKKs, particularly by MKK4/SEK1 and MKK7/SEK2. These MAPKKs in turn are activated by several MAPKKKs including MEKK1-4, the mixed-lineage kinases (MLKs), and the TGF-β-activated kinase 1 (TAK1) (Davis, 2000). Nonetheless, the precise molecular mechanism underlying TCR-induced JNK activation is still not well understood. A number of *in vitro* studies as well as studies from various knock-out mice have suggested a crucial role of the PKCθ-dependent Carma1-Bcl10-MALT1 (CBM) signalosome in TCR-induced JNK activation (see 1.3.5). First, the ability of the PKC-activating phorbolester 12-myristate 13-acetate (PMA) to induce phosphorylation of JNK proteins has implicated PKCs in TCR-induced JNK activation (Isakov and Altman, 2002). Second, overexpression of PKCθ, but not PKCα in Jurkat T cells mediates robust induction of AP-1 activity whereas, *vice versa*, PKCθ-deficient T cells lack TCR or PMA-induced c-Jun activation (Baier-Bitterlich et al., 1996; Sun et al., 2000). This is in line with reports showing that T cells deficient for the downstream signaling mediators Carma1 or Bcl10 are defective in TCR-induced JNK1/2 phosphorylation although the involvement of different JNK isoforms remains controversial (Blonska et al., 2007; Hara et al., 2003; Rebeaud et al., 2007). Moreover, TAK1 which operates downstream of the CBM complex (see 1.3.5) was shown to be mandatory for TCR-induced JNK activation (Wan et al., 2006).

(ii) TCR-induced p38 activation

The p38 MAPK family consist of four members (p38 α, β, γ, and δ) of which p38α, p38β, and p38δ are expressed in T lymphocytes (Rincon and Davis, 2009). A prominent target of p38 kinases is the activating transcription factor 2 (ATF2) that is activated upon phosphorylation. Akin to JNK activation, induction of p38 kinase activity is dependent on dual phosphorylation of threonine 180 and tyrosine 182 within its activation loop. Direct phosphorylation of p38 was shown to be mediated by the dual specificity kinases MKK3 and MKK6 which in turn are phosphorylated by the upstream activators MEKK3 and MEKK6. These signaling constituents are part of the so-called classical MAPK cascade that is initiated by the activity of small RHO-family GTPases such as Rac1 and Rac2 (Ashwell, 2006). However, recently it has been demonstrated that TCR-induced p38 activation occurs *via* an MEKK-independent alternative pathway that bypasses the MAPK cascade. This alternative pathway relies on direct Lck and ZAP-70-mediated phosphorylation of p38 on tyrosine 323 which results in p38 (mono-)autophosphorylation on threonine 180 to induce full kinase activity (Mittelstadt et al., 2009; Salvador et al., 2005). Furthermore, this pathway involves the scaffold protein discs large homolog 1 (Dlgh1) that inducibly associates with p38 and selectively channels TCR signals towards p38, but not JNK or ERK. Interestingly, knock-down of Dlgh1 in T cells does not only block TCR-induced p38 activation, but also affects the NFAT signaling pathway in response to TCR engagement (Rebeaud et al., 2007; Round et al., 2007).

1.3 Signaling to NF-κB

The transcription factor nuclear factor-kappaB (NF-κB) is a crucial determinant of various biological processes comprising inflammatory reactions, proliferation, cell death, embryonic and tissue development, and tumorigenesis. However, its most important functions refer to the regulation of innate and adaptive immune responses. Originally, NF-κB was identified in the laboratory of David Baltimore more than two decades ago as a transcription factor with inducible activity that selectively binds to specific DNA motifs, known as κB sites, within the kappa light-chain enhancer in B cells (Baeuerle and Baltimore, 1988; Sen and Baltimore, 1986). Since then, the role of NF-κB in diverse cellular processes and in different cellular contexts, including non-immune cells, became more and more evident, and NF-κB served as a model transcription factor whose regulation revealed some generic principles of receptor-induced signaling cascades (Hayden and Ghosh, 2008). In T lymphocytes NF-κB plays a critical role in activation,

differentiation, proliferation, and homing by regulating a wide variety of target genes such as different cytokines (*e.g.* IL-2, IFNγ, and TNFα), chemokines (*e.g.* IL-8), as well as cell adhesion molecules (*e.g.* ICAM-1) (Bonizzi and Karin, 2004; Ghosh and Karin, 2002). The mechanisms and molecular components governing NF-κB signaling are subject of the following sections with particular emphasis on NF-κB regulation in T lymphocytes.

1.3.1 The NF-κB core signaling machinery

(i) The NF-κB family of transcription factors

In mammals the NF-κB family of transcription factors consists of five conserved and structurally related members: NF-κB1 (p50 and its precursor p105), NF-κB2 (p52 and its precursor p100), RelA (p65), RelB, and c-Rel, encoded by *NFKB1*, *NFKB2*, *RELA*, *RELB*, and *REL*, respectively (Hayden and Ghosh, 2008). All NF-κB proteins share an homologous 300 amino acid long N-terminal Rel homology domain (RHD) that contains sequences responsible for homo- and heterodimerization, sequence-specific DNA binding to κB sites, interaction with inhibitory proteins (see below), as well as nuclear translocation (Hayden and Ghosh, 2004). Regulation of NF-κB-dependent transcription occurs *via* NF-κB homo- or heterodimers that bind to promoter or enhancer regions of target genes and the recruitment of transcriptional co-activators and co-repressors (Hoffmann et al., 2006). The co-association with trans-acting factors is mediated through unrelated C-terminal transactivation domains (TADs) that are only present in RelA, c-Rel, and RelB. By contrast, the p50 and p52 subunits lack TADs and might therefore either contribute to transcriptional repression as homodimers or to transcriptional activation as transcriptionally competent heterodimers *via* interaction with TAD-containing NF-κB family members or other TAD-containing proteins (Ghosh and Hayden, 2004). In principle, the ability to undergo homo- and heterodimerization generates a substantial combinatorial complexity among NF-κB transcription factors with up to 15 different dimer combinations. However, the physiological existence and relevance for all possible dimers has not been elucidated yet. Clearly, the heterodimer RelA:p50 is the most abundant transcriptionally active NF-κB complex that is detectable in many cell types (Oeckinghaus and Ghosh, 2009). Besides the possibility of dimer formation another layer of complexity is added by several posttranslational modifications such as phosphorylation and acetylation that have been shown to modulate the DNA sequence specificity as well as the transcriptional competence of NF-κB subunits (Viatour et al., 2005; Perkins, 2006). Moreover, several

auxiliary proteins have been identified that function as nuclear regulators of NF-κB. A particularly intriguing example in T lymphocytes is a recently discovered non-Rel integral subunit of NF-κB, the ribosomal protein S3 (RPS3), that has been shown to co-translocate with RelA into the nucleus upon TCR stimulation and to cause synergistic binding of p65 to κB sites. Consequently, RPS3 deficiency impaired TCR-induced NF-κB activity and upregulation of target genes (Wan et al., 2007).

(ii) The IκB family

In most unstimulated cells NF-κB proteins are sequestered in the cytoplasm by inhibitors of NF-κB proteins, the IκB proteins. The IκB protein family includes classical IκBs, such as IκBα, IκBβ, and IκBε, as well as the inducibly expressed atypical IκB proteins IκBζ, B cell lymphoma 3 (Bcl-3) and IκBNS. All IκB proteins are characterized by the presence of five to seven ankyrin repeat motifs that mediate binding to the RHD of NF-κB dimers. The precursor proteins p100 and p105, which can be proteolytically processed to the NF-κB subunits p52 and p50, respectively, also contain several C-terminal ankyrin repeats that allow them to serve IκB-like functions. The prototypical and most prominent IκB family member is IκBα. Upon various stimuli IκBα is rapidly degraded *via* the proteasome thereby releasing NF-κB dimers to enter the nucleus. p65:p50 heterodimers are most likely the primary target of IκBα (Oeckinghaus and Ghosh, 2009; Vallabhapurapu and Karin, 2009). Retention of NF-κB dimers in the cytosol is mediated by masking of a conserved nuclear translocation sequence (NLS) within the RHD of NF-κB subunits. For IκBα this masking is incomplete, but a nuclear export sequence (NES) within IκBα mediates rapid export of NF-κB:IκBα complexes under steady-state conditions. However, stimulation-induced degradation of IκBα drastically shifts this dynamic equilibrium in favour of nuclear localization of NF-κB transcription factors (Hayden and Ghosh, 2008).

(iii) The IκB kinase complex

Phosphorylation-induced proteasomal degradation of IκB proteins is a hallmark of all NF-κB signaling pathways and an indispensable prerequisite for NF-κB activation. Phosphorylation of IκB proteins is catalyzed by IκB kinases (IKKs) that are organized in a multimeric complex, known as IKK complex.

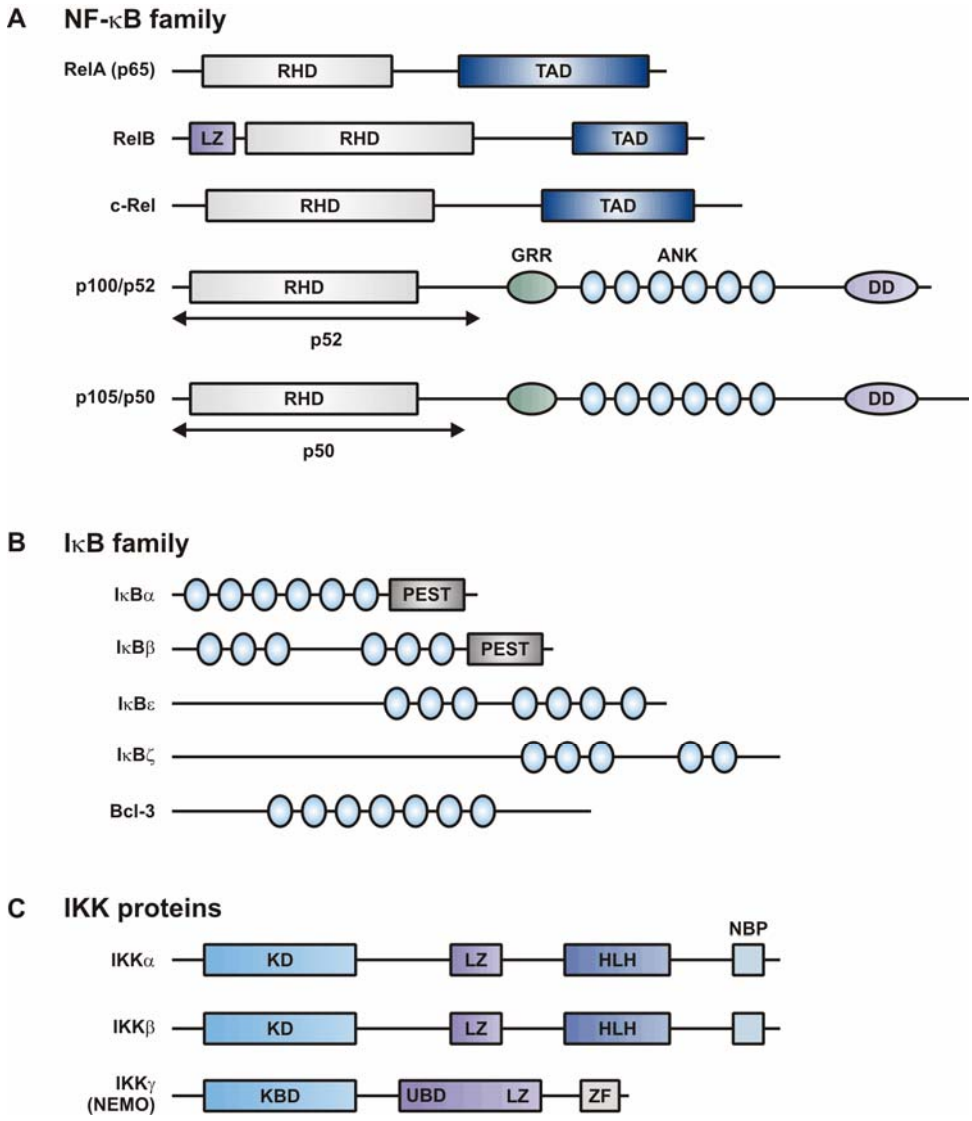

Figure 1.2 | Molecular architecture of NF-κB, IκB, and IKK family members. (A) In mammalian cells NF-κB exists as a group of 5 related transcription factors. All NF-κB family members share a Rel homology domain (RHD) responsible for dimerization, nuclear export, DNA binding and sequestration by IκB proteins. The transactivation domain (TAD) is only found in RelA (p65), RelB, and c-Rel and mediates transcription initiation at κB sites-containing promoters. RelB is unique in harbouring an N-terminal leucine zipper (LZ) motif that plays an important transcriptional regulatory role. p50 and p52 are generated by proteolytic processing of p105 and p100, respectively. The N-termini of these precursor proteins contain the RHD of p50 or p52, followed by a glycine rich region (GRR), multiple ankyrin repeat motifs (ANK), and a C-terminal death domain (DD). **(B)** IκB proteins are characterized by the presence of multiple ANK motifs mediating interactions with NF-κB dimers. Therefore, p100 and p105 can be assigned to both the NF-κB and IκB families. Proline (P), glutamic acid (E), serine (S), and threonine (T) residues within IκBα and IκBβ are indicated as PEST. **(C)** The IKK complex contains the catalytic kinase subunits IKKα and IKKβ, and the regulatory subunit NEMO. The kinase domain (KD) of IKKα or IKKβ is followed by a LZ and a helix-loop-helix (HLH) motif required for kinase dimerization. The C-terminal NEMO-binding peptide (NBP) mediates interaction with the kinase-binding domain (KBD) of NEMO. In addition to its LZ and zinc finger (ZF) motifs NEMO harbours a central Ub-binding domain that mediates binding to K63-linked pUb chains and is indispensable for NEMO signaling functions.

Initially, cytosolic IKK activity had been assigned to a large protein complex of 700-900 kDa with specificity for serines 32 and 36 within the destruction box of IκBα (Chen et al., 1996). Subsequently, biochemical experiments revealed the presence of two highly homologous kinases, IKKα (IKK1) and IKKβ (IKK2), and a regulatory subunit termed IKKγ or NF-κB essential modulator (NEMO) (DiDonato et al., 1997; Mercurio et al., 1997; Rothwarf et al., 1998; Woronicz et al., 1997). This trimolecular IKK complex forms a central nodal point in the receptor-induced activation of the so-called classical or canonical NF-κB signaling pathway. By contrast, an alternative IKK complex composed of IKKα homodimers is crucial for activation of a second NF-κB pathway, termed the alternative or non-canonical pathway (Bonizzi and Karin, 2004) (see 1.3.2).

IKKα and IKKβ, together with IKKi (IKKε) and TBK1, belong to the IKK family of serine-threonine kinases. IKKα and IKKβ both contain an N-terminal kinase domain followed by a C-terminal portion that harbours a conserved leucine-zipper and putative helix-loop-helix (HLH) motifs. IKKα and IKKβ display large sequence identity of 52%, with a greater extent of homology (65%) in the catalytic domain (Woronicz et al., 1997; Hacker and Karin, 2006). Dimerization of IKKα and IKKβ is required for kinase activity and dependent on the leucine zipper domain (Karin, 1999). The HLH is dispensable for kinase dimerization, yet crucial for full kinase activity (Zandi et al., 1998). Apparently, IKKα and IKKβ preferentially form heterodimers *in vivo*, and *in vitro* studies demonstrated that IKKα/IKKβ heterodimers posses a higher catalytic activity than either homodimer (Huynh et al., 2000). Both kinases can be inactivated by a point mutation of lysine 44 within the ATP-binding site (Hayden and Ghosh, 2004). However, there are important biochemical differences between IKKα and IKKβ, especially with respect to substrate specificity. IKKβ is responsible for phosphorylation of most NF-κB-bound IκB proteins, whereas IKKα confers p100 phosphorylation (Scheidereit, 2006). Both kinases are able to phosphorylate IκBα and IκBβ, although IKKβ is both necessary and sufficient to phosphorylate IκBα on serine 32 and serine 36, as well as IκBβ on serine 19 and serine 23 (Hayden and Ghosh, 2004). Moreover, in knock-out studies IKKα could not compensate for IKKβ deficiency. Yet, in the absence of IKKβ, IKKα is able to mediate some residual IκB kinase activity (Li et al., 1999), whereas, *vice versa*, IKKα deficiency has no impact on canonical IκB phosphorylation (Hu et al., 1999).

The third component of the trimolecular IKK complex is NEMO, a regulatory subunit of 48 kDa that lacks intrinsic catalytic activity and is not structurally related to IKKα and IKKβ

(Rothwarf et al., 1998; Yamaoka et al., 1998). It is composed of N- and C-terminal coiled-coil (CC) domains, a leucine-zipper motif, and an N-terminal zink finger-like domain. The C-terminal portion of NEMO is important for IKK activation and interactions with upstream signaling constituents whereas the N-terminus mediates the physical association with IKKα and IKKβ (Oeckinghaus and Ghosh, 2009). A recently identified ubiqutin (Ub)-binding domain (UBD) classifies NEMO as a receptor for K63-linked Ub chains and is mandatory for its signaling functions (Israel, 2010; Wu et al., 2006). IKKs themselves bind to NEMO *via* a short hexapeptide sequence (LDWSWL), known as NEMO binding domain (NBD). Competition experiments using a NBD peptide indicated that IKKβ has a higher affinity to NEMO than IKKα which is consistent with the idea that IKKβ is the dominant IKK in the NEMO-dependent canonical NF-κB pathway (May et al., 2000; May et al., 2002). The stoichiometry of the IKK complex is still controversially discussed. The high apparent molecular weight of 700-900 kDa of the natively purified IKK complex suggests that the IKK complex either contains additional molecules or exists in an oligomeric state. Tegethoff et al. have proposed tetrameric oligomers of NEMO *in vitro* (Tegethoff et al., 2003) while other studies have shown that IKKγ is able to form dimers and trimers, but no tetramers, in a cell type-specific manner (Agou et al., 2004). It has also been assumed that NEMO is monomeric in resting cells while upon stimulation multimeric structures of the stoichiometry $IKK\gamma_3$/IKKα/IKKβ are assembled (Hayden and Ghosh, 2004). However, recent models support the idea of an octameric IKK complex composed of two IKKα/IKKβ heterodimers each bound to two IKKγ molecules with the stoichiometry $(IKK\gamma_2 IKK\alpha_1 IKK\beta_1)_2$ (Hayden and Ghosh, 2008).

Although IKKα, IKKβ, and IKKγ are considered as the core elements of the IKK complex, there is evidence for two other proteins potentially being part of the IKK complex, including the chaperone HSP90/Cdc37 (Chen et al., 2002) and ELKS (Ducut Sigala et al., 2004). Both proteins have been co-purified with the IKK complex; however, their exact IKK-related functions have not been precisely defined yet (Hayden and Ghosh, 2004).

1.3.2 Activation of IKK: the canonical and non-canonical NF-κB signaling pathway

Two distinct NF-κB activation pathways have been described: the classical or canonical and the alternative or non-canonical NF-κB activation pathway. These signaling cascades proceed *via* activation of IKKs and phosphorylation and degradation of IκBs although they differ with regard to the triggering stimuli, IKK components involved and the targeted NF-κB subunits.

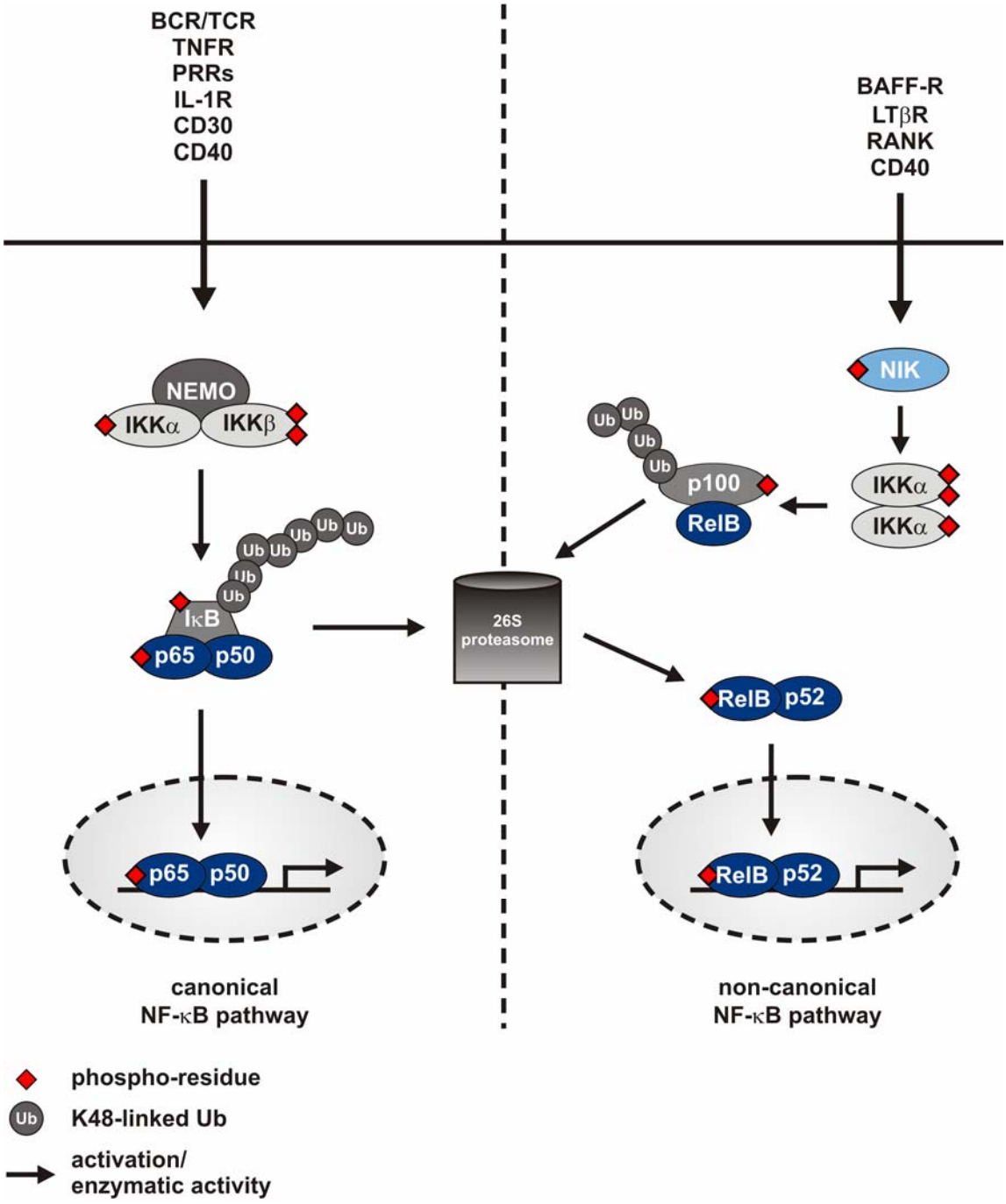

Figure 1.3 | The canonical and non-canonical pathway of NF-κB activation. The canonical pathway (left) is induced by a variety of surface receptors, such as antigen receptors on lymphocytes or the TNFR1, that converge on the activation of the trimeric IKK complex composed of IKKα, IKKβ, and NEMO. IKK activity leads to phosphorylation of IκB proteins which, in turn, induces K48-linked polyubiqitination of IκBs and their subsequent proteasomal degradation. Liberated p65/p50 dimers then traffic into the nucleus to turn on transcription of target genes. The non-canonical pathway (right) depends on NIK-induced activation of IKKα homodimers. Activated IKKα phosphorylates p100 to induce its partial proteolysis to p52 by the proteosome. Transcriptionally active p52 preferentially heterodimerizes with RelB to translocate into the nucleus and to promote transcription of target genes.

(i) The canonical NF-κB pathway

The canonical NF-κB signaling pathway is the major activation pathway triggered by most proinflammatory cytokines (*e.g.* TNFα, IL-1), PRRs, and antigen receptors (Bonizzi and Karin, 2004) (see 1.3.4 and 1.3.5). This pathway centers around the trimolecular IKK complex composed of IKKα, IKKβ, and NEMO and primarily involves activation of RelA:p50 NF-κB transcription factors (Vallabhapurapu and Karin, 2009). In the context of canonical signaling IKKβ is the predominant IκB-targeting IKK, although there are exceptions, for instance receptor activator of NF-κB ligand (RANKL)-stimulated mammary epithelial cells, which rely on IKKα for stimulation-induced IκBα phosphorylation (Cao et al., 2001). The overall role of IKKα in this pathway remains unclear. It has been speculated that IKKα serves structural functions within the IKK complex. Furthermore, IKKα plays an important nuclear role in NF-κB dependent gene expression in all canonical NF-κB pathways (Hayden and Ghosh, 2008). The general importance of the canonical pathway in the immune system has been revealed by genetic studies demonstrating that conditional IKKβ or RelA knock-out mice show a significantly higher susceptibility to infections (Gerondakis et al., 1999; Pasparakis et al., 2006).

Receptor-induced IKK activation primarily results in IκBα phosphorylation leading to its recognition and polyubiquitination at lysine 19 by the Skp1, Cdc53/Cullin1, and F-box protein β transducin repeat-containing protein (βTRCP)$SCF^{I\kappa B}$ E3 Ub ligase complex. K48-linked polyubiquitin (pUb) chains mark IκBα for degradation *via* the 26S proteasome, thereby liberating NF-κB dimers (Karin and Ben-Neriah, 2000).

(ii) The non-canonical pathway

The non-canonical pathway is triggered by a more restricted number of receptors including TNFR family receptors such as BAFF-R (B cell activating factor receptor), CD40 and RANK on B cells, as well as the lymphotoxin β receptor (LTβR) on splenic stromal cells (Bonizzi and Karin, 2004). In marked contrast to the canonical pathway, it does not rely on IKKβ and NEMO but depends on the activity of IKKα (Senftleben et al., 2001). Although still substantial evidence is missing, it is generally assumed that an alternative IKK complex composed of IKKα homodimers that are not bound to NEMO forms the receptor-activated IKK signaling entity in analogy to the trimeric IKK complex in the canonical pathway (Scheidereit, 2006; Hayden and Ghosh, 2008). The primary IκB-like target of IKKα is p100 which upon phosphorylation on serines within its C-terminal ankyrin

repeat domain is polyubiquitinated by the $SCF^{I\kappa B}$ E3 Ub ligase complex (Amir et al., 2004; Senftleben et al., 2001). This in turn leads to the limited proteasomal proteolysis of p100, a process with some similarity to the proteasomal editing of p105, and to the generation of active RelB/p52 heterodimers. However, generation of p50 subunits by proteasomal processing of the precursor protein p105 is a constitutive co-translational process (Oeckinghaus and Ghosh, 2009). Interestingly, there is cross talk between the canonical and non-canonical pathways as the former leads to upregulated expression of RelB and p100 and therefore feeds into the non-canonical pathway (Scheidereit, 2006).

1.3.3 Mechanisms and principles of IKK activation

Activation of the IKK complex requires phosphorylation of two serine residues within the activation T loop of both kinases which presumably induces a conformational change leading to kinase activation. Mutation of these residues in IKKβ (S177/S181) and IKKα (S176/180), respectively, to alanines prevents kinase activation, whereas the replacement with phosphomimetic glutamates in IKKβ (IKKβ(SS/EE)) results in a constitutively active enzyme (Delhase et al., 1999; Hacker and Karin, 2006). However, the mechanisms through which these phosphorylation events occur are still controversially discussed. A crucial question that remains to be answered is whether IKK activation depends on transautophosphorylation and/or phosphorylation by upstream IKK kinases (IKK-Ks).

The most compelling evidence for the existence and action of an IKK-K comes from the non-canonical pathway. The NF-κB-inducing kinase (NIK) is a MAPKKK family member and directly phosphorylates IKKα on its T loop serines leading to IKKα activation (Regnier et al., 1997). Although NIK has been shown to associate with IKKβ and NEMO (Bouwmeester et al., 2004; Lin et al., 1998), genetic studies from NIK knock-out mice and transgenic mice expressing a dominant negative version of NIK clearly proof an exclusive role of NIK in the alternative pathway (Shinkura et al., 1999).

Other studies have provided evidence for a role of the upstream MAPKKKs MEKK3 and TAK1 as IKK-Ks. MEKK3 phosphorylates and activates IKKα and IKKβ at their activation loops, and murine embryonic fibroblasts (MEFs) lacking MEKK3 exhibit impaired IκBα degradation upon TNFα stimulation (Yang et al., 2001a). MEKK3 inducibly associates with IKKs and is required for the assembly of the active IKK complex with IκBα (Schmidt et al., 2003). However, a direct phosphorylation of IKKβ by MEKK3 has not been shown yet, and it is conceivable that MEKK3 serves different functions, for example by bridging of IKK with IκBα, phosphorylation of IKK-activating substrates (*e.g.* ELKS), or by directly acting

as a scaffold protein. Moreover, a role of MEKK3 as an essential IKK-K in immune cells remains elusive (Hayden and Ghosh, 2004). TAK1 is another putative IKK-K that has been particularly implicated in TCR-induced NF-κB signaling. Akin to MEKK3, TAK1 overexpression induces NF-κB activation although TAK1 needs co-expression of its regulatory subunits TAB1, TAB2, or TAB3. TAK1 seems to be recruited to the activated TNF receptor (TNFR) and to phosphorylate the activation loops of the IKK catalytic subunits (Ishitani et al., 2003; Wang et al., 2001). Moreover, small interfering RNA (siRNA)-mediated silencing of TAK1 reduced IκBα phosphorylation and blocked IL-2 production upon TCR triggering in Jurkat T cells *in vitro* (Sun et al., 2004). However, the analysis of TAK1-deficient mice did not support a general role of TAK1 in antigen receptor-dependent IKK activation. BCR-induced NF-κB activation in the absence of TAK1 is not impaired (Sato et al., 2005), and TAK1 seems to selectively control TCR-induced NF-κB activation in thymocytes, but not in effector T cells (Liu et al., 2006; Wan et al., 2006). In concert, these data suggest a cell type-specific role for TAK1 and MEKK3 in NF-κB activation, and these kinases might rather lead to the amplification of IKK activity following initial IKK activation *via* transautophosphorylation.

Indeed, the concept of transautophosphorylation of IKKs by induced proximity and/or conformational changes has attracted more and more attention with the description of macromolecular scaffolding platforms that recruit IKK complexes, leading to their oligomerization and thereby activation. In this context, the discovery of non-degradative K63-linked polyubiquitination has led to a substantial improvement of the understanding of canonical IKK activation (Chen et al., 1996; Chen, 2005; Wertz and Dixit, 2010). Stimulation-dependent K63-linked ubiquitination of NEMO and various upstream signaling mediators in the canonical NF-κB signaling pathway is thought to mediate the assembly and stabilization of multi-protein complexes which in turn provide a scaffold for IKK oligomerization (Inohara et al., 2000). In support of this concept, it was recently demonstrated that even free and unanchored K63-linked pUb chains are sufficient to promote activation of TAK1 and IKKs *in vitro* (Xia et al., 2009). The assembly of these high-molecular IKK-containing complexes substantiates a role for transauto-phosphorylation of IKKs; however it is possible and not mutually exclusive that in a cell type and pathway-specific manner these signalosomes integrate IKK-Ks to catalyze IKK activation.

1.3.4 TNFR-induced NF-κB activation

Signaling by TNFα has long been a prototypic model for receptor-induced canonical IKK activation. TNFα binds to two receptors, TNFR1 and TNFR2, of which TNFR1 plays a much more prominent role in the immune system. TNFR1 is expressed on haematopoietic and non-haematopoietic cells with the strongest expression on epithelial cells whereas its ligand, TNFα, is secreted by activated DCs, macrophages, and T cells. TNFR1 ligation induces receptor trimerization and recruitment of the adapter protein TNFR1-associated death domain protein (TRADD). TRADD in turn enables binding of the serine threonine kinase receptor-interacting protein 1 (RIP1) and of the E3 ligases TNFR-associated factor 2 (TRAF2) and TRAF5 to the activated TNFR. Finally, these molecules co-recruit the E3 ligases cellular inhibitor of apoptotic proteins 1 (c-IAP1) and c-IAP2. Together, this conglomerate of molecules at the engaged TNFR1 forms the so-called complex 1 or TNFR-signaling complex (TNF-RSC) (Micheau and Tschopp, 2003). RIP1 is important for NF-κB activation downstream of TNFR1 although its kinase activity is completely dispensable (Meylan et al., 2004; Ting et al., 1996). Upon recruitment into the TNF-RSC RIP1 is covalently modified by the attachment of K63-linked pUb chains (Ea et al., 2006). Initially, TRAF2 was assumed to be the E3 ligase for RIP1; however novel studies support a role for TRAFs as adaptors for c-IAPs that in turn serve E3 ligase functions in TNFR1 signaling (Bianchi and Meier, 2009; Wu et al., 2007). The K63-linked pUb chains associated with RIP1 then induce the recruitment of two Ub-binding complexes, the TAK1/TAB complex (TAK1/TAB2/TAB3), and the IKK complex *via* the Ub receptors TAB2 and NEMO, respectively (Ea et al., 2006; Kanayama et al., 2004; Li et al., 2006a; Wu et al., 2006). Subsequently, TAK1 is believed to activate IKKβ, most probably through proximity-induced phosphorylation. However, two recent studies have led to a substantial refinement of the current dogma of TNFR1-induced IKK activation. Haas et al. and Tokunaga et al. reported independently the identification of an additional E3 ligase complex within the TNF-RSC, termed the linear Ub chain assembly complex (LUBAC) (Haas et al., 2009; Tokunaga et al., 2009). Unlike c-IAPs this complex catalyzes the polyubiquitination and attachment of linear Ub chains to NEMO and most likely other components of complex 1. In addition to initial K63-linked ubiquitination, this novel mode of linear ubiquitination has been suggested to stabilize the TNF-RSC and to support the recruitment, retention, and ubiquitination of the IKK complex (Bianchi and Meier, 2009).

1.3.5 TCR-induced NF-κB activation

Activation of NF-κB following triggering of antigen receptors is a crucial step for the regulation of antigen-specific proliferation, survival, maturation, and the effector functions of lymphocytes. Genetic deficiencies in the activation pathway coupling the TCR to NF-κB has been linked to immune deficiencies, whereas aberrant and constitutive NF-κB activity in lymphocytes is associated with autoimmune disorders and causative for the development of lymphoid malignancies (Li and Verma, 2002) (see section 1.5).

Antigen receptor-induced NF-κB activation involves the canonical machinery of NF-κB signaling. Engagement of the TCR/CD3 complex leads to the recruitment of the IKK complex into the immunological synapse (IS) (Khoshnan et al., 2000). However, the molecular events coupling the activated TCR to the IKK complex remained elusive until the identification of three interacting proteins known as Carma1 (caspase recruitment domain (CARD), membrane-associated guanylate kinase (MAGUK) protein 1), Bcl10 (B cell lymphoma10), and MALT1 (mucosa-associated lymphoid tissue lymphoma translocation protein 1). The PKCθ-dependent Carma1-Bcl10-MALT1 (CBM) complex is a central gateway in TCR-induced NF-κB activation. Deficiencies of either proteins cause profound defects in BCR- and TCR-induced NF-κB signaling and lymphocyte activation (for review see Thome, 2004).

Immunofluoresence studies using Carma1 knock-out mice demonstrated that the IKK complex is recruited into the IS in a Carma1-dependent manner (Hara et al., 2004). Carma1 belongs to the MAGUK family that is characterized by the presence of several protein interaction (PDZ) domains, an SH3 domain and guanylate kinase (GUK) domain (Dimitratos et al., 1999). Additionally, Carma1 possesses a CARD domain and a coiled-coil motif at its N-terminus that is separated by an extended linker region from the C-terminal MAGUK domains (Thome, 2004). A small fraction of Carma1 constitutively resides in lipid rafts and becomes further enriched upon stimulation (Gaide et al., 2002). The linker region of Carma1 is a major substrate of PKCθ. Following TCR engagement PKCθ-mediated phosphorylation of critical residues within the Carma1 linker region, also known as PKC-regulated domain (PRD), is thought to impose a conformational change within Carma1 that enables the direct and inducible interaction with Bcl10 (Matsumoto et al., 2005; Sommer et al., 2005; Wang et al., 2004). The association between Carma1 and Bcl10 is based on a homophilic interaction between the CARD domains of both proteins. Bcl10 operates downstream of Carma1 since deletion of the Carma1 CARD domain interferes with Bcl10 recruitment into lipid rafts and TCR-induced NF-κB activation (Gaide

et al., 2001). Bcl10 in turn is constitutively associated with MALT1 involving the Ig-like domains of MALT1 and a short C-terminal sequence within Bcl10. Both proteins are targets of chromosomal rearrangements linked to development of MALT1 lymphomas, underscoring their functional interaction in a common pathway (Lucas et al., 2001; Uren et al., 2000) (see 1.5.2).

Activation of the Carma1 signalosome is thought to induce an oligomerization cascade (Sun et al., 2004) which is substantiated by the observation that overexpression of Carma1, Bcl10, or MALT1 alone is sufficient to induce their activation and NF-κB signaling (Rawlings et al., 2006). The E3 ligases TRAF2 and TRAF6, which were predominantly implicated in TNFR- and IL-1R-induced IKK activation, are important downstream targets of MALT1 linking the CBM complex with the IKK complex. Oligomerization and recruitment of TRAF6 to the CBM complex leads to TRAF6 activation and K63-linked ubiquitination of TRAF6 itself and its major target NEMO (Sun et al., 2004). Moreover, recently MALT1 has been reported to contain an E3 ligase activity that catalyzes both its K63-linked autoubiquitination as well as Bcl10-dependent transubiquitination of NEMO (Oeckinghaus et al., 2007; Zhou et al., 2004a), although this activity is enhanced in the presence of TRAF6 (Sun et al., 2004). Ubiquitination of NEMO as well as recruitment and oligomerization of the IKK complex to the polyubiquitinated CBM signalosome then trigger IKK activation, most probably involving IKK transautophosphorylation and TAK1-mediated IKK phosphorylation (Rawlings et al., 2006). The complexity of the NF-κB-activating signalosome is further increased by the fact that caspase-8 is required for TCR-induced NF-κB activation. Caspase-8 binds to the activated CBM complex, and T lymphocytes lacking caspase-8 show diminished NF-κB activation (Bidere et al., 2006; Su et al., 2005). Interestingly, the rare disorder caspase-8 deficiency (CED) is due to a lack of caspase-8 expression and is associated with several immune defects (Chun et al., 2002).

Phosphorylation of Carma1 by PKCθ is a critical step in activation of the CBM complex, but the molecular details of the interactions between these upstream components have long been elusive. However, the finding that the 3-phosphoinositide-dependent kinase 1 (PDK1) mediates PKCθ phosphorylation and itself inducibly associates with Carma1 has significantly contributed to a more precise understanding of this signaling pathway (Lee et al., 2005). PDK1 is a plasma membrane-associated serine threonine kinase that is activated and recruited to the TCR *via* a CD28 co-stimulation-dependent mechanism involving phosphoinositide-3 kinase (PI3K) and Vav1 (Park et al., 2009).

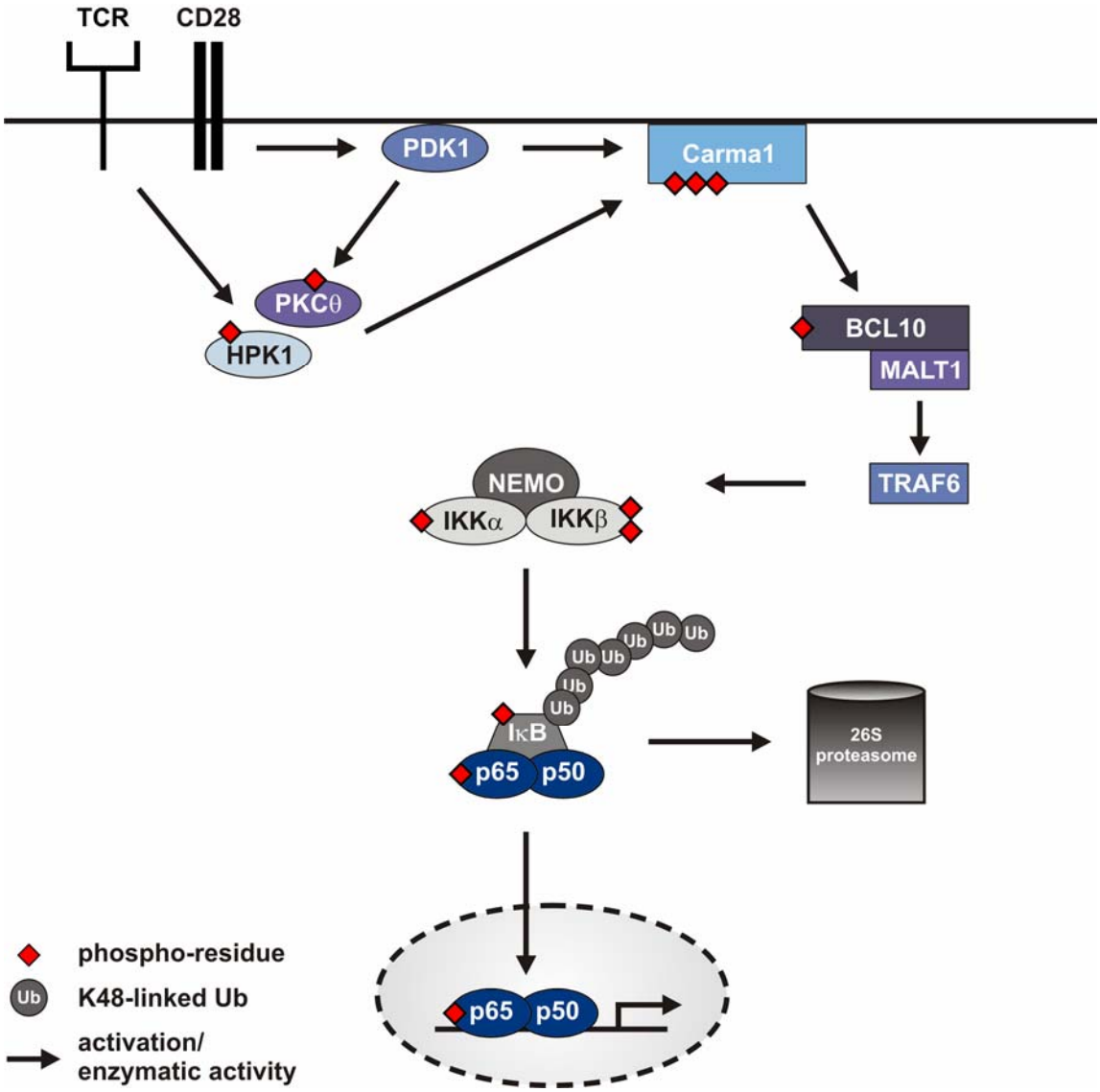

Figure 1.4 | TCR-induced signaling to NF-κB. Triggering of the TCR results in the activation of a receptor proximal core signalosome leading to activation of serine/threonine kinases PKCθ and HPK1. In addition, co-engagement of CD28 results in the activation and membrane recruitment of PDK1. PDK1 phosphorylates and activates PKCθ and inducibly associates with Carma1 in lipid rafts. Recruitment of the scaffold Carma1 to the plasma membrane facilitates its phosphorylation by PKCθ and HPK1 unleashing its adaptor functions. Activated Carma1 presumably undergoes a conformational change allowing for the association with BCL10 and MALT1 and the formation of a stable macromolecular signaling platform, known as CBM complex. Assembly of the CBM complex, in turn, leads to the recruitment, oligomerization and activation of the E3 ligase TRAF6. TRAF6-dependent K63-linked polyubiquitination of MALT1, NEMO, and TRAF6 itself facilitates the recruitment and activation of the IKK complex, most likely involving transautophosphorylation of IKKs by induced-proximity. The activated IKK complex then phosphorylates and marks IκBα for proteasomal degradation leading to nuclear translocation of transcriptionally active p65/p50 NF-κB heterodimers.

PDK1 phosphorylates and activates PKCθ. PKCθ-dependent phosphorylation of Carma1 results in membrane recruitment of the CBM complex; however, PDK1 seems to contribute to this process by interacting with Carma1 independently of PKCθ (Lee et al., 2005). Thus, PDK1 is a linker between PKCθ and the CBM complex and integrates TCR and CD28-induced signals to mediate NF-κB activation in T lymphocytes.

Although PKCθ seems to be the most dominant kinase targeting Carma1, other kinases have been described to contribute to CBM-dependent NF-κB signaling. Recently, a kinase-independent adaptor function of the casein kinase 1α (CK1α) has been shown to be important for antigen receptor-induced NF-κB activation (Bidere et al., 2008). Moreover, stimulation-dependent phosphorylation of the Carma1 linker region by HPK1 on serine residues that are different from PKCθ-phosphorylated sites seems to be crucial for TCR-induced CBM activation *in vitro*, although HPK1 might play a role as modulator rather than as indispensable trigger of TCR-induced NF-κB signaling (Brenner et al., 2009).

1.4 Mechanisms of negative regulation and signal termination

Signal initiation and propagation are based on rapid biochemical reactions that can be categorized into some generic themes of signaling such as phosphorylation, ubiquitination, localization, oligomerization, conformational regulation, and degradation. The reversion of these processes by counteracting negative regulatory mechanisms is a fundamental cell-intrinsic principle of signal transduction ensuring proper signal shaping, control, and termination (Acuto et al., 2008). Aberrations of these opposing mechanisms in T cells and other immune cells are associated with autoimmune disorders and cancer (see also section 1.5).

1.4.1 The human phosphatasome and its expression in T cells

Since its discovery by Edmond Fischer and Erwin Krebs more than 50 years ago it has become clear that reversible protein phosphorylation – catalyzed by kinases and their opposing counterparts phosphatases, respectively – is one of the most versatile posttranslational modifications that pervades nearly all aspect of cell physiology (reviewed in Bennett et al., 2006). Whereas kinases predominantly serve activating functions within diverse signaling cascades, phosphate removal by phosphatases is often, albeit not generally involved in negative regulation of signaling events. The human genome encodes in minimum 518 protein kinases with 90 PTKs and 428 protein serine/threonine kinases (PSKs) (Manning et al., 2002). By contrast, the number of phosphatase genes is

significantly lower and not yet precisely defined. Strikingly, 107 protein tyrosine phosphatases (PTPs) have been identified, whereas far fewer protein serine/threonine phosphatases (PSPs) (about 30) are known (Alonso et al., 2004; Shi, 2009). The dichotomy in the numbers of PSKs and catalytic subunits of PSPs can be explained by the combinatorial formation of PSP holoenzymes that are composed of one catalytic subunit and several non-enzymatic regulatory subunits. The most prominent class of PSPs are the phosphoprotein phosphatases (PPPs). There are only 13 genes encoding for catalytic subunits of PPPs in the human genome (Virshup and Shenolikar, 2009). However, by proteomic and genetic approaches interactions between more than 160 regulatory subunits and their corresponding PPP catalytic subunits have been already mapped (Bennett et al., 2006). Regulatory subunits are thought to govern phosphatase activity by regulating substrate targeting, subcellular localization, and enzymatic activity (Janssens et al., 2005; Mumby, 2007). Furthermore, small subfamilies of PTPs are known that catalyze the dephosphorylation of phospholipids (Wishart and Dixon, 2002). Whereas most PPP catalytic subunits are ubiquitously expressed, about 40 different gene products of PTPs have been detected in T lymphocytes (Mustelin et al., 2004).

1.4.2 Negative regulation of proximal TCR signaling by phosphatases

The assembly of the TCR proximal signalosome (see section 1.2) primarily involves the activation and activity of an array of protein tyrosine kinases (PTKs). Consequently, most phosphatases found to be associated with the upstream TCR signaling machinery are phosphatases of the PTP family (reviewed in Mustelin et al., 2004). The most prominent TCR proximal phosphatases will be shortly discussed in the following.

CD45 is the most abundantly expressed transmembrane PTP on T cells that has been primarily implicated in the positive regulation of Lck activity. In resting cells Lck is rendered inactive through phosphorylation on its inhibitory tyrosine residue by the C-terminal Src kinase (Csk). This inhibitory phosphorylation is counteracted by CD45 although it has been shown that CD45 also contributes to negative regulation of Lck by dephosphorylating its active site (Hermiston et al., 2003). Protein tyrosine phosphatase, receptor type, A (PTPRA) is a homologue of CD45 that, similar to CD45, appears to regulate Fyn activity in thymocytes (Maksumova et al., 2005). In addition, protein tyrosine phosphatase, non-receptor type 22 (PTPN22) has been shown to inhibit Lck activity (Hasegawa et al., 2004), and PTPN22 mutations have been linked to an increased risk for several autoimmune diseases in humans (Vang et al., 2005).

Another prominent cytoplasmic PTP in lymphocytes is the SH2 domain-containing phosphatase 1 (SHP1, also termed PTPN6). SHP1 contributes to the negative regulation of Lck (Stefanova et al., 2003), but has been implicated in the dephosphorylation and inactivation of ITAM-bound ZAP-70 as well (Acuto et al., 2008). SHP1-deficient (so-called motheaten) mice display aberrant lymphocyte development, T cell hyperactivation, and autoimmunity (Tsui et al., 1993). Furthermore, the suppressor of TCR signaling (Sts) family of proteins consisting of Sts1 and Sts2 play an important role in negative regulation of the TCR signalosome. Sts1 and Sts2 contain phosphatase activity to ZAP-70, Syk and SFKs although their precise mode of action is still unclear. Sts1 and Sts2 double-deficient mice show increased phosphorylation of ZAP-70, LAT, and SLP-76 which is likely to explain their phenotype of T cell hyperproliferation and increased susceptibility to autoimmunity (Carpino et al., 2004; Mikhailik et al., 2007).

The inositol phosphatases phosphatase and tensin homolog (PTEN) and the SH2 domain-containing inositol phosphatase 1 (SHIP1) dephosphorylate the second messenger PtdIns(3,4,5)P_3 within the plasma membrane and thereby counteract activation of PI3K and downstream signaling pathways (Harris et al., 2008). PTEN plays a rather ubiquitous role as tumor suppressor (Cully et al., 2006). T cell-specific PTEN knock-out mice exhibit splenomegaly and enlargement of the thymus (Suzuki et al., 2001) while the impact of SHIP1 deletion on T cell biology is less well studied (Helgason et al., 1998; Liu et al., 1998b). Importantly, the human model T cell line Jurkat lacks expression of both proteins although the PI3K-Akt pathway is still inducible upon TCR stimulation (Abraham and Weiss, 2004). This argues for a role of both phosphatases in defining thresholds of lymphocyte activation (Harris et al., 2008).

1.4.3 The NF-κB-regulating phosphatasome

The negative regulation of MAPK signaling cascades by a number of MAPK phosphatases (MKPs) – among which members of the dual specificity phosphatase (DUSP) family play the most prominent role – is well-established (Liu et al., 2007). In contrast, only few phosphatases have been implicated in the regulation of NF-κB activity. These phosphatases have been characterized in the context of different cellular systems and NF-κB-triggering stimuli, and most studies rely on overexpression of phosphatases and the use of phosphatase inhibitors. However, only scattered reports have provided genetic data that help to understand the role of phosphatases in the dephosphorylation of specific substrates within the NF-κB signaling pathway.

The most prominent phosphatase implicated in the regulation of NF-κB activity is PP2A. PP2A is an ubiquitously expressed phosphatase entity that exists as a collection of holoenzymes composed of one catalytic subunit PP2Ac (PP2Acα or PP2Acβ) and a regulatory A subunit (PR65 α or β isoform) that together form the core dimer, as well as multiple associated B subunits conferring and increasing substrate specificity (Janssens and Goris, 2001).

Several early reports have associated PP2A activity with negative regulation of NF-κB based on the observation that PP2A inhibitors induced activity and phosphorylation of the IKK complex and RelA, respectively, and led to enhanced and prolonged TNFα-dependent phosphorylation of IκBα. *Vice versa*, purified PP2A was shown to inhibit IKK kinase activity and to promote RelA dephosphorylation *in vitro* (DiDonato et al., 1997; Fu et al., 2003; Sun et al., 1995; Yang et al., 2001b). Moreover, PP2A seems to operate at different levels since physical interactions between PP2A and components of the IKK complex or RelA have been described (Fu et al., 2003; Yang et al., 2001b). Consistent with these results, a recent study has shown that siRNA-mediated silencing of PP2A catalytic or regulatory subunits enhanced TNFα-induced NF-κB activation (Li et al., 2006b). Whereas PP2Acβ and PP2R1A subunits were demonstrated to directly impinge on IKKβ phosphorylation and activation, PP2Acα/PP2R1B entities were shown to dephosphorylate RelA on serine 536, thereby inhibiting NF-κB activity *in vitro*. In addition, the PP2Acα/PP2R1A/ PP2R5C module was shown to interact with TRAF2 and to inhibit its activity by dephosphorylation of threonine 117 (Li et al., 2006b). However, this report did not provide evidence for a direct interaction and dephosphorylation of endogenous IKK and other NF-κB signaling constituents by PP2A. Indeed, more recently it has been suggested that PP2A-mediated IKK inhibition is rather due to direct dephosphorylation and inactivation of the upstream IKK-K MEKK3 (Sun et al., 2010). Instead, the magnesium-dependent phosphatases PPM1A and PPM1B were described as IKKβ phosphatases (Prajapati et al., 2004; Sun et al., 2009). Interestingly, PP2A has also been implicated in positive regulation of IKK activity, presumably by removing inhibitory phosphate groups (Kray et al., 2005).

Moreover, a recent study demonstrated that the PSP PP1 negatively regulates TNFα-induced phosphorylation and activation of IKKβ in murine macrophages and is inducibly recruited to the IKK complex (Li et al., 2008). IKK dephosphorylation was shown to depend on a ternary complex composed of the catalytic subunit PP1c, the PP1 regulatory subunit GADD34, and the adapter protein CUEDC2. The same authors, however, could

not verify a role for PP2A in negative regulation of IKK activity. Although all experimental systems were based on TNFα-induced NF-κB activation, these discrepancies might be explained by cell type-specific expression and/or functions of different phosphatase subunits.

Few other phosphatases have been linked to the negative regulation of NF-κB. The PSP catalytic subunit PP6c has been shown to interact with and to dephosphorylate IκBε, thereby interfering with TNFα-induced NF-κB activation (Bouwmeester et al., 2004; Stefansson and Brautigan, 2006). More recently, the phosphatase WIP1 (also known as PPM1D) has been identified as a negative regulator of nuclear RelA activity, probably by promoting its specific dephosphorylation on serine 536 (Chew et al., 2009). However and in contrast to these results, WIP1-deficient T cells exhibited even decreased TCR-induced proliferation arguing against a general and non-redundant negative regulatory function of WIP1 (Choi et al., 2002).

So far, most studies have been conducted using non-immune epithelial cell lines on the basis of TNFα-mediated stimulation. Hence, the involvement of these and most likely other phosphatases in the regulation of NF-κB activity in T lymphocytes still remains to be addressed.

1.4.4 Non-phosphatase-based negative regulation of canonical NF-κB

Besides the regulatory functions of phosphatases a number of distinct mechanisms are involved in terminating the NF-κB response that operate on different levels within the NF-κB pathway. Most of these mechanisms rely on rapid and highly efficient negative feedback inhibition of NF-κB.

Perhaps the most prominent example of IKK proximal feedback inhibition of NF-κB involves the transcriptional control of IκB proteins. For instance, IκBα is a *bona fide* NF-κB target gene, and NF-κB activity promptly causes upregulated expression of IκBα (Sun et al., 1993). *De novo* synthesized unphosphorylated IκBα then enters the nucleus and associates with DNA-bound p50:RelA dimers to promote their export into the cytosol (Vallabhapurapu and Karin, 2009).

A20 is another NF-κB target gene that in turn acts as negative feedback regulator of NF-κB (Coornaert et al., 2009; Hymowitz and Wertz, 2010). A20 is an Ub-editing enzyme that serves dual functions. On the one hand, it contains a deubiquitinase domain (DUB) that catalyzes removal of activating K63-linked Ub chains from NF-κB signaling proteins,

such as RIP1 and MALT1. On the other hand, it mediates destructive K48-linked ubiquitination of NF-κB effector proteins thereby shutting down the NF-κB response (Duwel et al., 2009; Lee et al., 2000; Wertz et al., 2004). A20 deficiency in T cells causes enhanced and prolonged TCR-induced IKK and IκBα phosphorylation *in vitro* (Duwel et al., 2009), and T cells from A20-deficient mice display a hyperactivated phenotype *in vivo* (Song et al., 2008). Similar to A20, the familial cylindromatosis tumor suppressor (CYLD) acts a deubiquitinating enzyme that inhibits NF-κB by removing K63-linked pUb chains from NEMO and TRAF proteins (Brummelkamp et al., 2003; Kovalenko et al., 2003; Trompouki et al., 2003). Unlike A20, CYLD exerts constitutive activity and, therefore, it might predominantly control basal NF-κB activity, whereas A20 operates in a stimulation-dependent manner (Sun, 2008).

Another IKK-regulating negative feedback mechanism in T lymphocytes involves the proteolytic processing of HPK1. In resting T cells HPK1 exists in its full length form while *in vitro* expansion of primary T cells is accompanied by cleavage of HPK1 giving rise to its non-catalytic cleavage product HPK1-C. Whereas HPK1 acts as Carma1-activating kinase, HPK1-C sequesters the IKK complex and blocks NF-κB activation in a dominant negative manner (Brenner et al., 2005; Brenner et al., 2009).

In addition to these negative regulatory mechanisms that mainly target receptor and IKK proximal components, several other modes of NF-κB inhibition have been described, including the nuclear degradation of RelA and the disruption of NF-κB transcriptional complexes (Wan and Lenardo, 2010).

1.5 NF-κB and lymphoid malignancies

1.5.1 Target genes of NF-κB and their implications in tumorigenesis

Besides its crucial physiological role in the immune system, a large body of evidence has clearly established a connection between NF-κB and cancer development and progression. It is now widely accepted that NF-κB activity predominantly serves pro-oncogenic functions since the majority of NF-κB target genes promote cell survival, proliferation and apoptosis resistance, as well as cell adhesion, migration, invasion, and tumor angiogenesis (Karin, 2009). Dysregulated and constitutive NF-κB activity results in aberrant expression of these target genes conferring or promoting the independency on

paracrine growth factors for survival and the capability to evade programmed cell death, or apoptosis. Indeed, these events have been identified as hallmarks of cancer (Hanahan and Weinberg, 2000) establishing a causative role of NF-κB not only in immune physiology, but also in tumorigenesis.

Apoptosis is a fundamental physiological process that regulates cellular and tissue homoestasis through removal of superfluous, damaged, or transformed cells (Vaux and Korsmeyer, 1999). Induction and execution of apoptosis are mediated and regulated by a variety of pro- and anti-apoptotic gene products. Relative expression and activity of these proteins determine the balance between apoptosis sensitivity and apoptosis resistance. Apoptosis can be induced *via* the so-called extrinsinc pathway that relies on engagement of death receptors, such as TNFR and CD95, by cognate ligands (Krammer, 2000). In addition, the intrinsic apoptosis-inducing pathway is triggered by a variety of stimuli, such as DNA damage and UV-irradiation, and involves the permeabilization of the outer mitochondrial membrane and cytochrome c (cyt c) release. However, both pathways converge on the activation of a related family of proteases, known as cysteine-aspartate-specific proteases (caspases) that execute the apoptotic program (Hengartner, 2000).

NF-κB target genes encoding for anti-apoptotic proteins include c-IAP1 and c-IAP2, XIAP, the cellular FLICE inhibitory protein (c-FLIP), Bcl-2, Bcl-X_L, survivin, TRAF1, as well as TRAF2 (Braun et al., 2006).

As outlined above, TRAF proteins are important for TNFα-induced NF-κB activation, and their anti-apoptotic functions might rather be attributed to their NF-κB-activating effects than to a direct intervention in the apoptosis-inducing machinery (Baud and Karin, 2001). By contrast, c-IAPs directly interfere with apoptosis induction *in vitro* by inhibition of the initiator and effector caspases caspase-9, and caspase-3, respectively (Deveraux et al., 1999). The c-IAP2 promoter contains two κB-sites which explains the NF-κB dependent expression of c-IAP2 (Hong et al., 2000). c-IAP inhibition causes c-IAP autoubiquitination and degradation leading to sensitization towards TNFα-dependent apoptosis (Varfolomeev et al., 2007). Transgenic overexpression of XIAP, another IAP family member, however, was shown to confer resistance of thymocytes towards multiple death stimuli (Conte et al., 2001). Moreover, overexpression of c-FLIP directly impinges upon death receptor-induced apoptosis (Scaffidi et al., 1999), and MEFs from FLIP-deficient mice exhibit hypersensitivity towards TNFα and CD95 ligand (CD95L)-induced apoptosis (Yeh et al., 2000). The Bcl-2 family members Bcl-2A1 and Bcl-X_L oppose the intrinsic mitochondrial pathway by blocking of mitochondrial membrane permeabilization and

prevention of subsequent caspase 9 activation (Strasser, 2005; Wang et al., 1999). The *bfl1* promoter, which controls expression of Bcl-2A1, contains one κB element, and Bcl-2A1 expression is inducible *via* the canonical NF-κB pathway (Grumont et al., 1998; Zong et al., 1999). Moreover, NF-κB target genes that drive proliferation include cyclin D1, cyclin D2, c-Myc, c-Myb, as well as cytokines, such as IL-2 and IL-6, that act as lymphocyte growth factors (Duyao et al., 1992; Hinz et al., 1999; Sasaki et al., 2006; Toth et al., 1995).

In addition, overactivation of the NF-κB pathway seems to be involved in invasion of tumor cells by upregulation of genes encoding for matrix metalloproteinases (MMPs) (Bond et al., 1998) and angiogenic factors (Levine et al., 2003).

1.5.2 Mutations associated with constitutive NF-κB activity

Mutations of NF-κB regulators and/or aberrant NF-κB activity have been described for cell lines and primary patient material both derived from lymphoid tumors and solid cancers. The role of NF-κB in tumorigenesis and malignant progression is based on cell-intrinsic and cell-extrinsic mechanisms. So far, oncogenic mutations that lead to constitutive NF-κB activity have only been identified in a variety of lymphoid cancers (see below). However, NF-κB activation has also been observed for many solid tumors although no tumor-intrinsic NF-κB-activating mutations have been detected (Karin, 2009). In these types of solid cancers NF-κB activity is often induced by inflammatory cytokines in an autocrine and/or paracrine manner as the result of the formation of an inflammatory microenvironment promoting tumor maintenance and progression (Ammirante et al., 2010; Karin, 2006).

Given the crucial role of NF-κB in lymphocyte physiology, it is not surprising that constitutive NF-κB activity has been implicated in a number of lymphoid malignancies. The first link between NF-κB and cancer came from studies showing that expression of the viral oncogene v-Rel (the viral homolog of c-Rel) can cause aggressive leukemia and lymphoma (Gilmore et al., 2003). Subsequently, constitutive NF-κB activity and genetic aberrations affecting NF-κB activity have been identified in a variety of B and T cell malignancies (reviewed in Jost and Ruland, 2007; Karin, 2009; Staudt, 2010).

Disease	Dysregulated/mutated genes	Reference
Activated B cell-like diffuse large B cell lymphoma (ABC-DLBCL)	Carma1; A20; CD79A; CD79B	(Compagno et al., 2009; Davis et al., 2010; Davis et al., 2001; Lenz et al., 2008)
Adult T cell lymphoma/ leukemia (ATL)	Tax (HTLV-1 oncogene)	(Cann et al., 1985; Carter et al., 2001; Ross et al., 1996; Sun and Ballard, 1999)
Childhood/T cell acute lymphoblastic leukemia (ALL/T-ALL)	Notch1; p100; RelB	(Kordes et al., 2000; Vilimas et al., 2007)
Cutanous T cell lymphoma (CTCL)	p100	(Sors et al., 2006; Zhang et al., 1994)
Hodgkin lymphoma (HL)	CD30; CD40; RANK/RANKL IκBα; IκBε; c-Rel; A20 ; LMP1 (EBV protein)	(Bargou et al., 1996; Bargou et al., 1997; Barth et al., 2003; Cabannes et al., 1999; Deacon et al., 1993; Emmerich et al., 2003; Fiumara et al., 2001; Horie et al., 2002; Joos et al., 2002; Martin-Subero et al., 2002)
MALT lymphoma	MALT1; Bcl10; A20	(Akagi et al., 1999; Dierlamm et al., 1999; Lucas et al., 2001; Willis et al., 1999)
Multiple myeloma (MM)	CD40; NIK; p100; p105; LTβR; TRAF2; TRAF3; c-IAP1/2; CYLD	(Annunziata et al., 2007; Bharti et al., 2004; Keats et al., 2007; Ni et al., 2001)

Table 1.1 | Lymphoid malignancies that are associated with constitutive NF-κB activity. Listed are different types of lymphomas and leukemias for which constitutive NF-κB activity has been reported in cell lines and/or primary patient material. As far as identified, genetic lesions, mutated gene products, and oncogenes that are associated with aberrant NF-κB signaling are depicted (for details see text). EBV: Epstein-Barr virus; LMP1: latent membrane protein 1.

Multiple myeloma (MM) is a prominent example of a neoplastic disorder, for which constitutive NF-κB activity has been described, both in cell lines as well as in MM patient samples (Ni et al., 2001). Two recent reports demonstrated that 10-20% of several hundred MM cell lines and patient samples have mutations which lead to activation of NF-κB. These genetic alterations comprise gain-of-function mutations of NF-κB activators,

as well as loss-of-function mutations of negative regulators of NF-κB, both inducing chronic NF-κB signaling in MM tumor cells (Annunziata et al., 2007; Keats et al., 2007).

In marginal zone lymphomas of mucosa-associated lymphoid tissue (MALT) that is predominantly seen in the gastric mucosa, several specific genetic alterations have been identified that cause constitutive NF-κB activity. These mutations primarily include chromosomal translocations affecting genes encoding for MALT1 and Bcl10 (see 1.3.5). Translocations either cause the generation of a chimeric cIAP2-MALT1 fusion protein or increased expression of MALT1 and Bcl10 genes under control of the Ig heavy chain enhancer, both leading to Bcl10-MALT1 complex formation and NF-κB activation independent of antigen receptor engagement (Liu et al., 2001; Lucas et al., 2001).

Similarly to MALT lymphomas, aberrant activity of the IKK-inducing CBM complex has been identified as a frequent event in the development of diffuse large B cell lymphoma (DLBCL), the most common type of non-Hodgkin lymphoma (NHL) (Lenz and Staudt, 2010). Based on correlations of microarray gene expression profiling and clinical outcome Staudt and colleagues have classified the majority of DLBCLs into three subentities termed activated B cell-like DLBCL (ABC-DLBCL), germinal centre B cell-like DLBCL (GCB-DLBCL), and an unclassified group of DLBCLs (Alizadeh et al., 2000; Wright et al., 2003). Relative to the GCB subtype, ABC-DLBCL is a much more aggressive disease (Wright et al., 2003). Importantly, the ABC-DLBCL subtype displays upregulation of a large series of NF-κB target genes, consistent with the observation that ABC-DLBCL cell lines exhibit constitutive NF-κB activity in contrast to cells derived from GCB-DLBCLs (Davis et al., 2001). The strict dependence of ABC-DLBCL cells on chronic NF-κB signaling for survival, a phenomenon known as “oncogenic addiction” (Luo et al., 2009b; Weinstein, 2002), was demonstrated by an RNA interference (RNAi) screen showing that knock-down of either Carma1, Bcl10, or MALT1 specifically causes spontaneous cell death of ABC-DLBCL cells (Ngo et al., 2006). Constitutive NF-κB activity in these cells is largely due to somatic mutations of genes encoding for positive and negative regulators of the BCR-induced NF-κB signaling machinery. For instance, activating mutations of Carma1 have been found in 7 out of 73 ABC-DLBCL biopsies rendering Carma1 a *bona fide* oncogene in lymphocytes (Lenz et al., 2008). *Vice versa*, biallelic inactivation of the negative regulator A20 was demonstrated to be a frequent pathogenetic event in ABC-DLBCL biopsies (Compagno et al., 2009), although inactivation of the A20 gene has also been implicated in the pathogenesis of other types of B cell malignancies (Kato et al., 2009). More recently, somatic mutations in CD79A and CD789B, both detected in ABC-

DLBCL biopsy samples and cell lines, were shown to increase BCR surface expression, thereby leading to receptor clustering and chronic active BCR signaling in ABC-DLBCL cells (Davis et al., 2010).

Adult T cell lymphoma/leukaemia (ATL) is an aggressive malignant disease of T cells caused by the human T-lymphotropic virus type I (HTLV-1) (Poiesz et al., 1981). In HTLV-1-infected T cells the viral oncoprotein Tax drives constitutive activation of the IKK complex and upregulation of NF-κB-dependent genes (Sun and Ballard, 1999). In the case of T cell acute lymphocytic leukaemia (T-ALL), it could be shown that activating mutations in Notch1 resulted in direct activation of the IKK complex (Vilimas et al., 2007). Moreover, Notch1 activity leads to increased transcription of *NFKB2* and *RELB*, activating the non-canonical pathway (Vilimas et al., 2007).

In summary, aberrant NF-κB activation is a frequent pathogenic event in leukemogenesis and lymphomagenesis. Targeting the NF-κB pathway might open up new avenues for the treatment of lymphoid malignancies, and a number of recently developed NF-κB inhibitors are already subject of clinical studies (Karin and Lin, 2002; Karin et al., 2004).

1.5.3 The Sézary syndrome and its link to NF-κB

The Sézary syndrome and mycosis fungoides belong to a rare group of lymphoproliferative disorders, called cutaneous T cell lymphoma (CTCL). The more common variant mycosis fungoides (MF) is confined to the skin and characterized by skin plaques and tumors. MF is a slowly progressive disease defined through indolent clinical behaviour compared to the more aggressive and systemic Sézary syndrome that can be considered as a leukemic subtype of CTCL (Booken et al., 2008; Diamandidou et al., 1996; Dippel et al., 2003; Kim et al., 2005; Klemke et al., 2005).

The Sézary syndrome was first described by Albert Sézary (1880-1956) in 1938 and is characterized by the triad of generalized erythoderma, lymphadenopathy, and the presence of 5% or more malignant T cells with cerebriform nuclei (known as Sézary cells) in peripheral blood lymphocytes (Hwang et al., 2008). However, it is now proposed by the International Society for Cutaneous Lymphoma (ISCL) that the diagnosis of Sézary syndrome is made by flow cytometric evidence of a clonal population of T cells in the blood in addition to erythroderma (Hwang et al., 2008). Sézary syndrome runs an aggressive course with a high mortality rate and a median survival of 2-4 years. A confining criteria for the survival of patients is the breakdown of the T cell repertoire together with the clonal expansion of Sézary cells leading to a state of immune

suppression and high susceptibility to infections which ultimately result in lethal systemic infections (sepsis) (Hwang et al., 2008).

The first hint that the pathogenesis of the Sézary syndrome is associated with abnormal regulation of NF-κB was reported more than one decade ago (Zhang et al., 1994). This report described a rearrangement of chromosomes in the CTCL cell line Hut78 which led to a truncated p100 protein devoid of the C-terminus. The truncated p100 protein accumulated abnormally in the nucleus indicating that it lost cytoplasmatic retention and thereby contributes to chronic NF-κB signaling (Zhang et al., 1994). These observations were further corroborated by a study showing constitutive activation of NF-κB by electrophoretic mobility gel shift assay (EMSA) in the CTCL cell lines HH, Hut-78, MyLa, and SeAx, as well as in peripheral blood lymphocytes from patients with Sézary syndrome (Izban et al., 2000; Sors et al., 2006). Further, overexpression of IκBα and treatment with a proteasome inhibitor induced apoptosis in cell lines and patient cells. Moreover, targeting NF-κB by a specific IKKβ inhibitor prevented the nuclear translocation of p65 and induced apoptosis of both, CTCL cell lines MyLa and SeAx, and malignant T cells from patients suffering from Sézary syndrome (Sors et al., 2006). Interestingly, viability of both peripheral blood lymphocytes from healthy donors and of non-malignant T cells derived from Sézary patients remained unchanged, indicating that the constitutively activated NF-κB pathway in tumor cells can be targeted specifically (Sors et al., 2008).

Recently, Kiessling et al. provided a molecular explanation for the selective apoptosis sensitivity of CTCL cells in response to NF-κB inhibition (Kiessling et al., 2009). Targeting of the NF-κB pathway by chemical compounds immediately led to the downregulation of ferritin heavy chain (FHC), an iron storage protein whose expression critically depends on NF-κB. Subsequently, the increase in the free intracellular iron pool led to the massive generation of reactive oxygen species (ROS), and to ROS-dependent cell death *in vitro* and *in vivo* (Kiessling et al., 2009). Nonetheless, the molecular and genetic mechanisms underlying constitutive NF-κB activity in CTCL cells still remain largely elusive.

2 Aims of the study

TCR-induced activation of the NF-κB signaling cascade involves a plethora of kinases and phosphorylated substrates, ranging from upstream protein complexes to the IKK core signaling machinery and transcriptionally active NF-κB dimers. Whereas in some cases phosphorylation is followed by protein degradation, most phosphorylation events are transient, implying the activity of phosphatases in shaping and reversing the phosphorylation signal. However, to date only little is known about the existence and identity of NF-κB-modulating phosphatases, their targeted phospho-substrates, and their putative functions in regulating and terminating NF-κB activity in T lymphocytes.

Therefore, the current study aimed at gaining a comprehensive and systematic understanding of the role of individual phosphatases in the regulation of TCR-induced NF-κB activity. To this end, an RNAi-based genetic screening approach was adopted in order to identify NF-κB-modulating phosphatases in T lymphocytes. Subsequently, physical and functional interactions between validated phosphatases and components of the T cell NF-κB signaling machinery were elucidated. In detail, the current experimental study included the following objectives:

(i) Generation of a cell-based NF-κB activity reporter system that allows for high throughput screening on a subgenome-wide scale in T cells.

(ii) Design and implementation of an RNAi-based screen for phosphatases that regulate TCR-induced NF-κB activity.

(iii) Validation of primary candidate phosphatase genes by secondary screening.

(iv) Genetic and biochemical analysis of individual phosphatases with respect to physiology, function and mechanism underlying NF-κB regulation.

(v) Investigation of expression and function of NF-κB-regulating phosphatases in malignant Sézary T cells and potential implications in disease pathogenesis.

3 Materials

3.1 Chemicals, reagents, and kits

3.1.1 Chemicals

Unless otherwise indicated, chemicals were purchased from Serva (Heidelberg), Fluka (Neu-Ulm), Sigma (München), Roth (Karlsruhe), and Merck (Darmstadt). Radioactive reagents were purchased from Amersham (Braunschweig).

3.1.2 Consumables

Consumables	Company
96-well plates for qRT-PCR	Applied Biosystems
Amersham Hyperfilm™ ECL	Amersham Bioscience
Cell culture plates and flasks	TPP/Greiner
Electropuration cuvettes (4 mm)	BioRad
ELISA 96-well plates	costar®
LS columns	Miltenyi Biotec
Nitrocellulose membrane Hybond™-ECL™	Amersham Bioscience
Pipette tips	TipOne
Reaction tubes (1.5, 2 ml)	Eppendorf
Reaction tubes (5, 15, 50 ml)	BectonDickinson/Nunc/TPP
Reaction tubes for PCR	TipOne
Sealing foil	Roche
Sealing strips	Applied Biosystems
Serological pipettes	Becton Dickinson/Greiner
Sterile filters (0.22 µm, 0.45 µm)	Millipore
Whatman Blotting paper	Biorad/Schleicher & Schuell

3.1.3 Commercial kits and reagents

Kit	Company
Cell Line 96-well Nucleofector® Kit SE	Lonza
Cell Line Nucleofector® Kit V	Lonza
CellTiter-Glo® Luminescent Cell Viability Assay	Promega
Dual-Light® System	Applied Biosystems
Gaussia-Glow Juice	p.j.k.
Gene Ruler™ 1 kb DNA ladder	Fermentas
High Capacity cDNA Reverse Transcription Kit	Applied Biosystems
Human IFNγ, IL-2, TNFα ELISA	BD Bioscience
Human IL-8 ELISA	Immunotools
Human T Cell Nucleofector® Kit	Lonza
KOD Hot Start DNA Polymerase Kit	Novagen®
LightCycler® 480 Probes Master Kit	Roche
o-Phenylenediamine dihydrochloride tablets for ELISA	Sigma
Power SYBR® Green PCR Master Mix	Applied Biosystems
Protein A sepharose beads	Sigma
Protein molecular weight standard	New England Biolabs (NEB)
Proteinase Inhibitor Cocktail Tablets	Roche
QIAEX II Gel extraction Kit	Qiagen
Qiagen® Plasmid Maxi Kit	Qiagen
Qiagen® Plasmid Mini Kit	Qiagen
QIAquick PCR Purification Kit	Qiagen
RealTime ready Custom Panel 386	Roche
RNAqueous®-Micro Kit	Applied Biosystems
Roti®-Quant Bradford assay	Roth
SensoLyte® pNPP Protein Phosphatase Assay	AnaSpec

TNT® T7 Coupled Reticulocyte Lysate System	Promega
Transcriptor High Fidelity cDNA Synthesis Kit	Roche
Western Lightning™ Plus-ECL reagent	PerkinElmer

3.1.4 Reagents and kits for isolation of T cells

Reagent/Kit	Company
CD4 MicroBeads	Miltyenyi Biotec
$CD4^+$ T cell isolation kit II, human	Miltyenyi Biotec
CD25 MicroBeads	Miltyenyi Biotec
Ficoll	Biochrom

3.1.5 Reagents for treatment of cells

Reagent	Company/Reference
Ionomycin	Sigma
NEMO binding peptide (NBP)	Calbiochem; (May et al., 2000)
NF-κB activation inhibitor	Calbiochem; (Kiessling et al., 2009)
Phorbol 12-myristate 13-acetate (PMA)	Sigma
Phytohemagglutinin (PHA)	Sigma
Polybrene	Millipore
Recombinant human IL-2	Cell line LBRM-33 5A4; (Gillis et al., 1980)
Recombinant human TNFα	BASF/Invitrogen

3.2 Buffers and solutions

All solutions and buffers were made in double destilled water (ddH_2O). Lysis buffers for lysis of eukaryotic cells were freshly supplemented with Proteinase Inhibitor Cocktail Tablets (Roche) with 1 tablet per 50 ml of lysis buffer.

Buffer	**Composition**
ACK buffer (10x)	41.45 g NH_4Cl 5.0 g $KHCO_3$ 0.186 g EDTA pH 7.27 ad 500 ml ddH_2O
Citrate buffer (ELISA)	6.9 g Citric acid 20.95 g Sodium citrate dihydrate pH 5.0 ad 1 l ddH_2O
Coating Buffer (ELISA)	8.4 g $NaHCO_3$ 3.56 g Na_2CO_3 pH 9.6 ad 1 l ddH_2O
DNA sample buffer (6x)	30 % (v/v) glycerine 0.36 % (w/v) bromophenol blue (BPB) or orange G
FACS buffer	5% FCS 0.1% NaN_3 in PBS
HBS (10x)	1.4 M NaCl 100 mM KCl 500 mM HEPES 20 mM Na_2HPO_4 22.2 mM Glucose pH 6.5
KCM buffer (5x)	500 mM KCl 150 mM $CaCl_2$ 250 mM $MgCl_2$
Kinase buffer	50 mM Tris/HCl pH = 8.0 5 mM $MgCl_2$ 2 mM $MnCl_2$ 0.5 mM DTT
Lysis buffer (for phospho-blots)	50 mM Tris/HCl pH 7.8 137 mM NaCl 0.5 mM EDTA 1 mM NaF 1 mM Na_3VO_4

	10% (v/v) glycerol 1% NP-40
MACS buffer	0.5% BSA 2 mM EDTA in PBS
PBS	137 mM NaCl 8.1 mM Na_2HPO_4 2.7 mM KCl 1.5 mM KH_2PO_4 pH 7.4
PBST	PBS 0.05% (v/v) Tween
Reducing sample buffer (3x)	62.5 mM Tris/HCl pH 6.8 2 % (w/v) Sodium dodecylsulfate (SDS) 2 mM EDTA 20 % (v/v) glycerol 0.025 % (w/v) BPB 5 % (v/v) 2-mercaptoethanol
Phosphatase buffer (Marley et al., 1996)	50 mM Tris-HCL pH 7.5 0.1 mM EDTA 60 mM $MgCl_2$ 0.5 mM DTT
RIPA lysis buffer (2x)	120 mM NaCl 50 mM Tris/HCl pH 7.5 0.5% (w/v) Desoxycholate 1 mM Dithiothreitol
SDS PAGE running buffer	25 mM Tris 0.19 M Glycin 1% (w/v) SDS
SDS separating gel buffer	37.5 mM Tris-HCl pH = 8.8 8-12% (w/v) Acrylamid/Bisacrylamid 37,5:1 0.1% (w/v) SDS 0.03% (w/v) Ammonium persulfate (APS) 0.1% (w/v) Tetramethylethylendiamin (TEMED)
SDS stacking gel buffer	24 mM Tris-HCl pH 6,8 5 % (w/v) Acrylamid/Bisacrylamid 37,5:1 0.1% (w/v) SDS 0.1% (w/v) APS 0.1% (w/v) TEMED
Stripping buffer	62.5 mM Tris/HCl pH 6.8 2% (w/v) SDS 100 mM 2-mercaptoethanol
TAE buffer (1x)	40 mM Tris/HCl 20 mM Acetic acid 1 mM EDTA

	pH 8.3
Transfer buffer (immunoblotting)	25 mM Tris/HCl 0.19 M Glycine 20% (v/v) Methanol 0.037% (w/v) SDS
Triton lysis buffer	150 mM NaCl 30 mM Tris-HCl, pH 7,5 1 mM Phenylmethylsulfonyl fluorid (PMSF) 10% (w/v) Glycerol 1% (w/v) Triton X-100
TSB solution	10 mM $MgCl_2$ 10 mM $MgSO_4$ 5% (v/v) DMSO 10% (v/v) PEG 6000 in LB medium

3.3 Culture media

3.2.1 Media for bacteria

Media for *E. coli* were autoclaved and stored at 4°C. Autoclavation of liquids was carried out at 125°C for 30 min. To ensure plasmid propagation LB medium and LB agar plates were supplemented with 50-100 µg/ml ampicillin or 30 µg canamycin.

Medium	**Composition**
LB medium	10 g tryptone 5 g yeast extract 10 g NaCl pH 7.0 ad 1 l ddH_2O
LB agar	20 g agar per 1 l LB medium

3.3.2 Media and supplements for eukaryotic cell culture

Unless otherwise indicated, media were supplemented with 10% (v/v) heat-inactivated FCS. IMDM medium for Jurkat cell lines was supplemented with 1.0% (v/v) penicillin/streptomycin. For selection of stably transfected/transduced Jurkat cells, media were supplemented with 2.0 µg/ml G418 (neomycin) and 1.0 µg/ml puromycin, respectively. All media were stored at 4°C until use.

Reagent	Company
Dulbecco's Modified Eagle Medium (DMEM)	Gibco/Sigma
Fetal calf serum (FCS)	Biochrom/Gibco
Freezing medium	90 % (v/v), 10 % (v/v) DMSO
G418 (neomycin)	Roth
Iscove's Modified Dulbecco's Medium (IMDM)	Gibco
Penicillin/Streptomycin	Sigma
Puromycin	Roth
Roswell Park Memorial Institute (RPMI) 1640 medium	Gibco/Sigma
Trypsin/EDTA	Gibco
X-Vivo 15 medium	Cambrex

3.4 Biological material

3.3.1 Bacteria

For plasmid propagation the *E. coli* strains DH5α and TOP10F' were utilized.

E. coli strain	Company
DH5α	Invitrogen
TOP10F'	Invitrogen

3.3.2 Mammalian cell lines

Cell line (ATCC number)	Description/Reference
CEM (CRL-2265)	Human T lymphoblastic cell line derived from acute lymphoblastic leukemia (Kapoor et al., 1995).
Gluc-J16	Reporter T cell line derived from J16-145 with stable genomic integration of a NF-κB-dependent Gaussia luciferase cassette (this study).
HEK293T (CRL-11268)	Human embryonic kidney cell line (Pear et al., 1993).
HeLa (CCL-2)	Human cervix adenocarcinoma cell line (Boshart et al., 1984).
Hep3B (HB-8064)	Human epithelial cell line derived from hepatocellular carcinoma (Aden et al., 1979).
HH (CRL-2105)	Human CTCL dell line derived from a patient with Sézary syndrome (Starkebaum et al., 1991).
HT (CRL-2260)	Human Non-Hodgkin lymphoma cell line (diffuse mixed small and large cell) (Beckwith et al., 1990).
Hut78 (TIB-161)	Human CTCL cell line derived from a patient with Sézary syndrome (Gootenberg et al., 1981).
J16-145	Subclone of the human lymphoblastoid cell line J16
JE6.1 (TB-152)	Human lymphoblastoid cell line derived from acute T cell leukemia cell line (Schneider et al., 1977).
MyLa	Human CTCL cell line (Dummer et al., 1994).
OCI-Ly3	Human DLBCL cell line (ABC subtype) (Tweeddale et al., 1987).
Phoenix ampho	HEK293T-derived packaging cell line engineered for rapid production of retroviruses (Swift et al., 2001).
Raji (CCL-86)	Human Burkitt's lymphoma cell line (Epstein et al., 1966).
SeAx	Human CTCL cell line derived from a patient with Sézary syndrome (Kaltoft et al., 1984).
SUDHL-5	Human DLBCL cell line (ABC subtype) (Epstein et al., 1976).
SUDHL-6 (CRL-2959)	Human DLBCL cell line (GC subtype) (Epstein et al., 1978).

3.5 Materials for molecular biology

3.5.1 Phosphatase siRNA library

For RNAi screening the *Silencer® Select Human Phosphatase siRNA Library V4* (Applied Biosystems) was used. The library contained three single siRNA oligos targeting 298 known or predicted phosphatases. siRNAs were dissolved in RNase-free H_2O with a final concentration of 20 µM. Three independent, pre-aliquoted siRNAs sets (894 individual siRNAs for 298 genes) were stored in 96-well plates at -80°C until use.

3.5.2 siRNA sequences

siRNA	Gene targeted	Sequence (5'→3')	Company
siA20#1	*TNFAIP3*	CCGAGCTGTTCCACTTGTTAA	Qiagen
siA20#2	*TNFAIP3*	CAGATGTATGGCTAACCGGAA	Qiagen
siCarma1#1	*CARD11*	ACUCGAGAUCGAUCAGCUATT	Qiagen
siCarma1#2	*CARD11*	Not available	Qiagen
siCarma1#3	*CARD11*	Not available	Qiagen
siCtrl	nontargeting	UUCUCCGAACGUGUCACGUTT	Qiagen
siCYLD	*CYLD*	GAUUGUUACUUCUAUCAAATT	Applied Biosystems
siPP4R1#1	*PPP4R1*	GCCGCAUCUGCUAACCUUATT	Applied Biosystems
siPP4R1#2	*PPP4R1*	GGAUAGGUGUUCUUAAACATT	Applied Biosystems
siPP4R1#3	*PPP4R1*	GGAGCUCAUUGAACGAUUUTT	Applied Biosystems
siPP4R1#4	*PPP4R1*	CCUACAAGUUGGUCAGCGA	Dharmacon
siPP4R1#5	*PPP4R1*	UGUGAGAUGUGCUGCGAUU	Dharmacon
siPP4R1#6	*PPP4R1*	GAUUAUAAUUGUCACCGAA	Dharmacon
siPP4R1#7	*PPP4R1*	GCCCGGAGUUUGCUCGAUA	Dharmacon
siRelA	*RELA*	CCAUCAACUAUGAUGAGUUTT	Applied Biosystems
siTNFR1	*TNFRSF1A*	CAAAGGAACCUACUUGUACUU	Dharmacon

3.5.3 shRNA sequences

All shRNA clones encoding for shRNAs targeting PP4R1 were obtained as glycerol stocks from Sigma. As a negative control a *Non-Target shRNA Control Vector* was used. All shRNA vectors are pLKO.1-puro derivatives.

shRNA	TRC#	Sequence (5'→3')
shPP4R1#1	TRCN0000052763	CCGGGCGTTGTTAGATCAGTATTTACTCGAGTAAATACT GATCTAACAACGCTTTTTG
shPP4R1#2	TRCN0000052764	CCGGCGGACCAAATTATCAGCACTTCTCGAGAAGTGCT GATAATTTGGTCCGTTTTTG
shPP4R1#3	TRCN0000052765	CCGGCCCAGAGATGTTTATGACTATCTCGAGATAGTCAT AAACATCTCTGGGTTTTTG
shPP4R1#4	TRCN0000052766	CCGGGCAGCTAGTAATGAGAATGATCTCGAGATCATTCT CATTACTAGCTGCTTTTTG
shPP4R1#5	TRCN0000052767	CCGGGCTGCAAGTGAGAACATATTTCTCGAGAAATATGT TCTCACTTGCAGCTTTTTG

3.5.4 PCR primers for gene cloning

For cloning of HA-tagged versions of human PP4R1, HA-tagged human PP4c, FLAG-tagged PP4c as well as HA-tagged PP2Ac the primers listed below were used. Amplicons were *BamHI*/*NotI*-digested and ligated into derivatives of the pEF4 expression vector (Invitrogen) containing 5'-HA or 5'-FLAG-epitope tags (pEF4:HA/pEF4:FLAG) (see 4.5.7). PP4R1 cDNA, cloned into the pEF4:HA expression vectors, was used as a template for generation of various HA-tagged PP4R1 deletion mutants. In addition, cDNA of PP4R1, PP4c, and PP2Ac , cloned into the pEF4:HA vector, served as a template for cloning of HA-tagged gene sequences into the pMX-IRES-GFP vector using a pMX-specific universal forward primer (pMX-univ-for) and gene-specific pMX-reverse PCR primers *via EcoRI/NotI* restriction digests of PCR amplicons. PCR primers were synthesized by MWG Biotech or Sigma.

Primer	Target vector	Sequence (5'→3')
P4R1-for	pEF4:HA	CGCGGATCCGCGGGCGCGGACCTCTCGCTGCTTCAG
P4R1-rev	pEF4:HA/ pMX-IRES-GFP	ATAGTTTAGCGGCCGCCTACTAGTAGGTTGAGGACGCTG
P4R1(133)-for	pEF4:HA	CGCGGATCCGCGGGCCTACCTATTGTGGTTAGATACC
P4R1(213)-for	pEF4:HA	CGCGGATCCGCGGGCATCCTCCCTAGGTTTTGTG
P4R1(663)-rev	pEF4:HA	ATAGTTTAGCGGCCGCCTAGCAGTGCCAATTCTGTCTTCC
P4R1(313)-rev	pEF4:HA	ATAGTTTAGCGGCCGCCTACTGAAAAGCTGCTTGGCGAAC
P4R1(314)-for	pEF4:HA	CGCGGATCCGCGGGCTCTCTGGGACCTTTCATATC
P4c-for	pEF4:HA/FLAG	CGCGGATCCGCGGGCGCGGAGATCAGCGACCTG
P4c-rev	pEF4:HA/FLAG/ pMX-IRES-GFP	ATAGTTTAGCGGCCGCTCACAGGAAGTAGTCGGCCACGG
P2Ac-for	pEF4:HA	CGCGGATCCGCGGGCGACGAGAAGGTGTTCACCAAG
P2Ac-rev	pEF4:HA/ pMX-IRES-GFP	ATAGTTTAGCGGCCGCCTATTACAGGAAGTAGTCTGGG
pMX-univ-for	pMX-IRES-GFP	CCGGAATTCCGGGGCCCCAAGCTGGCTAGTTAAGC
P4R1-pMX-rev	pMX-IRES-GFP	ATAGTTTAGCGGCCGCCTACTAGTAGGTTGAGGACGCG
P4c-pMX-rev	pMX-IRES-GFP	ATAGTTTAGCGGCCGCTCACAGGAAGTAGTCGGCCACGG
P2Ac-pMX-rev	pMX-IRES-GFP	ATAGTTTAGCGGCCGCCTATTACAGGAAGTAGTCTGGG

3.4.5 qRT-PCR primers

Primers for SYBR Green qRT-PCR were designed using the online primer designing tool Primer-BLAST (http://www.ncbi.nlm.nih.gov/tools/primer-blast/). For UPL-based qRT-PCR assays the Universal ProbeLibrary Assay Design Center (https://www.roche-applied-science.com/sis/rtpcr/upl/index.jsp?id=UP030000) provided by Roche was used. In general, all primer pairs were designed to be intron-spanning with primer efficiencies between at least 1.7 and 2.0. Al primers for qRT-PCR were synthesized by MWG Biotech or Sigma.

(i) SYBR Green qRT-PCR primer pairs

Gene	Primer	Sequence (5'→3')
CYLD	forward reverse	CTAAACACTGCACCCGTCCAA CAATGAGCCCACTTCTAGACCAT
GAPDH	forward reverse	GCAAATTCCATGGCACCGT TCGCCCCACTTGATTTTGG
HPRT1	forward reverse	TGACACTGGCAAAACAATGCA GGTCCTTTTCACCAGCAAGCT
IFNG	forward reverse	TTCAGCTCTGCATCGTTTTGG TCCGCTACATCTGAATGACCTG
IL2	forward reverse	AAGTTTTACATGCCCAAGAAG AAGTGAAAGTTTTTGCTTTGAGCT
IL8	forward reverse	GAATGGGTTTGCTAGAATGTGATA CAGACTAGGGTTGCCAGATTTAAC
NFKBIA	forward reverse	CGCCCAAGCACCCGGATACA AGGGCAGCTCGTCCTCTGTGA
PPP2CA	forward reverse	CTTGGTGGATGGGCAGAT TCTTGTAGGCGATCAAGTGC
PPP4R1	forward reverse	GACAAAGTTTCTTCTGTTCGTTGGA TCCGAACGTTGGTGGTGTT
RELA	forward reverse	CGGGATGGCTTCTATGAGG CTCCAGGTCCCGCTTCTT
TNFAIP3	forward reverse	TGCGGCACCCTTGGAAGCAC TGCGCTGGCTCGATCTCAGTT
TNFRSF1A	forward reverse	GAGAGGCCATAGCTGTCTGG GAGGGGTATATTCCACCAAC

(ii) Primer pairs for UPL assays

Gene	Primer	UPL probe#	Sequence (5'→3')
CYLD	forward reverse	11	CAGTCTCCGGAATATTCTTTGG CAGTGAAACCTTGACCACGA
GAPDH	forward reverse	60	AGCCACATCGCTCAGACAC GCCCAATACGACCAAATCC
HPRT1	forward reverse	73	TGACCTTGATTTATTTTGCATACC CGAGCAAGACGTTCAGTCCT
IFNG	forward reverse	21	GGCATTTTGAAGAATTGGAAAG TTTGGATGCTCTGGTCATCTT
IL2	forward reverse	65	AAGTTTTACATGCCCAAGAAGG AAGTGAAAGTTTTTGCTTTGAGCTA
IL8	forward reverse	72	AGACAGCAGAGCACACAAGC ATGGTTCCTTCCGGTGGT
NFKBIA	forward reverse	38	GTCAAGGAGCTGCAGGAGAT GATGGCCAAGTGCAGGAA
PPP2CA	forward reverse	47	CTTGGTGGATGGGCAGAT TCTTGTAGGCGATCAAGTGC
PPP4R1	forward reverse	56	CCCCACATTGATGATCCAG CAGGCTGGAAGCACGTAGT
RELA	forward reverse	47	CGGGATGGCTTCTATGAGG CTCCAGGTCCCGCTTCTT
TNFAIP3	forward reverse	74	TGCACACTGTGTTTCATCGAG ACGCTGTGGGACTGACTTTC
TNFRSF1A	forward reverse	59	GAGAGGCCATAGCTGTCTGG GAGGGGTATATTCCACCAAC

3.4.6 Enzymes

All restriction endonucleases were purchased from Fermentas or New England Biolabs (NEB). *KOD* DNA polymerase was from Novagen®. T4 DNA ligase as well as calf intestinal phosphatase (CIP) were obtained from Fermentas. All enzymes were used according to the manufacturer's instructions.

3.4.7 Vectors

Vector	Description	Origin/Reference
pEF4:HA	Derivative of the pEF4 eukaryotic expression vector with a 5' single HA tag	Invitrogen/ J. Hoffmann, DKFZ
pEF4:FLAG	Derivative of the pEF4 eukaryotic expression vector with a 5' single FLAG tag	Invitrogen/ J. Hoffmann, DKFZ
pMX-IRES-GFP	Retroviral expression vector containing an IRES-controlled EGFP reporter cassette	A. Cerwenka, DKFZ Hozumi et al., 2000
EGFP-C1	Eukaryotic expression vector for C-terminal Enhanced Green Fluorescent Protein (EGFP)	Clontech
pEF4:HA-PP4R1-wt	pEF4:HA derivative encoding for HA-tagged human PP4R1, full-length protein (aa 1-950)	This study
pEF4:HA-PP4R1-133-950	pEF4:HA derivative encoding for HA-tagged human PP4R1, deletion mutant (aa 133-950)	This study
pEF4:HA-PP4R1-213-950	pEF4:HA derivative encoding for HA-tagged human PP4R1, deletion mutant (aa 213-950)	This study
pEF4:HA-PP4R1-1-663	pEF4:HA derivative encoding for HA-tagged human PP4R1, deletion mutant (aa 1-663)	This study
pEF4:HA-PP4R1-1-313	pEF4:HA derivative encoding for HA-tagged human PP4R1, deletion mutant (aa 1-313)	This study
pEF4:HA-PP4R1-314-950	pEF4:HA derivative encoding for HA-tagged human PP4R1, deletion mutant (aa 314-950)	This study
pEF4:HA-PP4R1-314-663	pEF4:HA derivative encoding for HA-tagged human PP4R1, deletion mutant (aa 314-663)	This study
pEF4:HA-PP4R1-664-950	pEF4:HA derivative encoding for HA-tagged human PP4R1, deletion mutant (aa 664-950)	This study
pEF4:HA-PP4c-wt	pEF4:HA derivative encoding for HA-tagged human PP4c, full-length protein	This study/ T. Mock, DKFZ
pEF4:FLAG-PP4c-wt	pEF4:FLAG derivative encoding for FLAG-tagged human PP4c, full-length protein	This study/ T. Mock, DKFZ
pEF4:HA-PP2Ac-wt	pEF4:HA derivative encoding for HA-tagged human PP2Ac, full-length protein	This study
pMX-PP4R1-wt	pMX-derivative encoding for HA-tagged human PP4R1, full-length protein	This study
pMX-PP4c-wt	pMX-derivative encoding for HA-tagged human PP4c, full-length protein	This study

pMX-PP2Ac-wt	pMX-derivative encoding for HA-tagged human PP2Ac, full-length protein	This study
pGluc basic	*Gaussia* luciferase vector without promoter sequences	New England Biolabs
8xNF-κB-pGluc	pGluc basic derivative with a *Gaussia* reporter cassette under control of the mouse c-fos promoter and eight κB sites	This study/ Arnold et al., 2001
8xNF-κB-pGL	pGL derivative with a *firefly* reporter cassette under control of the mouse c-fos promoter and eight κB sites	Arnold et al., 2001
3xAP-1-Luc	Derivative of the pTATA-Luc vector encoding for *firefly* luciferase under control of three copies of the AP-1 binding site from the SV40 enhancer	Li-Weber et al., 2002
pfosLacZ	pSDK derivative encoding for β-galactosidase under control of the mouse c-fos promoter	Arnold et al., 2001
FLAG:IKKα	pCR derivative encoding for FLAG-tagged murine IKKα	D. Goeddel
FLAG:IKKβ	pCR derivative encoding for FLAG-tagged murine IKKβ	D. Goeddel
FLAG:NEMO	pCMV derivative encoding for FLAG-tagged human NEMO	R. Marienfeld
FLAG:IKKβ (SS/EE)	Expression vector for a FLAG-tagged dominant active kinase mutant of IKKb with SS/EE T loop mutations	D. Goeddel
HA:HPK1	pcDNA3 derivative encoding for HA-tagged HPK1	Arnold et al., 2001
HA:HPK1 (K46E)	pcDNA3 derivative encoding for a HA-tagged kinase inactive mutant of HPK1 with a K46E mutation	Arnold et al., 2001
pIκBα	pDNA3 derivative encoding for IκBα	Weil et al., 1997/ M. Kiessling, DKFZ

3.5 Antibodies

3.5.1 Antibodies for immunoblotting (IB) and immunoprecipitation (IP)

For IB analysis primary antibodies were diluted, as indicated, in PBST, containing 1% BSA and 0.01% NaN_3. Secondary, horseradish peroxidase (HRP)-conjugated antibodies were diluted 1:10,000-1:20,000 in PBST containing 1% milk powder. Unless otherwise indicated, all antibodies are mouse monoclonal antibodies.

(i) Primary antibodies for IB and antibodies for IP

Name/Clone	Species/Isotype	Antigen	Application/Reference
Anti-β-actin	Mouse, IgG2a	β-actin	IB (1:10,000), Sigma
Anti-Carma1	Rabbit, polyclonal	Carma1	IB (1:1,000), ProSci
Anti-ERK1/2 (MK12)	Mouse, IgG1	ERK1/2	IB (1:1,000), BD Bioscience
Anti-FLAG (M2)	Mouse, IgG1	FLAG epitope	IB (1:1,000), IP (2 µl per IP), Sigma
Anti-HA (12CA5)	Mouse, IgG2b	HA epitope	IP (100 µl of hybridoma supernatant per IP)
Anti-HA (3F10)	Rat, monoclonal	HA epitope	IB (1:1,000), Roche
Anti-IκBα (C-21)	Rabbit, polyclonal	IκBα	IB (1:500), Santa Cruz Biotechnology
Anti-IKKα	Rabbit, polyclonal	IKKα	IB (1:1,000), Cell Signaling
Anti-IKKβ (10A9B6)	Mouse, IgG1	IKKβ	IB (1:500), Imgenex
Anti-NEMO (FL-419)	Rabbit, polyclonal	NEMO (IKKγ)	IP (10-20 µl per IP), Santa Cruz Biotechnology
Anti-p-ERK1/2 (E10)	Mouse, IgG1	Phospho-thr202/tyr204 and phospho-thr185/tyr187 of ERK1/2	IB (1:1,000-1:2,000), Cell Signaling
Anti-p-IκBα (5A5)	Mouse, IgG1	Phospho-ser32/36 of IκBα	IB (1:1,000), Cell Signaling

Anti-p-IκBα (14D4)	Rabbit, monoclonal IgG	Phospho-ser32 of IκBα	IB (1:1,000), Cell Signaling
Anti-p-IKKα/β	Rabbit, polyclonal	Phospho-ser180/181 of IKKα/β	IB (1:1,000), Cell Signaling
Anti-PP1α (4G3)	Mouse, IgG2a	PP1α	IB (1:2,000), Santa Cruz Biotechnology
Anti-PP2Ac	Rabbit, polyclonal	PP2Ac	IB (1:1,000), Thermo Scientific
Anti-PP4c (#A300-893A)	Rabbit, polyclonal	PP4c	IB (1:1,000), Bethyl
Anti-PP4R1 (#A300-836A)	Rabbit, polyclonal	PP4R1 (N-terminus)	IB (1:2,000), Bethyl
Anti-PP4R1 (#A300-837A)	Rabbi, polyclonal	PP4R1 (C-terminus)	IB (1:1,000), Bethyl
Anti-RelA (A)	Rabbit, polyclonal	RelA	IB (1:300), Santa Cruz Biotechnology
Anti-TNFR1 (H-5)	Mouse, IgG2b	TNFR1	IB (1:1,000), Santa Cruz Bioctenology
Anti-Tubulin (B-5-1-2)	Mouse, IgG1	Tubulin	IB (1:2,000-1:5,000), Sigma

(ii) Conjugated antibodies for IB and flow cytometry

Name/Clone	**Species/Isotype**	**Antigen**	**Application/Reference**
Anti-CD69-PE	Mouse, IgG1	CD69	Flow cytometry (1:25), BD Bioscience
Anti-IgG-HRP	Goat, polyclonal	Mouse IgG	IB, Southern Biotechnology
Anti-IgG1-HRP	Goat, polyclonal	Mouse IgG1	IB, Southern Biotechnology
Anti-IgG2a-HRP	Goat, polyclonal	Mouse IgG2a	IB, Southern Biotechnology
Anti-IgG2b-HRP	Goat, polyclonal	Mouse IgG2b	IB, Southern Biotechnology
Anti-rabbit IgG-HRP	Goat, polyclonal	Rabbit IgG	IB, Santa Cruz Biotechnology
Anti-rat IgG-HRP	Goat, polyclonal	Rat IgG	IB, Santa Cruz Biotechnology

3.5.2 Antibodies for T cell stimulation

Name/Clone	Species/Isotype	Antigen	Reference
Anti-CD3 (OKT3)	Mouse IgG	CD3	Prepared from hybridoma
Anti-CD28	Mouse IgG	CD28	Prepared from hybridoma
C305	Mouse IgM	Jurkat TCR β chain	Upstate/ Weiss and Stobo, 1984
Goat anti-mouse	Goat, polyclonal	Mouse IgG	Southern Biotechnology

3.6 Instruments

Instrument	Company
Agarose gel electrophoresis apparatus	Gibco BRL
Analytical and precision balances	Mettler
Bacteria culture incubator/shaker CH-403	Infors AG
Centrifuges: - Biofuge Fresco 17 - Biofuge A - Megafuge 3.0R - Sorvall Evolution RC	 Heraeus Heraeus Heraeus Heraeus
Chemilumescence detector Chemi-Smart 5100	Vilber Lourmat
CO_2-cell culture incubator Stericult	Forma Scientific
Developing system for Roentgen films Curix 160	Agfa-Gevaert
Electrophoresis power supply PS 500	Renner
Electroporation System Gene Pulser II	Bio-Rad
FACSCantoII	Becton Dickinson
Freezer: - -20°C - -80°C	 Liebherr Forma Scientific
Gel documentation system	Bio-Rad

Laminar chambers SG600	Baker Company
Luminometer: - Orion L Microplate Luminometer - Mithras LB940 plate reader	 Berthold Detection Systems Berthold Technologies
Microplate Reader Model 680	BioRad
Microscopes: - Fluorescence microscope Labovert FS - Light microscope ID 02	 Leica Zeiss
Microwave oven HMG 730B	Bosch
Neubauer cell-counting chamber	Brand
pH-meter Calimatic	LHD Labortechnik
Polyacrylamide gel electrophoresis apparatus PROTEAN II Cell	Bio-Rad
Quartz cuvettes Suprasil	Hellma
Semi-Dry blotting system: - Power supply, Consort E865 600V-500mA - Semi-dry transfer cell Trans-Blot SD	Bio-Rad
Spectrophotometer BioPhotometer	Eppendorf
Thermocycler DNA Engine DYAD	MJ Research
Thermomixer Compact	Eppendorf
Thermostated hot-block 5320	Eppendorf
Water baths	Köttermann

3.7 Software

Software	Company
Bio-1D	Vilber Lourmat
Chemi-Capt	Vilber Lourmat
CorelDraw 14	Corel Cooperation
FACSDIVA	Becton Dickinson
Light cycler 480® software	Roche
MS Office 2007	Microsoft
Photoshop CS4	Adobe
Simplicity 4.10	Berthold Detection Systems
Windows XP	Microsoft
7.500 Software version 2.0.1	Applied Biosystems

4 Methods

4.1 Methods in Molecular Biology

4.1.1 Cultivation and storage of bacteria

Bacteria were cultured aerobically at 37°C and 180 rpm in a rotary shaker. Therefore, LB-medium, supplemented with either ampicillin (100 µg/ml) or kanamycin (30 µg/ml), was inoculated with cells of a single colony of transformed bacteria. For the long term strain storage 1-2 ml of a freshly saturated bacterial culture were centrifuged at 3000 g for 5 min. The supernatant was removed and the bacteria were resuspended in ¼ volume of LB/ampicillin. Then, ¼ volume of 87 % glycerol was added and the cell suspension was mixed. The bacteria were stored at -80°C until use.

4.1.2 Generation of KCM-competent bacteria

For the generation of transformation competent *E. coli* cells 100 ml LB medium without antibiotics were inoculated with 1 ml overnight culture. The culture was grown until an OD_{600} value of 0.5-0.6 was reached. Subsequently, the bacteria suspension was incubated on ice for 10 min and then harvested at 1,500 g and 4°C for 15 min. The supernatant was removed and the bacterial pellet was resuspended in 7.5 ml TSB solution. After incubation on ice for 1 h the bacteria were shock-frozen with liquid nitrogen, and aliquots of 100 µl were stored at -80 °C until use.

4.1.3 Transformation of KCM-competent bacteria

For transformation aliquots of KCM-competent *E. coli* were thawed on ice for 2 min. Subsequently, 100 µl of 1x KCM solution containing an appropriate amount of plasmid DNA (100-500 ng) or a complete ligation sample were added. Bacteria were carefully resuspended. The transformation sample was incubated on ice for 20 min, followed by 10 min of incubation at RT. For regeneration, 1 ml of RT LB medium without antibiotics was added. Cells were incubated at 37°C for 30-60 min on a rotary shaker. Subsequently, the bacteria were centrifuged at 2,000 g and resuspended in 100 µl of remaining medium. The suspension was spread onto LB plates containing appropriate antibiotics and incubated at 37°C overnight.

4.1.4 Plasmid preparation on analytical scale (miniprep)

For the analytical plasmid isolation 5 ml of LB medium, supplemented with an appropriate antibiotic, were inoculated with a single bacterial colony and the culture was grown at 37°C in a shaker overnight. The next day the plasmid DNA was isolated using the *Qiagen® Plasmid Mini Kit* according to the manufacturer's instructions.

4.1.5 Plasmid preparation on preparative scale (maxiprep)

For the production of larger amounts of plasmid DNA, 100-250 ml of LB medium containing appropriate antibiotics were inoculated and the cultures were grown at 37°C in a shaker overnight. The preparation of plasmid DNA was carried out with the *Qiagen® Plasmid Maxi Kit* according to the manufacturer's instructions.

4.1.6 Photometric determination of DNA concentrations

DNA concentrations were determined photometrically using a *Biophotometer* (Eppendorf). DNA concentrations can be approximately calculated by the following formula: OD_{260} = 1 refers to 50 µg/ml DNA (layer thickness of the cuvette: 1 cm). The ratio OD_{260}/OD_{280} characterizes the purity of DNA with values between 1.7 and 2.0 for pure DNA.

4.1.7 Isolation of total cellular RNA

Total cellular RNA was isolated using the *RNAqueous®-Micro Kit* (Applied Biosystems) according to the manufacturer's protocol. Essentially, approximately 1-2x10^5 cells were pelleted (1,500 rpm, 5 min), the supernatant was discarded, and cells were resuspended in 100 µl lysis buffer. Subsequently 50 µl of 100% ethanol were added, followed by brief vortexing of the sample.The lysate/ethanol mixture was passed through a micro silica filter and centrifuged for 2 min at 14,000 g. The filter was then washed once with 180 µl of wash solution 1 and twice with 180 µl of wash solution 2/3. After each wash the filter was centrifuged at 14,000 g for 2 min. Subsequently, the flow through was discarded and the filter was centrifuged at 14,000 g for 2 min to remove residual fluid and to dry the filter. For elution of RNA the filter was transferred into a micro elution tube. In a first step, 15 µl of elution buffer – pre-heated to 75°C – was applied to the center of the filter and incubated for 2 min before centrifugation for 2 min at 14,000 g. In a second step, the procedure was repeated with 10 µl of elution buffer. To remove traces of contaminating genomic DNA the RNA elution was treated with recombinant DNase I. Therefore, 2.6 µl of 10x DNase I buffer and 1 µl of DNase I were added to 25 µl of RNA solution and incubated for 30 min

at 37°C. To inactivate DNase I, 2.8 µl of DNase Inactivation reagent was added. The mix was briefly vortexed, incubated for 1 min at RT, vortexed again and incubated for another minute. Finally, the DNase inactivation reagent was pelleted by centrifuging at 14,000 g for 2 min. The RNA-containing supernatant was transferred into a fresh tube and stored at -20°C until use. All steps were done on ice and centrifuges were pre-cooled to 4°C. Optionally, RNA content was measured photometrically at a wavelength of 260 nm using a *Biophotometer* (Eppendorf). RNA purity was assayed by measurement of the 260/280 nm ratio.

4.1.8 Reverse transcription of RNA into cDNA

To synthesize cDNA from total RNA the *High Capacity cDNA Reverse Transcription Kit* (Applied Biosystems) was used according to the manufacturer's protocol. For one reaction 0.5-1.0 µg total RNA or 10 µl of RNA elution were employed in a total reaction volume of 20 µl. 10 µl of 2x RT master mix containing 2.0 µl 10x RT buffer, 0.8 µl 25x dNTP mix (100 mM), 10x random primers, 1.0 µl of *MultiScribe*^{TM} reverse transcriptase, 1.0 µl of RNase inihibitor, and 3.2 µl nuclease-free H_2O were mixed with 10 µl of RNA sample. RT reactions were performed using the conditions below. Synthesized cDNA was stored at -20^{o}C and used for quantification of gene expression by qRT-PCR (see 4.1.10).

Step	Temperature/Time
Annealing	25°C; 10 min
Elongation	37°C; 120 min
Denaturation	85°C; 5 min

Table 4.1 | Standard protocol for reverse transcription.

For cloning of genes total RNA was extracted from Jurkat T cells (see 4.1.7) and cDNA was synthesized using the *Transcriptor High Fidelity cDNA Synthesis Kit* (Roche). The Transcriptor High Fidelity Transcriptase is a recombinant reverse transcriptase conferring proofreading activity for high accuracy of transcription of RNA. 10 µl of RNA elution was mixed with 1 µl of anchored-oligo$(dT)_{18}$ primers (50 pmol/µl) and filled up with 0.4 µl ddH_2O to make a total volume of 11.4 µl. For denaturation the template-primer mixture was heated for 10 min at 65°C. Subsequently, the sample was cooled on ice, and the following components of the RT mix were added to get a final volume of 20 µl: 10 µl 5x RT

buffer, 0.5 µl Protector RNase inhibitor, dNTP mix (10 mM each), DTT (100 mM) and 1.1 µl Transcriptor High Fidelity Reverse Transcriptase (10 U). Reagent were mixed and RT reactions were performed using the conditions below.

Step	Temperature/Time
Elongation	50°C; 30 min
Denaturation	85°C; 5 min

Table 4.2 | Conditions for high accuracy reverse transcription.

4.1.9 Polymerase chain reaction (PCR)

The polymerase chain reaction (PCR) enables the cyclic enzymatic amplification of defined DNA fragments *in vitro* (Mullis et al., 1986). Short oligonulceotide fragments which anneal to the complementary strains of the DNA template in an inverse orientation determine the ends of the amplified DNA fragment. In the presence of dNTPs thermostable DNA polymerases extend these forward- and reverse-primers along the denaturated single stranded DNA generating a complementary DNA strand.

For cloning of tagged versions of human PP4R1, PP4c, and PP2Ac as well as for mutagenesis of PP4R1 the *KOD Hot Start DNA Polymerase Kit* (Novagen®) was used. The *KOD* polymerase is a thermostable DNA polymerase derived from the hyperthermophilic archaeon *Thermococcus kodakaraensis (KOD)* (Benson et al., 2003). *KOD* Hot Start DNA Polymerase is a pre-mixed complex of the high fidelity *KOD* DNA Polymerase and two monoclonal antibodies that inhibit the DNA polymerase at ambient temperatures (Mizuguchi et al., 1999). Similar to the *Pfu* DNA polymerase *KOD* DNA polymerase possess a 3'→5' proofreading capacity which replaces mismatched 3'-terminal nucleotides from primer-template complexes. The following standard protocol was applied according to the manufacturer's recommendations:

Component	Amount/Volume	Final concentration
Template DNA	30 ng (1 µl)	30 ng/50 µl
Primer fwd (50 µM)	0.5 µl	0.75 µM
Primer rev (50 µM)	0.5 µl	0.75 µM
dNTPs (2 mM each)	5 µl	0.2 µM (each)
25 mM $MgSO_4$	3 µl	1.5 mM
KOD buffer (10x)	5 µl	1x
ddH_2O	34 µl	
KOD Hot Start DNA Polymerase (1 U/µl)	1 µl	0.02 U/µl
Total reaction volume	**50 µl**	

Table 4.3 | Standard protocol for PCR.

The following cycling conditions were applied:

Step	Temperature/Time	Cycles
Polymerase activation	95°C; 2 min	1
Denaturation	95°C; 20 sec	35
Annealing	Lowest primer Tm°C for 10 sec	
Elongation	70°C; 1for 20 sec/kB	
Storage	4°C; ∞	

Table 4.4 | Standard cycling conditions for PCR.

Oligonucleotides were designed with about 40-60 % GC content, no internal secondary structure, and complementarities at the 3'-ends. PCRs were prepared on ice. Optionally, gradient PCRs were performed to determine optimal annealing temperatures.

4.1.10 Quantitative Real Time-PCR (qRT-PCR)

Similar to conventional PCR quantitative real-time PCR (qRT-PCR) enables the amplification of specific DNA sequences. However, by use of fluorescent reporter molecules DNA amplification products are already detected during synthesis and therefore allow for the relative or absolute quantification of the amplified DNA.

(i) SYBR Green-based qRT-PCR

In general, relative gene expression levels were determined by SYBR Green-based qRT-PCR. This method relies on the detection of the incorporated DNA-intercalating fluorescent dye SYBR Green. SYBR Green specifically fluoresces upon light excitation when bound to double-stranded DNA. During PCR the detectable fluorescence is amplified by each PCR cycle. Gene expression was analyzed using the *Power SYBR® Green PCR Master Mix* in combination with the 7.500 Real-Time PCR System and the 7.500 Software version 2.0.1 (Applied Biosystems). Relative expression was determined from cycle threshold (Ct) values by normalization to hypoxanthine phosphoribosyl-transferase 1 (HPRT1) and/or glyceraldehyde-3-phosphate dehydrogenase (GAPDH) levels as reference genes. Fold expression was calculated according to the $\Delta\Delta$Ct method (Pfaffl, 2001).

Reactions were carried out in 96-well plates in triplicates with a final volume of 25 µl per reaction. Master mixes for triplicate measurements were prepared according to the following protocol:

Component	Amount/Volume
Template cDNA	1-2 µl
SYBR Green PCR master mix (2x)	42.5 µl
Primer mix (5 µM each)	10.2
ddH_2O	30.3 µl
Total reaction volume	**85 µl**

Table 4.5 │ Standard protocol for SYBR Green qRT-PCR.

The *Power SYBR® Green PCR Master Mix* contains 300 µl 110x SYBR Green buffer, 360 µl 25 mM $MgCl_2$, 240 µl dNTP (10 mM each), 15 µl U/µl Hot Gold Star Taq polymerase and 30 µl U/µl uracil-N-glycosylase.

(ii) Universal probe library assays

For some experiments *Univeral Probe Libray (UPL)* assays (Roche) were designed using the ProbeFinder Software (www.universalprobelibrary.com), and qRT-PCR was performed using the *LightCycler® 480 Probes Master Kit* and the *LightCycler ® 480. System* (Roche). UPL assays rely on a probe-based qRT-PCR, also known as TaqMan PCR. In contrast to SYBR Green qRT-PCR, this method requires a set of transcript-specific PCR primers and an additional fluorogenic 3' non-extendable hydrolysis probe for real-time PCR detection. The hydrolysis probe consists of a sequence-specific oligonucleotide that is covalently labeled with a fluorescent reporter dye at the 5'-end and a quencher label at the 3'-end. As long as the probe is intact any fluorescence signal is quenched. During PCR the probe hybridizes to the amplified sequence and the 5'→3'-exonuclease activity of the *Taq* DNA polymerase cleaves the hydrolysis probe. As a result, the fluorophore is liberated and fluorescence is detected. The amount of detectable fluorophore is directly proportional to the amount of template and can be used for quantification of transcript levels. Relative gene expression was calculated according to the ΔΔCt method as described before using the *LightCycler® 480* software with normalization to HPRT1 levels as endogenous reference.

qRT-PCR reactions were performed in 384-well plates in triplicate with a final volume of 11 µl per reaction according to the following protocol:

Component	Amount/Volume
Template cDNA	25 ng (1.1 µl)
Probes Master mix	4.5 µl
UPL probe	0.114 µl
Primer mix (20 µM each)	0.436 µl
ddH_2O	3.85 µl
Total reaction volume	**11 µl**

Table 4.6 | Standard protocol for UPL-based qRT-PCR.

For the *LightCycler® 480 System* the following qRT-PCR program was used:

Step	Temperature/Time	Cycles
Initial denaturation	95°C; 10 min	1
Denaturation	95°C; 10 sec	45
Annealing	55°C; 20 sec	
Elongation	72°C; 1 sec	
Final cooling	40°C; 20 sec	1

Table 4.7 | Standard cycling conditions for qRT-PCR using the *LightCycler® 480* System.

4.1.11 Gene expression profiling

cDNA from Jurkat, SeAx, Hut78, and HH cells was prepared (see 4.1.7 and 4.1.8). Gene expression was measured using a customized *RealTime ready* expression panel based on UPL assays (see 4.1.10) and the *LightCycler® 480 System* (Roche) according to the manufacturers' instructions. Relative expression was calculated using the *LightCycler® 480* software with triple normalization to HPRT1, GAPDH, and 18S rRNA levels.

4.1.11 Enzymatic manipulation of DNA

(i) Digestion of DNA with restriction endonucleases

For the sequence-specific cleavage of DNA molecules the samples were incubated with restriction endonucleases under appropriate reaction conditions. The amount of enzyme and DNA, the choice of buffer, temperature and duration of the reaction were adjusted according to the manufacturer's instructions.

(ii) Dephosphorylation of linearized vector DNA

Restriction of vector DNA with a single enzyme may lead to subsequent religation. Therefore, 5' termini of vector DNA were dephosphorylated using calf intestinal phosphatase (CIP) according to the manufacturer's instructions.

(iii) Ligation of DNA fragments

For the ligation of linearized vectors with DNA-fragments the T4 DNA ligase was used. This enzyme catalyzes the formation of phosphodiester bonds between adjacent 3'-OH

and 5'-P ends in double-stranded DNA. For ligations of cohesive ends a molar ratio between 1:3 and 1:5 (vector *vs.* insert DNA) was chosen.

4.1.12 Agarose gel electrophoresis

DNA samples were separated, characterized and purified by agarose gel electrophoresis. For preparation of agarose gels 1% agarose (w/v) was dissolved in 1x TAE buffer by boiling and supplemented with 6 µl ethidium bromide/100 ml solution. Prior to loading DNA samples were mixed with 6x DNA loading buffer. Additionally, 5-10 µl of a DNA molecular weight standard (*Gene Ruler*^{TM} 1 kB DNA ladder, Fermentas) was loaded. The voltage was set to 5 V/cm electrode distance and electrophoresis was performed in a horizontal gel chamber filled with TAE buffer. DNA fragments stained with ethidium bromide were visualized by UV-excitation at λ = 312 nm (fluorescence at λ = 590 nm).

4.1.13 Extraction of DNA from agarose gels

DNA fragments and linearized vectors for transfections were isolated from agarose gels and purified using the *QIAEX II Gel extraction Kit* (Qiagen). Alternatively, double-stranded DNA fragments from PCR or other enzymatic reactions were purified using the *QIAquick PCR Purification Kit* (Qiagen).

4.1.14 DNA sequencing

DNA sequencing was conducted by Seqlab or GATC Biotech according to the didesoxy method (Sanger et al., 1977).

4.2 Methods in mammalian cell culture

4.2.1 General culture conditions

All used cell lines were cultured at 37°C in an atmosphere with a relative humidity of 90% and a CO_2 content of 5%. For the inactivation of complement factors FCS was heated to 56°C for 30 min before use. Unless otherwise indicated, all media contained 10% (v/v) FCS and were supplemented with antibiotics. Cells were harvested by centrifugation for 4 min at 1,500 rpm and 4°C. Cell culture work was performed under sterile conditions using a laminar flow hood.

4.2.2 Culture of adherent cells

Adherent growing cell lines HEK293T, HeLa, Hep3B, and Phoenix were maintained in DMEM medium. At a confluence of about 80% cells were split in a ratio of 1:3-1:10. To this end, the supernatant was discarded and 2-5 ml of trypsin/EDTA solution were added for 3-5 min at RT. Detached cells were resuspended in fresh DMEM medium and seeded with a confluence of 10-25% onto new plates.

4.2.3 Culture of suspension cell lines

For the culture of suspension cell lines or primary human T lymphocytes the following media were used.

Cell line/type	Cell culture medium
Jurkat-derivatives JE6.1, J16-145, Gluc-J16	IMDM
CEM, SeAx, MyLa, Hut78, HH, SUDHL-5, BJAB, SUDHL-6, HT, Raji	RPM1 1640
OCI-Ly3	RPM1 1640 (with 20% FCS)
Primary human peripheral blood T lymphocytes	RPMI 1640 with IL-2 (25 U/ml) or X-Vivo 15 medium with IL-2 (25 U/ml) and 1% Glutamax

Table 4.8 | Media for mammalian cell culture.

Media were replaced every 2-3 days. The suspension cell lines JE6.1, J16-145, and Gluc-J16 were cultured with a density of 1.5-4x10^5 cells/ml.

4.2.4 Thawing and freezing of eukaryotic cells

The cells were harvested and resuspended in freezing medium containing 90% (v/v) FCS and 10% (v/v) DMSO. The cell density was adjusted to 1-1.5x10^7 cells/ml. 1 ml cell suspension was transferred into a cryo-tube and immediately stored at -80 °C (-140°C for long term storage). Cells were rapidly thawed at 37°C and immediately resuspended in 10 ml of RPMI or IMDM medium to dilute the DMSO. Afterwards, cells were centrifuged at 1,500 rpm for 4 min at 4°C and resuspended in an appropriate volume of fresh culture medium.

4.2.5 Determination of the cell density

The cell density of a culture was determined by use of a Neubauer chamber slide. If necessary, cells were diluted prior to counting.

4.2.6 Preparation of AET-erythrocytes

A solution of 2-aminoethylisothiouroniumbromide (AET) (pH=9.0) was prepared using pyrogen-free, sterile water (0.5 g of AET diluted in 12.5 ml of water). Sheep blood erythrocytes were suspended in a 1:1 ratio in Alsever solution. After washing with PBS for three times, 25 ml of the sheep blood erythrocytes were mixed with 12.5 ml of the AET solution and incubated for 15 min at 37°C. Cells were then washed four times with PBS. Finally, cells were diluted in FCS-containing RPMI medium to prepare a 4% suspension. All centrifugation steps were performed at 500 g and 20°C for 10 min. AET-treated sheep blood erythrocytes were stored at 4°C for up to three days.

4.2.7 Ficoll gradient isolation of human mononuclear cells

Primary human mononuclear cells were isolated from 500ml total blood or buffy coats according to the following protocol. 1 ml of heparin was added to 500 ml of whole blood to inhibit coagulation. Buffy coats were adjusted to 300ml with PBS. 50ml tubes filled with 15 ml Ficoll were slowly overlayed with 35 ml blood and centrifuged at 650 g and 20°C for 20 min without break. Peripheral blood leukocytes (PBLs) were collected from the interphase and washed twice with PBS and resuspended in RPMI medium. PBLs were transferred into cell culture flasks and cultured for 30-45 min in the incubator for the depletion of adherent cells (*i.e.* monocytes and macrophages). Non-adhering lymphocytes were collected, spun down (500 g, 10 min, RT) and suspended in RPMI medium with a cell density adjusted to $1x10^7$ cells/ml. Lymphocytes were used for the further purification of human peripheral blood T lymphocytes by rosetting with 2-amino-ethylisothyo-uronium-bromide-treated sheep red blood cells as described before (Gulow et al., 2005). Alternatively, $CD4^+CD25^-$ T lymphocytes were purified by magnetic sorting (see 4.2.8).

4.2.8 Isolation and culture of human peripheral T cells

(i) T cell isolation by T cell rosetting with AET-erythrocytes

PBLs were mixed in a 2:1 ratio with 4% AET-erythrocytes for a “rosetting” reaction. The mixture was centrifuged (500 g, 10 min, RT, slow breaking). The pellet (containing “rosettes”) was resuspended, carefully layered on top of pre-warmed Ficoll solution

(15 ml) and centrifuged for 20 min at 2420 rpm and RT (without breaks). The pellet, consisting of T cells and erythrocytes, was washed with pre-warmed PBS or medium (500 g, 10 min, RT, slow breaking). The erythrocytes were lysed by addition of 4x volume (acc. to the pellet) of ACK buffer. The lysis is indicated by a colour change of the mixture from turbid light red to clear dark red. Subsequently, cells were washed twice with pre-warmed PBS or medium, resuspended in 50 ml of RPMI, counted and diluted to a concentration of $2x10^6$ cells/ml.

(ii) Magnetic-activated cell separation of $CD4^+$ T lymphocytes

The isolation of T cells was accomplished by means of magnetic-activated cell separation (MACS). Cells can be separated by MACS either by positive or negative selection.

In a first step, $CD25^+$ T cells were removed by positive selection. For that, the PBL suspension was incubated with a limiting amount (2 µl/10^7 cells) of bead-coupled anti-CD25 monoclonal antibodies. After a subsequent washing step, the cell suspension was loaded onto a column in a magnetic field. The magnetic beads retain the $CD25^+$ cells in the column, while the remaining cell types flow through. Outside of the magnetic field, $CD25^+$ cells were eluted from the column. In a second step, $CD4^+CD25^-$ T cells were isolated from the $CD25^+$-depleted fraction using the CD4 Isolation kit II and additionally depleted from $CD25^+$ cells with 6 µl of anti-CD25 MACS beads per 10^7 cells.

Alternatively, bulk $CD4^+$ T cells were isolated from total PBLs by positive selection using *CD4 MicroBeads* (Miltyenyi Biotec) according to the manufacturer's protocol. Briefly, PBLs were resuspended in 80 µl of buffer per $1x10^7$ total cells. 20 µl of CD4 MicroBeads conjugated to anti-CD4 monoclonal antibodies were added per $1x10^7$ total cells. The suspension was mixed and incubated for 15 min at 4°C. Subsequently, cells were washed by addition of 2 ml of buffer per $1x10^7$ cells, followed by centrifugation at 300 g for 10 minutes. Finally, up to $1x10^8$ cells were resuspended in 2 ml of buffer. Magnetic separation of bead-labeled $CD4^+$ cells was performed as described before. Isolated T cells were rested overnight in X-Vivo 15 medium and diluted to a concentration of $2x10^6$ cells/ml.

4.2.9 *In vitro* expansion of T lymphocytes

For activation, resting peripheral blood T lymphocytes were cultured at a concentration of $2x10^6$ cells/ml in the presence of 1 µg/ml PHA for 16 h. Alternatively, T cells were stimulated by soluble anti-CD3 (0.5 µg/ml) and anti-CD28 (2 µg/ml) agonistic antibodies.

T cells were then cultured in RPMI medium supplemented with 10% FCS and 25 U/ml IL-2 for 6-8 days (day 6 T cells). In general, all experiments were performed with T cells isolated from 2-3 independent healthy donors.

4.2.10 T cells from Sézary patients

T lymphocytes were isolated from peripheral blood of patients suffering from Sézary syndrome and PP4R1 mRNA levels were analyzed by SYBR Green qPCR with dual normalization for GAPDH and HPRT1 expression. For transcriptional analyses only those samples were included that showed tumor loads of generally at least 60% as determined by microscopical evaluation of blood smears. At large, the percentage of Sézary T cells relative to whole lymphocytes in peripheral blood samples was about 70% with $CD4^+$ to $CD8^+$ T cell ratios between 11 and 99 as evaluated by flow cytometry (Klemke et al., 2008). As controls, T cells from 10 age-matched normal healthy donors were investigated. cDNAs were kindly provided by N. Booken and C.-D. Klemke (University Hospital Mannheim). CTCL was diagnosed according to the WHO-EORTC classification of cutaneous lymphomas (Willemze et al., 2005) and the criteria of the international society of cutaneous lymphomas (Vonderheid et al., 2002). The study was conducted according to the ethical guidelines of German Cancer Research Center (DKFZ, Heidelberg) and the Helsinki Declaration, and approved by the ethics committee II of the Ruprecht-Karls-University of Heidelberg, Germany.

4.3 Cell biological methods

4.3.1 Transient and stable transfections by electroporation

Electroporation is a method for the direct transfer of macromolecules (*i.e.* DNA) into target cells by perforating the plasma membrane with a short electric pulse.

For generation of stably-transfected Gluc-J16-15 reporter cells the 8xNF-κB pGluc vector was linearized by *ScaI* restriction digest. For transient transfection of Jurkat and HH cells circular plasmid DNA was used. For each sample about 5-30 µg of plasmid DNA were transfected. 1-3x10^7 cells were harvested and washed once with cold and sterile PBS. Cells were resuspended in 400 µl of IMDM medium without FCS and antibiotics and mixed with the plasmid sample. Subsequently, the cell-plasmid mixture was transferred into an electroporation cuvette. Cells were electroporated at 250 V and 950 µF. Then, cells were resuspended in 5-10 ml of pre-warmed medium in 6-well plates or 10 cm

dishes. After 24-48 h cells were subjected to further analyses. For selection of stable integrants Gluc-J16-156 cells were cultured in IMDM medium supplemented with 2-4 mg/ml G418 in 96-well plates. Single clones were subloned twice by limiting dilutions according to Poisson statistics.

4.3.2 Nucleofection and siRNA-mediated gene silencing

For siRNA-mediated gene silencing J16-145 T cells as well as primary human T lymphocytes were transiently transfected by nucleofection using the *Cell Line Nucleofector® Kit V* and the *Human T Cell Nucleofector® Kit* (Amaxa), respectively, according to the manufacturer's instructions. $2x10^6$ J16-145 T cells or $5x10^6$ primary human T cells were resuspended in appropriate nucleofection solutions containing 1µM siRNA. Nucleofection was performed using program X-01 for J16-145 cells or program U-14 for primary human T lymphocytes. After 72 h, knock-down efficacy was assessed and cells were subjected to further analyses.

4.3.3 Nucleofection of siRNA under HTS conditions

For large-scale RNAi screening and subsequent validation experiments Gluc-J16 reporter cells or J16-145 cells were nucleofected in a 96-well plate format. siRNA transfections were performed using the *Nucleofector® 96-well Shuttle®* system in combination with the *Cell Line 96-well Nucleofector® Kit SE* (Lonza). Cells were kept in logarithmic growth phase prior to transfection. For one nucleofection well 5×10^5 cells, resuspended in 20 µl of Cell Line 96-well *Nucleofector® Solution SE*, were transfected with 1 µl of 20 µM siRNA solution. Before transfection 1 µl of siRNA solution was pre-spotted into 96-well V-bottom plates. For transfection of one 96-well plate the content of five T75 flasks grown to a density of 2×10^5 cells/ml was centrifuged at 1.500 rpm for 5 min and cell pellets were subsequently pooled to obtain a total cell number of about 5×10^7 cells. Residual medium was completely removed from the cell pellet and cells were resuspended in 2.2 ml *Nucleofector® Solution SE*. Next, cells 20 µl of the cell-nucleofector suspension were transferred to the 96-well V-bottom plate and mixed gently with the pre-spotted siRNAs by carefully pipetting up and down. Subsequently, the siRNA-cell suspension was transferred into *Nucleocuvette™* plates and transfection was immediately initialized using program 96-CL-120. After transfection 100 µl of pre-warmed medium per 96-well was added, cells were resuspended and divided into two technical replicates. Cells were grown in 200 µl medium in 96-well plates for about 72 h and then subjected to further analyses.

4.3.4 siRNA library screening

Primary RNAi screening was based on Gluc-J16 NF-κB reporter cells and the commercially available *Silencer® Select Human Phosphatase siRNA Library V4* (Applied Biosystems) targeting 298 known or putative phosphatase genes encoding for regulatory or catalytic phosphatase subunits. The library contained three single, independent siRNA oligos per gene yielding a total of 894 phosphatase-specific siRNAs. Each individual siRNA was arrayed in a 96-well plate format and transfected in biological dublicates. For the phosphatase RNAi screen the HTS siRNA transfection protocol was applied using the *Nucleofector® 96-well Shuttle®* system as described before (see Fig. 4.1 and section 4.3.3). For each 96-well transfection plate a constant panel of positive and negative control siRNAs (*i.e.* siRNA oligos specific for CYLD, RelA, and Carma1, as well as non-targeting siRNA) and mock transfections (H_2O) were included. In total, 22 96-well plates were transfected with more than 2,000 consecutive single transfections. Subsequent to the transfection procedure, cells were divided into equivalent fractions (two technical replicates per biuological replicate), incubated for about 72 h and then subjected to different stimulation conditions. To this end, cells from each well (technical replicate) were again separated into equivalent fractions and were either left untreated (medium control) or stimulated with agonistic anti-CD3, anti-CD28 and goat-anti-mouse antibodies (0.1 µg/mL final concentration each) for 5 h. Subsequently, Gluc activity in cell supernatants determined (see section 4.4.9). In addition, cell viability was measured for normalization of the luciferase signal (see section 4.4.10).

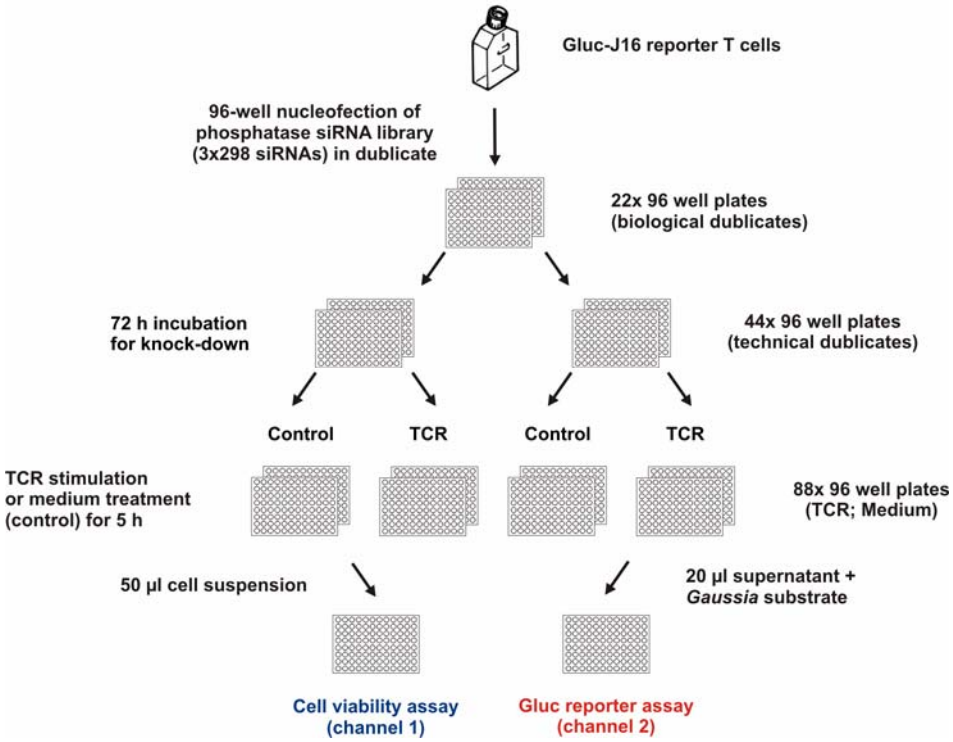

Figure 4.1 | Schematic representation of work-flow for primary siRNA library screening. Gluc-J16 reporter cells, transfected with 1 µM of phosphatase-specific siRNA or control siRNA, were either left untreated (medium control) or stimulated with agonistic anti-CD3, anti-CD28, and anti-goat-anti-mouse antibodies (TCR; 0.1 µg/ml final concentration each). For details see text.

4.3.5 Transfection of HEK293T cells by the $Ca_3(PO_4)_2$ method

Cells were grown to 70-80% confluence in 10 cm cell culture dishes. 5-20 µg plasmid DNA were mixed with 1 ml 1x HBS and 50 µl 2.5 M $CaCl_2$ were carefully added. After 10 min of incubation the mix was added dropwise to the cells. After 24 h the transfection efficiency was analyzed by fluorescence microscopy using cells that had been (co-)transfected with cDNA encoding for the green fluorescent protein (GFP) as control. After additional 24 h cells were harvested, lysed and exogenous protein expression was examined.

4.3.6 Production of recombinant retroviruses

Retroviral supernatants were prepared by transfection of pMX IRES-GFP expression vectors into amphotropic Phoenix cells. The Phoenix cell line is a HEK293T-derived helper cell line for the production of recombinant retroviruses (Swift et al., 2001). For production of lentiviral particles HEK293T cells were used.

Phoenix-Ampho cells and 293T cells were seeded with a density of $1.5x10^6$ and $1.0x10^6$ cells/ml, respectively, in 4 ml of DMEM medium in T25 flasks and cultured overnight up to

a confluence of about 75%. Prior to transfection 293T cells were pre-treated for 1 h with 25 µM chloroquin. Cells were transfected by the $Ca_3(PO_4)_2$ method as described before using 600 µl 1x HBS and 30 µl 2.5 M $CaCl_2$. For transfection of Phoenix cells 10 µg of pMX-based expression vector were transfected. 293T cells were transfected with 6.3 µg of TRC-derived shRNA vectors, 4.3 µg of psPAX2 (encoding for gag, pol, and env proteins), and 2.3 µg of pMD2 (encoding for VSV-G) for pseudotyping. 8 h post transfection the medium was removed from packaging cells and replaced by 4 ml of fresh DMEM medium. Virus production was continued for additional 24 h.

4.3.7 Viral transduction of target cells

Two days after transfection of packaging cells, the supernatant was collected and centrifuged at 1,500 rpm for 4 min at 4°C to remove cell debris. In addition, the supernatant was passed through a 0,45 µM filter. $1x10^5$ target cells resuspended in 100 µl of RPM1 1640 medium were added to 1 ml of viral supernatant supplemented with Polybrene (8 µg/ml). Cells were infected in 24-well plates by spin occulation. To this end, cells were centrifuged at 2.500 rpm for 2 h and 30°C. 24 h later cells were collected, washed three times with medium, resuspended in fresh medium, and transferred into fresh tissue culture flasks. 48 h post transduction, stably shRNA-transduced Jurkat cells were selected by puromycin resistance (1 µg/ml puromycin).

4.3.8 Retroviral reconstitution assays

The toxicity of ectopic phosphatase expression was examined by retroviral reconstitution of the CTCL lines SeAx, MyLa, Hut78, and HH. For the reconstitution assay CTCL cell lines were retrovirally transduced with pMX-IRES GFP vectors either expressing GFP alone (ctrl) or co-expressing wild type human PP4R1, PP4c, or PP2Ac. The frequency of transduced (GFP-positive) cells was monitored over time by flow cytometry. For a single assay cells were transduced and analyzed in triplicate. The percentage of phosphatase-reconstituted cells was normalized to that of control-transduced cells at the same day. In addition, the ratio of GFP-positive cells at various time points was normalized to the initial ratio at day 3-5 post transduction.

4.3.9 Determination of CD69 cell surface expression

Cell surface expression of CD69 on J16-145 cells was analyzed by immunofluorescence staining and flow cytometry. $1\text{-}2x10^6$ J16-145 cells, that had been transiently co-

transfected with plasmid DNA and a GFP-encoding control plasmid (10 µg each) (see 4.3.1), were stimulated with anti-CD3, anti-CD28 and goat-anti-mouse antibodies (1µg/mL each) in 6-well plates for 8 h. Subsequently, cells were collected and incubated one ice for 30 min with a PE-conjugated anti-human CD69 antibody (diluted 1:25 in FACS buffer) in a total volume of 20 µl per sample. To remove unbound antibodies cells were washed twice with 1 ml of PBS. Finally, cells were resuspended in 200 µl of FACS buffer and subjected to FACS analysis. CD69 levels of plasmid-transfected cells were determined by gating on GFP-positive viable cells. Fluorescence intensities were monitored on a flow cytometer (*FACSCanto II*) and the analysis was accomplished using the software *FACSDIVA*. Fluorescence emission was detected on the FL1-H and FL2-H channel. For each diagram $2x10^4$ cells were analyzed on a logarithmic scale.

4.4 Biochemical and immunological methods

4.4.1 *In vitro* stimulation of T cells

Cells were harvested and resuspended in fresh culture medium. Cells were stimulated with agonistic soluble anti-CD3 (Okt3), anti-CD28, and anti-goat-anti-mouse monoclonal antibodies (TCR stimulation) with final concentrations between 0.1 and 1.0 µg/ml. Alternatively, cells were stimulated with PMA (10 ng/ml), ionomycin (10 µM), and recombinant TNFα (20 ng/ml), respectively. For stimulations in 96-well plates, $1\text{-}2x10^5$ Jurkat or Gluc-J16 cells were resuspended in 100 µl medium and 100 µl of 2-fold-concentrated stimulation medium was added. For biochemical experiments, $1\text{-}5x10^7$ cells were resuspended in 4-5 ml of medium in 6-well plates or T25 flasks. For stimulation 1 ml of 4-5-fold-concentrated stimulation mix was added. Cells were stimulated for the indicated time periods. To stop stimulation, cells were transferred into 1,5 ml Eppendorf tubes or into 15 ml tubes and centrifuged at 5,000 rpm for 1 min or at 1,500 rpm for 4 min at 4°C. The supernatant was drawn off and cells were lysed as described in 4.4.2.

4.4.2 Cell lysis

Cells were harvested and the supernatant was drawn off. Then, 20 µl of ice-cold lysis buffer per $1x10^6$ cells were added, and the lysates were incubated on ice for at least 20 min. The lysates were cleared from insoluble cell debris by centrifugation at 14,000 g and 4°C for 10 min. Protein concentrations of whole cell lysates were measured by *Roti®-Quant* Bradford assay (Roth) according to the manufactures' instructions and adjusted to

equal levels. For gel electrophoresis lysates were mixed with 10 µl of 3x reducing SDS sample buffer per 1x10^6 cells (Laemmli et al., 1970) and heated to 95°C for 5 min or subjected to immunoprecipitation (see 4.4.3).

4.4.3 Immunoprecipitation

For immunoprecipitation (IP) cleared lysates of 1-6x10^7 cells were incubated with the desired antibody at 4°C on a rotator for 1 h. Subsequently, 40 µl of protein A-sepharose beads were added and the suspension was incubated at 4°C on a rotator for at least 3 h or overnight. The matrix was washed 1-5 times with 1 ml of ice-cold lysis buffer or PBS to remove unspecifically adsorbed proteins. Subsequently, beads were resuspended in 50 µl of lysis buffer and heated in 25 µl 3x sample buffer at 95°C for 5 min. (Co-)purified proteins were detected by SDS-PAGE and immunoblotting (see 4.4.4 and 4.4.5).

4.4.4 SDS polyacrylamide gel electrophoresis (SDS-PAGE)

The analytical separation of proteins was accomplished by discontinous SDS-PAGE under reducing conditions (Laemmli et al., 1970). Sodium dodecyl sulphate (SDS) is an anionic detergent. SDS denatures proteins and concomitantly confers to them a net negative charge. On average, proteins bind 1.4 g SDS per gram of protein. Thus, migration of the SDS-protein complexes through polyacrylamide gels in an electric field largely depends on their molecular mass.

For electrophoresis 8-12% polyacyrlamide separating gels and 5 % polyacrylamide stacking gels were prepared. The polymerisation was started by adding 0.1% (v/v) TEMED and the polymerizing solution was used immediately. The separating gel was covered with isopropanol. After 15 min the isopropanol was removed by washing with water, the gel surface was dried and the stacking gel was added. Proteins were electrophoretically separated at a constant current of 25-30 mA/gel for 1-1.5 h.To estimate apparent molecular weights of analyzed proteins an appropriate molecular weight marker (NEB) was used. Subsequent to SDS-PAGE, the polyacrylamide gel was subjected to immunoblotting (see 4.4.5).

4.4.5 Immunoblot analysis

For immunoblot (IB) analysis, proteins separated by SDS-PAGE were electrophoretically transferred onto a nitrocellulose membrane (Amersham Bioscience) using a semidry-transfer system (Biorad) (transfer conditions: 0.8 mA/cm^2; 2 h). Gel and membrane were

pre-incubated in transfer buffer. After electroblotting the transferred proteins are bound to the membrane providing access for the detection by specific antibodies. To avoid unspecific binding the membrane was incubated in blocking solution (5 % (w/v) nonfat dried milk in PBST or 5 % (w/v) BSA in PBST) at RT for 1 h on a shaker. The membrane was briefly washed three times with PBST. For specific detection of proteins the membrane was incubated with a primary antibody solution for at least 1 h at RT or overnight at 4°C on a shaker. After washing three times with PBST the membrane was incubated with a HRP-conjugated α-immunoglobulin secondary antibody for 0.5-1 h at RT on a shaker. Finally, the membrane was washed three times with PBST for 20 min each time. Detection of membrane bound HRP was performed by enhanced chemiluminescence (ECL) using the *Western Lightning™ Plus-ECL* reagent (PerkinElmer) according to the manufacturer's instructions. Chemiluminescence was detected using a digital chemiluminescence acquisition system (Vilber Lourmat). Analysis was accomplished using the software Chemi-Capt (Vilber Lourmat) and Photoshop CS4. Protein quantification was performed using the Bio-1D software (Vilber Lourmat). For specific detection of further proteins the enzymatic activity of the HRP was inactivated by incubation with 0.01 % (w/v) NaN_3 in PBST at RT for 1 h. Thereafter, the membrane was incubated with the subsequent primary antibody and the visualization procedure was continued as described above. Alternatively, the nitrocellulose membrane was incubated for 15 min at 55°C in stripping buffer to denaturate primary and secondary antibodies, followed by extensive washing with ddH_20 and PBST. Then, the membrane was blocked again for 1 h and the procedure was continued as described above.

4.4.6 *In vitro* kinase assay

All *in vitro* kinase assays were performed as described previously (Brenner et al., 2005). FLAG:IKKβ or the endogenous IKK complex were immunoprecipitated by anti-FLAG and anti-NEMO antibodies, respectively. Immunoprecipitates were washed 1-3 times with lysis buffer, followed by a final washing step with kinase buffer. Immune complexes were resuspended in 100 µl kinase buffer in divided into equivalent 50 µl aliquots. One part was used to control for protein input by SDS-PAGE and immunoblotting, while the other part was subjected to the *in vitro* kinase reaction. 5 µg of recombinant GST:IκBα, serving as a IKK-specific kinase substrate, were added together with 10 µCi [^{32}P-γ]ATP. The reaction was performed for 30 min at 30°C on a shaker. Subsequently, proteins were separated by SDS-PAGE. The gel was dried and subjected to autoradiography.

4.4.7 *In vitro* phosphatase assay

To obtain phosphorylated FLAG-tagged IKK substrates, FLAG:IKKα and FLAG:IKKβ expression plasmids were transiently transfected into HEK293T cells. After 24 h, cells were stimulated with PMA/ionomycin for 15 min. Subsequently, IKKs were immunoprecipitated from whole cell lysates by anti-FLAG immunoprecipitation. Alternatively, the endogenous IKK complex was immunoprecipitated by anti-NEMO antibodies from Jurkat T cells that were either unstimulated or stimulated by treatment with PMA/ionomycin for 15 min. Phosphorylated IKK proteins were recombined and served as substrates in a subsequent phosphatase reaction. For this purpose, HA:PP4R1 or HA:PP4c were separately overexpressed in HEK293T cells and purified by anti-HA immunoprecipitation. Anti-HA immunoprecipitates were then co-incubated with equivalent portions of FLAG-tagged IKK substrates for 1 h in phosphatase buffer. Subsequently, combined immune complexes were resolved by SDS-PAGE and IKK phosphorylation was analyzed by immunoblotting. For cell lysis and immunoprecipitation, a lysis buffer without phosphatase inhibitors was used. To measure phosphatase activity of exogenous or endogenous PP4R1 and anti-PP4c immunoprecipitates the colorimetric *SensoLyte® pNPP Protein Phosphatase Assay* (AnaSpec) was used according to the manufacturer's instructions. For this, phosphatase reactions were performed for 1 h or overnight at 30°C in a shaker. For end-point reading the absorbance signal was measured at 415 nm using the *Microplate Reader Model 680* (Biorad). Relative phosphatase activity was calculated as (induced phosphatase activity – background activity)/(background activity)x100.

4.4.8 *In vitro* translation

HA-tagged PP4R1 as well as FLAG-tagged versions of IKKα, IKKβ, or PP4c were *in vitro* translated in the presence of radioactively labeled ^{35}S-methionine using the *TNT® T7 Coupled Reticulocyte Lysate System* (Promega) according to the manufactures' instructions.

4.4.9 *Gaussia* luciferase reporter assay

0.5-2x10^5 GLuc reporter cells or T cells that had been transiently transfected with the Gluc expression plasmid were stimulated in 96 well plates. For each sample, 20 µl of supernatant was subjected to a *Gaussia* luciferase assay (p.j.k.) according to the manufactures' instructions. Luciferase activity was measured in 96-well plates using a *Orion L Microplate Luminometer* (Berthold Detection Systems) with an integration time of

3.0 sec. In parallel, cell viability was determined (see 4.4.10) and normalized Gluc activity was calculated as the ratio between Gluc activity and cell viability counts.

4.4.10 Cell viability assay

To normalize luciferase expression for variations in cell numbers, cell viability was measured in a 96-well format using the *CellTiter-Glo® Luminescent Cell Viability Assay* (Promega). This method determines the number of viable cells based on the relative quantification of the intracellular ATP content. The amount of ATP present correlates with the amount of metabolically active cells. To perform the *CellTiter-Glo®* assay, cells were resuspended in the remaining medium and 50 µl of the cell suspension were added to 50 µl of the CellTiter-Glo reagent (1:1 diluted with medium). Subsequently, plates were incubated for 20 min at 37 °C in the dark. Luminescence was measured using a *Mithras LB940 plate reader* (Berthold Technologies) (integration time 0.1 sec) or an *Orion L Microplate Luminometer* (Berthold Detection Systems) (integration time 1.0 sec).

4.4.11 Transient reporter assay

For transient reporter assays $1x10^7$ Jurkat T cells or $2x10^5$ HEK293T cells were co-transfected with NF-κB- or AP-1-specific transcriptional reporter plasmids (pGL8xNF-□B-fos or p3xAP-1-Luc) and pfos-LacZ as described previously (Arnold et al., 2001). Jurkat cells were co-transfected with 8 µg of reporter plasmid and 1.5 µg of pfos-LacZ. HEK293T cells were co-transfected with 2 µg of reporter plasmid and 0.5 µg of pfos-LacZ. Transfection efficiency was normalized to LacZ expression. 24-48 h post transfection cells were lysed and luciferase activity was measured using the *Dual-Light® System* (Applied Biosystems) and an *Orion L Microplate Luminometer* (Berthold Detection Systems) according to the manufactures' instructions.

4.4.12 Enzyme-linked immunosorbent assay (ELISA)

To measure cytokine secretion of siRNA-transfected or shRNA-expressing Jurkat T cells or primary human T lymphocytes, cells were stimulated in 96-well plates with anti-CD3, anti-CD28, and anti-goat-anti-mouse monoclonal antibodies overnight or with PMA/ionomycin for 8 h. Subsequently, the supernatant was collected, and the levels of secreted IFNγ, IL-2, IL-8, or TNFα were determined by enzyme-linked immunosorbent assays (ELISA) according to the manufactures' instructions. For all TCR stimulations, 50 µl of supernatant was applied, whereas supernatants from PMA/ionomycin-stimulated

Jurkat cells were diluted 1:4-1:20 with IMDM medium without supplements, depending on the tested cytokine (1:4 for IFNγ and IL-8, 1:10-1:20 for IL-2). For end-point reading the absorbance signal was measured at 490 nm using the *Microplate Reader Model 680* (Biorad). Optionally, the remaining cell suspension was subjected to a cell viability assay (see 4.4.10) to normalize cytokine levels to cell numbers.

4.5 Computational and statistical analysis

4.4.1 Statistical normalization

Statistical analysis of the primary RNAi screen and data pre-processing were conducted using the *cellHTS2* Bioconductor/R software package (in collaboration with D. Nickles, DKFZ) (Boutros et al., 2006; Pelz et al., 2010). For each 96-well two reporter signals were measured: channel 1 was representative of overall cell viability and cell numbers, whereas channel 2 was based on measurement of NF-κB-driven Gluc activity (see also 5.1.5). Computational analysis of raw data from each channel revealed in part considerable interplate variations as well as systematic intraplate effects (positional effects, such as column, row, or edge effects). Therefore, values were statistically normalized using the stringent *B* score algorithm that is suitable to standardize for intraplate and plate-to-plate variability (Birmingham et al., 2009; Brideau et al., 2003; Malo et al., 2006). *B* score normalization yielded accurate and similar distributions of median normalized signal intensities between replicates and across different plates as assessed by box plot analysis (Boutros et al., 2006; data not shown). In addition to statistical normalization, pre-processed data from either channel were combined in order to calculate values for NF-κB-specific Gluc activity normalized to cell numbers (channel 2/channel 1; biological normalization). Subsequently, mean Gluc activity of two biological replicates for each siRNA transfection was determined. Mean values, in turn, were transformed into the statistical *z* score for hit selection and post-screen analysis (see 4.4.2).

4.4.2 Candidate selection by analysis of statistical normality

For identification of candidate phosphatases (hits) quantified RNAi phenotypes (*i.e.* mean values of normalized NF-κB activity) were scored for statistical significance. To this end, normalized measurements were transformed into the statistical *z* score (Boutros et al., 2006). Data transformation helps to further minimize data variability and allows for the

analysis of statistical normality which is instrumental in defining appropriate thresholds for hit selection. Using a quantile-quantile (QQ) plot analysis (Ramadan et. al., 2007) *z* scores assigned to individual phosphatase siRNAs (sample quantiles) were plotted against values from a theoretical normal distribution (theoretical quantiles) (Fig. 5.5 A). *z* score deviations from normally (randomly)-distributed values indicated statistically significant RNAi phenotypes. For hit selection *z* scores > +1.5 and < -1.5 were defined as cut-offs values (Fig. 5.5 A and B).

4.4.3 Student's t-test

The unpaired Student's *t*-test (independent two-sample t-test; unequal sample sizes and unequal variance) was used for statistical analysis of *PPP4R1* mRNA expression in Sézary patients (12 samples) *vs.* normal healthy donors (10 samples). A *p* value of less than 0.05 was considered statistically significant.

5 Results

Activation and regulation of NF-κB signaling in T cells proceed *via* the orchestrated action of a number of adapter and effector molecules. While multiple kinases and phosphorylated target proteins that induce NF-κB activity have been identified, the molecular machinery involved in the termination of antigen receptor-mediated NF-κB activation still remains only poorly understood. Since signal transmission emanating from engaged cell surface receptors (*e.g.* TCR and TNFR) to transcriptionally active NF-κB largely relies on phosphorylation events, it is generally assumed that phosphatases play an important role in the modulation and termination of NF-κB activity. Yet, the role of phosphatases in regulation of TCR-induced NF-κB signaling is still not well understood.

The following study has been conducted with the aim to elucidate the potential role of phosphatases in regulation of TCR-induced NF-κB signaling. To this end, an RNAi-based genetic screening strategy has been adopted in order to systematically uncover phosphatase genes that shape the TCR-dependent NF-κB signal. Subsequent experiments were performed to characterize individual NF-κB-modulating phosphatases with respect to physiological relevance, biological function as well as the biochemical mechanism underlying NF-κB regulation.

5.1 Design and implementation of a large-scale RNAi screen for phosphatases that regulate TCR-induced NF-κB activity

With the discovery of RNAi-based gene silencing it has become possible to adopt large-scale reverse genetic screens in mammalian cells in order to identify genetic components and interactions underlying basic biological programs or specific signaling pathways. Cell-based RNAi screens rely on siRNA-mediated silencing of specific target genes and provide an efficient and unbiased approach to systematically study loss-of-function phenotypes *in vitro* (Boutros and Ahringer, 2008; Moffat and Sabatini, 2006).

The quality of information that can be extracted from RNAi-based high throughput screening (HTS) experiments critically depends on a number of general technical considerations. These include: (i) appropriate means to monitor and quantify RNAi phenotypes, (ii) efficient siRNA delivery (transfection) and gene silencing, (iii) screening design and procedure under large-scale conditions, and (iv) statistical methods for primary hit selection and post-screen analysis (Sharma and Rao, 2009). The optimization and adaptation of these experimental parameters was subject of the following analyses.

5.1.1 Generation of a novel luciferase-based NF-κB activity reporter system

The activity of specific signaling pathways can be monitored by transcriptional reporter assays. Luciferase-based reporter assays are particularly applicable for large-scale RNAi screens since they facilitate the rapid quantification of transcriptional activity under HTS conditions (Moffat and Sabatini, 2006).

In order to establish a cell-based NF-κB-specific screening system a novel luciferase reporter cassette was generated that allows for the NF-κB-dependent transcription of the *Gaussia* luciferase (Gluc) reporter gene under control of the basal mouse c-fos promoter and eight NF-κB-binding (κB) sites (Arnold et al., 2001) (Fig. 5.1 A). Importantly, Gluc harbours a natural N-terminal secretion sequence mediating quantitative secretion of the nascent protein in an active form (Badr et al., 2007; Tannous et al., 2005). Unlike conventional luciferase reporter systems, secreted Gluc can be measured directly in the cell supernatant omitting the need for cell lysis and allowing for additional cell-based assays (Tannous, 2009).

First, in order to examine the sensitivity and specificity of the *Gaussia* NF-κB reporter system, Jurkat T cells were transiently transfected with the Gluc reporter plasmid and luciferase activity was determined in response to various NF-κB-triggering stimuli (Fig. 5.1). As shown in Fig. 5.1 B, treatment of Jurkat cells with the potent TCR-mimicking stimulus PMA/ionomycin yielded a massive induction of *Gaussia* reporter activity by more than 120-fold compared to unstimulated cells. In marked contrast, Jurkat T cells that had been transfected with a *Gaussia* plasmid lacking NF-κB-specific promoter sequences virtually displayed no luciferase activity, both in the absence and presence of stimulating conditions. Furthermore, stimulation of Jurkat T cells with agonistic antibodies targeting the TCR or CD3/CD28 surface proteins led to a clear induction of Gluc activity, albeit to a significantly lesser extend compared to PMA/ionomycin-stimulated cells (Fig. 5.1 C). In order to directly proof the specificity of the reporter system towards NF-κB activity, Jurkat T cells were transiently co-transfected with the *Gaussia* reporter plasmid in combination with expression vectors encoding for tagged versions of the NF-κB-activating kinases HPK1 (Arnold et al., 2001; Brenner et al., 2005) or IKKβ (Delhase et al., 1999). 24 h post transfection luciferase activity was measured without additional stimulation. As expected, overexpression of HPK1 or IKKβ alone was already sufficient to stimulate *Gaussia* activity, whereas overexpression of a kinase inactive mutant form of HPK1 (HPK1:K46E) failed to induce any luciferase expression (Fig. 5.1 D).

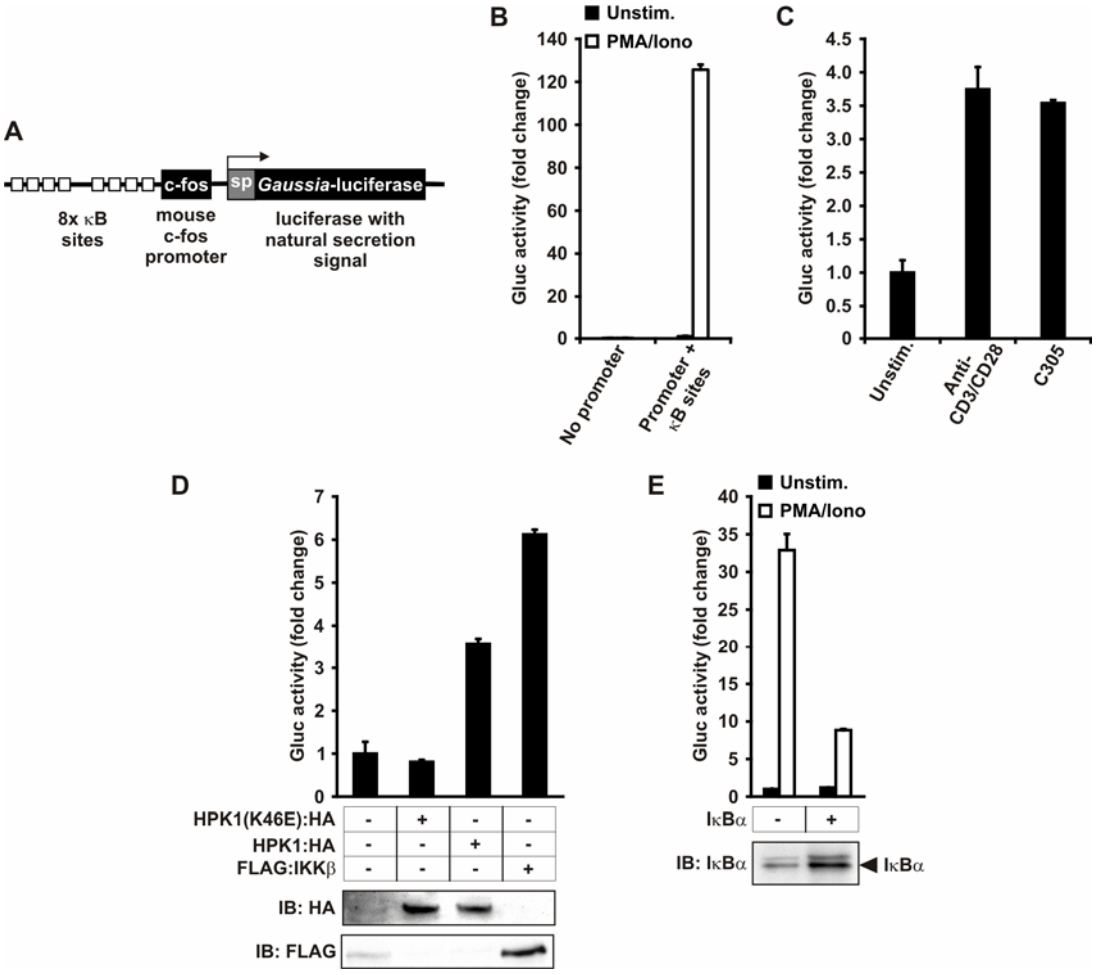

Figure 5.1 | NF-κB-dependent induction of *Gaussia* luciferase (Gluc) reporter activity in transiently transfected Jurkat T cells. (A) Schematic representation of the NF-κB dependent Gluc reporter cassette (sp: secretion peptide). **(B)** Jurkat T cells were transiently transfected with the Gluc reporter plasmid or a control *Gaussia* plasmid lacking NF-κB-targeted promoter sequences. Subsequently, cells were stimulated with PMA/ionomycin (PMA/Iono) and luciferase activity was measured. **(C)** Jurkat cells were transfected as in **(B)** and luciferase activity was determined in response to stimulation using anti-CD3/CD28 antibodies or an idiotype-specific anti-TCRβ chain antibody (C305). **(D)** Jurkat cells were co-transfected with the Gluc NF-κB reporter system and expression vectors encoding for tagged versions of HPK1 or IKKβ or empty vector for control. 24 h post transfection Gluc activity was determined and expression of exogenous proteins was verified by SDS-PAGE and immunoblotting. **(E)** Similar to **(D)** Jurkat cells were either co-transfected with an expression vector encoding for IκBα or with empty vector for negative control. Subsequently, cells were stimulated with PMA/Iono for 8 h followed by measurement of luciferase activity and determination of IκBα protein levels in whole cell lysates by SDS-PAGE and immunoblotting. Mean and SD of luciferase activity are representative of dublicate measurements.

Specific induction of NF-κB-dependent Gluc reporter activity was further demonstrated in a reverse experiment in which co-overexpression of the *bona fide* NF-κB inhibitor IκBα led to a marked decrease in Gluc activity in the supernatant of Jurkat T cells upon stimulation with PMA/ionomycin (Fig. 5.1 E).

In summary, the *Gaussia* reporter system was shown to be applicable for the detection and relative quantification of NF-κB activity in Jurkat T cells stimulated with PMA/ionomycin and TCR/CD3-triggering antibodies, respectively. Moreover, based on transient overexpression experiments, it could be demonstrated that the Gluc reporter system properly responds to both specific activation and inhibition of the NF-κB signaling pathway.

5.1.2 Generation of a NF-κB-dependent reporter Jurkat T cell line

Previous results had established the Gluc reporter system as an appropriate method to specifically quantify NF-κB activity in Jurkat T cells. So far, all luciferase assays were based on transient transfection of Jurkat T cells, thereby limiting the applicability of the Gluc reporter system for large-scale RNAi experiments due to two major technical constraints. (i) The sensitivity of the transiently transfected reporter system towards TCR-induced NF-κB activity turned out to be rather moderate with about 4-fold induction of Gluc activity compared to a more than 120-fold change in luciferase activity upon PMA/ionomycin simulation (Fig. 5.1 B,C). (ii) Fluctuations in cell viability and transfection efficiency are likely to superimpose the NF-κB-dependent Gluc signal associated with a specific loss-of-function phenotype.

In order to circumvent these limitations, a NF-κB reporter T cell line with stable genomic integration of the Gluc reporter cassette was engineered (Fig. 5.2 A). This cell line was derived from the Jurkat variant J16-145 (Gulow et al., 2005) and is hereafter referred to as Gluc-J16. Therefore, stable transfectands were positively selected *via* antibiotic resistance and subcloned twice in order to obtain a genetically homogenous cell population. Several distinct NF-κB-responsive Gluc-J16 reporter subclones were obtained (data not shown) of which one clone was characterized in more detail and utilized for all subsequent experiments. As seen in Fig. 5.2, treatment of reporter cells with anti-CD3/CD28 agonistic antibodies or the PKC-activating phorbolester PMA similarly caused considerable induction of luciferase activity by more than 100-fold (Fig. 5.2 B). Whereas the Ca^{2+} ionophore ionomycin alone was insufficient to stimulate any luciferase response, co-treatment of Gluc-J16 cells with PMA and ionomycin synergistically induced NF-κB activity, which is in accordance with published observations (Dolmetsch et al., 1997). The high sensitivity of Gluc reporter T cells to NF-κB-activating reagents was further demonstrated by anti-TCR antibodies that induced Gluc activity up to 60-fold in a dose-dependent manner (Fig. 5.2 C).

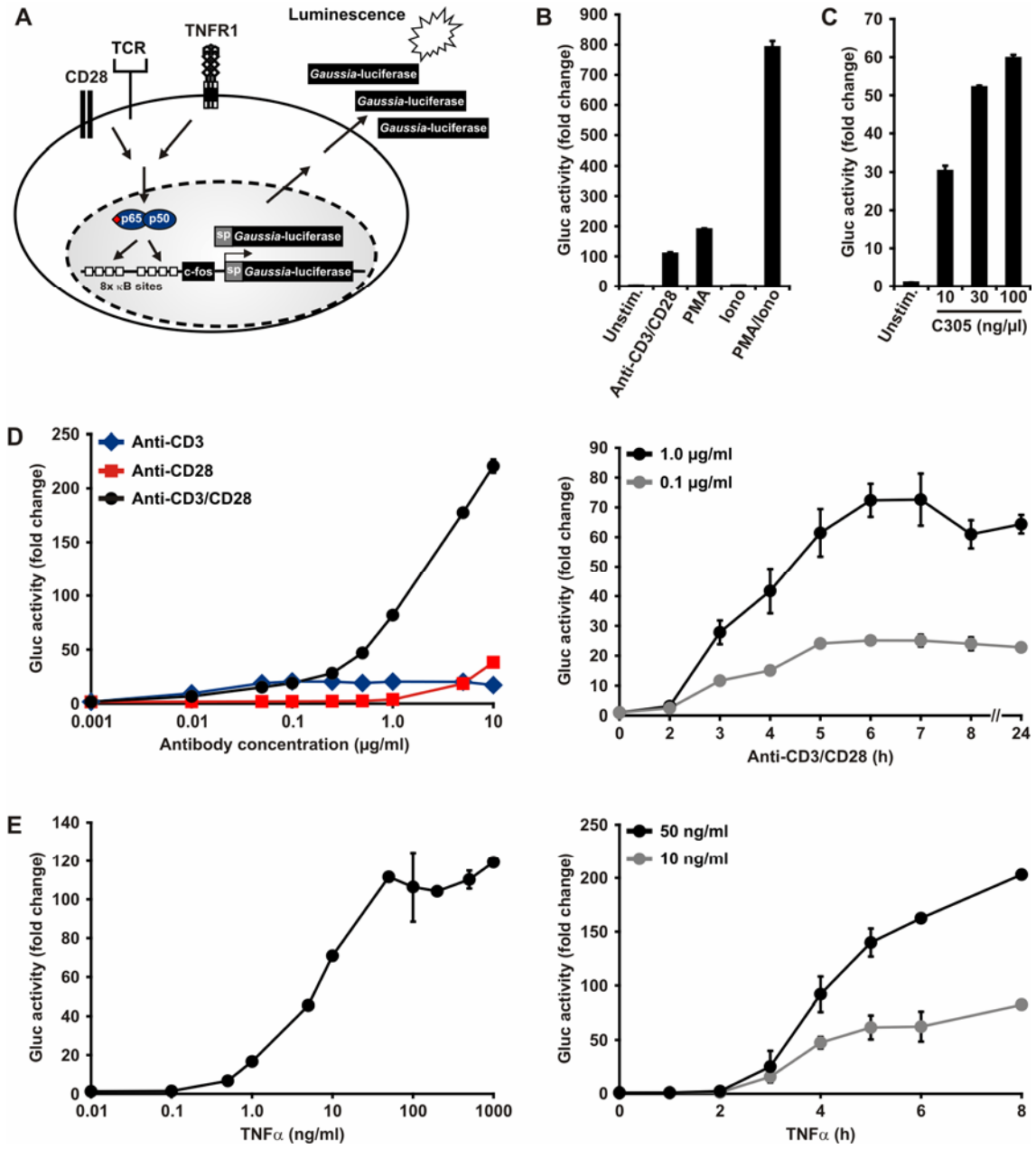

Figure 5.2 | Gluc-J16 NF-κB reporter Jurkat T cells are highly responsive to TCR and TNFR-induced NF-κB activation. (A) Gluc-J16 cells with stable genomic integration of the NF-κB-dependent Gluc reporter cassette were generated allowing for inducible secretion of *Gaussia* luciferase. **(B)** and **(C)** Reporter cells were stimulated with PMA and ionomycin (Iono), alone or in combination, as well as with agonistic anti-CD3/CD28 and C305 antibodies for 5 h. Luciferase was measured and quantified as fold induction relative to unstimulated cells. **(D)** Gluc-J16 cells were treated with increasing concentrations of anti-CD3 and anti-CD28 antibodies, alone or in combination for 5 h (left panel) or were co-stimulated with anti-CD3/CD28 antibodies for the indicated time periods (right panel). Luciferase activity is shown as fold induction. **(E)** Similar to **(D)** Gluc-J16 cells were stimulated with indicated concentrations of TNFα for 5 h (left panel) and for different time periods (right panel). Subsequently, NF-κB-dependent Gluc activity was determined. Mean and SD of luciferase activity are representative of triplicate measurements.

In order to assess the sensitivity and temporal dynamics of the Gluc reporter system towards TCR-induced NF-κB activation, Gluc-J16 reporter cells were stimulated with anti-CD3/CD28 antibodies over a broad range of concentrations and for various time periods (Fig. 5.2 D). Anti-CD3 or anti-CD28 antibodies alone caused only moderate luciferase expression with maximal inductions of about 20 to 40-fold. Gluc activation in response to treatment with anti-CD3 antibodies reached its plateau at already low concentrations, whereas the maximal anti-CD28 response required higher titers of antibody. In marked contrast, combined crosslinking of CD3 and CD28 surface proteins synergized to induce a massive luciferase response by more than 200-fold at highest concentrations (Fig. 5.2 D left panel). These results are consistent with the well-proven concept that integration of TCR and CD28-delivered signals is required for maximal NF-κB activity (Kane et al., 2002) (see 1.3.5). Moreover, luciferase induction in response to CD3/CD28 engagement occurred rapidly with maximal Gluc activity after already 5-6 h post stimulation. Thereafter, the Gluc response reached a plateau and did not significantly change over time (Fig. 5.3 D right panel).

In addition to TCR engagement the responsiveness of Gluc-J16 cells towards TNFR-induced NF-κB activation was investigated. Stimulation of reporter cells with increasing concentrations of TNFα resulted in a sigmoid dose-response curve of Gluc activity (Fig. 5.2 E left panel). Significant luciferase activity was already detected at TNF concentrations as low as 0.5 ng/ml, and reached its maximum of about 120-fold induction at concentrations of about 50 ng/ml. As for CD3/CD28 stimulation, Gluc activity was rapidly induced in a dose-dependent manner with maximal luciferase expression after 5-8 h of TNF stimulation (Fig. 5.2 E right panel).

Collectively, these data show that the reporter T cell line Gluc-J16 reacts to a variety of well-established NF-κB-triggering stimuli. The luciferase response is highly sensitive and synergistic to CD3/CD28 co-crosslinking, and proceeds in a dose-dependent manner with rapid kinetics. Thus, Gluc-J16 cells provide an efficient reporter system to study stimulation-dependent NF-κB activity in T cells *in vitro*.

5.1.3 Gluc-J16 reporter cells allow for efficient gene silencing and adopt robust NF-κB-specific RNAi phenotypes

RNAi screens are based on the systematic generation of loss-of-function phenotypes that can be assigned to specific activities and functions of genes or gene products. The successful implementation of such a strategy requires (i) appropriate tools for efficient

gene silencing and (ii) the availability of a reporter system that precisely responds to signal manipulation by adopting distinct and quantifiable RNAi phenotypes.

As reported for most non-adherent mammalian cells, T cells are difficult to transfect and largely refractory to lipofection-based transfection methods (data not shown). Therefore, a siRNA transfection protocol was optimized that relies on nucleofection of Jurkat T cells (Brenner et al., 2009) (see 5.3.3 and 5.3.4). In a first step, it was aimed to (i) assess knock-down efficacies, and (ii) to test whether siRNA-mediated silencing of *bona fide* regulators of the TCR-induced NF-κB signaling pathway translates into a measurable and robust RNAi phenotype. To this end, reporter cells were transfected with siRNA oligos targeting A20 and CYLD, respectively, (Fig. 5.3 A) as well as with oligos specific for Carma1 and RelA (Fig. 5.3 B). In addition, non-targeting control siRNA was included. Subsequently, cells were stimulated *via* the TCR with indicated concentrations of anti-CD3/CD28 antibodies and Gluc activity was measured.

A20 and CYLD are well-established negative regulators of NF-κB activity, while Carma1 and RelA are known to be indispensable components of the TCR-induced NF-κB signaling apparatus (Fig. 5.3 D, see 1.3 and 1.4). Indeed, knock-down of both A20 by two independent siRNA oligos as well as CYLD similarly resulted in a hyperactivated luciferase phenotype with an increase in Gluc activity by almost 2-fold compared to control-transfected cells (Fig. 5.3 A left panel). *Vice versa*, RNAi-mediated decrease in Carma1 or RelA protein expression dramatically impaired TCR-dependent luciferase activity, irrespective of the strength of the applied stimulus (Fig. 5.3 B left panel). Specific knock-down of A20 and CYLD mRNA levels was verified by qPCR (Fig. 5.3 A right panel), and efficient silencing of Carma1 and RelA was confirmed by immunoblotting of endogenous proteins (Fig. 5.3 B right panel). For Carma1 three independent siRNAs were transfected with different knock-down efficacies. Of note, there was a tight positive correlation between Carma1 protein levels and Gluc activity, proving a specific and graded phenotypic response of the reporter system.

Moreover, specific inhibition of NF-κB activity in Gluc-J16 cells was demonstrated by administration of two chemical inhibitors, the NEMO binding peptide (NBP) (May et al., 2000) (see also 1.3.1) and a synthetic NF-κB activation inhibitor (Kiessling et al., 2009). As expected, pre-treatment of Gluc reporter cells with either inhibitor caused significant reduction of Gluc expression upon stimulation with anti-CD3/CD28 antibodies and PMA/ionomycin, respectively (Fig. 5.3 C).

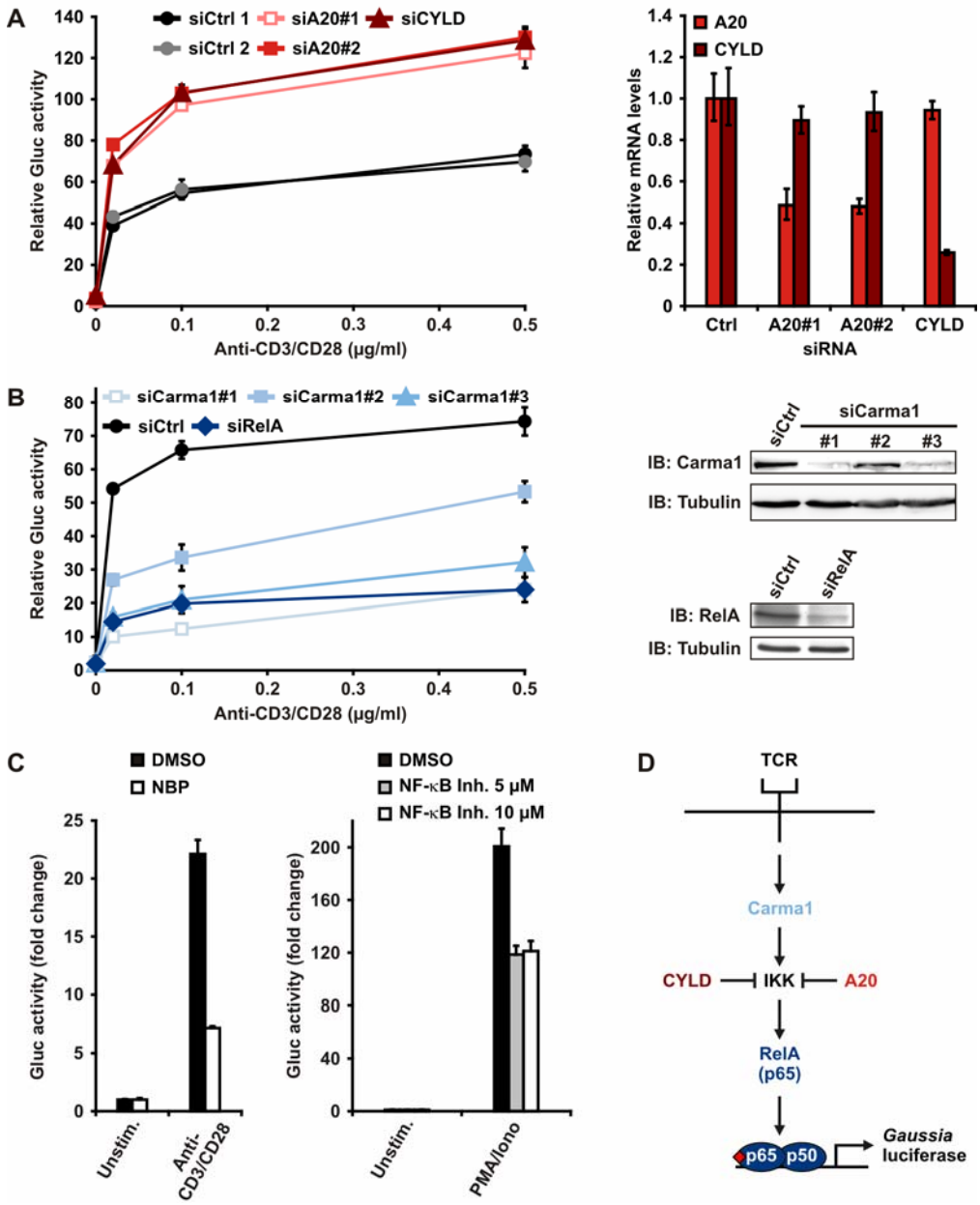

Figure 5.3 | Manipulation of the TCR-induced NF-κB pathway in Gluc-J16 reporter T cells by RNAi or chemical inhibitors translates into a robust phenotypic response. (A) and **(B)** Gluc-J16 cells were transfected with non-targeting control siRNA (siCtrl) or with siRNA specific for A20 (siA20#1 and #2), CYLD, Carma1 (siCarma1#1-3), and RelA, respectively. 72 h post transfection cells were stimulated with indicated concentrations of anti-CD3/CD28 antibodies for 5 h and Gluc activity was assayed. In parallel, cell viability was measured for normalization of the luciferase signal. Right panels: for knock-down control relative mRNA levels of A20 and CYLD were determined by qPCR. Carma1 and RelA protein expression was assessed by SDS-PAGE and immunoblotting of endogenous proteins using primary antibodies as indicated. Reprobing with anti-Tubulin antibodies verified equal loading. **(C)** Gluc-J16 cells were pre-treated with 40 µM NEMO binding peptide (NBD) (left panel) or with indicated concentrations of an NF-κB activation inhibitor (NF-κB Inh.) (right panel) for 1 h followed by stimulation with anti-CD3/CD28 antibodies or PMA/ionomycin for 5 h. Luciferase activity was measured as fold induction relative to untreated cells. Mean and SD of Gluc assays are representative of triplicate measurements. **(D)** Schematic illustration of functional interactions between established NF-κB pathway components in T cells.

Collectively, these data demonstrate (i) efficient siRNA-mediated gene silencing, and (ii) a highly sensitive and specific phenotypic response of the Gluc reporter system with respect to functional manipulation of TCR-induced NF-κB activity.

5.1.4 Optimization of RNAi screening conditions in a multi-well format

Next, in preparation for large scale RNAi screening, both the siRNA transfection protocol and conditions for stimulation and measurement of reporter activity were optimized in a multi-well format.

For high throughput transfection of siRNA a 96-well shuttle nucleofection system was used (see Material and Methods). Again, reporter cells were transfected with siRNAs targeting CYLD, Carma1 or RelA. In addition, siRNA specific for TNFR1 was included. For negative control, cells were either transfected with non-targeting siRNA or were mock-transfected (H_2O). 72 h post transfection cells were stimulated with anti-CD3/CD28 antibodies and TNFα, respectively, or were left untreated. Subsequently, luciferase was measured and normalized to cell numbers. To define optimal conditions for reporter activity, Gluc-J16 reporter cells were transfected with various amounts of siRNA and subjected to different concentrations of NF-κB-triggering stimuli (data not shown).

As depicted in Fig. 5.4, transfection of Carma1 and TNFR1 siRNA did not affect basal luciferase activity compared to control-transfected cells. By contrast, RelA-silenced cells exhibited reduced NF-κB activity, whereas knock-down of the negative regulator CYLD triggered substantial NF-κB activation even in the absence of stimulation (Fig. 5.4 A). Stimulation of control-transfected reporter cells with anti-CD3/CD28 antibodies led to an induction of NF-κB activity by about 10-fold (Fig. 5.4 B). As expected and in line with preceding experiments, knock-down of Carma1 significantly attenuated the TCR-induced luciferase signal, and RelA silencing completely abolished Gluc expression. Conversely, CYLD knock-down led to a marked increase in TCR-dependent luciferase activity. Of note, silencing of TNFR1 did not affect the TCR-induced reporter signal, but almost completely prevented TNF-mediated Gluc upregulation. Analogously, the effect of Carma1 knock-down was specific for TCR stimulation, while silencing of RelA or CYLD caused similar RNAi phenotypes regarding TCR and TNFR1 stimulation (Fig. 5.4 B,C). These results are consistent with general functions of RelA and CYLD as positive and negative regulators of NF-κB signaling, respectively. By contrast, Carma1 and TNFR1 operate in a pathway-specific manner (Fig. 5.4 D).

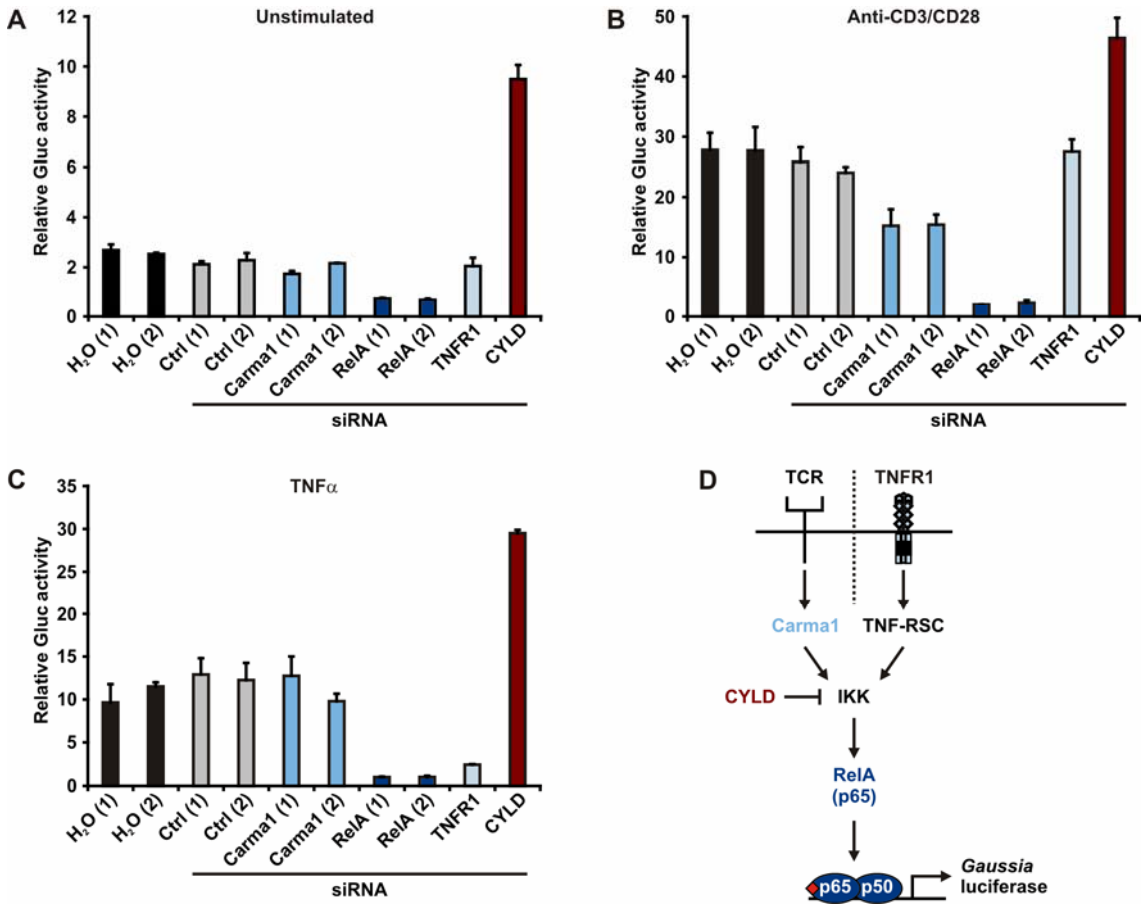

Figure 5.4 | The Gluc-J16 reporter system allows for RNAi-based manipulation of TCR and TNFR-induced NF-κB signaling under large-scale screening conditions. Gluc-J16 reporter T cells were transiently transfected with indicated siRNAs or were mock-transfected in a 96-well format. 72 h post nucleofection cells were either left untreated **(A)** or were stimulated with anti-CD3/CD28 antibodies (0.1 µg/ml) **(B)** and 20 ng/ml TNFα **(C)**, respectively. Subsequently, Gluc activity in the supernatant was measured and normalized to cell viability. If indicated, transfections were performed in two independent replicates (1) and (2). Mean and SD of single Gluc assays are representative of dublicate measurements. **(D)** Synoptic illustration of known regulators of TCR and TNFR1-induced NF-κB signaling triggering Gluc secretion in Gluc-J16 cells (TNF-RSC: TNFR signaling complex).

Importantly, RNAi phenotypes turned out to be highly reliable since deviations of normalized Gluc activity between single replicates of siRNA transfection and stimulation were marginal.

In conclusion, a cell-based NF-κB luciferase reporter system has been established and validated that is well applicable for large-scale RNAi screening strategies in order to identify genetic modifiers of NF-κB activity in T lymphocytes.

5.1.5 Systematic large-scale RNAi screen identifies phosphatases that regulate TCR-induced NF-κB activity

In order to identify phosphatase genes that play a role in the regulation of TCR-induced NF-κB activity a large-scale RNAi screen was performed. To this end, Gluc-J16 reporter cells were transfected with a subgenomic, commercially available siRNA library targeting 298 known or putative phosphatase genes encoding for regulatory or catalytic phosphatase subunits. The library contained three single, independent siRNA oligos per gene yielding a total of 894 phosphatase-specific siRNAs. Each individual siRNA was arrayed in a 96-well plate format and transfected in dublicate (see also 4.3.3 and 4.3.4). For each transfection plate several positive and negative control siRNAs encompassing siRNA oligos specific for CYLD, RelA, Carma1, and TNFR1 as well as non-targeting siRNA and mock transfections (H_2O) were included. Subsequent to the transfection procedure, cells were incubated for about 72 h and then subjected to different stimulation conditions. For this purpose, cells from each well were separated into equivalent fractions and were either left untreated or stimulated with anti-CD3/CD28 antibodies. In addition, cells were stimulated with TNFα. This dual stimulation protocol allowed for the simultaneous and synoptical analysis of phosphatase genes involved in the regulation of TCR- and/or TNFR1-induced NF-κB signaling. The results of the TNFR1-specific phosphatase screen are published elsewhere (Frey, 2009). For all stimulation assays cell viability was measured for normalization of the luciferase signal (see below).

The primary RNAi screen yielded two numerical data sets either indicative of TCR-induced luciferase activity (channel 2) or cell viability (channel 1). Statistical analysis for tentative hit selection was conducted using the *cellHTS2* software package (Boutros et al., 2006; Pelz et al., 2010) (for details see 4.5). In order to compensate for systematic inter- and intraplate variations, the raw data from each channel was normalized using the iterative *B* score normalization algorithm (Birmingham et al., 2009; Brideau et al., 2003; Malo et al., 2006; Ramadan et al., 2007). In addition to statistical normalization, the ratio of processed raw data from channel 2 and 1 was calculated for each individual well to obtain values for NF-κB-specific Gluc activity normalized to cell viability. Subsequently, mean Gluc activity of two biological replicates was determined. Mean values, in turn, were transformed into the statistical *z* score for hit selection and post-screen analysis.

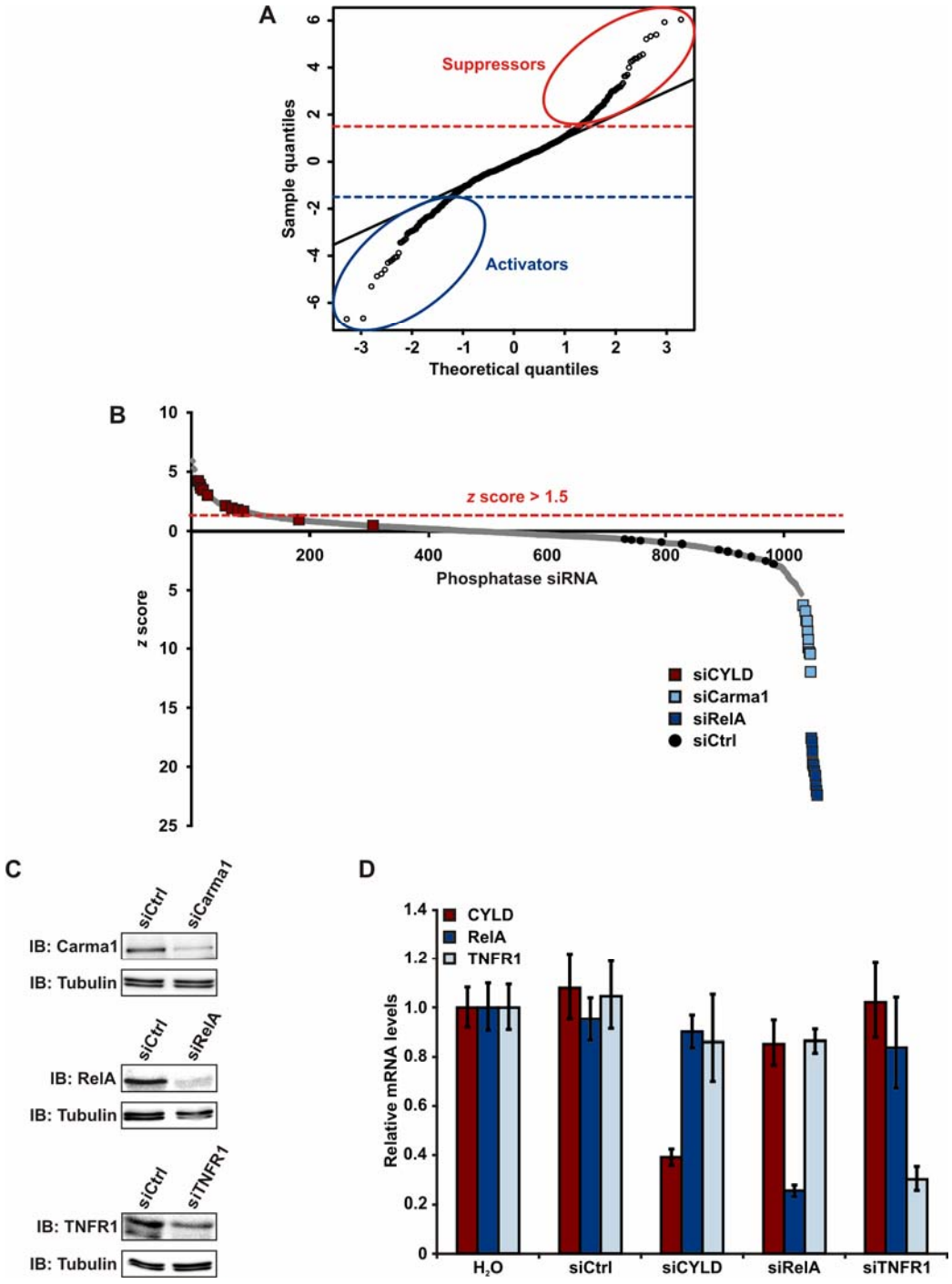

Figure 5.5 | Summary of results of primary RNAi screen for phosphatases regulating TCR-induced NF-κB signaling. (A) Quantile quantile (QQ) plot analysis of *z* scores from primary RNAi screen. *z* scores higher +1.5 or lower -1.5 were non-normally distributed indicating RNAi phenotypes of enhanced (suppressors, red ellipse) or attenuated (activators, blue ellipse) NF-κB activity upon TCR stimulation. **(B)** Graph of *z* score distribution for individual phosphatase-specific siRNAs and control siRNAs. **(C)** In parallel to the RNAi screen, transfection and knock-down efficacy of control siRNA oligos targeting Carma1, RelA, or TNFR1 were determined by SDS-PAGE and immunoblotting of endogenous proteins using primary antibodies as indicated. Reprobing with anti-Tubulin antibodies verified equal loading. **(D)** Alternatively or in addition, gene silencing of CYLD, RelA or TNFR1 was assessed by quantification of mRNA levels by qPCR.

The *z* score provides a statistical mean to quantify the relative strength of an RNAi phenotype (Birmingham et al., 2009; Malo et al., 2006; Ramadan et al., 2007). It indicates how many standard deviations an individual sample of interest deviates from the population mean and thereby allows for comparison of data from different normal distributions. Negative and positive *z* values are indicative of reduced and enhanced reporter activity, respectively. The identification of screening-positive RNAi phenotypes was based on a quantile-quantile (QQ) plot statistical analysis (Falschlehner et al., 2010; Ramadan et al., 2007). Using this method, one can determine thresholds for hit selection based on the discrimination of numerical values that are statistically normally or non-normally distributed. *z* scores that are non-normally distributed convey RNAi phenotypes that might be associated with a real biological effect of signal perturbation.

According to the QQ plot analysis depicted in Fig. 5.5 A RNAi phenotypes with *z* scores higher +1.5 or lower -1.5 were considered statistically significant, whereas intermediate values followed a statistically normal distribution (solid line). To minimize the rate of false positives, only those phosphatase genes were qualified as potential hits that scored with at least two independent siRNA oligos beyond pre-defined *z* score thresholds. Based on these criteria six phosphatase genes were identified as negative regulators of TCR-induced NF-κB activity (suppressors), whereas six phosphatases were assigned to positively regulate NF-κB activity (activators) (data not shown and Table 5.1). Fig. 5.5 B shows the complete distribution of mean *z* values for individual siRNAs. Importantly, almost all positive control siRNAs, *i.e.* siRNA specific for CYLD, Carma1, or RelA, scored reproducibly demonstrating both the validity and sensitivity of primary RNAi screen and statistical analysis. Nonetheless, a number of phosphatases that had been previously implicated in regulation of TCR and NF-κB signaling, such as PP2Ac, PTPN6, and PTPN22, were not identified as regulators of NF-κB activity. Similarly, siRNAs specific for PTEN did not yield any significant RNAi phenotype, which is consistent with the fact that Jurkat T cells lack endogenous PTEN expression (Abraham and Weiss, 2004) (Table 5.1). Moreover, a fraction of control-transfected reporter cells was used to determine transfection and knock-down efficacies of CYLD, Carma1, RelA, and TNFR1-specific siRNA oligos on mRNA and protein levels under real-time HTS conditions. As demonstrated in Fig. 5.5 C and D, gene silencing was again proven to be highly efficient which is consistent with strong RNAi phenotypes observed for all positive controls (Fig. 5.5 B and Frey, 2009).

Gene ID	Gene Symbol	Name/Description	Mean *z* scores	Specificity/ Function
Negative regulators (suppressors)				
9989	PPP4R1	Protein phosphatase 4, regulatory subunit 1	3,6; 2,1; -0,5	Regulatory
5786	PTPRA	Protein tyrosine phosphatase, receptor type, A	2,56; 2,32; 0,91	Tyr
Positive regulators (activators)				
5780	PTPN9	Protein tyrosine phosphatase, non-receptor type 9	-4,07; -4,77; -6,69	Tyr
5798	PTPRN	Protein tyrosine phosphatase, receptor type, N	-1,46; -1,6; *(3,34)*	Tyr
Reference phosphatases				
5515	PPP2CA	Protein phosphatase 2, catalytic subunit (PP2Ac), alpha isozyme	1,69; 0,82; 0,65	Ser/Thr
5777	PTPN6	Protein tyrosine phosphatase, non-receptor type 6 (SHP1)	-0,2; -0,35; -1,83	Tyr
26191	PTPN22	Protein tyrosine phosphatase, non-receptor type 22 (lymphoid)	-0,26; 1,33; 1,49	Tyr
5728	PTEN	Phosphatase and tensin homolog	-0,25; -0,29; -0,38	Inositol/Tyr

Table 5.1 | Candidate phosphatase genes associated with TCR-induced NF-κB activity. Data represent mean *z* scores of biological dublicates for each three individual siRNAs per phosphatase gene. Only those phosphatases were considered potential hits and selected for secondary analyses for which two independent siRNAs scored at least twice above (suppressors) and below (activators) *z* scores of +1.5 and -1.5, respectively. Parenthesized *z* scores indicate outliers with inverse phenotypes. A number of reference phosphatases are listed that had been previously identified as regulators of TCR and NF-κB signaling (PP2Ac, PTPN6, PTPN22), but that were not confirmed in the primary screen. In addition, *z* scores for the negative control phosphatase PTEN are depicted that is not expressed in Jurkat T cells. Ser/Thr indicates serine/threonine phosphatase; Tyr, tyrosine phosphatase; Inositol, inositol phosphatase; Regulatory; regulatory (non-catalytic) phosphatase subunit.

5.2 Genetic and biochemical characterization of PP4R1 as a negative regulator of NF-κB activation in T lymphocytes

Primary RNAi screening revealed several phosphatases as being potentially involved in negative regulation of TCR-induced NF-κB activity (suppressors; Table 5.1). Among these tentative candidates PP4R1 (protein phosphatase 4, regulatory subunit 1), a regulatory subunit of the protein ser/thr phosphatase 4 holoenzyme, was identified as a potent negative regulator of TCR-induced NF-κB activity. Validation and the detailed functional and biochemical characterization of PP4R1 as a negative regulator of NF-κB in T lymphocytes were subject of the following analyses.

5.2.1 Validation of PP4R1-associated RNAi phenotype by secondary NF-κB activity assays

In a first step, it was aimed to confirm the primary PP4R1-associated RNAi phenotype in order to exclude non-specific phenotypic effects potentially owing to the luciferase-based screening system, the large-scale screening procedure or to off-target effects of siRNA oligos directed against PP4R1. For this purpose, Jurkat T cells were transfected with a broad panel of PP4R1-targeting siRNAs, including three sequences that had been already used for primary library screening (siPP4R1#1-#3) and four additional independent siRNAs (siPP4R1#4-#7). Subsequently, cells were stimulated *via* the TCR or with PMA/ionomycin and upregulation of different NF-κB target genes as well as stimulation-dependent secretion of NF-κB-regulated cytokines were examined. To correlate the strength of individual RNAi phenotypes with knock-down efficacies, gene silencing of PP4R1 was monitored on mRNA level by qPCR.

As seen in Fig. 5.6 A, individual PP4R1-specific siRNAs differed drastically in mediating efficient gene silencing. Two independent sequences (siPPP4R#2 and #7) yielded best knock-down efficacies of about 60% mRNA reduction compared to control-transfected cells (Fig. 5.6 A left panel). Overall, there was a tight inverse correlation between knock-down efficacies and phenotypic outcome as assessed by TCR-induced upregulation of mRNA levels of *bona fide* NF-κB target genes (Fig. 5.6 B). Of note, knock-down efficacies of PP4R1 screening oligos (siPP4R1#1-#3) correlated well with *z* scores obtained for the primary screen (Table 5.1). Specific induction of NF-κB target genes was controlled by knock-down of RelA (Fig. 5.6 A right panel and data not shown). Interestingly, residual PP4R1 mRNA levels of more than 60% were equally insufficient to induce any phenotypic response irrespective of individual siRNAs.

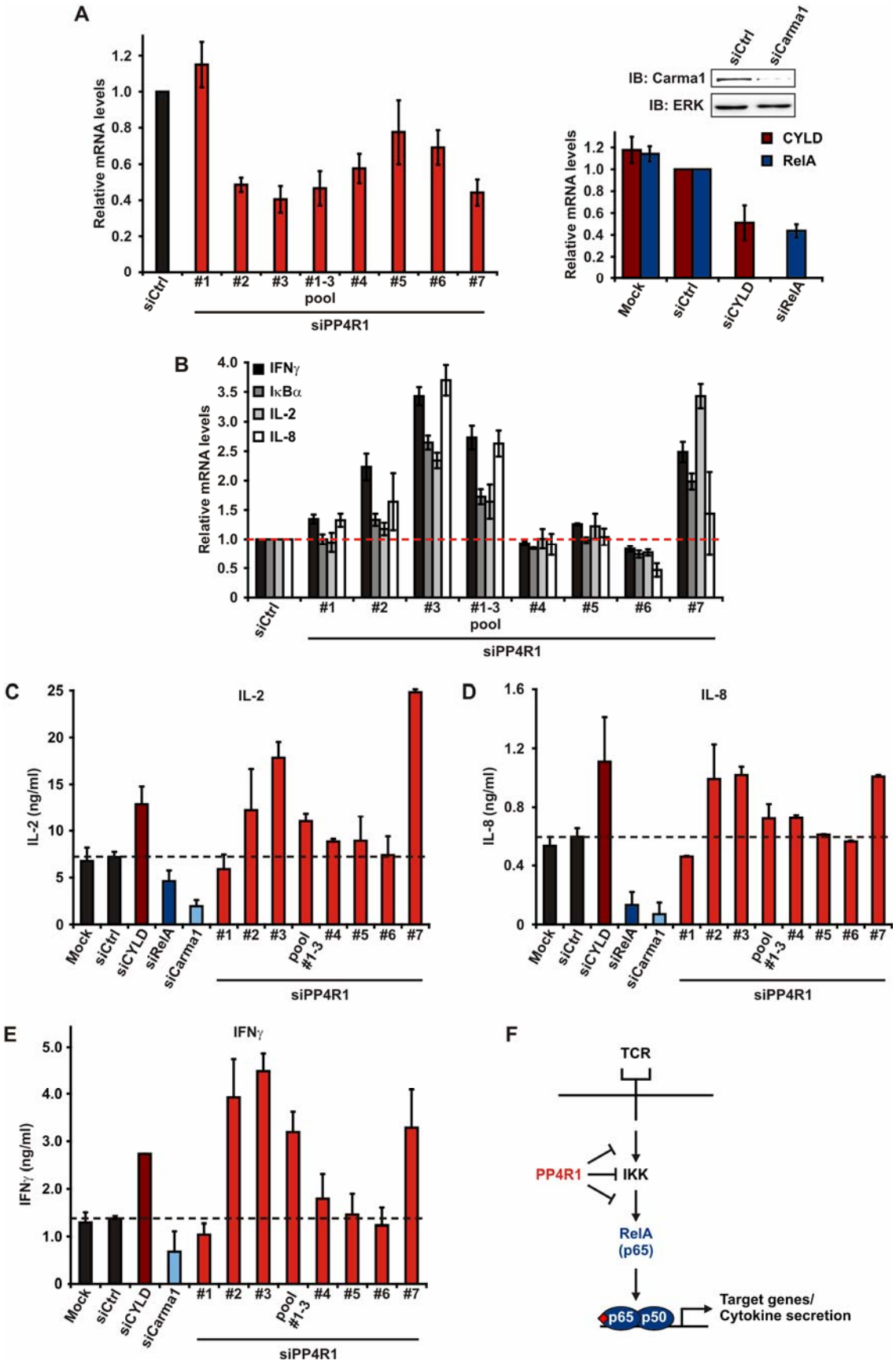
A
Relative mRNA levels
siCtrl
#1
#2
#3
#1-3 pool
#4
#5
#6
#7
siPP4R1
siCtrl
siCarma1
IB: Carma1
IB: ERK
CYLD
RelA
Relative mRNA levels
Mock
siCtrl
siCYLD
siRelA
B
IFNγ
IκBα
IL-2
IL-8
Relative mRNA levels
siPP4R1
C
IL-2
IL-2 (ng/ml)
Mock
siCtrl
siCYLD
siRelA
siCarma1
pool #1-3
siPP4R1
D
IL-8
IL-8 (ng/ml)
E
IFNγ
IFNγ (ng/ml)
F
TCR
PP4R1
IKK
RelA (p65)
p65
p50
Target genes/ Cytokine secretion

Figure 5.6 | Validation of PP4R1 as a negative regulator of TCR-induced NF-κB activity. Jurkat T cells were transfected with 7 independent siRNAs targeting PP4R1 (siPP4R1#1-#7) of which oligos siPP4R1#1-#3 were already included in the siRNA screening library. In addition, these oligos were transfected as equimolar pool. Moreover, mock transfections (H_2O) as well as transfections of non-targeting siRNA (negative control) or siRNA specific for RelA, Carma1, and CYLD, respectively, (positive controls) were included. **(A)** Knock-down of PP4R1 and control genes was assessed by qPCR (left: PP4R1 knock-down; right: knock-down of positive controls). Knock-down of Carma1 was monitored by immunoblotting of endogenous protein. Reprobing with anti-ERK antibodies verified equal loading. **(B)** Cells were stimulated *via* the TCR with agonistic anti-CD3/CD28 antibodies for 1 h or were left untreated. Subsequently, relative mRNA levels of NF-κB target genes were analyzed by qPCR. mRNA expression is shown as fold induction compared to stimulated control-transfected cells. Induction of cytokine transcription was controlled using unstimulated control cells (data not shown). **(C)**-**(E)** A fraction of transfected cells was stimulated with PMA/ionomycin for 8 h and concentrations of IL-2, IL-8, and IFNγ, respectively, in the supernatants were determined by ELISA. In addition, cell numbers and viability were determined for normalization of cytokine secretion. Dashed lines indicate mRNA and cytokine levels of control-transfected cells. **(F)** Schematic representation of PP4R1 and its potential role in the TCR-induced NF-κB pathway.

Next, it was tested whether upregulated mRNA levels of IL-2, IL-8, and interferon γ (IFNγ) were reflected by enhanced cytokine secretion on the protein level. Therefore, a fraction of siRNA-transfected Jurkat T cells was subjected to PMA/ionomycin stimulation and cytokine levels were determined. Indeed, knock-down of PP4R1 led to a marked increase in stimulation-dependent secretion of all tested cytokines (Fig. 5.6 C-E). Again, enhanced cytokine secretion closely correlated with knock-down efficacies of single siPP4R1 oligos. Compared to control-transfected cells, protein secretion of IL-2, IL-8, and IFNγ was increased up to 3-fold, depending on knock-down efficacy and the type of cytokine, and even exceeded levels of CYLD-silenced cells for positive control. In contrast, siRNA oligos that yielded reduction of PP4R1 mRNA levels to less than 40% did not mediate any significant phenotypic changes. As expected, RelA or Carma1 knock-down drastically impaired cytokine secretion upon stimulation.

In summary, these results confirm primary screening data and substantiate a role of PP4R1 as a negative regulator of TCR-induced NF-κB activation (Fig. 5.6 F). Efficient knock-down of PP4R1 both by screening and independent siRNA oligos resulted in enhanced stimulation-dependent upregulation of NF-κB target genes and cytokine secretion. Thereby, phenotypic outcome and PP4R1 mRNA levels demonstrated a tight inverse correlation.

5.2.2 Knock-down of PP4R1 protein results in enhanced NF-κB reporter activity upon TCR, PMA, and TNFR1 stimulation

Previous experiments demonstrated a tight inverse correlation between PP4R1 mRNA levels and enhanced NF-κB signaling activity in Jurkat T cells. Next, it was examined whether the PP4R1-specific RNAi phenotype similarly correlated with reduced PP4R1 expression on the protein level. Therefore, Gluc-J16 reporter cells were transfected with control siRNA as well as with four independent siPP4R1 oligos that had been shown before to be most potent in gene silencing (siPP4R1#2, #3, #4, and #7). Subsequently, cells were stimulated *via* the TCR and NF-κB-dependent luciferase activity was determined. In addition, cells were lysed and knock-down of PP4R1 was assessed by SDS-PAGE and immunoblotting of endogenous proteins. Consistent with preceding experiments, knock-down efficacies of individual PP4R1 siRNAs differed considerably (Fig. 5.7 A). As seen for mRNA levels, two independent siPP4R1 oligos (siPP4R1#3 and #7) were shown to be most efficient in gene silencing and similarly blocked PP4R1 protein expression by about 80% (Fig. 5.7 right panel). Moreover, there was again a remarkable inverse correlation between PP4R1 protein quantities and TCR-dependent Gluc expression with a maximal increase in NF-κB reporter activity by almost 2-fold.

In extension of the previous experiment it was tested next whether the effect of PP4R1 silencing on NF-κB activity was dependent on the strength of the TCR stimulus. To this end, reporter cells were transfected with control siRNA or siRNA specific for PP4R1, CYLD, and RelA, respectively, followed by TCR stimulation using a broad range of concentrations of anti-CD3/CD28 agonistic antibodies. Again, efficient knock-down of PP4R1 was confirmed both by immunoblotting (Fig. 5.7 B upper panel) and qPCR (Fig. 5.7 B lower panel). Moreover, knock-down of CYLD and RelA was verified by qPCR (Fig. 5.7 B lower panel). Consistent with previous results, PP4R1-silenced cells displayed highly increased NF-κB reporter activity irrespective of the strength of TCR stimulation (Fig. 5.7 C). The increase in NF-κB activity by about 2-fold was similar to that of CYLD-transfected cells, whereas, as expected, RelA knock-down almost completely blunted Gluc expression. Interestingly, lack of PP4R1 expression in Jurkat T cells did not affect basal NF-κB, but also enhanced NF-κB activation in response to treatment with PMA, a strong PKC-activating compound, and TNFR1 stimulation by recombinant TNFα (Fig. 5.7 D). As for TCR stimulation, the effect of NF-κB hyperactivation upon PMA or TNFα treatment was well-pronounced and similar to that of CYLD-silenced cells.

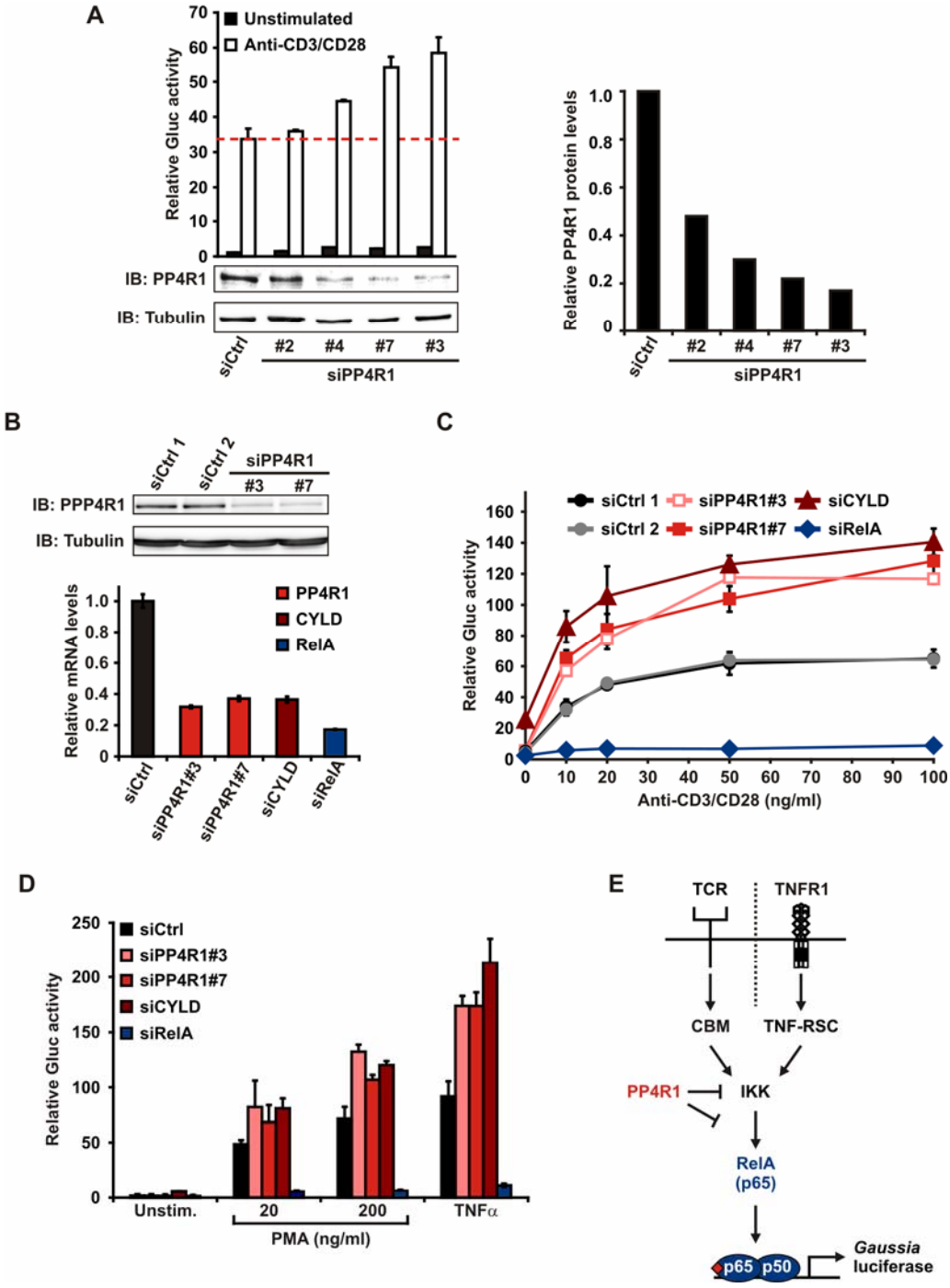

Figure 5.7 | PP4R1 negatively regulates NF-κB activation triggered by TCR, PMA, or TNFR1 stimulation of Jurkat T cells. (A) Gluc-J16 reporter cells were transfected with four independent siRNA oligos specific for PP4R1 (siPP4R1) or non-targeting control siRNA. Subsequently, cells were stimulated with anti-CD3/CD28 antibodies for 5 h or were left untreated. Normalized NF-κB-dependent luciferase activity was determined as described before. PP4R1 knock-down was assessed by SDS-PAGE of endogenous proteins and immunoblotting using primary antibodies as indicated (left panel). Reprobing with anti-Tubulin antibodies verified equal loading. In addition, normalized PP4R1 expression relative to control-transfected cells was quantified (right panel). **(B-D)** Cells were transfected as in **(A)**, including siRNAs for PP4R1, CYLD, or RelA. For negative control cells were transfected with non-targeting siRNA in two independent replicates (siCtrl1+2).

For knock-down control, relative mRNA levels of PP4R1, CYLD, and RelA were determined by qPCR. Gene expression is shown as percent of negative control (B, lower panel). Carma1 expression was assessed by SDS-PAGE and immunoblotting of endogenous proteins using primary antibodies as indicated (B, upper panel). **(C)** Cells were stimulated *via* the TCR with indicated concentrations of anti-CD3/CD28 antibodies for 5 h or were left untreated **(D)**. In addition, cells were treated with indicated concentrations of PMA or were stimulated with 20 ng/ml TNFα for 5 h. Normalized luciferase activity was determined as described before. **(E)** Schematic illustration of TCR and TNFR1-induced NF-κB signaling and its negative regulation by PP4R1.

In summary, these data demonstrate proper expression and efficient siRNA-mediated knock-down of endogenous PP4R1 protein in Jurkat T cells and further confirm a role of PP4R1 as negative regulator of TCR-induced NF-κB activation. Importantly, PP4R1 function was not selectively assigned to TCR-induced signaling, but was also shown to be involved in negative regulation of NF-κB downstream of PKC and TNFR1 activation (Fig. 5.7 E). However, basal activity of NF-κB did not significantly change in transiently silenced cells. Hence, PP4R1 seems to be a shared signaling modulator in activation-induced canonical NF-κB signaling.

5.2.3 Transient and stable knock-down of PP4R1 results in increased TCR-induced upregulation of NF-κB target genes and cytokine secretion

Preceding experiments have shown enhanced upregulation of NF-κB target genes upon TCR stimulation as a result of PP4R1 deficiency in Jurkat T cells. However, so far cells were only stimulated for one hour which does not cover the whole temporal dynamics of TCR-induced gene regulation. Therefore, it was aimed to gain a more extended and detailed picture of the kinetics of TCR-induced NF-κB dependent gene expression in PP4R1-silenced *vs.* non-silenced T cells.

To this end, Jurkat T cells were again transiently transfected with two independent siRNAs targeting PP4R1 or control siRNA. Subsequently, cells were stimulated *via* the TCR for various time periods and mRNA levels of a panel of *bona fide* NF-κB target genes, such as IL-2, IL-8, A20, and IκBα, were determined by qPCR. As shown in Fig. 5.8 A, maximal mRNA induction of all tested genes was detected after about 1.5 - 2 h of TCR stimulation. However, in PP4R1-silenced cells mRNA upregulation was dramatically increased with 2-3-fold higher levels for the cytokines IL-2 and IL-8 (upper panels). Enhanced mRNA upregulation was also seen for A20 and IκBα (lower panels). The increase in mRNA levels both applied to the kinetics of upregulation and the maximal magnitude of gene expression. Of note, this effect was transient since increased mRNA expression was not significantly prolonged in PP4R1-silenced cells, but rapidly declined to basal levels at later

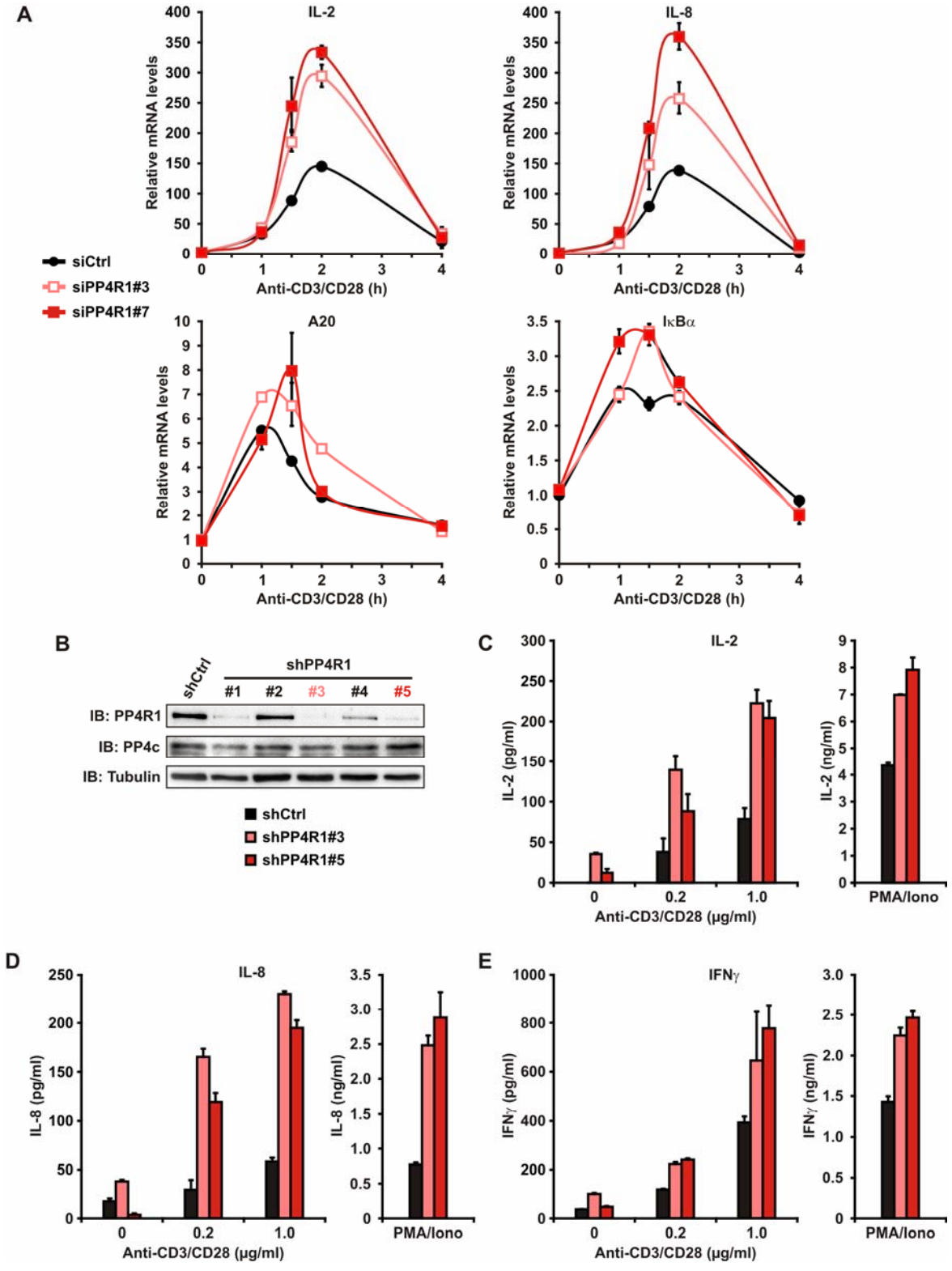

Figure 5.8 | Transient and stable PP4R1 silencing in Jurkat T cells causes enhanced stimulation-dependent upregulation of NF-κB target genes and cytokine secretion. (A) Jurkat T cells were transiently transfected with siRNAs specific for PP4R1 or non-targeting siRNA. 72 h post transfection cells were stimulated *via* the TCR for different time periods as indicated. Subsequently, mRNA levels of NF-κB target genes, such as IL-2 and IL-8 (upper panel) as well as

A20 and IκBα (lower panel) were assessed by qPCR. **(B)** Jurkat T cells were retrovirally transduced with five independent shRNAs targeting PP4R1 or non-targeting control shRNA. Stably transduced cells were selected *via* antibiotic resistance and levels of endogenous PP4R1 and PP4c proteins were determined by SDS-PAGE of whole cell lysates and immunoblotting using primary antibodies as indicated. Reprobing with anti-Tubulin antibodies verified equal loading. **(C-E)** shRNA-expressing Jurkat T cells were stimulated with indicated concentrations of anti-CD3/CD28 antibodies overnight or were treated with PMA/ionomycin for 8 h. Subsequently, levels of secreted IL-2, IL-8, and IFNγ were measured by ELISA. In addition, cell numbers and viability were determined for normalization.

time points. Moreover, no significant changes in basal transcription of NF-κB target genes were observed.

As yet, all functional analyses were based on transient siRNA-mediated knock-down of PP4R1 in Jurkat T cells. To achieve more efficient and sustained PP4R1 gene silencing and to further confirm the PP4R1 RNAi phenotype by an independent knock-down approach, Jurkat T cells were lentivirally transduced with vectors encoding for small hairpin RNA (shRNA) against PP4R1. Five independent shPP4R1-transduced Jurkat clones were obtained of which two displayed most efficient knock-down of endogenous protein and were selected for further analyses (Fig. 5.8 B). To corroborate and complement previous data, stably PP4R1-silenced cells were stimulated *via* the TCR with indicated concentrations of agonistic antibodies or were left unstimulated. In addition, a fraction of cells was again subjected to stimulation with PMA/ionomcyin. Subsequently, levels of secreted cytokines IL-2, IL-8, and IFNγ were measured by ELISA. Consistent with previous findings, stable knock-down of PP4R1 led to a substantial increase in cytokine secretion, both in response to TCR stimulation and treatment with PMA/ionomcyin (Fig. 5.8 C-E). With respect to TCR-stimulated cells, levels of secreted IL-2 and IL-8 were almost 3-4-fold increased compared to controls, and secretion of IFNγ was twice as high. In accordance with augmented cytokine secretion, PP4R1-silenced Jurkat T cells displayed enhanced TCR-dependent induction of a variety of NF-κB target genes encoding for IL-8, TNFα, the T cell activation marker CD69, or the anti-apoptotic Bcl2-family member Bcl2A1 (data not shown).

In summary, these data demonstrate that NF-κB hyperactivation in T cells lacking PP4R1 expression is reflected by enhanced transcriptional upregulation and secretion of NF-κB-responsive genes and cytokines, respectively. In contrast to transient siRNA-mediated gene silencing, sustained deficiency for PP4R1 by shRNA transduction was shown to result in enhanced basal cytokine secretion. These findings provide evidence for a critical physiological role of PP4R1 as a negative regulator of T cell activation *in vitro*.

5.2.4 Overexpression of PP4R1 selectively attenuates TCR-induced NF-κB, but not AP-1 activation

The functional importance of PP4R1 in negative regulation of NF-κB signaling and T cell activation had been systematically defined by a number of different loss-of-function studies. In complementation of these data, it was tested next in a reverse approach whether overexpression of PP4R1 hampers TCR-induced NF-κB activation.

Therefore, Jurkat T cells were transiently transfected with an expression plasmid encoding for haemagglutinin (HA)-tagged human PP4R1 or with empty vector for control (Mock). Cells were stimulated with increasing amounts of agonistic antibodies, and NF-κB activity was determined using a co-transfected NF-κB luciferase reporter system. As shown in Fig. 5.9 A, Jurkat T cells readily expressed exogenous HA-tagged PP4R1 protein upon transient transfection. As expected, overexpression of PP4R1 attenuated NF-κB activation in response to TCR stimulation (Fig. 5.9 B, left panel) or PMA/ionomycin treatment (Fig. 5.9 B, right panel). Moreover, inhibition of TCR stimulation-dependent NF-κB reporter activity by PP4R1 occurred in a dose-dependent manner and was already seen for low quantities of overexpressed exogenous protein (Fig. 5.9 C). Intriguingly, PP4R1 overexpression specifically inhibited NF-κB, but had no significant impact on TCR- or PMA/ionomycin-induced activity of the transcription factor AP-1, as assessed by analogous co-transfection of an AP-1-specific reporter system (Fig. 5.9 D).

PP4R1-mediated inhibition of NF-κB signaling was further demonstrated by analysis of TCR-induced surface expression of the NF-κB-dependent T cell activation marker CD69. For this purpose, exogenous PP4R1 and GFP were co-overexpressed in Jurkat T cells, followed by analysis of CD69 surface expression in response to TCR stimulation using flow cytometry. Simultanous expression of GFP in PP4R1-overexpressing cells allowed for the indirect tracing of cells with different expression levels of exogenous PP4R1 protein. Indeed, overexpression of PP4R1 reduced CD69 cell surface levels by more than 40% compared to control-transfected cells (Fig. 5.9 E). Similarly to NF-κB reporter activity, increasing expression levels of exogenous PP4R1, as assessed by GFP positivity, caused a more profound effect of inhibition.

In concert, these data show that forced overexpression of PP4R1 attenuates TCR-induced NF-κB-activation and, therefore, corroborate preceding loss-of-function data. Moreover, these results provide the first hint that PP4R1 is specifically involved in negative regulation of NF-κB signaling, but does not control AP-1 activity.

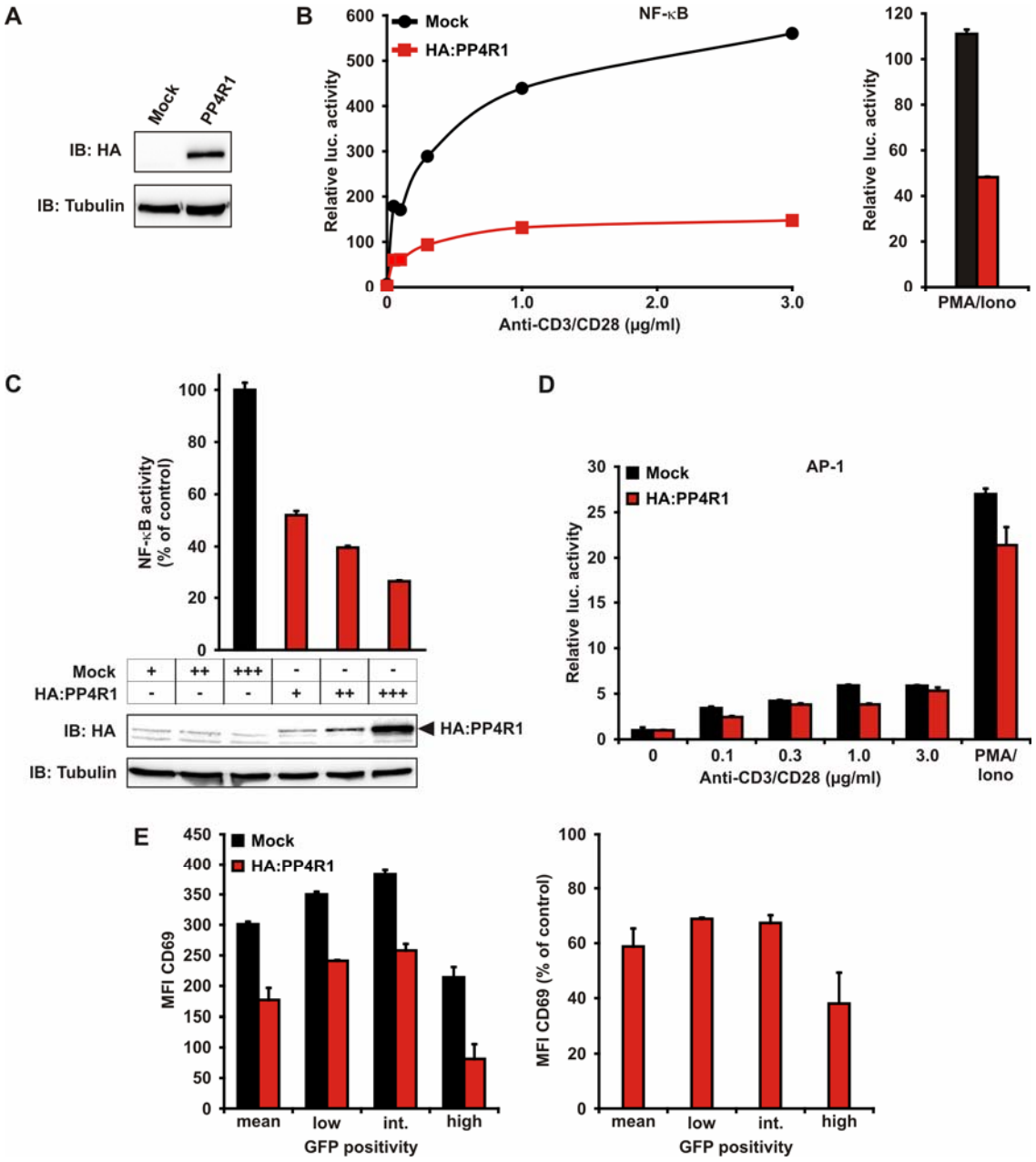

Figure 5.9 | Overexpression of PP4R1 in Jurkat T cells impedes T cell activation by specifically counteracting NF-κB, but not AP-1 signaling. (A) Jurkat T cells were transiently transfected with an expression plasmid encoding for HA-tagged PP4R1 or empty vector (Mock) for control. In addition, cells were co-transfected either with a NF-κB **(B)** or AP-1 **(D)** specific luciferase reporter system. 36 h post transfection cells were lysed and expression of exogenous PP4R1 was assessed by SDS-PAGE and immunoblotting. Reprobing with anti-Tubulin antibodies verified equal loading. **(B)** NF-κB luciferase assay of Jurkat T cells transiently overexpressing HA:PP4R1, and stimulated with indicated concentrations of anti-CD3/CD28 antibodies or treated with PMA/ionomycin for 8 h. **(C)** Jurkat T cells were transfected as in **(A)**, but with increasing concentrations of cDNA encoding for HA:PP4R1 or empty vector for control. NF-κB-dependent luciferase activity was determined as in **(B)**. NF-κB activity of PP4R1-expressing cells was normalized to that of mock-transfected cells. SD for mock-transfected cells refers to the geometric mean of SDs of individual mock transfections with different cDNA concentrations. For expression control, whole cell lysates were subjected to SDS-PAGE followed by immunoblotting of exogenous

protein. Reprobing with anti-Tubulin antibodies verified equal loading. **(D)** AP-1 luciferase assay of Jurkat T cells analogous to that in **(B)**. Mean and SD of all luciferase assays are representative of dublicate measurements. **(E)** Jurkat T cells were transiently transfected with cDNA encoding for PP4R1 or empty vector together with an expression vector encoding for GFP. 36 h post transfection, cells were stimulated *via* the TCR for 8 h and CD69 surface expression of GFP-positive cells was determined by flow cytometry. Mean fluorescence intensity (MFI) was determined for transfected cells with low, intermediate (int.), and high GFP co-overexpression (left panel). MFI of PP4R1-expressing cells was normalized to that of mock-transfected cells (right panel). Mean and SD are representative of triplicate measurements.

5.2.5 PP4R1 is upregulated in expanded primary human T cells and affects NF-κB activity and TCR-induced cytokine secretion *in vitro*

So far, the functional importance of PP4R1 had been extensively documented for the human T cell line Jurkat, but expression and function of PP4R1 in non-malignant primary human T lymphocytes remained elusive. In order to address this question, primary human T cells were isolated, stimulated, and expanded *ex vivo* over the course of 8 days in the presence of IL-2. To assess PP4R1 protein expression, cells were lysed before (day 0) and at different time points post stimulation (day 1-8). Subsequently, lysates were subjected to SDS-PAGE and expression of endogenous proteins was assessed by immunoblotting. Surprisingly, endogenous PP4R1 protein was not detectable in resting T cells (Fig. 5 A). At about day 2 post stimulation, PP4R1 expression became visible and continuously increased in the course of expansion. Compared to its rather modest expression at day 2, PP4R1 protein levels were induced by more than 30-fold in T cells at day 8 of *in vitro* culture (Fig. 5.10 A, right panel). In marked contrast, the catalytic subunit of the PP4 holoenzyme (PP4c) was already well-expressed in unstimulated T cells and its expression level did not significantly change over time.

To further elucidate whether the differential expression of PP4R1 in resting *vs.* activated T cells is a generic or gene-specific phenomenon, expression profiles of two different protein phosphatase catalytic subunits, PP2Ac and PP1c, that do not form part of the PP4 holoenzyme were examined. Akin to PP4c, PP1c expression remained unchanged upon T cell activation and expansion, whereas expression of the PP2A catalytic subunit PP2Ac was strongly induced upon T cell activation (Fig. 5.10 A). In contrast to PP4R1 however, maximal protein levels were detected earlier and thereafter remained constant.

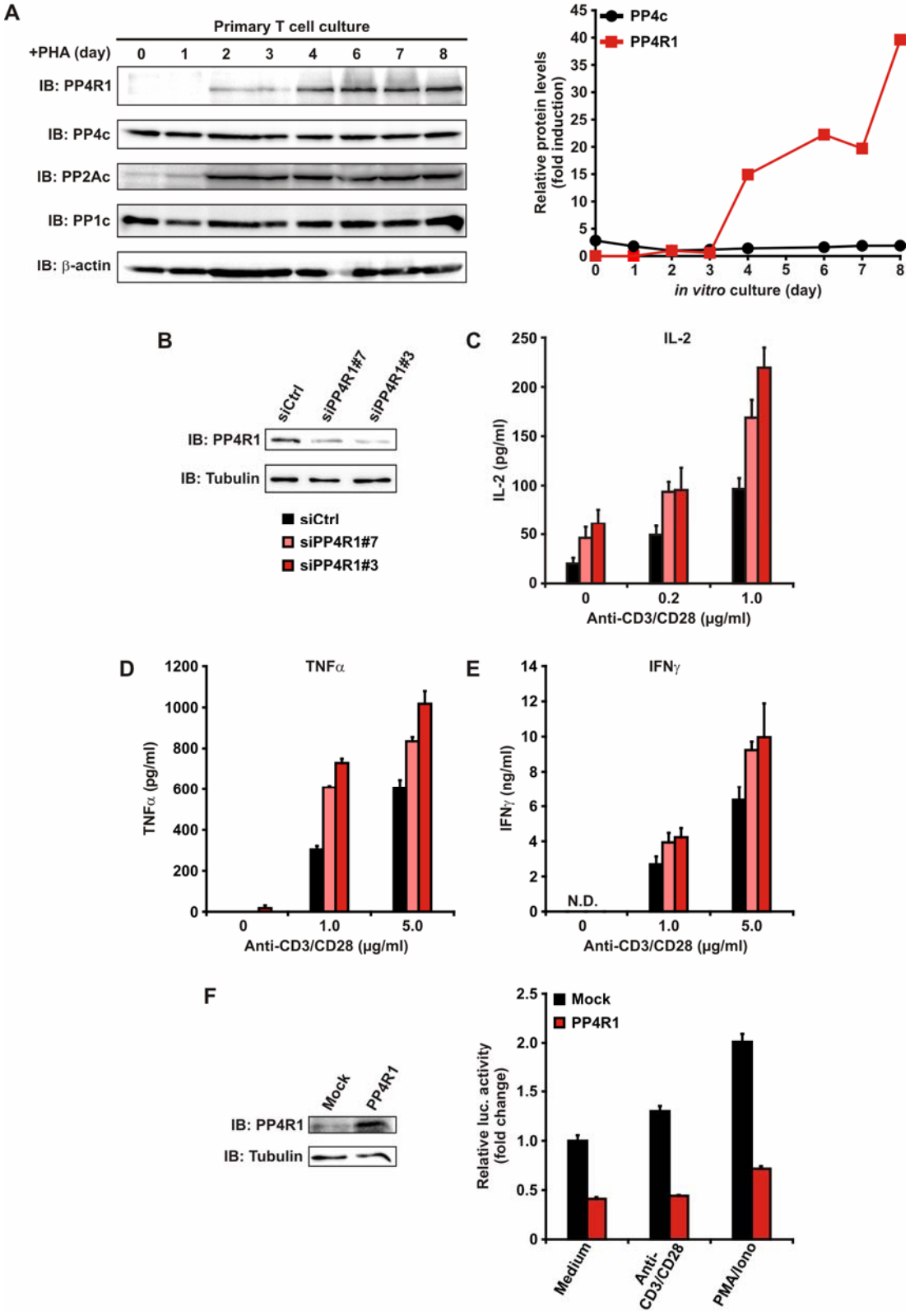

Figure 5.10 | PP4R1 suppresses TCR-induced cytokine secretion and NF-κB signaling in pre-stimulated primary human T lymphocytes *in vitro*. (A) Primary human T lymphocytes were isolated from peripheral blood, stimulated with PHA, and expanded in the presence of IL-2. Before and during *in vitro* expansion whole cell lysates of T lymphocytes were collected and subjected to

SDS-PAGE. Endogenous proteins were detected by immunoblotting using primary antibodies as indicated (left panel). PP4R1 and PP4c protein levels were quantified using β-actin levels for normalization. Relative PP4c and PP4R1 expression is shown as fold induction relative to levels of day 2 of *in vitro* expansion (right panel). **(B)** Pre-stimulated peripheral blood T cells were transfected with indicated siRNAs at day 4 of *in vitro* expansion. 72 h post transfection, cells were lysed and PP4R1 and PP4c protein levels were determined by SDS-PAGE and immunoblotting. Reprobing with anti-Tubulin antibodies verified equal loading. **(C-E)** Transiently silenced cells were stimulated with indicated concentrations of anti-CD3/CD28 antibodies and secretion of IL-2, TNFα, and IFNγ was measured by ELISA. **(F)** $CD4^+$ primary peripheral blood T cells were isolated and expanded *in vitro* by TCR stimulation. At day 3 of *in vitro* expansion cells were co-transfected with cDNA encoding for PP4R1 or empty vector (Mock) for control together with a NF-κB-specific luciferase reporter system. 24 h post transfection cells were stimulated as indicated and NF-κB-dependent luciferase was measured. Results are shown as fold induction relative to untreated control-transfected cells. Mean and SD of luciferase activity are representative of triplicate measurements (right panel). To confirm PP4R1 overexpression a fraction of cells was lysed, followed by SDS-PAGE of whole cell lysates and immunoblotting. Reprobing with anti-Tubulin antibodies verified equal loading. (N.D.: not detectable).

The differential regulation of PP4R1 protein expression in primary human T lymphocytes *in vitro* raised the question whether, analogous to Jurkat T cells, PP4R1 plays a role as negative regulator of NF-κB specifically in pre-activated, expanded T cells. To answer this question, primary human T lymphocytes were isolated and expanded *in vitro* as described before. At day 4 post stimulation cells were transfected with siRNA specific for PP4R1 or non-targeting control siRNA. Subsequently, cells were stimulated with increasing concentrations of anti-CD3/CD28 antibodies or were left unstimulated. T cell activation was monitored based on measurement of cytokine secretion by ELISA. Knock-down of endogenous PP4R1 protein by two independent siPP4R1 oligos was confirmed by SDS-PAGE and immunoblotting (Fig. 5.10 B). As already seen for Jurkat T cells, transient siRNA-mediated down-regulation of PP4R1 protein in expanded primary T lymphocytes substantially augmented production of the NF-κB-regulated cytokines IL-2, TNFα, and IFNγ in response to anti-CD3/CD28 treatment (Fig. 5.10 C-E). Moreover, basal IL-2 secretion was already markedly increased in PP4R1-silenced cells indicative of enhanced T cell activation and expansion even without TCR re-stimulation. As seen before, cytokine secretion and PP4R1 protein levels showed a tight inverse correlation.

To directly confirm negative regulation of NF-κB activity, expanded primary human T cells at day 3 of *in vitro* culture were transfected with a PP4R1 expression plasmid or empty vector for negative control. Subsequently, cells were stimulated by treatment with anti-CD3/CD28 antibodies and PMA/ionomycin, respectively, or were left untreated. NF-κB activity was measured using a co-transfected NF-κB-dependent luciferase system. Pre-stimulated expanded T lymphocytes displayed already high basal NF-κB activity that was

further increased by up to 2-fold in response to stimulation (Fig. 5.10 F). However, overexpression of PP4R1 considerably inhibited basal NF-κB activity compared to control-transfected cells and almost completely prevented further luciferase upregulation upon TCR stimulation or PMA/ionomycin treatment.

Collectively, these data suggest that PP4R1 counterbalances activation of pre-stimulated primary human T cells by negatively regulating NF-κB signaling. Upregulated PP4R1 expression in expanded pre-stimulated T lymphocytes implies a mechanism of activation-induced negative feedback that limits NF-κB signaling upon TCR re-stimulation.

5.2.6 PP4R1 physically interacts with the IKK complex in a TCR stimulation-dependent manner

So far, genetic and functional analyses had clearly established an important role for PP4R1 in regulating NF-κB activation in Jurkat T cells and primary human T lymphocytes. However, the precise molecular mechanism governing PP4R1-dependent NF-κB modulation as well as potential effector molecules targeted by PP4R1 remained elusive. The fact that PP4R1 does not only impinge upon TCR-induced NF-κB activity but similarly affects PKC-driven and TNFR-mediated NF-κB signaling gave rise to the assumption that PP4R1 operates on a shared level within the canonical pathway downstream of PKCθ and the TNFR signaling complex (TNF-RSC) (see Fig. 5.7 E). A central point of convergence in canonical signaling is the IKK complex.

To test for a potential physical interaction between PP4R1 and individual components of the IKK complex, HA-tagged PP4R1 was transiently overexpressed in HEK293T cells alone or in combination with FLAG-tagged versions of IKKα, IKKβ, and IKKγ (NEMO), respectively. Exogenous proteins were subjected to immunoprecipitation using either anti-FLAG antibodies (Fig. 5.11 A) or anti-HA antibodies (Fig. 5.11 B). Subsequently, immune complexes were resolved by SDS-PAGE, and (co-)immunoprecipitated proteins were detected by immunoblotting using anti-HA or anti-FLAG antibodies. Indeed, PP4R1 was demonstrated to be a potent interaction partner of IKKα as revealed both by anti-FLAG and anti-HA co-immunoprecipitation experiments (Fig. 5.11 A,B). Of note, the interaction between exogenous PP4R1 and IKKα seemed to be highly specific. PP4R1 did not interact with NEMO and only showed a weak interaction with IKKβ in anti-HA immuno-precipitations (Fig. 5.11 B). IKKα is an integral part of the heterotrimeric IKK complex, but also serves separate functions, *e.g.* by mediating non-canonical NF-κB activation or by controlling nuclear NF-κB activity (Ghosh and Hayden, 2008; Senftleben et al., 2001).

Therefore, it is conceivable that PP4R1 specifically interacts with IKKα to be recruited to the endogenous IKK complex. Alternatively, the PP4R1-IKKα interaction might occur independently of additional IKK compounds and IKK complex formation. So far, interaction data were based on concomitant overexpression of exogenous proteins in HEK293T cells, thereby limiting conclusions regarding the specificity of possible interactions under physiological conditions in T cells.

To test for an endogenous interaction between PP4R1 and the IKK complex, Jurkat T cells (Fig. 5.11 C) as well as expanded primary human T lymphocytes at day 7 of culture (Fig. 5.11 D) were stimulated with anti-CD3/CD28 antibodies for various time periods. Cells were lysed and the IKK complex was immunoprecipitated using anti-NEMO antibodies. The immunoprecipitated material was then subjected to SDS-PAGE and endogenous proteins were detected by immunoblotting. Both in Jurkat T cells and in primary human T cells a small fraction of PP4R1 pre-associated with the endogenous IKK complex under resting conditions (Fig. 5.11 C,D). Importantly, TCR engagement led to a transient, but marked increase in IKK-associated PP4R1. Thereby, enhanced association of PP4R1 with the IKK complex became apparent at later time points and peaked at about 45-90 minutes of stimulation. Proper assembly and pull-down of the endogenous IKK complex was confirmed by immunoblotting of IKKα and IKKβ, respectively. In addition, T cell activation was monitored by determining levels of phospho-ERK in whole cell lysates.

In summary, these data demonstrate a physical interaction between PP4R1 and the IKK complex in T cells. This association is regulated and transiently increased in a TCR stimulation-dependent manner and presumably involves specific binding of PP4R1 to IKKα. Delayed recruitment of PP4R1 to the IKK complex upon TCR triggering suggests a role of PP4R1 in activation-induced termination of IKK activity.

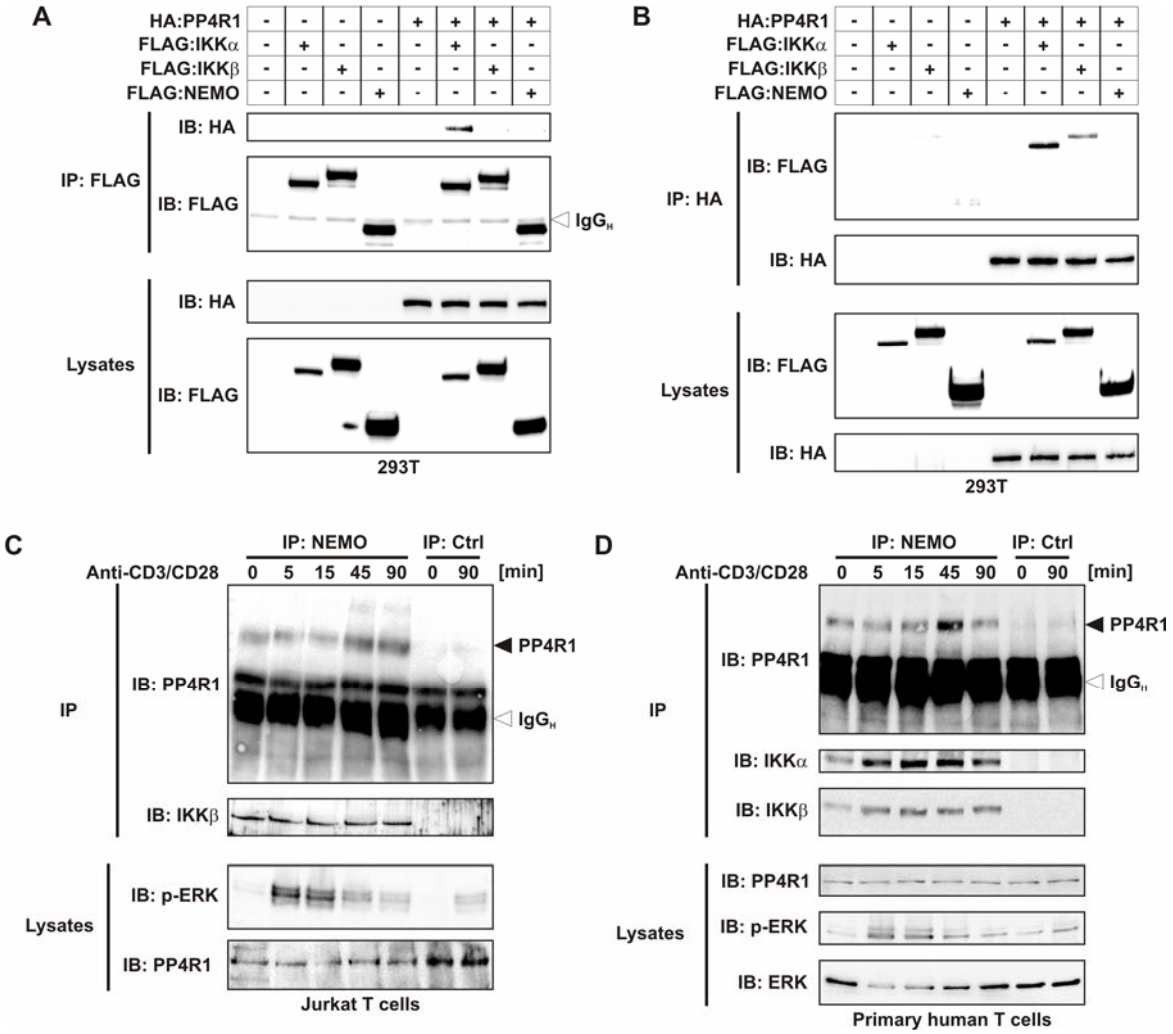

Figure 5.11 | PP4R1 interacts with IKKα and associates with the IKK complex in a TCR stimulation-dependent manner. (A) and **(B)** HA-tagged PP4R1 was overexpressed in HEK293T cells alone or in combination with FLAG-tagged versions of IKKα, IKKβ, or NEMO. Cells were lysed and exogenous proteins were immunoprecipitated using anti-FLAG **(A)** or anti-HA **(B)** antibodies. Whole cell lysates and immune complexes were resolved by SDS-PAGE and (co)immunoprecipitated proteins were detected by immunoblotting using primary antibodies as indicated. **(C,D)** Jurkat T cells **(C)** or primary human day 6 T lymphocytes **(D)** were stimulated with 1.0 µg/ml of anti-CD3/CD28 antibodies for indicated time periods. Cells were lysed and the IKK complex was immunoprecipitated using anti-NEMO antibodies. A non-precipitating antibody was used to control for specificity. Whole cell lysates and immune complexes were resolved by SDS-PAGE followed by immunoblotting using primary antibodies as indicated. Reprobing with anti-phospho-ERK antibodies verified proper stimulation of cells. Results are representative of at least three independent experiments. (Filled and open arrowheads indicate specific proteins and IgG_H, respectively).

5.2.7 PP4R1 and the catalytic subunit PP4c constitutively interact with each other and pre-associate with the IKK complex

The stimulation-dependent interaction of PP4R1 with the IKK complex provided a first hint for the molecular basis of PP4R1-mediated NF-κB inhibition. However, PP4R1 itself does not contain intrinsic enzymatic activity, rendering its precise molecular function elusive. Instead, several earlier reports indicated – based on proteomics approaches – that PP4R1 forms a stable complex with the PP4 catalytic subunit PP4c and thereby might function as a regulatory subunit of the PP4 holoenzyme (Bennett et al., 2006; Ewing et al., 2007; Gingras et al., 2005; Kloeker and Wadzinski, 1999).

To confirm the PP4R1-PP4c interaction, HEK293T cells were transiently transfected with expression plasmids encoding for HA-tagged PP4R1 or FLAG-tagged PP4c, either alone or in combination. Subsequently, overexpressed proteins were specifically pulled-down using anti-HA or anti-FLAG antibodies. Immune complexes were resolved by SDS-PAGE and (co-)immunoprecipated exogenous proteins were probed by anti-FLAG and anti-HA antibodies, respectively. In accordance with published observations, a strong interaction between exogenous PP4R1 and PP4c proteins was demonstrated both by anti-FLAG immunoprecipitations and, *vice versa*, anti-HA pull-down (Fig. 5.12 A).

To confirm an association of endogenous proteins and to further test whether this interaction is subject to regulation by TCR-stimulation, Jurkat T cells (Fig. 5.12 B) as well as primary human T cells at day 6 of *in vitro* culture (Fig. 5.12 C) were stimulated with anti-CD3/CD28 antibodies for different time points, followed by cell lysis and immunoprecipitation of endogenous PP4R1 protein using anti-PP4R1 antibodies. Endogenous proteins were detected by immunoblotting. PP4R1 and PP4c were shown to constitutively interact with each other irrespective of TCR stimulation (Fig. 5.12 B,C). In contrast to binding of PP4R1 to the IKK complex, there was a strong pre-association of both proteins that was maintained in stimulated cells. Of note, the PP4R1-PP4c interaction seemed to be highly specific since PP2Ac, a structurally related catalytic subunit of the PP2A holoenzyme (Bennett et al., 2006), did not co-purify with endogenous PP4R1 protein in Jurkat T cells, neither before nor post TCR stimulation (Fig. 5.12 C).

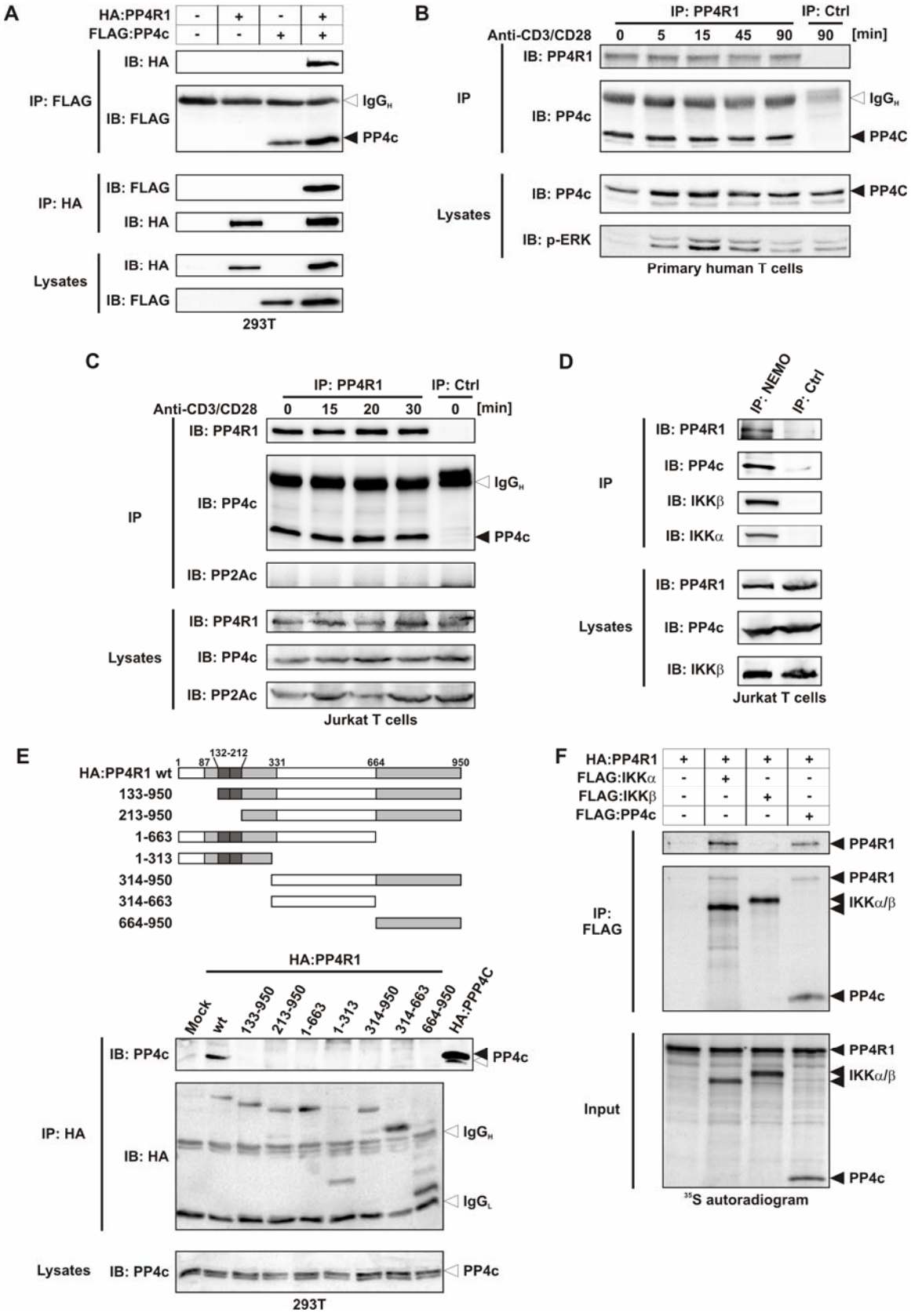
A
HA:PP4R1
FLAG:PP4c
IB: HA
IP: FLAG
IB: FLAG
IgG$_H$
PP4c
IP: HA
IB: FLAG
IB: HA
Lysates
IB: HA
IB: FLAG
293T
B
IP: PP4R1
IP: Ctrl
Anti-CD3/CD28
0 5 15 45 90 90 [min]
IB: PP4R1
IP
IB: PP4c
IgG$_H$
PP4C
Lysates
IB: PP4c
PP4C
IB: p-ERK
Primary human T cells
C
IP: PP4R1
IP: Ctrl
Anti-CD3/CD28
0 15 20 30 0 [min]
IB: PP4R1
IP
IB: PP4c
IgG$_H$
PP4c
IB: PP2Ac
Lysates
IB: PP4R1
IB: PP4c
IB: PP2Ac
Jurkat T cells
D
IP: NEMO
IP: Ctrl
IB: PP4R1
IP
IB: PP4c
IB: IKKβ
IB: IKKα
Lysates
IB: PP4R1
IB: PP4c
IB: IKKβ
Jurkat T cells
E
HA:PP4R1 wt
1 87 132-212 331 664 950
133-950
213-950
1-663
1-313
314-950
314-663
664-950
HA:PP4R1
Mock wt 133-950 213-950 1-663 1-313 314-950 314-663 664-950 HA:PPP4C
IB: PP4c
PP4c
IP: HA
IB: HA
IgG$_H$
IgG$_L$
Lysates
IB: PP4c
PP4c
293T
F
HA:PP4R1
FLAG:IKKα
FLAG:IKKβ
FLAG:PP4c
PP4R1
IP: FLAG
PP4R1
IKKα/β
PP4c
Input
PP4R1
IKKα/β
PP4c
^{35}S autoradiogram

Figure 5.12 | PP4R1 and PP4c form a stable complex in T lymphocytes that pre-associates with the IKK complex in T lymphocytes. (A) HA-tagged PP4R1 and PP4c were overexpressed in HEK293T cells alone or in combination. Exogenous proteins were pulled-down either by anti-FLAG or by anti-HA antibodies. Whole cell lysates and immune complexes were resolved by SDS-PAGE and (co-)immunoprecipitated proteins were detected by immunoblotting using primary antibodies as indicated. **(B,C)** Primary human day 6 T cells **(B)** or Jurkat T cells **(C)** were stimulated with 1.0 µg/ml of anti-CD3/CD28 antibodies and endogenous PP4R1 was immunoprecipitated using anti-PP4R1 antibodies. A non-precipitating antibody was used to control for specificity. Whole cell lysates and immune complexes were resolved by SDS-PAGE and (co-)immunoprecipitated proteins were detected by immunoblotting using primary antibodies as indicated. Reprobing with anti-phospho-ERK antibodies confirmed T cell stimulation. **(D)** Resting Jurkat T cells were lysed and the IKK complex was immunoprecipitated by anti-NEMO antibodies. A non-precipitating antibody was used to control for specificity. (Co)immunoprecipitated proteins were detected by SDS-PAGE and immunoblotting using primary antibodies as indicated. Whole cell lysates were included to confirm equal input. **(E)** Schematic representation of PP4R1 domain structure and HA-tagged deletion mutants. Light grey boxes indicate regions with homology to the A subunit of PP2A. Dark grey boxes represent *in silico* predicted "heat" repeats (upper panel). Full length HA-tagged PP4R1 (wt) or different PP4R1 deletion mutants were overexpressed in HEK293T cells. In addition, HA-tagged PP4c was overexpressed. Exogenous proteins were immunoprecipitated by anti-HA antibodies from whole cell lysates. Immune complexes and lysates were subjected to SDS-PAGE followed by immunoblotting using primary antibodies as indicated. **(F)** HA-tagged PP4R1 and FLAG-tagged versions of IKKα, IKKβ, and PP4c, respectively, were *in vitro* translated in the presence of radioactively labeled ^{35}S-methionine. *In vitro* translated HA:PP4R1 protein was recombined with anti-FLAG *in vitro* translates followed by anti-FLAG immunoprecipitations. (Co-)immunoprecipitated recombinant proteins were detected by autoradiography. In addition, equal input of *in vitro* translated proteins was confirmed. (Filled and open arrowheads indicate specific proteins and IgG_H, or IgG_L respectively. For anti-PP4c immunoblotting open arrowheads indicate endogenous protein).

Given the strong complex formation between PP4R1 and PP4c it was next examined whether PP4c, analogously to PP4R1, associates with the IKK complex in T cells. To this end, the IKK complex was again immunoprecipitated from lysates of resting Jurkat T cells using anti-NEMO antibodies. Immune complexes were resolved by SDS-PAGE and the presence of purified proteins was analyzed by immunoblotting. Indeed, PP4c was found to pre-associate with the IKK complex in T cells prior to stimulation, as observed for PP4R1 (Fig. 5.12 D). Consistent with this finding, PP4c was shown to interact with IKKα upon overexpression in HEK293T cells (data not shown).

PP4R1 harbours two N-terminal and C-terminal regions, respectively, that display homology to the A subunit of PP2A (Chen et al., 2008; Kloeker and Wadzinski, 1999). In addition, the N-terminal domain was predicted *in silico* to contain two so-called "heat" repeats – specific motifs that have been proven to be involved in protein protein interactions (Andrade and Bork, 1995; Groves et al., 1999) (Fig. 5.12 E). To test for minimal structural requirements underlying PP4R1-PP4c complex formation, a series of HA-tagged PP4R1 deletion mutants was cloned and overexpressed in HEK293T cells. In addition, full-length HA:PP4R1 was overexpressed for positive control. Exogenous

proteins were pulled-down by anti-HA immunoprecipitation and co-association of endogenous PP4c was analyzed by SDS-PAGE and anti-PP4c immunoblotting. To control for specificity, HEK293T lysates containing overexpressed HA-tagged PP4c were included. Surprisingly, none of the PP4R1 deletion mutants showed interaction with PP4c, while the full-length protein mediated again strong co-pull-down of endogenous PP4c (Fig. 5.12 E). This result indicated that separated or already partially disrupted PP2A homology regions within PP4R1 are insufficient for PP4c association implying the involvement of multiple PP4R1 domains in PP4c binding.

To test whether the dual interactions of PP4R1 with IKKα on the one hand, and with PP4c on the other hand occur in a direct manner, HA-tagged PP4R1 as well as FLAG-tagged versions of IKKα, IKKβ, or PP4c were recombinantly expressed and radioactively labeled using an *in vitro* translation system in the presence of ^{35}S-methionine. Subsequently, recombinant HA-tagged PP4R1 was immunoprecipitated from *in vitro* translates containing either PP4R1 alone or in combination with individual and separately expressed FLAG-tagged proteins. Immunoprecipitation of proteins was detected by autoradiography. Again, PP4R1 specifically interacted with FLAG-IKKα, but not with FLAG-IKKβ (Fig. 5.12 F). Furthermore, PP4R1 was confirmed as a ligand of recombinant PP4c *in vitro*.

In conclusion, these data reveal stable and TCR stimulation-independent complex formation between PP4R1 and PP4c. Most likely, PP4c is co-recruited to the IKK complex *via* binding to PP4R1, probably involving direct interactions between PP4R1 and IKKα and PP4c, respectively.

5.2.8 PP4R1 negatively regulates TCR-induced IKK signaling and kinase activity

The observation that TCR stimulation is followed by a transient increase in IKK-associated PP4R1 suggested that PP4R1 directly impedes IKK activation and thereby negatively regulates NF-κB signaling in T lymphocytes. To test this hypothesis and to further analyze at which stage PP4R1 interferes with the NF-κB signaling cascade, the impact of PP4R1 deficiency or overexpression on IKK signaling was elucidated in detail.

First, Jurkat T cells were transiently transfected with siRNA specific for PP4R1 or control siRNA. 72 h post transfection cells were stimulated by treatment with PMA/ionomycin for various time periods and the IKK complex was immunoprecipitated from whole cell lysates using anti-NEMO antibodies. To directly measure IKK activity, a fraction of anti-NEMO immunoprecipitates was subjected to an *in vitro* kinase assay using recombinant GST:IκBα as a substrate. In addition, an equivalent portion of the immunoprecipitated

material was subjected to SDS-PAGE and proper co-purification as well as the phosphorylation status of IKKα and IKKβ was determined by immunoblotting. As seen in Fig. 5.13 A, siRNA-mediated knock-down of PP4R1 caused a marked increase in stimulation-dependent IKK activity as visualized by IκBα and IKK autoradiography. Thereby, IKK activation occurred more rapidly, with a considerably higher peak of kinase activity after 25 minutes of stimulation and seemed to be more sustained. No changes in basal IKK activity were observed. Interestingly, T loop phosphorylation of IKKs, as assessed by immunoblotting with phospho-specific antibodies, was already heavily increased in unstimulated PP4R1-deficient cells compared to control-transfected cells. Constitutive IKK phosphorylation did not change substantially in response to stimulation but was highly sustained – in marked contrast to transient IKK phosphorylation observed in control-transfected cells. PP4R1 knock-down did not alter PMA/ionomcyin-induced PKCθ phoshorylation and kinase activity (data not shown) indicating that PP4R1 directly inhibits the IKK complex. Accordingly and further supporting its IKK-specific function, transient or stable knock-down of PP4R1 did not alter ERK phosphorylation (Fig. 5.13 A and data not shown).

In a reverse experiment, the impact of PP4R1 overexpression on TCR-induced IKK activity was determined. To this end, exogenous FLAG:IKKβ was transiently overexpressed in Jurkat T cells with or without HA-tagged PP4R1. Cells were stimulated *via* the TCR with agonistic antibodies and exogenous IKKβ was immunoprecipitated from whole cell lysates. Subsequently, FLAG:IKKβ kinase activity was analyzed in an *in vitro* kinase assay as described before. Conversely to PP4R1 silencing, ectopic PP4R1 completely blunted TCR-induced IKK activation (Fig. 5.13 B). Whereas in control-transfected cells maximal IKK and IκBα phosphorylation were detected at 20 minutes post stimulation, PP4R1-overexpressing cells exhibited almost no induction of IKK activity. Overexpression of HA-tagged PP4R1 and equivalent pull-down of IKKβ were confirmed by anti-HA and anti-IKKβ immunoblotting, respectively.

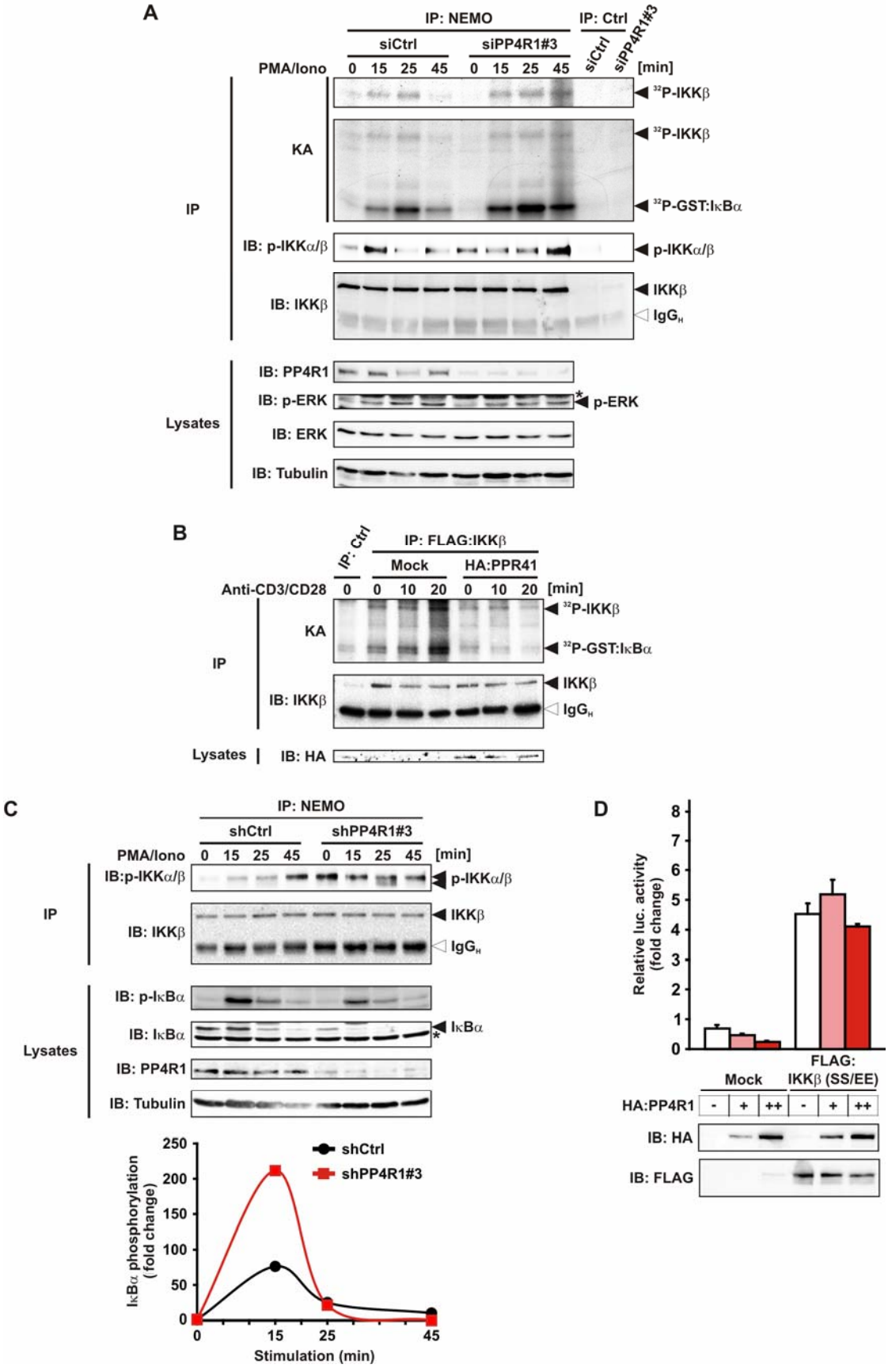
A
IP: NEMO
IP: Ctrl
siCtrl
siPP4R1#3
siCtrl
siPP4R1#3
PMA/Iono
0 15 25 45 0 15 25 45
[min]
IP
KA
32P-IKKβ
32P-IKKβ
32P-GST:IκBα
IB: p-IKKα/β
p-IKKα/β
IB: IKKβ
IKKβ
IgGH
Lysates
IB: PP4R1
IB: p-ERK
p-ERK
IB: ERK
IB: Tubulin
B
IP: Ctrl
IP: FLAG:IKKβ
Mock
HA:PPR41
Anti-CD3/CD28
0 0 10 20 0 10 20
[min]
IP
KA
32P-IKKβ
32P-GST:IκBα
IB: IKKβ
IKKβ
IgGH
Lysates
IB: HA
C
IP: NEMO
shCtrl
shPP4R1#3
PMA/Iono
0 15 25 45 0 15 25 45
[min]
IP
IB:p-IKKα/β
p-IKKα/β
IB: IKKβ
IKKβ
IgGH
Lysates
IB: p-IκBα
IB: IκBα
IκBα
IB: PP4R1
IB: Tubulin
shCtrl
shPP4R1#3
IκBα phosphorylation (fold change)
250
200
150
100
50
0
0 15 25 45
Stimulation (min)
D
Relative luc. activity (fold change)
8
7
6
5
4
3
2
1
0
FLAG:
Mock
IKKβ (SS/EE)
HA:PP4R1
- + ++ - + ++
IB: HA
IB: FLAG

Figure 5.13 | PP4R1 negatively regulates IKK activation in resting and stimulated T cells. Jurkat T cells were transiently transfected with PP4R1-specific siRNA or control siRNA. 72 h post transfection cells were stimulated with PMA/ionomcyin for indicated time periods and the IKK complex was immunoprecipitated by anti-NEMO antibodies. A non-precipitating antibody was used to control for specificity. A fraction of immunoprecipitates was subjected to an *in vitro* kinase assay (KA) in the presence of radioactively labeled [γ-^{32}P]ATP and GST:IκBα as a substrate. Remaining immunoprecipitates together with whole cell lysates were subjected to SDS-PAGE followed by immunoblotting using primary antibodies as indicated. Reprobing with anti-PP4R1 and anti-Tubulin antibodies verified efficient knock-down and equal loading, respectively. **(B)** Jurkat T cells were transfected with cDNA encoding for FLAG:IKKβ together with an expression vector for HA:PP4R1 or empty vector (Mock). 48 h post transfection exogenous IKKβ was pulled-down by anti-FLAG immunoprecipitation. A non-precipitating antibody was used to control for specificity. Immunoprecipitates were subjected to an *in vitro* kinase assay or, in parallel, to SDS-PAGE and anti-IKKβ immunoblotting. Overexpression of HA:PP4R1 was confirmed by SDS-PAGE and anti-HA immunoblotting of whole cell lysates. **(C)** Jurkat cells stably expressing PP4R1-specific shRNA (shPP4R1#3) or control shRNA were stimulated with PMA/ionomcyin for different time periods. Cells were lysed and the IKK complex was immunoprecipitated by anti-NEMO antibodies. Immune complexes and whole cell lysates were subjected to SDS-PAGE followed by immunoblotting using primary antibodies as indicated. Reprobing with anti-PP4R1 and anti-Tubulin antibodies verified efficient knock-down and equal loading, respectively (upper panel). IκBα phosphorylation was quantified as fold induction compared to unstimulated control-transduced cells (lower panel). (Asterisks indicate non-specific bands, filled and open arrowheads specific proteins and IgG_H, respectively). **(D)** Increasing amounts of HA:PP4R1 were overexpressed in HEK293T cells either alone or together with a dominant-active kinase mutant of FLAG:IKKβ (FLAG:IKKβ SS/EE). 48 h post transfection cells were lysed and NF-κB activity was measured by use of a co-transfected NF-κB-specific luciferase reporter system. Overexpression was confirmed by SDS-PAGE and immunoblotting. Mean and SD of luciferase activity are representative of dublicate measurements.

To further confirm and analyze the role of PP4R1 in negative regulation of IKK signaling, stably PP4R1-silenced Jurkat T cells were stimulated with PMA/ionomycin and IKK phosphorylation was assessed as described before. In parallel, the phosphorylation status and expression levels of IκBα were analyzed by immunoblotting. In accordance with transient PP4R1 silencing, stable shRNA-mediated knock-down of PP4R1 caused again a dramatic increase in basal IKKβ phosphorylation compared to control-transduced cells (Fig. 5.13 C upper panel). Furthermore, IKKβ phosphorylation seemed to be constitutive and sustained in PP4R1-deficient cells and did not change significantly upon stimulation. In contrast, phosphorylation of IKKα peaked at about 25 minutes post stimulation, but was markedly increased in cells lacking PP4R1 expression. Constitutive IKKβ phosphorylation correlated well with significantly less IκBα protein in resting PP4R1-deficient Jurkat T cells. Moreover, residual IκBα protein was rapidly degraded upon stimulation, while in control cells IκBα protein levels decreased later after about 25 minutes of stimulation. Despite low IκBα protein expression, relative phosphorylation of IκBα was much higher in PP4R1-deficient cells and precisely paralleled IκBα degradation (Fig. 5.13 C lower panel).

To determine whether PP4R1 affects signaling events downstream of IKK activation, HA-tagged PP4R1 was overexpressed in HEK293T cells, alone or in combination with a constitutively active mutant of FLAG-tagged IKKβ, IKKβ S177E/S181E (IKKβ SS/EE) (Mercurio et al., 1997). NF-κB activity was measured by means of a co-transfected NF-κB-specific luciferase reporter system. As seen in Fig. 5.13 D, forced overexpression of HA:PP4R1 inhibited basal NF-κB activity in a dose-dependent manner, but had no impact on IKKβ SS/EE-dependent NF-κB signaling. Thus, constitutive kinase activity that is uncoupled from inducible phosphorylation of T loop serines within IKKβ was sufficient to bypass PP4R1-mediated NF-κB inhibition.

Collectively, the combined data demonstrate that PP4R1 negatively regulates IKK phosphorylation and kinase activity. Increased levels of phospho-IKK in PP4R1-silenced cells correlated well with enhanced *in vitro* kinase activity and IκBα phosphorylation and degradation upon stimulation. Constitutive IKKβ phosphorylation was reflected by significantly decreased IκBα protein levels in resting PP4R1-deficient cells, although no changes in basal IKK activity were observed in an *in vitro* kinase assay. Importantly, PP4R1 deficiency did not cause any alterations in stimulation-dependent ERK phosphorylation. The specificity of PP4R1 on IKK phosphorylation and activation was further substantiated by epistasis analysis on the basis of overexpression of a constitutively active version of IKKβ.

5.2.9 The PP4R1/PP4c module exerts TCR stimulation-dependent phosphatase activity and mediates dephosphorylation of IKK proteins *in vitro*

Functional and biochemical analyses had clearly established PP4R1 as a negative and most likely direct regulator of the IKK complex in T lymphocytes. Since PP4R1 and the catalytic subunit PP4c form part of a stable holoenzyme and similarly associate with the IKK complex, it is conceivable that PP4R1 regulates and directs PP4c phosphatase activity towards dephosphorylation of IKK proteins, thereby limiting and terminating kinase activation.

First, the question was addressed whether PP4R1 functions as a co-regulator of PP4c enzymatic activity. Therefore, HA-tagged versions of PP4R1 and PP4c, respectively, were overexpressed in HEK293T cells, either alone or in combination. Subsequently, exogenous proteins were pulled-down from whole cell lysates using anti-HA antibodies.

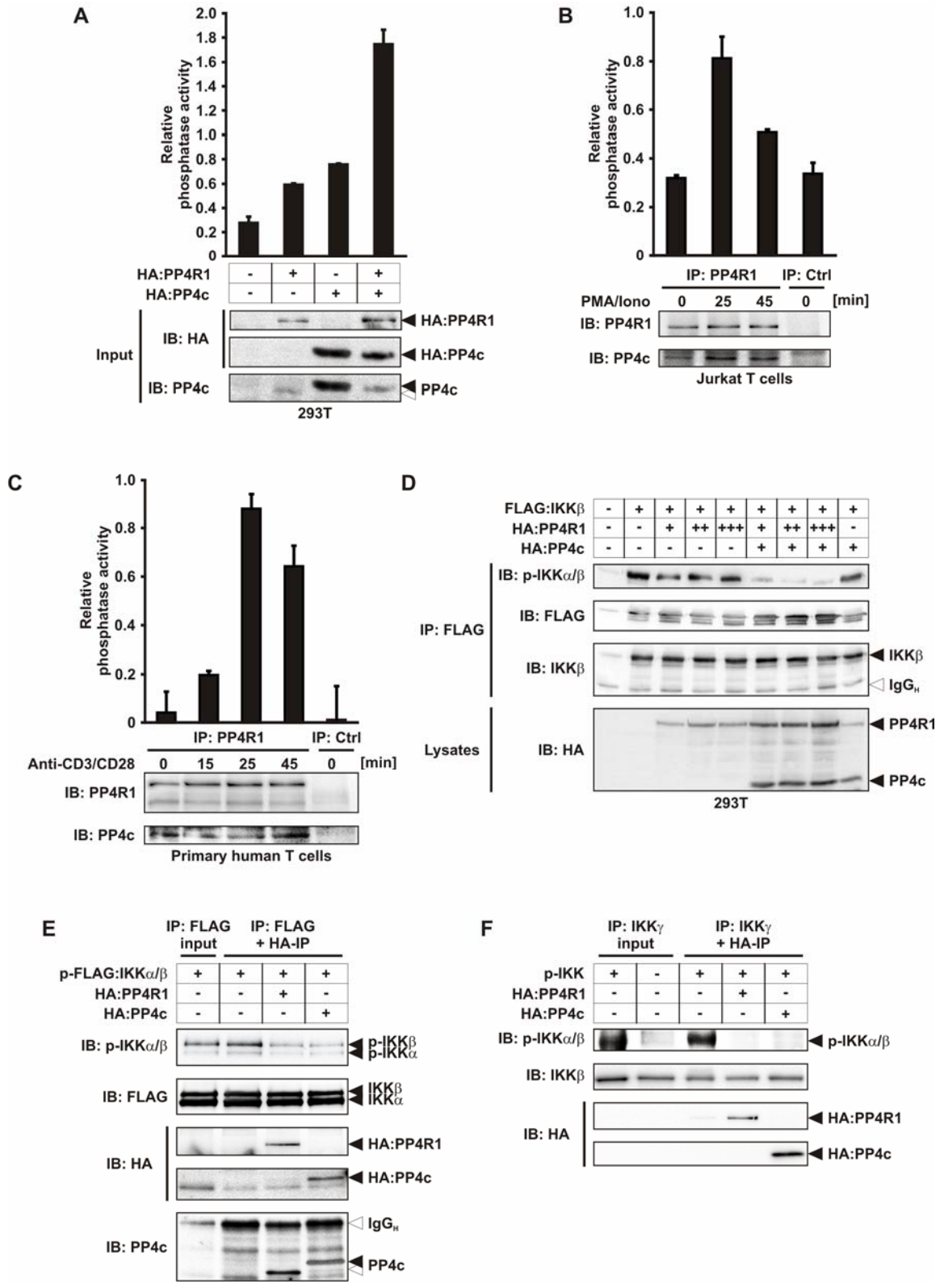

Figure 5.14 | The PP4R1/PP4c module exerts TCR stimulation-dependent phospholytic activity and dephosphorylates IKKs *in vitro*. (A) HA-tagged versions of PP4R1 and PP4c were overexpressed in HEK293T cells alone or in combination. Exogenous proteins were pulled-down by anti-HA antibodies and subjected to a colorimetric phosphatase activity assay. Mean and SD of

relative phosphatase activities are representative of triplicate measurements. **(B,C)** Jurkat T cells **(B)** or primary human day 6 T cells **(C)** were stimulated by treatment with PMA/ionomycin or anti-CD3/CD28 antibodies for various time periods as indicated. Cells were lysed and endogenous PP4R1 was immunoprecipitated. A non-precipitating antibody was used to control for specificity. Immunoprecipitates were subjected to an *in vitro* phosphatase activity assay as described in **(A)**. In parallel, to control equal input, a fraction of immunoprecipitates was subjected to SDS-PAGE and immunoblotting using primary antibodies as indicated. **(D)** FLAG:IKKβ together with increasing amounts of HA:PP4R1 and/or HA:PP4c was overexpressed in HEK293T cells. 48 h post transfection FLAG:IKKβ was pulled-down from whole cell lysates by anti-FLAG immuno-precipitation. Immune complexes were resolved by SDS-PAGE followed by immunoblotting using primary antibodies as indicated. In addition, expression of HA-tagged proteins in whole cell lysates was confirmed by SDS-PAGE and anti-HA immunoblotting. **(E)** To generate phospho-substrates for a reconstituted *in vitro* phosphatase assay, FLAG-tagged versions of IKKα or IKKβ were overexpressed in HEK293T cells. Following PMA/ionomycin stimulation for 15 min cells were lysed and FLAG:IKKs were pulled down by anti-FLAG immunoprecipitation. In parallel, HA:PP4R1 and HA:PP4c were separately overexpressed in HEK293T cells and exogenous proteins were immunoprecipitated by anti-HA antibodies. Subsequently, anti-HA immunoprecipitates and FLAG:IKKs were recombined in a phosphatase reaction for 1 h. Dephosphorylation of IKKs was monitored by SDS-PAGE of immunoprecipitates followed by immunoblotting using phospho-IKKα/β (ser180/ser181)-specific antibodies. Reprobing with anti-FLAG, anti-HA, and anti-PP4c antibodies confirmed equal input and proper expression of FLAG:IKKs and HA-tagged proteins, respectively. **(F)** The endogenous IKK complex was pulled-down from resting or PMA/ionomycin-stimulated Jurkat T cells using anti-NEMO antibodies. The immunoprecipitated material was then subjected to an *in vitro* phosphatase reaction as described in **(E)**. (Filled and open arrowheads indicate specific proteins and IgG_H, respectively. For anti-PP4c immunoblotting open arrowheads indicate endogenous protein).

To determine phospholytic activity, anti-HA immune complexes were subjected to an *in vitro* phosphatase activity assay. In parallel, to confirm proper expression and pull-down of HA-tagged proteins, equivalent fractions of anti-HA immunoprecipitates were subjected to SDS-PAGE followed by immunoblotting. As seen in Fig. 5.14 A, concomitant expression of PP4R1 and PP4c caused a synergistic increase in phosphatase activity compared to separate expression of either protein. Of note, modest PP4R1-associated phosphatase activity in the absence of co-overexpressed PP4c was most likely due to an interaction between exogenous HA-tagged PP4R1 and endogenously expressed PP4c as assessed by anti-PP4c immunoblotting.

The observation that TCR triggering transiently increased binding of PP4R1 to the IKK complex gave further rise to the question whether the PP4R1/PP4c module exerts phosphatase activity in a TCR stimulation-dependent manner. To test this hypothesis, Jurkat T cells or primary human T cells at day 6 of *in vitro* expansion were stimulated for different time periods by treatment with PMA/ionomycin and anti-CD3/CD28 antibodies, respectively. Subsequently, the PP4R1-PP4c complex was immunoprecipitated from whole cell lysates using anti-PP4R1 antibodies. To measure phosphatase activity, a fraction of the immunoprecipitated material was subjected to an *in vitro* phosphatase

assay as described before. In parallel, proper pull-down of endogenous PP4R1 and PP4c proteins was assessed by SDS-PAGE of immune complexes and immunoblotting. Indeed, TCR stimulation led to a strong and transient rise in PP4R1-associated phosphatase activity that reached its maximum at about 25 minutes post stimulation indicating that the PP4R1/PP4c module is itself subject to regulation by TCR triggering (Fig. 5.14 B,C).

PP4R1 physically interacts with the IKK complex while PP4c forms the catalytically active subunit of the PP4 holoenzyme. Moreover, activating mutations of IKKβ T loop serine residues to phosphomimetic glutamate prevented NF-κB inhibition by PP4R1 (Fig. 5.13 D). To examine whether PP4R1 and PP4c cooperate to catalyze dephosphorylation of IKKβ T loop serines *in vitro*, HEK293T cells were transfected with expression plasmids encoding for FLAG:IKKβ either alone or in combination with increasing cDNA concentrations of HA-tagged PP4R1 and/or expression plasmids encoding for HA-tagged PP4c. Overexpression of exogenous IKKs is known to cause kinase transautophosphorylation and activation by induced-proximity. To monitor IKKβ phosphorylation, cells were lysed and exogenous IKKβ was pulled-down by anti-FLAG immunoprecipitation followed by immunoblotting with phospho-specific antibodies. As seen in Fig. 5.14 D, the presence of either ectopic PP4R1 or PP4c was already sufficient to mediate a slight reduction in IKKβ phosphorylation. However, combined PP4R1 and PP4c overexpression completely blunted IKKβ phosphorylation. Overexpression of HA-tagged versions of PP4R1 and PP4c was confirmed by immunoblotting.

To test whether IKKα and IKKβ are similarly targeted and dephosphorylated by the PP4R1/PP4c holoenzyme, a reconstituted *in vitro* phosphatase assay was established. For this, FLAG-tagged forms of IKKα or IKKβ were separately overexpressed in HEK293T cells. IKK-overexpressing cells were then stimulated with PMA/ionomycin and IKKs were immunoprecipitated from whole cell lysates by anti-FLAG immunoprecipitation. Phosphorylated exogenous IKK proteins were recombined and served as substrates in a subsequent phosphatase reaction. For this purpose, HA:PP4R1 or HA:PP4c were separately expressed in HEK293T cells and purified by anti-HA immunoprecipitation. Anti-HA immunoprecipitates were then co-incubated with equivalent portions of FLAG-tagged IKK substrates. Subsequently, combined immune complexes were resolved by SDS-PAGE and IKK phosphorylation was analyzed by immunoblotting. As seen in Fig. 5.14 E, purified PP4R1 and PP4c proteins were equally sufficient to mediate dephosphorylation of both recombinant phospho-IKKα and phospho-IKKβ. Of note, exogenous PP4R1 was associated with endogenous PP4c which most likely conferred catalytic activity.

In a similar experiment, it was examined whether PP4R1 and PP4c mediate dephosphorylation of the endogenous activated IKK complex *in vitro*. Therefore, the phosphorylated IKK complex was immunoprecipitated by anti-NEMO antibodies from whole cell lysates of Jurkat T cells that had been stimulated by treatment with PMA/ionomycin. Purified endogenous phospho-IKK proteins were then subjected to a reconstituted *in vitro* phosphatase activity assay as described before. Again, immunoprecipitated PP4R1 and PP4c proteins mediated complete dephosphorylation of IKKα/β and reversed the phospho-IKK signal to basal levels (Fig. 5.14 F).
In summary, these data demonstrate that (i) PP4R1 regulates and potentiates PP4c phosphatase activity, (ii) that phospholytic activity exerted by the endogenous PP4R1/PP4c complex is transiently increased by TCR stimulation, and (iii) that PP4R1 synergizes with PP4c to catalyze dephosphorylation of IKK proteins *in vitro*.

5.3 Expression and function of PP4R1 in Sézary T cells

The Sézary syndrome is an aggressive version of CTCL that is characterized by the presence of highly proliferating malignant T cells in the blood of Sézary patients (Klemke et al., 2005). Recent studies provided evidence for constitutive NF-κB activation in Sézary T cells that is crucial for CTCL survival (Izban et al., 2000; Kiessling et al., 2009; Sors et al., 2006). Hence, deregulation of NF-κB is most likely a central event that is required for the maintenance of the malignant phenotype of Sézary T cells. However, the molecular aetiology and genetic aberrations underlying constitutive NF-κB signaling in this subtype of CTCL remain largely enigmatic. The present study identified PP4R1 as an important negative regulator of NF-κB signaling in T lymphocytes. Therefore, the following analyses were conducted with the goal to elucidate a potential role of PP4R1 in the molecular pathogenesis of the Sézary syndrome.

5.3.1 Diminished expression of PP4R1 in a fraction of Sézary T cells

Forced RNAi-mediated PP4R1 deficiency in Jurkat T cells as well as in primary human T lymphocytes had been demonstrated to cause constitutive IKK phosphorylation and hyperactivation as well as enhanced IκBα degradation. Therefore, it was tempting to speculate whether chronic NF-κB signaling in Sézary T cells, at least for a subgroup of cells, occurs as a result of diminished PP4R1 expression.

To test this hypothesis, whole cell lysates of four different CTCL cell lines, SeAx, MyLa, Hut78, and HH, as well as lysates derived from the leukemic and non-CTCL T cell lines Jurkat, or CEM, or from non-malignant *in vitro* expanded primary human T cells were subjected to SDS-PAGE and endogenous protein levels were determined by immunoblotting using primary antibodies as indicated. As seen in Fig. 5.15 A, two different Sézary T cell lines showed significantly diminished PP4R1 protein levels compared to Jurkat T cells. PP4R1 expression in Hut78 cells was reduced by about 50% and HH cells completely lacked PP4R1 protein expression (Fig. 5.15 A right panel). By contrast, SeAx and MyLa cells expressed PP4R1 similar to Jurkat, CEM and primary T cells. Interestingly, PP4c and the related phosphatase subunit PP2Ac as well as other T cell signaling components were equally abundant in all tested cell lines, indicating specific dysregulation of PP4R1 protein expression in a subset of CTCL cell lines. Solely, IKKβ expression levels seemed to be elevated in PP4R1-deficient HH cells.

Decreased or absent PP4R1 protein expression in Hut78 and HH cells, respectively, was reflected by diminished PP4R1 mRNA levels as determined by qPCR (Fig. 5.15 B). Hut78 cells displayed about 40% of PP4R1 mRNA expression relative to Jurkat T cells, and HH cells virtually lacked PP4R1-specific transcripts. Again, SeAx and MyLa cells exhibited a similar expression pattern compared to Jurkat cells. Moreover, defective mRNA expression was specifically assigned to PP4R1, since expression of PP2Ac was largely unaffected.

To investigate PP4R1 expression in primary Sézary cells, T lymphocytes were isolated from peripheral blood of a number of patients suffering from Sézary syndrome and PP4R1 mRNA levels were analyzed by qPCR. For transcriptional profiling only those samples were included that showed tumor loads of generally at least 60% as determined by microscopical evaluation of blood smears. At large, the percentage of Sézary T cells relative to whole lymphocytes in peripheral blood samples was about 70% with $CD4^+$ to $CD8^+$ T cell ratios between 11 and 99 as evaluated by flow cytometry (Klemke et al., 2008). Indeed, compared to peripheral T cells from normal healthy donors, peripheral blood T cells of Sézary patients exhibited a reduced expression of PP4R1 mRNA (Fig. 5.15 C). Overall, median expression of PP4R1 was reduced by more than 50% in patient samples relative to control samples.

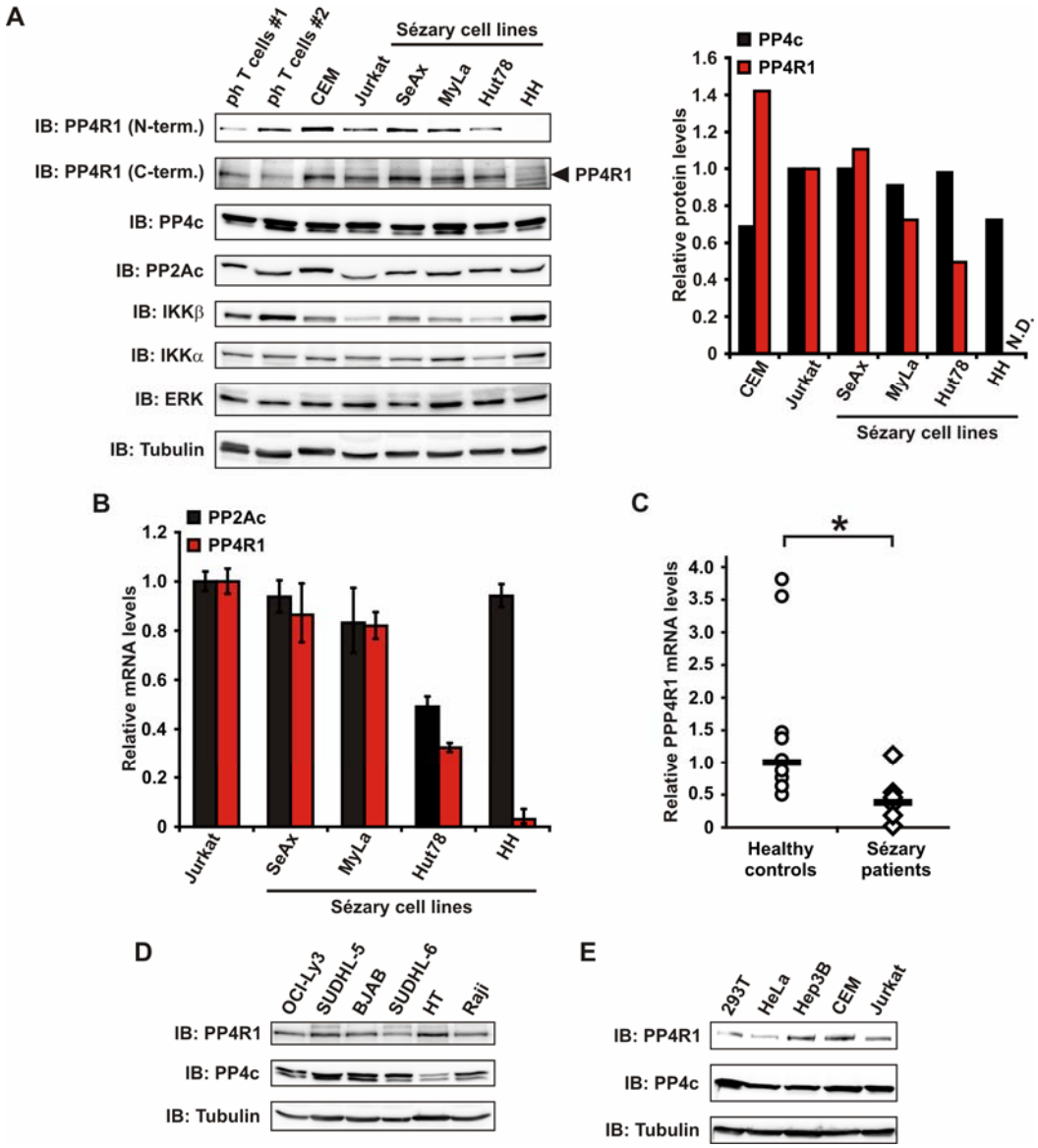

Figure 5.15 | Subgroups of Sézary cell lines and primary Sézary cells display diminished PP4R1 protein and mRNA expression. (A) Whole cell lysates derived from expanded day 6 primary human T lymphocytes (two independent donors), Jurkat, CEM or different CTCL cell lines were subjected to SDS-PAGE followed by immunoblotting using primary antibodies as indicated. For anti-PP4R1 immunoblotting two different PP4R1-specific antibodies, either recognizing N-terminal or C-terminal epitopes, were used. (Filled arrowhead indicates PP4R1). Reprobing with anti-Tubulin antibodies verified equal loading (left panel). Endogenous PP4c and PP4R1 expression was normalized to Tubulin levels and quantified as fold levels relative to Jurkat cells (right panel). **(B)** mRNA levels of PP2Ac and PP4R1 in CTCL cell lines were determined by qPCR. Levels are shown as fold change relative to Jurkat cells. (N.D.: not detectable). **(C)** Similar to **(B)** mRNA levels of peripheral blood T cells derived from normal healthy controls (10 donors) or Sézary patients (12 donors) were quantified by qPCR. Bars indicate median values. Expression was calculated as fold change to median expression of controls (Student's t-test, p=0.01699). **(D,E)** Analogous to **(A)** whole cell lysates of different human B cell lines **(D)** or epithelial cell lines in addition to lysates of CEM and Jurkat cells **(E)** were subjected to SDS-PAGE. Expression of PP4R1 and PP4c proteins was assessed by immunoblotting. Reprobing with anti-Tubulin antibodies verified equal loading.

Similarly to Sézary T cells, aberrant NF-κB activity has been reported for a number of clinically distinct B cell lymphomas among which the DLBCL plays a prominent role (Alizadeh et al., 2000; Ngo et al., 2006; Rosenwald et al., 2002). Whereas the ABC-DLBCL subtype critically relies on constitutive NF-κB signaling for lymphoma survival, the GCB-DLBCL subtype does not (Davis et al., 2001). To examine the expression of PP4R1 in different NF-κB-dependent or independent B cell lines, whole cell lysates from ABC-DLBCL (OCI-Ly3, SUDHL-5) and GCB-DLBCL (BJAB, SUDHL-6) cell lines, respectively, as well as lysates from the diffused mixed lymphoma line HT or the Burkitt lymphoma cell line Raji were subjected to SDS-PAGE and PP4R1 and PP4c expression were assessed by immunoblotting. Although expression of both PP4 phosphatase subunits differed slightly among the different cell lines, no specific reduction in expression of either phosphatase protein was observed for NF-κB-dependent ABC-DLBCL cells (Fig. 5.15 D). Moreover, expression of PP4R1 and PP4c was further investigated in a number of non-lymphoid epithelial cell lines. Interestingly, the human cell lines HeLa and HEK293T displayed low PP4R1 protein levels, while PP4R1 was similarly abundant in the hepatic cell line Hep3B compared to CEM or Jurkat T cells (Fig. 5.15 E).

In summary, it was demonstrated that a fraction of Sézary T cells derived from Sézary patients as well as a subgroup of CTCL cell lines exhibit defective or completely lack endogenous PP4R1 expression. Abrogration of PP4R1 expression was observed both on protein and mRNA levels and was highly gene-specific, since expression of PP2Ac was almost not altered.

5.3.2 Overexpression of PP4R1 reverses constitutive IKK activity and limits survival of PP4R1-deficient Sézary T cells

To confirm and examine on a genetic level whether CTCL Sézary T cells display enhanced basal NF-κB signaling, the transcription profile of a variety of different NF-κB target genes was determined. For this, basal mRNA levels of selected target genes in different Sézary cell lines, such as SeAx, Hut78, and HH, were quantified using a qPCR expression array. As a control, mRNA expression in Jurkat T cells, a non-CTCL leukemic T cell line, was determined. In accordance with published observations (Izban et al., 2000; Sors et al., 2006), Sézary cells showed a specific NF-κB target gene expression signature that was most pronounced for Hut78 and HH cells (Fig. 5.16 A). Interestingly, HH cells lacked expression of anti-apoptotic Bcl2 family members Bcl2A1 and Bcl2L11, but showed strongly upregulated expression of c-IAP1 (*BIRC2*) and c-IAP2 (*BIRC3*). Even more

strikingly, expression of the *bona fide* NF-κB target genes IκBα (*NFKBIA*) and A20 (*TNFAIP3*) was increased by more than 10-fold in HH cells compared to Jurkat T cells. Moreover, Hut78, HH, and to a lesser extend SeAx cells exhibited significantly increased expression of *NFKB1*, *NFKB2*, and *RELB*. Remarkably, expression of *STAT5A* was uniformly increased in all Sézary cell lines by up to 70-fold.

Consistent with constitutive NF-κB signaling inhibition of the NF-κB pathway in Sézary T cells, either derived from cell lines or primary patient material, had been recently shown to cause spontaneous cell death *in vitro* (Kiessling et al., 2009). However, for most Sézary cell lines it has not been clarified yet at what stage within the TCR or NF-κB signaling cascade constitutive signaling activity is exerted. To examine IKK activity in Jurkat T cells and Sézary T cells under resting conditions, the IKK complex was immunoprecipitated by anti-NEMO antibodies from whole cell lysates of unstimulated cells. Subsequently, kinase activity and phosphorylation were measured by autoradiography. As seen in Fig. 5.16 B, Jurkat T cells as well as SeAx and MyLa cells exhibited weak IKK phosphorylation in the absence of stimulation. By contrast, increased basal IKK phosphorylation was observed for Hut78 cells and was even more striking for PP4R1-deficient HH cells.

So far, inverse correlation between PP4R1 expression and enhanced basal IKK activity implied but did not formally prove a causative role of PP4R1 deficiency in constitutive IKK signaling in Sézary T cells. To directly address this question, it was tested whether aberrant IKK activity was rescued by reconstitution of PP4R1 expression in PP4R1-deficient HH cells. To this end, FLAG-tagged IKKβ was transiently overexpressed with or without exogenous HA-tagged PP4R1, and IKKβ phosphorylation was monitored by anti-FLAG immunoprecipitation and autoradiography. Intriguingly, overexpressed exogenous IKKβ in HH cells was highly phosphorylated, consistent with constitutive activation of the endogenous IKK complex in this cell line (Fig. 5.16 C). However, co-overexpression of PP4R1 completely prevented IKKβ activation, demonstrating that re-expression of PP4R1 is sufficient to reverse the phenotype of IKK hyperactivation in HH cells. In line with these results, basal NF-κB luciferase reporter activity in PP4R1-deficient HH cells was substantially elevated compared to PP4R1-sufficient Jurkat T cells, and this NF-κB phenotype was again reversed by re-expression of exogenous PP4R1 (Fig. 5.16 D).

Preceding experiments had uncovered PP4R1 as a potent negative regulator of the NF-κB pathway in T lymphocytes. Moreover, PP4R1 expression is reduced in a subset of primary Sézary cells and CTCL cell lines that exhibit and rely on chronic NF-κB signaling for survival.

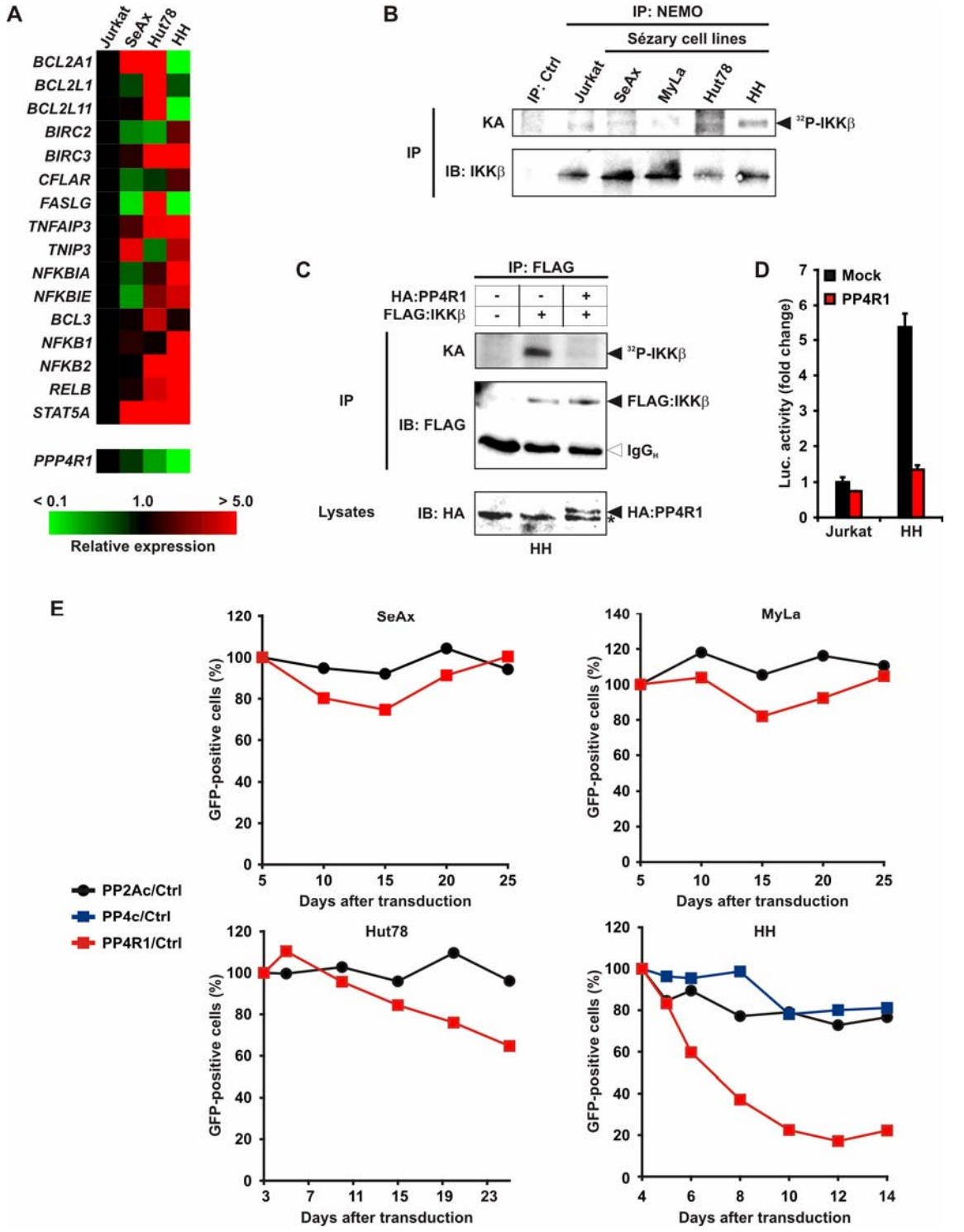

Figure 5.16 | PP4R1 overexpression reverses constitutive IKK activity and causes spontaneous cell death specifically in PP4R1-deficient Sézary cells. (A) Basal mRNA expression levels of various NF-κB target genes were examined in Sézary cell lines using a qPCR gene expression array. In addition, PP4R1 mRNA levels were determined. Relative expression is shown as fold change compared to Jurkat cells. Decreased and increased relative expression levels are shown in green and red, respectively, according to the colour scale shown. **(B)** The IKK complex was immunoprecipitated from whole cell lysates of unstimulated cells by anti-NEMO antibodies as indicated. In addition, immunoprecipitation of Jurkat lysates by a non-precipitating

antibody was included to control for specificity. Immune complexes were divided and subjected either to an *in vitro* kinase assay using radioactively labeled [γ-^{32}P]ATP or to SDS-PAGE followed by anti-IKKβ immunoblotting. **(C)** HA:PP4R1 was transiently overexpressed in HH cells, alone or together with FLAG:IKKβ. 24 h post transfection cells were lysed, followed by anti-FLAG immunoprecipitation of whole cell lysates. Immunoprecipitates were subjected to an *in vitro* kinase assay as described in **(B)** or subjected to SDS-PAGE and immunoblotting. Overexpression of HA:PP4R1 was assessed by SDS-PAGE and anti-HA immunoblotting of whole cell lysates. **(D)** PP4R1 was transiently overexpressed in Jurkat and HH cells. NF-κB activity in resting cells was measured using a co-transfected NF-κB-specific reporter luciferase system. Fold activity is shown relative to that of control-transfected Jurkat cells. Mean and SD of luciferase activity are representative of dublicate measurements. **(E)** Indicated CTCL cell lines were retrovirally transduced with overexpression vectors encoding for PP4R1, PP4c, and PP2Ac, respectively. Frequency of transduced cells was monitored over time by flow cytometry based on IRES-driven co-expression of GFP. Percentage of GFP-positive cells was normalized to that of control-transduced cells.

Therefore, it was tested next whether PP4R1-mediated IKK inhibition is sufficient to induce spontaneous cell death of Sézary T cells *in vitro*. To this end, cDNA encoding for HA-tagged PP4R1 was cloned into a GFP-expressing retroviral vector and four different Sézary cell lines were retrovirally transduced. In addition, empty vector and retroviral vectors for overexpression of PP2Ac or PP4c were included. Co-overexpression of GFP by means of an internal ribosome entry site (IRES) sequence allowed for the tracing of retrovirally transduced cells by flow cytometry. Indeed, re-expression of PP4R1 reduced the frequency of GFP-positive PP4R1-expressing Hut78 and HH cells relative to control-infected cells over time (Fig. 5.16 E lower panels). Remarkably, HH cells that completely lack endogenous PP4R1 were highly sensitive towards PP4R1 overexpression, whereas the frequency of PP4R1-expressing Hut78 cells declined continuously, but less rapidly. By contrast, PP4R1-sufficient MyLa and SeAx Sézary cells were completely refractory to PP4R1 overexpression (Fig. 5.16 E upper panels). Intriguingly, lethality of PP4R1 overexpression was highly specific in HH cells since ectopic PP4c had almost no impact on cell survival. Moreover, there was no toxicity of forced PP2Ac expression in all tested cell lines.

Taken together, these data demonstrate that PP4R1 deficiency in a subset of Sézary cell lines is causative for constitutive IKK phosphorylation and activation. Consistently, PP4R1 re-expression was highly toxic for PP4R1-deficient Sézary cells while PP4R1-sufficient cells were largely resistant to forced overexpression of exogenous PP4R1. These results establish PP4R1 not only as a gatekeeper of IKK activity but also as physiological suppressor of T cell activation and lymphomagenesis.

6. Discussion

The transcription factor NF-κB plays a key role in the immune system by governing lymphocyte activation, proliferation, and survival (Vallabhapurapu and Karin, 2009). Physiological NF-κB activity requires precise control by positive and negative regulatory mechanisms. Whereas disruption of NF-κB signaling is known to cause severe immune defects, constitutive NF-κB activity has been implicated in several lymphoid malignancies and autoimmune diseases (Li and Verma, 2002; Staudt, 2010).

Signal transduction to NF-κB from engaged cell surface receptors, such as the TCR or TNFR1, proceeds rapidly and involves multiple well-characterized phosphorylation events (Mayya et al., 2009; Viatour et al., 2005). A large body of literature has described a plethora of kinases and phosphorylated target proteins as being indispensable for TCR-induced NF-κB activation, ranging from upstream signaling platforms to the IKK complex and NF-κB subunits themselves (Hacker and Karin, 2006; Hayden and Ghosh, 2008). In marked contrast, a detailed understanding of mechanisms controlling NF-κB signal termination is only starting to emerge. In this context, recent progress has been made with the identification of Ub-editing enzymes, such as A20 and CYLD, that counterbalance the activity of proximal signaling complexes downstream of several pro-inflammatory receptors (Brummelkamp et al., 2003; Lee et al., 2000). However, negative regulation of phosphorylation in NF-κB signaling is only partially understood – despite the abundance and critical role of the NF-κB-activating phospho-proteome.

In few cases, phosphorylation has been shown to mediate protein degradation, thereby promoting signal interception and termination in a negative feedback fashion (Bidere et al., 2008; Lobry et al., 2007; Moreno-Garcia et al., 2010; Wegener et al., 2006). Nonetheless, most stimulation-dependent phosphorylation events are transient and reversible, implying the opposing action of kinases and phosphatases in controlling the phosphorylation state of NF-κB signaling components. In support of the concept of reversible and site-specific protein (de)phosphorylation, several phosphatases have been already implicated in negative regulation of a number of distinct phosphorylation-dependent signaling pathways, such as in signal transducer and activator of transcription (STAT) signaling (Nakahira et al., 2007), JNK signaling (Eichhorn et al., 2007), or in the MAPK cascade (Liu et al., 2007). The role of individual phosphatases in NF-κB signaling is less well defined. Most studies were based on phosphatase inhibitors and overexpressed proteins, limiting conclusions regarding specificity and functional importance of endogenous proteins under

physiological conditions (see 1.4.3). Only few genetic studies demonstrated the selective involvement of different phosphatase entities in NF-κB inhibition and dephosphorylation of specific phosho-substrates (Chew et al., 2009; Li et al., 2008; Li et al., 2006b). However, the results of these studies do not allow for a generalized and comprehensive picture of NF-κB-modulating phosphatases, especially with regard to different receptor systems and cellular contexts (*e.g.* T lymphocytes). (i) Most studies were conducted on the basis of TNFα-induced NF-κB signaling and thereby did not address phosphatases specifically targeting signaling proteins of the TCR-induced NF-κB pathway. (ii) So far, genetic screens and functional analyses of phosphatase activity were uniformly performed using non-lymphoid cellular systems, such as human epithelial cell lines. Contradictory results among different approaches already suggested species and cell type-specific patterns of expression and/or activity of individual phosphatase components. Therefore, a systematic examination of NF-κB-modulating phosphatases in T lymphocytes is still elusive.

The current study has been conducted with the aim to functionally define phosphatases that are involved in TCR-induced NF-κB signaling. Using a novel NF-κB reporter system a large-scale RNAi-based loss-of-function screen in T cells has been adopted. Several novel phosphatases were uncovered as negative regulators of TCR-dependent NF-κB signaling. Subsequent experiments were performed to confirm candidate genes and to gain a more detailed understanding of the functional roles of individual phosphatases in lymphocyte biology.

6.1 Analysis and evaluation of the phosphatase RNAi screen: technical aspects and genetic understanding

6.1.1 RNAi screening in mammalian systems: strategies and restrictions

RNAi has emerged as a powerful technique of reverse genetics and has opened up new avenues for large-scale genetic screens aiming at identifying genetic components underlying specific cellular processes or signaling pathways (Boutros and Ahringer, 2008; Moffat and Sabatini, 2006). For mammalian systems, genome-scale RNAi screens have been largely hampered by lack of suitable tools for efficient gene silencing under HTS conditions. To date a number of subgenome-wide RNAi screens in human cells have been reported. Most of these screening approaches were based on morphology or viability phenotypes that are likely to integrate various signaling pathways. Examples include RNAi screens for genes regulating apoptosis sensitization (za-Blanc et al., 2003),

cell survival (Barbie et al., 2009; Luo et al., 2009a; MacKeigan et al., 2005), proliferation (Berns et al., 2004), and transformation (Kolfschoten et al., 2005) (for review see Boutros and Ahringer, 2008; Moffat and Sabatini, 2006). However, screening approaches in human cells that are based on directed transcriptional reporter assays and therefore allow for the systematic dissection of specific signaling pathways are technically challenging. Only few examples of reporter-based screens in human epithelial cell lines have been reported (Brummelkamp et al., 2003; Chew et al., 2009; Major et al., 2008).

RNAi-based loss-of-function screens in immune cells turned out to be even more difficult and require sophisticated strategies for efficient gene silencing. Lymphocytes are largely refractory to transient siRNA transfection. Usually, conventional electroporation of T lymphocytes requires high concentrations of siRNA and is further complicated by decreased cell viability (Sharma and Rao, 2009). Therefore, most screens were conducted on the basis of shRNA libraries delivered by viral transduction and selection of stable integrants (Root et al., 2006). Using this method several molecular targets required for proliferation and survival of B cell lymphoma cells have been successfully identified (Davis et al., 2010; Lenz et al., 2008). Recently, a shRNAi screen in T cells led to the discovery of a specific splicing factor involved in CD45 alternative splicing (Oberdoerffer et al., 2008). To date, only one shRNA library-based screen has been reported for primary T lymphocytes that revealed regulators of IL-10 secretion (Astier et al., 2010).

Design and implementation of systematic RNAi screens in mammalian systems require the optimization of several experimental conditions and involve a multi-step protocol that can be generalized as follows (Falschlehner et al., 2010; Moffat and Sabatini, 2006):

(i) *screen preparation* (development of appropriate cell-based reporter assays, optimization of transfection conditions, and library design)
(ii) *screen performance* (screen protocol under HTS conditions)
(iii) *screen and post-screen analysis* (data pre-processing, normalization, statistical analysis, as well as candidate selection, validation, and characterization)

The adaptation of these parameters provided the basis of the present RNAi screening strategy that led to the identification of several phosphatases regulating TCR-induced NF-κB activity. Major technical and biological aspects of the RNAi screen will be discussed in the following sections.

6.1.2 Gluc-J16 reporter cells: a novel NF-κB screening system in T cells

The development of an appropriate and validated phenotypic assay is the core element of a successful RNAi screening strategy. In order to measure transcriptional activity of a signal transduction pathway of interest, a primary assay system is needed that has to be robust, sensitive, and specific with respect to signal manipulation, as well as adoptable to HTS conditions. Luciferase-based transcriptional reporters are especially amenable to screening experiments since they allow for the rapid quantification of signaling activity on a large scale (Boutros and Ahringer 2008; Moffat and Sabatini, 2006).

In the present study a novel NF-κB dependent screening system based on expression of secreted luciferase in T lymphocytes has been generated. To this end, Jurkat-derived J16-145 T cells (Gulow et al., 2005) were engineered with stable genomic integration of a NF-κB-dependent *Gaussia* luciferase cassette (Gluc-J16 cells) (Fig. 5.1 and 5.2). The reporter system was highly sensitive towards TCR or TNFR stimulation and responded synergistically towards TCR and CD28 co-stimulation (Fig. 5.2).

RNAi-based gene silencing in reporter cells was based on transient siRNA delivery according to a novel nucleofection protocol that is suitable for siRNA transfections under HTS conditions (see 4.3.3 and 4.3.4). In pre-experiments transfection and stimulation conditions were optimized and established Gluc-J16 cells as a valuable tool for large-scale RNAi screening experiments (Fig. 5.3-5.5). As expected and in accordance with published observations, siRNA-mediated knock-down of *bona fide* positive or negative regulators of the TCR and/or TNFR1-induced NF-κB signaling pathway resulted in significant reduction and enhancement of luciferase secretion, respectively (Fig. 5.3 and 5.4, Frey, 2009). The fact that reporter cells similarly respond to TCR or TNFR1 stimulation was exploited by a dual screening strategy that enabled the synoptic analysis of phosphatases modulating TCR and/or TNFR-induced NF-κB activity (see section 5.1.5 and Frey, 2009). In addition to signal manipulation by RNAi, the reporter system was shown to be sensitive to NF-κB inhibition by chemical compounds (Fig. 5.4 and data not shown). Future applications of the Gluc-J16 NF-κB screening system might therefore not only comprise further subgenome-wide RNAi screens (*e.g.* targeting kinases or Ub-editing enzymes), but also small-molecule screens to identify (pathway-specific) pharmacological inhibitors of NF-κB (Fig. 6.1).

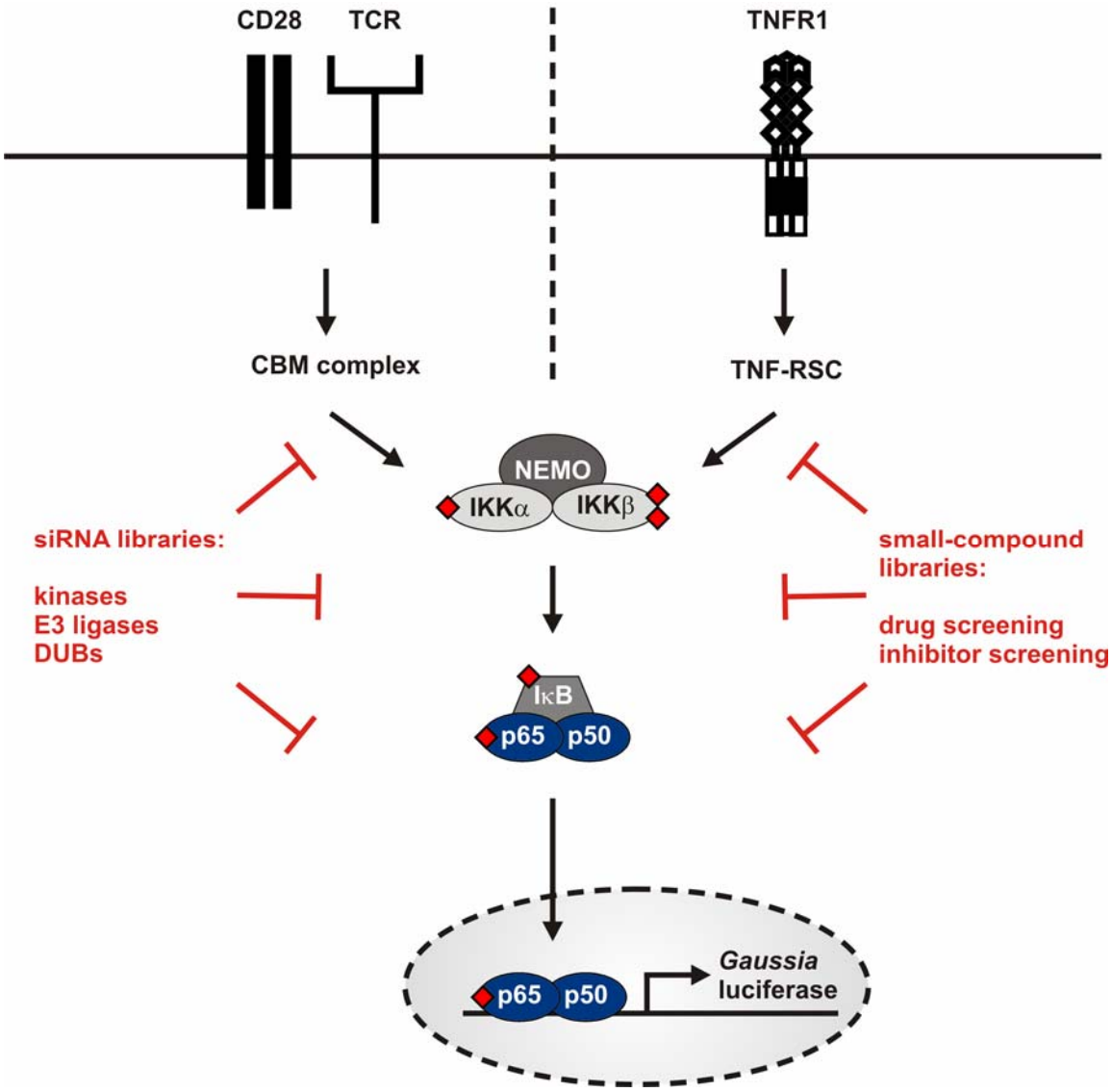

Fig. 6.1 | Possible screening applications of the Gluc-J16 NF-κB reporter system. The RNAi screening protocol that was designed for the Gluc-J16 reporter system may be suitable for further screening approaches based on siRNA libraries targeting specific classes of signaling modifiers, such as kinases, E3 ligases, or deubiquitinating enzymes (DUBs). Moreover, the application of large-scale small-compound libraries may enable drug screening to identify novel (pathway-specific) pharmacological inhibitors of the NF-κB pathway. Compound screening based on known chemical inhibitors of effector enzymes (*e.g.* kinase or phosphatase inhibitors) can complement RNAi screening strategies to confirm and validate candidate genes on a large scale.

6.1.3 Post-screen analysis of primary RNAi phosphatase screening

(i) Screen robustness and sensitivity: positive controls and hit selection

For identification of candidate phoshatase genes (hits) RNAi phenotypes – based on mean values of normalized NF-κB activity – were scored for statistical significance. To this end, normalized measurements were transformed into the statistical *z* score (Boutros et al., 2006). Data transformation allows for the analysis of statistical normality which is instrumental in defining appropriate thresholds for hit selection. Using a quantile-quantile (QQ) plot analysis (Ramadan et. al., 2007) (Fig. 5.5 A) *z* score deviations from normally (randomly)-distributed values indicated statistically significant RNAi phenotypes. For the present screen *z* scores > +1.5 and < -1.5 were defined as cut-offs values (Fig. 5.5 A,B). To facilitate secondary screening and to minimize the numbers of false-positives, only those phosphatase genes were categorized as tentative candidates that scored with at least two independent siRNAs beyond given *z* score thresholds (Table 5.1). Definition of cut-offs for hit selection depends on the individual screening system and is recommended to be adapted empirically to ensure a proper balance between sensitivity and specificity (Ramadan et. al., 2007). Too stringent definitions might lead to a high rate of false-negatives, whereas more permissive criteria might enrich for false-positive candidates (Echeverri et al., 2006).

A first step in assessing sensitivity of RNAi screening and statistical analysis involves the inspection of positive controls (Ramadan et. al., 2007). Remarkably, almost all positive control siRNAs were identified as statistically significant hits (Fig. 5.5 B). Knock-down of Carma1 and RelA, respectively, translated into robust and distinct RNAi phenotypes with low variability across individual plates. Similarly, siRNA-mediated silencing of CYLD led to significant NF-κB phenotypes. In general, CYLD-specific siRNAs uniformly scored with z scores above +1.5. The relative strength of RNAi phenotypes varied among positive controls. siRNAs targeting positive regulators conferred highly stable and significant phenotypes with Z scores < -10.0, whereas CYLD knock-down yielded less strong z scores in the range of +1.0 to +4.3. Robust phenotypes of positive controls were reflected by highly efficient silencing of control genes on mRNA and protein levels, further underscoring the validity of the HTS protocol (Fig. 5.5 C,D). Interestingly, non-targeting control siRNAs seemed to be biased towards negative z scores. Thus, the threshold for identification of positive regulators might be further decreased to minimize numbers of false-positive candidates.

In summary, the distributions of negative and positive control values showed significant and sufficient separation. Importantly, the dynamic range of phenotypes enabled bidirectional screening for positive and negative regulators of NF-κB. QQ plot-based statistical criteria for hit selection allowed for high screening sensitivity as reflected by scoring of almost all positive control siRNAs.

(ii) False-positive and false-negative candidate phosphatases

Another measure of screening sensitivity refers to the number of confirmed genes that were expected *a priori* to be identified as candidate modifiers (Ramadan et. al., 2007). The present screen identified six phosphatases as suppressors and six phosphatases as activators of TCR-induced NF-κB activity (Table 5.1).

Among NF-κB-activating candidate genes, two phosphatases, PTPN9 (MEG2) and PTPRN, were previously implicated in TCR and NF-κB signaling, respectively. Using a similar RNAi screening approach in murine astrocytes, Li et al. identified PTPRN as a NF-κB-activating phosphatase regulating both basal and TNFα-induced NF-κB activity (Li et al., 2006b). Interestingly, PTPN9 has not been specifically associated with NF-κB signaling before, but is required for lymphocyte activation by inducing secretory vesicle fusion (Huynh et al., 2003; Huynh et al., 2004; Wang et al., 2005). PTPN9-deficient T lymphocytes almost completely lack mature secretory vesicles and display impaired IL-2 secretion (Wang et al., 2005). The unexpected identification of a vesicle-modulating phosphatase was due to the primary assay system that relies on the ER-dependent secretion of the *Gaussia* luciferase reporter. Indeed, a Gluc secretion assay was recently reported as a highly sensitive HTS technique to monitor secretory pathway activity and ER stress (Badr et al., 2007).

Surprisingly, negative regulatory candidates did not include any known phosphatases that were previously implicated in NF-κB signaling. Solely, the tyrosine phosphatase PTPRA – that had been reported to serve CD45-like functions in T cells (Maksumova et al., 2005; Maksumova et al., 2007) – was identified as an inhibitor of TCR-induced NF-κB activation. Both PTPN6 (SHP1) and PTPN22 did not match the criteria for hit selection although two PTPN22-specific siRNAs yielded *z* scores that were only marginally below the selection threshold (Table 5.1, reference phosphatases). PP2Ac, the catalytic subunit α isoform of the PP2A holoenzyme, has been associated with negative regulation of NF-κB by several independent laboratories based on genetic approaches, expression of recombinant protein, and the use of PP2A inhibitors (see 1.4.3). However, primary screening failed to

confirm PP2Ac as a NF-κB-suppressing phosphatase. Strikingly, only one PP2Ac-specific siRNA significantly enhanced TCR-induced reporter activity, whereas PP2Ac showed highest scores and was amongst the top candidates of the TNFR1-specific subscreen (Frey, 2009). These apparently contradictory findings prompted closer reinvestigation of the effect of PP2Ac gene silencing on TCR-induced NF-κB activity. Indeed, PP2Ac knock-down by several independent siRNA oligos led to an enhancement of NF-κB reporter activity, TCR-induced upregulation of NF-κB-dependent gene expression, and cytokine secretion. Thereby, PP2Ac-specific siRNAs largely mediated efficient gene silencing. Consistent with these genetic data, treatment of Jurkat T cells with the PP2A inhibitor okadaic acid amplified NF-κB reporter activity in response to PMA/ionomcyin and TNFα treatment (data not shown), further proving an involvement of PP2Ac in negative regulation of TCR- and TNFR1-induced NF-κB signaling.

Collectively, these results suggest that several false-negative phosphatases were not identified by primary screening. Overall, the percentage of false-negatives is difficult to assess. In general, error rates of about 15% in genome-wide screens have been suggested (Ramadan et. al., 2007), but certainly depend on the individual screening design. Experimental factors affecting screening sensitivity might include (i) limitations of the phenotypic assay system, (ii) loss of biological information by stringent *B* score normalization of raw data, (iii) thresholds of NF-κB activity and rigid criteria for candidate selection, and (iv) poor knock-down efficacies by non-functional siRNAs.

6.1.4 The NF-κB-modulating phosphatasome: How much phosphatases do we need?

A brief survey of the current literature reveals more than 20 phosphatases that were previously suggested or proven to be involved in either negative or positive modulation of NF-κB. The complexity of the NF-κB-modulating phosphatasome was further increased by the present screen which identified several novel phosphatases associated with TCR-dependent NF-κB activation (Table 5.1). Certainly, caution is warranted with respect to the *in vivo* relevance and substrate specificity of endogenous proteins unless detailed genetic, functional, and biochemical analysis is provided. Nonetheless, several questions may arise: How many phosphatases can one expect to participate in NF-κB signaling? How can one explain the apparently high number of phosphatase genes associated with NF-κB? What are the implications for specificity, redundancy, and robustness in NF-κB signaling?

A first aspect lies in the species, cell type, and pathway-specific expression and/or activity of individual phosphatase components (see also 1.4.3). For instance, Li et al. uncovered PTPRN as a NF-κB-activating phosphatase in murine astrocytes, but could not confirm gene activity in mouse fibroblasts (Li et al., 2006b). The same authors reported several PP2A regulatory and catalytic subunits to be involved in negative regulation of TNFα-induced NF-κB signaling. In marked contrast, a recent study reported a crucial role of PP1 in negative regulation of IKK activity upon TNFα stimulation in murine macrophages as well as in human HeLa and HEK293T cells, but failed to confirm PP2A-mediated inhibition of IKK phosphorylation and activation (Li et al., 2008). The discrepancy in the function of PP1 *vs.* PP2A with respect to IKK inactivation was explained by tissue and cell type specificity of phosphatase activity. Moreover, PP2A regulatory subunits were shown to specifically impinge upon TNFR-induced, but not IL-1R-dependent NF-κB signaling (Li et al., 2006b). The TNF-RSC employs the TRAF2 adapter, whereas the IL-1R complex relies on TRAF6. The regulatory subunit PP2R5C was reported to specifically confer PP2A-dependent dephosphorylation of TRAF2, and consequently, PP2R5C silencing by RNAi enhanced TNFα-dependent, but not IL-1-stimulated NF-κB signaling. Indeed, evidence for pathway-specific phosphatase activity was also obtained by the present TCR/TNFR1-specific subcreening strategy. Several phosphatases were identified as specific modulators of either TCR- or TNFR-dependent NF-κB signaling although the overlap between both screens was still remarkable (see also Frey, 2009).

Substrate-specific phosphatase activity does not only confer pathway specificity, but also allows for the differential regulation of distinct signaling steps within a single signal transduction cascade. For instance, Li et al. provided evidence for distinct functions of PP2A modules in the NF-κB pathway, including dephosphorylation of TRAF2, IKK, and NF-κB proteins (Li et al., 2006b). Consistently, PP2A complexes were shown before to modulate both IKK activity (DiDonato et al., 1997; Fu et al., 2003) and p65 dephosphorylation (Yang et al., 2001b). Moreover, a recent report assigned PP2A-mediated inhibition of NF-κB signaling to dephosphorylation of the IKK-K MEKK3 (Sun et al., 2010), while PPM1 phosphatases were implicated in the direct dephosphorylation of IKK proteins (Prajapati et al., 2004; Sun et al., 2009).

Intriguingly, phosphatase specificity does not only refer to protein recognition, but also involves site-specific discrimination of single phospho-residues within a given phospho-substrate. The WIP1 phosphatase, for example, mediates specific dephosphorylation of serine 536 of p65, but does not affect the phosphorylation of adjacent phospho-acceptor

sites (Chew et al., 2009). Conversely, site-specific and non-redundant phosphorylation has been described for multiple TCR proximal and NF-κB signaling components and involves an increasing number of kinases. For instance, Carma1 contains 142 putative phospho-acceptor sides, and selective phosphorylation of Carma1 by PKCθ (Matsumoto et al., 2005), HPK1 (Brenner et al., 2009), and CK1α (Bidere et al., 2008; Moreno-Garcia et al., 2009) has been suggested to differentially contribute to Carma1 signaling. It is tempting to speculate that with the phylogenetic implementation and diversification of kinases and phospho-proteins phosphatase activity adaptively co-evolved to ensure precise control of phospho-signaling circuits in multicellular organisms (Breitkreutz et al., 2010; Tan et al., 2009). From a theoretical perspective however, it is reasonable to assume that the sensitivity of signaling systems to dephosphorylation depends (i) on the signaling activity and (ii) on the half life of targeted signaling compounds. Control of the phosphorylation status of central signaling hubs with high and sustained activity and high protein stability certainly provides a more efficient mechanism of signal termination than dephosphorylation of auxiliary signaling proteins with eventually redundant functions.

Another aspect of the present RNAi screen is the large number of regulatory relative to catalytic PSP subunits that were identified as regulators of TCR-induced NF-κB signaling (Table 5.1; see also Frey, 2009). Most likely, this dichotomy reflects the combinatorial complexity of PSP holoenzymes through which non-catalytic subunits modify catalytic core components by conferring and/or increasing enzymatic activity as well as substrate specificity (Bennett et al., 2006). Probably, pleiotropic functions of almost all catalytic subunits in diverse cellular processes masked or interfered with potential NF-κB-specific loss-of-function phenotypes. However, it cannot be formerly excluded that NF-κB modulation by regulatory PSP subunits occurs independently of phosphatase activity, but involves additional and unknown effector functions.

Given the cellular and molecular complexity of phospho-substrates and phosphorylation events in NF-κB signaling it is not surprising that the present RNAi screen identified several novel phoshatases as regulators of NF-κB activity in T lymphocytes. The possibility of false-negative candidates as well as redundant or compensatory functions among related phosphatase components might even cause additional underestimates of the numbers of NF-κB-regulating phosphatases in T lymphocytes.

6.2 PP4R1 as a novel negative regulator of NF-κB in T lymphocytes

Primary RNAi screening as well as subsequent validation experiments revealed PP4R1 as a potent negative regulator of NF-κB activity in T lymphocytes. PP4R1 silencing in Jurkat T cells caused enhanced NF-κB reporter activity, upregulation of NF-κB-dependent gene expression, as well as cytokine secretion in response to TCR stimulation or PMA/ionomcyin treatment. Similarly, siRNA-mediated knock-down of PP4R1 in expanded primary human T lymphocytes amplified stimulation-dependent cytokine secretion, whereas ectopic PP4R1 almost completely blunted basal and induced NF-κB activity (Fig. 5.6-5.10). These findings prompted closer investigation of the biochemical mechanism through which PP4R1 regulates NF-κB signaling in T lymphocytes.

6.2.1 Molecular mechanism of PP4R1-mediated NF-κB inhibition: experimental evidence and remaining questions

(i) Direct inhibition of IKK signaling by PP4R1

The IKK complex forms a central signaling hub in canonical NF-κB signaling that couples and integrates various receptor signals to NF-κB transcriptional activity (Hayden and Ghosh, 2008). Several lines of evidence suggest a role of PP4R1 in directly counteracting IKK phosphorylation and activation (Fig. 6.2).

(1) PP4R1 was shown to physically interact with the native IKK complex in T lymphocytes. PP4R1 pre-associated with IKK components in resting cells, and this association was transiently increased upon stimulation. Thereby, the PP4R1-IKK interaction profile closely followed the kinetics of IKK activation (Fig. 5.11).

(2) Knock-down of PP4R1 in Jurkat cells dramatically enhanced IKK activation upon stimulation, whereas ectopic PP4R1 largely abrogated IKKβ kinase activity. Congruently, PP4R1-silenced Jurkat cells displayed constitutive IKKβ and increased IKKα phosphorylation, reduced basal levels of IκBα protein, as well as accelerated IκBα phosphorylation and degradation following stimulation. Enhanced basal and induced NF-κB activity as well as IKK hyperactivation in PP4R1-silenced Jurkat cells and PP4R1-deficient HH cells, respectively, was rescued by overexpression of ectopic PP4R1 (Fig. 5.13, 5.16 and data not shown).

(3) PP4R1 associates with the catalytic PP4 subunit PP4C (see 6.2.2) thereby confering IKK-specific phosphatase activity (Fig. 5.12). PP4R1 and PP4C synergized to catalyze dephosphorylation of T loop serine residues within IKKα and IKKβ *in vitro*, and PP4R1-associated phosphatase activity was increased upon TCR stimulation. As for IKK association, maximal PP4R1-associated phosphatase sharply followed the peak of IKK activity (Fig. 5.14). Moreover, PP4C associated with the IKK complex in Jurkat cells in a PP4R1-dependent manner (data not shown).

(4) Constitutively active IKKβ (IKKβ SS/EE) was sufficient to bypass PP4R1-mediated NF-κB inhibition (Fig. 5.13 D), and PP4R1 deficiency had no effect on PKCθ phosphorylation and activation (data not shown).

Collectively, these results support a role of PP4R1 as a gatekeeper of IKK activity in T lymphocytes counterbalancing the strength and duration of IKK/NF-κB signaling. However, several aspects still remain to be addressed in detail.

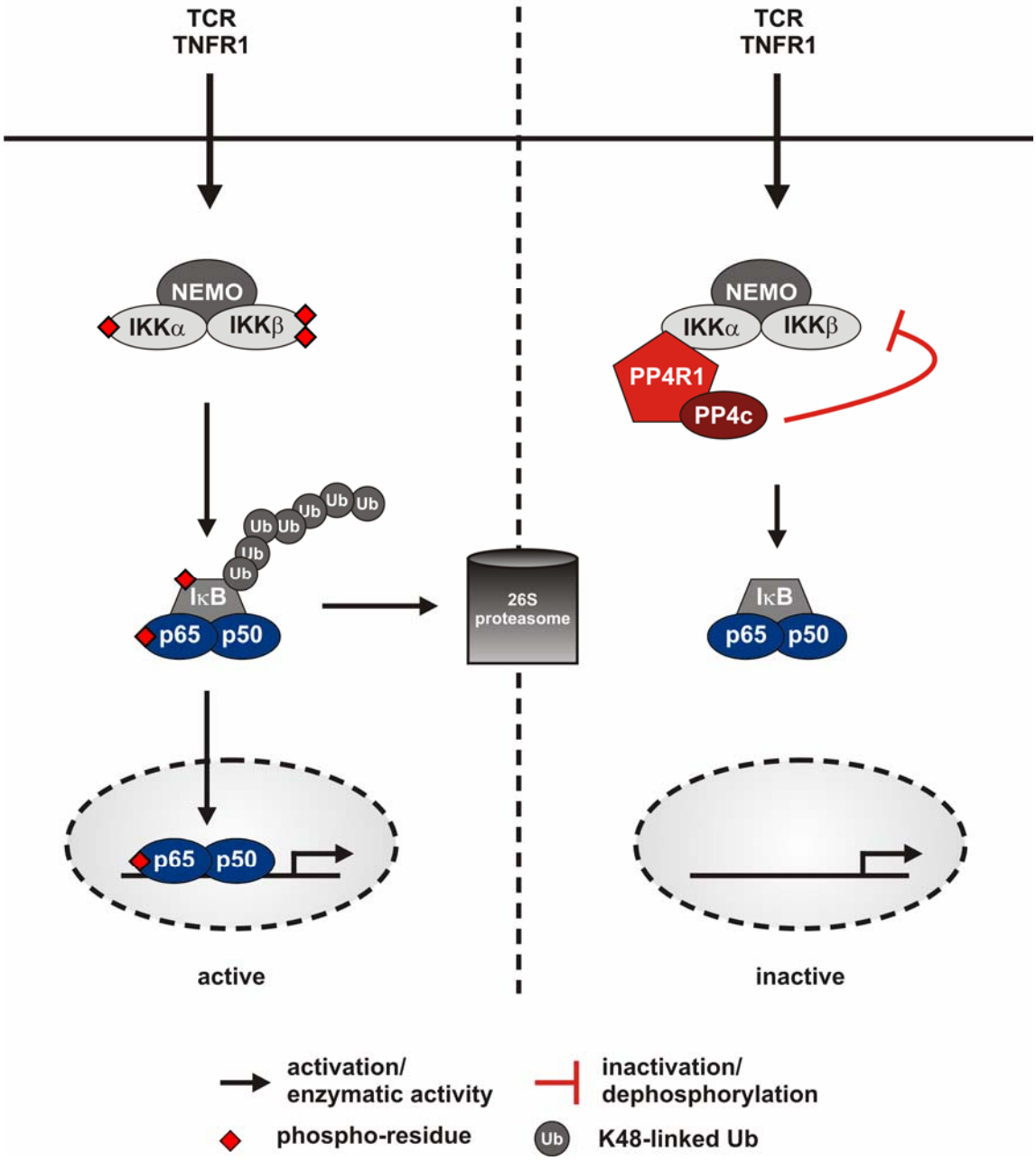

Figure 6.2 | Proposed mechanism of PP4R1-mediated IKK inhibition. TCR or TNFR1 engagement triggers phosphorylation and activation of the canonical IKK complex by upstream kinases and effector molecules. A phosphatase complex composed of PP4R1 and PP4c limits and terminates IKK activation through direct dephosphorylation of T loop ser residues within IKKα and IKKβ and most likely also inhibits spontaneous IKK (auto-)phosphorylation under resting conditions. Binding of the PP4R1/PP4c complex to the IKK complex involves most likely a direct interaction between IKKα and PP4R1 which act as adapter molecules to recruit the catalytically active PP4c subunit to its major substrate IKKβ (right side). Loss of PP4R1 expression results in deregulated IKK phosphorylation causing enhanced NF-κB dependent expression of target genes (left side).

(ii) Control of basal IKK phosphorylation and activity by PP4R1?

It is not yet precisely understood whether PP4R1 – in addition to inhibition of stimulation-dependent IKK activation – controls steady-state IKK activity. In transiently siRNA-transfected T cells no changes in basal NF-κB signaling were observed, neither with regard to NF-κB reporter activity, NF-κB-dependent gene expression or cytokine secretion, nor with respect to IKK kinase activity (Fig. 5.7, 5.8, 5.13 A). In contrast, stably silenced, shPP4R1-expressing Jurkat cells displayed constitutive IKKβ phosphorylation as well as reduced basal IκBα protein levels (Fig. 5.13 B). Moreover, PP4R1-deficient HH cells exhibited increased basal IKK and NF-κB activity which was reversed by PP4R1 re-expression (Fig. 5.16). However, basal IκBα phosphorylation did not seem to be increased, but was heavily triggered upon stimulation. Moreover, IKKα phosphorylation was not altered in unstimulated PP4R1-silenced cells, but was enhanced in response to PMA/ionomycin treatment. However, IKKβ was constitutively phosphorylated both in siRNA-transfected and shRNA-transduced Jurkat cells (Fig. 5.13 B). The discrepancy in IKKα *vs.* IKKβ phosphorylation may be explained by differential IKK substrate affinities of the PP4R1/PP4c complex. In addition, IKKβ is the dominant IKK component and its higher kinase activity may require tight control in activated and unstimulated cells. Furthermore, the observed experimental discrepancies might be due to differences in the efficacy of PP4R1 gene silencing. Residual PP4R1 protein upon transient siRNA-mediated silencing might be still sufficient to control basal IKK activity whereas stimulation-induced IKK activity is already markedly enhanced.

Moreover, it has been hypothesized that structural changes within the IKK complex – induced by NEMO serine 68 and IKK phosphorylation – may provide access for phosphatases to mediate IKK T loop desphosphorylation and inactivation (Palkowitsch et al., 2008). Stimulation-induced IKK-specific phosphatase activity is an attractive model of negative feedback regulation and may explain increased binding of PP4R1 to the IKK complex upon stimulation. However, it is likely that additional mechanisms exist to limit and prevent spontaneous IKK phosphorylation and activation under resting conditions.

(iii) Phospho-residue and pathway specificity of PP4R1?

Induction of IKK activity critically relies on phosphorylation of T loop serines of at least one IKK subunit. Activation of IKKβ involves phosphorylation of serine 177 and serine 181 within the activation T loop of the kinase domain, whereas in IKKα serine 176 and serine 180 need to be phosphorylated (Delhase et al., 1999; DiDonato et al., 1997).

Phosphorylation of these distinct residues is thought to impose conformational changes within IKKs thereby unleashing enzymatic activity (Hayden and Ghosh, 2008).

In the present study, enhanced phosphorylation of serine 180/181 of IKKα/β was observed as a result of PP4R1 deficiency (Fig. 5.13, 5.14). Whether PP4R1 analogously prevents or reverses serine 176/177 phosphorylation needs to be addressed by means of phospho-specific antibodies. The fact that PP4R1 silencing enhances overall IKK kinase activity, however (Fig. 5.13 A), makes it likely that phosphorylation of both IKK phospho-acceptor sides is negatively controlled by PP4R1. This assumption is further substantiated by the finding that dominant active IKKβ, in which serine 177 and serine 181 have been replaced by phospho-mimetic glumate residues (Mercurio et al., 1997), is uncoupled from PP4R1-mediated kinase inhibition (Fig. 5.13 D).

In contrast to T loop phosphorylation, several additional phospho-acceptor sides within IKK components have been described to mediate IKK inhibition. IKKβ contains several negative regulatory serine residues within a C-terminal autophosphorylation cluster, whose replacement by alanine residues confers increased basal and TNFα-induced IKKβ activity (Delhase et al., 1999). Moreover, phosphorylation of the IKK NBD serine residue 740 inhibits IKK activity by interfering with NEMO heterodimerization (May et al., 2002; Schomer-Miller et al., 2006). Autophosphorylation of these IKK serine residues is thought to provide an IKK intrinsic negative feedback mechanism (Hayden and Ghosh, 2008). Although PP4R1-associated phosphatase activity has been shown to counteract T loop phosphorylation and kinase activation it cannot be formerly ruled out that, in addition, PP4R1 interferes with phosphorylation of inhibitory serine residues within the IKK complex. Indeed, bifunctional IKK phosphatase activity has been already demonstrated for PP2A enzymes. Whereas PP2A has been shown to inhibit IKK phosphorylation and activation (DiDonato et al., 1997; Li et al., 2006b), PP2A inhibition following stimulation attenuated IKK activity, probably by interfering with removal of inhibitory phosphate groups (Kray et al., 2005).

PP4R1 silencing similarly enhanced NF-κB activity upon TCR stimulation or PMA/ionomycin and TNFα treatment, respectively (Fig. 5.7). Consistently, PP4R1 was shown to negatively regulate IKK activity which is a central point of convergence in canonical NF-κB signaling. However, it cannot be excluded that PP4R1 additionally acts at the level or downstream of PKCθ. For instance, the TAK1/TAB module is a shared positive regulator in TCR and TNFR1 signaling and is phosphorylated upon stimulation. Although it is unlikely that PP4R1 impedes TAK1 phosphorylation and activation because

AP-1 signaling was unaffected (Fig. 5.9, 5.13), this issue could be directly addressed by means of phospho-specific antibodies and TAK1 kinase activity assays. Moreover, investigation of Carma1 phosphorylation as well as Bcl10, MALT1, and NEMO ubiquitination could further confirm and extend epistasis analysis.

Given the fact that PP4R1 specifically interacts with IKKα and thereby associates with the canonical IKK complex it is conceivable that PP4R1 similarly interacts with IKKα homodimers to mediate negative regulation of NIK-induced phosphorylation and non-canonical IKKα activation. Investigation of the effect of PP4R1 knock-down in B cells on IKKα phosphorylation and non-canonical NF-κB activation in response to CD40, BAFF-R, or LTβR triggering might be a suitable approach to address this question in the future.

(iv) Redundancy and robustness in the control of IKK activity

Activation of IKK signaling is a transient event and is subject to several post-inductive negative feedback mechanisms (Hayden and Ghosh, 2008). These include deubiquitination and inactivation of proximal signal compounds by the negative regulators A20 and CYLD as well as the activity of several IKK-specific phosphatases (see 1.4.3 and 1.4.4). Given multiple layers of negative regulation it is surprising that targeted inactivation of single regulatory components is already sufficient to cause profound IKK phenotypes. Obviously, negative regulation of IKK activity involves an intricate network of signaling inhibitors that serve, at least in part, non-redundant functions and/or require co-suppression by additional factors to mediate complete and stable IKK inhibition. Combined knock-down of PP4R1 and A20, CYLD, PP2Ac, or other phosphatase components could address the question whether these inhibitors cooperate in suppressing IKK activity or whether they serve redundant or additive functions.

Interestingly, PP4R1 is not expressed in resting T cells, but its expression is heavily upregulated upon primary activation and expansion, implying a physiological mechanism of activation-induced feedback inhibition limiting NF-κB signaling upon TCR re-stimulation. However, the fact that resting T cells lack PP4R1 expression already suggests alternative mechanisms of IKK control in T lymphocytes. It will be interesting to analyze phosphatase expression in resting *vs.* pre-stimulated T cells and to investigate whether in resting cells distinct phosphatase entities are present that serve PP4R1-like functions. Nonetheless, it is tempting to speculate that – through differential expression of phosphatases – resting *vs.* pre-activated T lymphocytes differ in the kinetics and strength of IKK phosphorylation

and kinase activation and therefore exhibit differential sensitivities towards TCR stimulation.

6.2.2 The PP4 holoenzyme and the NF-κB-specific PP4c/PP4R1 module

(i) The PP4c interactome

Based on co-purification strategies PP4R1 was the first non-catalytic, regulatory phosphatase subunit to be identified as stable interactor of the catalytically active subunit PP4c (Kloeker and Wadzinski, 1999; Wada et al., 2001). Stable complex formation between PP4R1 and PP4c was confirmed by independent proteomic screening approaches (Chen et al., 2008; Gingras et al., 2005). Accordingly, the present study provided further evidence for a specific interaction between PP4R1 and PP4c in human T lymphocytes (Fig. 5.12).

PP4c (formerly known as PPX) is a highly conserved and ubiquitously expressed phosphatase that shares about 65% amino acid identity with PP2A catalytic subunits and therefore belongs, along with PP2Ac and PP6c, to the PP2A-type phosphatases (Brewis and Cohen, 1992; Brewis et al., 1993; Cohen et al., 2005; da Cruz e Silva OB et al., 1988). Given the large structural homology to PP2Ac it has been hypothesized that PP4c exists in distinct multimeric complexes with different subunit compositions and molecular functions. Indeed, to date several PP4c-interacting proteins have been reported, including PP4R1, PP4R2, PP4R3α, PP4R3β, PP4R4, and α4/IGBP1 (Carnegie et al., 2003; Chen et al., 2008; Gingras et al., 2005; Hastie et al., 2000) (see also Fig. 6.3). Whereas, PP4R1, PP4R2, and PP4R4 are likely to interact with PP4c in a direct manner and independently of other subunits (Fig. 5.12 F), PP4R3 isoforms depend on PP4R2 for association with PP4c (Chen et al., 2008; Chowdhury et al., 2008).

Both PP4R1 and PP4R4 are HEAT repeat-containing proteins with some homology to the A subunit of PP2A. PP2A A contains 15 repeat motifs, whereas PP4R1 and PP4R4 contain 14 and 3 canonical HEAT repeats, respectively (Chen et al., 2008; Kloeker and Wadzinski, 1999). HEAT repeats are structural elements that have been shown to mediate interactions between the PP2A A subunit and catalytic and regulatory B subunits of PP2A. Consistently, mutations or deletions of HEAT repeats within PP4R1 have been shown to impair or prevent binding to PP4c (Chen et al., 2008) (Fig. 5.12 E). Although PP4R1 and PP4R4 were suggested to display similar PP4c binding interfaces, related to the PP2Ac-PP2A A interaction, they seems to require different structural determinants of PP4c association (Chen et al., 2008). In contrast to the α4 subunit, PP4R1 and other PP4

regulatory subunits specifically bind to PP4c, but not to the structurally related phosphatase PP2Ac (Chen et al., 2008; Chowdhury et al., 2008) (Fig. 5.12 B). PP4c interactions, however, are specific for PP4 regulatory subunits, but not for PP2A A α or β isoforms (Chen et al., 2008).

Given the strong and most probably direct interaction between PP4c and PP4R1 or other PP4 regulatory subunits it is tempting to speculate that additional co-factors exist that, in analogy to various PP2A B subunits, modify PP4 core complexes and give rise to a wide collection of PP4 holoenzymes.

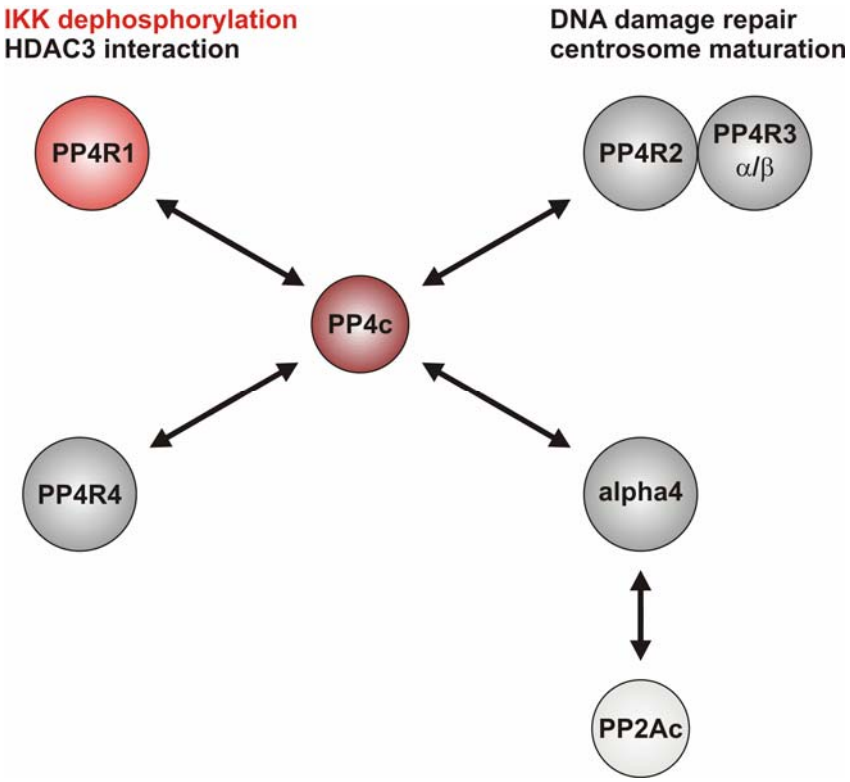

Figure 6.3 | Schematic representation of distinct PP4 complexes and functions. The PP4 catalytic subunit PP4c forms stable complexes with a number of distinct interaction partners, including PP4R1, PP4R2, PP4R3α/β, PP4R4, and alpha4. The interactions between PP4c and PP4R1, PP4R2, PP4R4, or alpha4 are likely to occur in a direct manner, whereas PP4R3 subunits depend on PP4R2 to associate with PP4c. The alpha subunit interacts with both PP4c and PP2Ac. All other PP4 regulatory subunits are specific for PP4c. The PP4c/PP4R2/PP4R3 module has been implicated in DNA damage repair and centrosome maturation. The PP4c/PP4R1 complex was previously shown to interact with HDAC3. Moreover, the present study identified PP4R1 as a direct interaction partner of IKKα, connecting the PP4c/PP4R1 complex with the IKK complex (highlighted in red). The functions of other distinct PP4c complexes are largely unknown.

(ii) PP4c complexes and functions

PP4c has been implicated in diverse cellular processes, including DNA damage checkpoint signaling, microtubule organization, spliceosome assembly and apoptosis regulation (reviewed in Cohen et al., 2005). The overall essential and non-redundant role of PP4c in ontogenesis and tissue development has been demonstrated by genetic studies using PP4c knock-out mice (Shui et al., 2007). Ablation of PP4c results in embryonic lethality of mice, and T cell-specific PP4c gene deletion causes abnormal thymic development and pre-TCR signaling (Shui et al., 2007). Pleiotropic functions of PP4c have been assigned to distinct PP4c-containing complexes with different compositions, subcellular localizations, substrate specificities, and activities (Fig. 6.3). Indeed, PP4c complexes are found throughout the cell, ranging from cytosolic to nuclear or centrosomal localizations (Brewis and Cohen, 1992; Brewis et al., 1993; Chen et al., 2008; Cohen et al., 2005; Toyo-oka et al., 2008). The molecular functions of different PP4R subunits are largely elusive and have been best defined for ternary PP4c-PP4R2-PP4R3 complexes that have been recently implicated in DNA damage repair (Chowdhury et al., 2008; Nakada et al., 2008).

In support of the concept of modular PP4c activity the present study has uncovered a distinct PP4 complex, composed of PP4c and PP4R1, as a negative regulator of NF-κB signaling in T lymphocytes (Fig. 6.2). PP4R1 and PP4c were shown to co-associate with the IKK complex in a stimulation-dependent manner (Fig. 5.11), and in preliminary experiments it could be shown that the PP4c co-association is largely abolished in PP4R1-silenced cells (data not shown). Therefore, it is concluded that PP4R1 acts as an adapter bridging the IKK complex and PP4c and directing PP4c catalytic activity to specifically mediate IKK dephosphorylation. Given the stimulation-dependent profile of the PP4R1-IKK interaction it is likely that auxiliary factors and/or posttranslational modifications are required to mediate IKK-PP4R1-PP4c complex formation and IKK dephosphorylation. Analysis of PP4R1-associated proteins by mass spectrometry might lead to the identification of additional basal or inducible interaction partners of PP4R1. However, it cannot be excluded that the PP4R1/PP4c module serves separate and IKK-independent functions, depending on the molecular and subcellular context. Indeed, a recent report demonstrated the PP4c-PP4R1 complex to physically associate with histone deacetylase 3 (HDAC3) and to negatively regulate HDAC3 activity (Zhang et al., 2005). Although the physiological relevance of this interaction is elusive it may imply a role of PP4 in epigenetic regulation of gene transcription.

(iii) PP4C and its controversial role in regulating NF-κB

Previous studies have linked PP4c to positive regulation of NF-κB activity. Based on a yeast-two-hybrid screening approach PP4c was identified as an interaction partner of c-Rel, and PP4c was shown to interact with recombinant c-Rel, RelA (p65), and p50 (Hu et al., 1998) and endogenous p65 (Yeh et al., 2004). Increased NF-κB signaling upon PP4c overexpression was suggested to be dependent on PP4c-mediated dephosphorylation of inhibitory threonine residues within p65 (Hu et al., 1998; Yeh et al., 2004). Moreover, knock-down of PP4c was shown to cause reduced basal and TNFα-induced NF-κB activity (Li et al., 2006b). In addition, it has been suggested that PP4c is a positive regulator of HPK1 (Zhou et al., 2004b) which, in turn, acts as a Carma1/IKK-activating kinase in T lymphocytes (Brenner et al., 2005; Brenner et al., 2009).

In contrast to these results, the present study has identified the PP4R1/PP4c module as negative regulator of IKK activity. How can one explain these apparently controversial findings? It is important to note that on the basis of the experimental systems employed in this study single knock-down of PP4c by RNAi did not yield any significant NF-κB phenotype, neither with respect to TCR nor with respect to TNFR1 signaling. Moreover and in contrast to other reports, overexpression of PP4c alone did not alter TCR-induced NF-κB signaling in Jurkat cells (data not shown). Obviously, PP4c serves ambivalent NF-κB signaling functions that are most likely determined by the co-action of different regulatory subunits. Moreover and as outlined above, PP4c plays important roles in a wide variety of cellular processes. It is reasonable to assume that pleiotropic and counteracting functions of PP4c mask and superimpose separate PP4c signaling roles and, therefore, complicate a functional analysis of PP4c. Analysis of IKK activity in the presence or absence of PP4c could omit downstream functions of PP4c and directly address its role in regulating IKK activity. Moreover, the analysis of T cell-specific PP4R1 knock-out mice will certainly shed more light on the biological functions of the PP4R1-PP4c complex in T cell activation and inflammation.

6.2.3 Regulation of the regulator: How is PP4R1-associated phosphatase activity controlled?

Based on *in vitro* phosphatase activity and IKK dephosphorylation assays using overexpressed proteins it could be demonstrated that (i) PP4R1 potentiates PP4c catalytic activity and (ii) that TCR stimulation results in a transient induction of PP4R1-associated phosphatase activity, peaking at around 25 minutes of stimulation (Fig. 5.14).

PP4R1-mediated modulation of PP4c activity may be due to structural changes within PP4c and allosteric regulation of phosphatase activity or to the PP4R1-dependent co-recruitment of additional PP4c-activating factors. Indeed, distinct PP4c complexes have been described to exhibit differential phosphatase activities (Chen et al., 2008). In contrast to PP4R1, however, PP4R2/PP4R3 and PP4R4-containing complexes were reported to be less active than unbound PP4c subunits.

Stimulation-dependent modulation of PP4c activity has been previously described for TNFα-stimulated HEK293T cells (Zhou et al., 2002). The authors reported induction of PP4c activity by about 4-fold in response TNFα treatment which was precisely paralleled by transient TNFα-induced serine/threonine phosphorylation of PP4c. Similarly, PP2Ac has been shown to be subject to tyrosine and threonine phosphorylation (Chen et al., 1994; Guo and Damuni, 1993), and IL-6 stimulation triggered PP2A phosphorylation and increased phosphatase activity (Kantrow et al., 2000). Regulation of PP4c phosphatase activity may involve different or additional reversible post-translational modifications. For instance, PP2A-type phosphatases have been described to undergo carboxy-methyl modifications at their C-termini, possibly modulating interactions with regulatory subunits (Bryant et al., 1999; Tolstykh et al., 2000). Further studies, including (phospho)-mass spectrometric analysis of PP4c/PP4R1 complexes in response to TCR or TNFR1 stimulation as well as phosphatase assays using purified recombinant PP4R1 and PP4c proteins, are required to gain more insights into the mechanisms regulating PP4c/PP4R1 phosphatase activity.

6.2.4 Implications for IKKα as a bifunctional signaling device

PP4R1 was shown to specifically interact with IKKα upon overexpression. In contrast, PP4R1 failed to interact with the structural IKK subunit NEMO and displayed only weak interaction with IKKβ. Moreover, *in vitro* translated PP4R1 associated with IKKα as efficiently as with the catalytic subunit PP4c indicative of a direct protein-protein interaction (Fig. 5.11).

Apart from its function in promoting NF-κB activation, several lines of evidence suggest an inhibitory role of IKKα in NF-κB activation. For example, IKKα-deficient mice exhibited exaggerated inflammatory responses, and IKKα-deficient macrophages displayed higher kinase activity of IKKβ (Li et al., 2005). Interestingly, IKKα-dependent repression of IKKβ activity was shown to be independent of IKKα kinase activity, indicating a negative regulatory adapter function of IKKα (Lawrence et al., 2005). In line with these data,

biochemical studies have demonstrated the presence of IKKβ/NEMO complexes activated by anti-CD3/CD28 antibodies in primary T cells (Khoshnan et al., 1999) and revealed the presence of an IKKβ-only complex lacking IKKα (Mercurio et al., 1999). Although these data demonstrated IKKα to be a bifunctional modulator of IKKβ activity and NF-κB signaling the molecular basis for these observations remained elusive.

The present study significantly contributes to a more precise understanding of the ambivalent signaling properties of IKKα and suggests a molecular mechanism for its negative regulatory function in IKK signaling. Through specific and direct binding to PP4R1 IKKα may serve as a PP4R1-specific adaptor bridging the IKK and PP4R1/PP4c complex to mediate IKK dephosphorylation and inactivation (Fig. 6.2). So far, the importance of the PP4R1/PP4c module in controlling IKK activity was revealed by knock-down of PP4R1 in Jurkat cells which caused enhanced and sustained IKK phosphorylation and abrogated the co-recruitment of PP4c. Analogously, it will be necessary to specifically knock-down IKKα in Jurkat T cells and primary T lymphocytes to directly investigate the effect of IKKα deficiency on IKKβ activation and PP4R1/PP4c co-association.

6.3 PP4R1 and its potential role in lymphomas

6.3.1 CTCL and oncogenic activation of NF-κB in lymphomas

CTCL is a clinically heterogeneous lymphoma entity among which the leukemic variant Sézary syndrome represents the most aggressive subtype (Diamandidou et al., 1996; Kim et al., 2005). A growing body of evidence has established a key role of NF-κB in CTCL progression and survival. Recent reports demonstrated constitutive activation of the canonical NF-κB pathway in the CTCL cell lines SeAx, MyLa, Hut78, and HH as well as in malignant peripheral blood T lymphocytes from patients with Sézary syndrome (so called Sézary cells) (Izban et al., 2000; Sors et al., 2006). Consistently, a specific NF-κB target gene expression signature was observed for the CTCL lines SeAx, Hut78, and HH in comparison to Jurkat T cells (Fig. 16 A).

Interestingly, constitutive activation of the NF-κB pathway does not seem to be a paraneoplastic event, but is indispensable for the continued proliferation and survival of CTCL cells *in vitro* and *in vivo*. Inhibition of NF-κB by IκBα overexpression or chemical compounds, such as an IKK activation inhibitor or proteasome inhibitors, selectively

induced apoptosis in CTCL cell lines and malignant Sézary cells, but not in non-malignant cells from Sézary patients or healthy donors (Kiessling et al., 2009; Sors et al., 2006; Sors et al., 2008).

The dependence of CTCL cells on chronic NF-κB signaling for survival reflects a general phenomenon of oncogenesis, known as oncogenic addiction. The term "oncogenic addiction" was introduced by Weinstein and conceptualizes the frequent observation that cancer cells are physiologically dependent on ("addicted to") the sustained activity of a certain oncogene or an oncogenic signaling pathway (*e.g.* the NF-κB pathway) for the maintenance of their transformed phenotype (Weinstein, 2002). Single oncogenic lesions are not sufficient to induce tumorigenesis and to bypass cell-intrinsic checkpoint mechanisms, but require the collaboration with other oncogenes or with loss of tumor suppressors for tumor initiation (oncogene collaboration). Single oncogene inactivation, in turn, is thought to lead to an imbalance between proapoptotic *vs.* antiapoptotic programs and to the restoration of physiological checkpoint mechanisms resulting in spontaneous apoptosis of tumor cells (Weinstein, 2002; Weinstein and Joe, 2008).

Physiological addiction to NF-κB signaling has also been reported for other lymphoid malignancies, such as ABC-DLBCL or Hodgkin lymphoma (reviewed in Staudt, 2010). In a subset of ABC-DLBCL cells a number of dominant active, oncogenic mutations for components of the BCR-induced NF-κB pathway, such as CD79A, CD79B, Carma1, TRAF2, and TAK1 have been identified, causing constitutive, ligand-independent NF-κB activity. In contrast to tumor initiation by direct oncogene activation, however, not every protein in a tumor-promoting pathway may be mutated or overexpressed although still being rate-limiting to oncogenic pathway activity. This phenomenon has been termed "non-oncogene addiction" (Luo et al., 2009b; Solimini et al., 2007). For instance, activating Carma1 mutations in a fraction of ABC-DLBCL cells have uncovered Carma as a *bona fide* NF-κB oncogene (Lenz et al., 2008). By contrast, mutations of Bcl10 or CK1α, two other crucial components of the CBM complex, have not been identified. Yet, targeting of Bcl10 or CK1α by RNAi caused cell death of ABC-DLBCL cells to a similar extent as downregulation of Carma1, revealing these signaling components as essential malignancy genes in ABC-DLBCL cells (Bidere et al., 2008; Ngo et al., 2006).

A central role of NF-κB-driven anti-apoptotic gene expression has also been reported for a number of non-lymphoid epithelial malignancies. Based on an RNAi screen to identify synthetic lethal partners of oncogenic K-Ras it was recently demonstrated that the non-canonical NF-κB-activating TANK-binding kinase 1 (TBK1) is selectively essential for the

survival of *KRAS* mutant tumors (Barbie et al., 2009). Moreover, mutant K-Ras overexpression was shown activate the canonical NF-κB pathway (Meylan et al., 2009). A co-dependence between MAPK and NF-κB signaling for tumor formation and maintenance was further demonstrated by a previous study that identified the IKK family member IKKε as a breast cancer oncogene (Boehm et al., 2007).

6.3.2 PP4R1: suppressor of NF-κB and tumor suppressor?

Conceptually, aberrant NF-κB activity in tumor cells can result from mutated or amplified signaling activators with oncogenic activity (*e.g.* Carma1; see 6.3.1) and/or from mutational inactivation or deficiency of NF-κB repressors. Indeed, recent studies provided evidence for a function of A20, a negative regulator of NF-κB signaling, as a central tumor suppressor in a wide variety of NF-κB-dependent B cell lymphomas. In ABC-DLBCL, MALT lymphoma, a large panel of additional non-Hodgkin lymphomas, Hodkin lymphoma, and primary mediastinal B cell lymphoma (PMBL) the A20 gene (*TNFAIP3*) was frequently inactivated by mutations and/or deletions affecting both *TNFAIP3* alleles which is a hallmark of tumor suppressor genes (Hymowitz and Wertz, 2010). A20 deficiency correlated with increased NF-κB-dependent gene expression, and reconstitution of A20-deficient lymphomas with wild-type A20 suppressed cell growth and promoted apoptosis (Compagno et al., 2009; Honma et al., 2009; Kato et al., 2009; Schmitz et al., 2009). Moreover, KEAP1, an E3 ligase for IKKβ that inhibits the NF-κB pathway, was recently shown to be frequently mutated or downregulated in several breast cancer cell lines and primary human breast cancer specimens (Lee et al., 2009).

In contrast, the molecular aetiology underlying constitutive NF-κB signaling in CTCL cells remains largely unknown. Although constitutive NF-κB activation was demonstrated to be predominantly IKKβ-dependent (Sors et al., 2006; Sors et al., 2008), a contribution of the alternative pathway is also discussed (Zhang et al., 1994). However, molecular lesions that promote constitutive IKK signaling in CTCL have not been described yet.

The present study revealed significant downregulation of PP4R1 expression in a fraction of CTCL cell lines and primary CTCL cells from Sézary patients (Fig. 5.15). Whereas SeAx and MyLa cell lines were PP4R1-sufficient, Hut78 displayed reduced PP4R1 protein levels, and HH cells completely lacked PP4R1 expression. PP4R1 deficiency correlated well with constitutive IKKβ activity in PP4R1-deficient CTCL cells. Forced re-expression of PP4R1 in HH cells reversed constitutive IKK activation and NF-κB signaling, indicating that PP4R1 deficiency is sufficient and causative for IKK hyperactivation in these cells (Fig.

5.16). This is in accordance with the physiological role of PP4R1 in negative regulation of IKK phosphorylation and T cell activation and implies a role of PP4R1 in lymphoma survival. Indeed, reconstitution of PP4R1 expression sensitized Hut78 and most prominently PP4R1-deficient HH cells to cell death, whereas the survival of PP4R1-sufficient SeAx and MyLa cells was not affected (Fig. 5.16 E). Collectively, these results provide genetic and functional evidence that PP4R1 is a suppressor of the NF-κB pathway whose downregulation unleashes constitutive IKK activity and is required for the continued survival of a subset of CTCL cells.

Whether PP4R1 – analogously to A20 – is a tumor suppressor or serves tumor suppressor-like functions remains to be addressed. Given its functional role in NF-κB signaling and CTCL survival it is likely that loss of PP4R1 expression does not reflect a tumor intrinsic program, but represents a pathogenetic event that is essential for the initiation or propagation of a specific, NF-κB-addicted malignant phenotype. To address this question, gene expression profile studies and mutational analyses of the *PPP4R1* locus using larger cohorts of CTCL or Sézary patients are required. Moreover, these genetic analyses have to be extended to examine whether deregulated PP4R1 expression is a CTCL-specific phenomenon or may also contribute to the pathogenesis of other types of lymphoid malignancies, such as ABC-DLBCL, Hodgkin lymphoma, and MM. So far, no defective PP4R1 expression in two tested ABC-DLBCL cell lines was detected (Fig. 5.15 D), although the possibility of inactivating point mutations cannot be ruled out. Expression screening and *PPP4R1* sequence analysis of a larger panel of available cell lines as well as of primary patient material are needed. Importantly, deregulation of PP4R1 expression is restricted to a subtype of CTCL cells and, therefore, most probably not the only molecular determinant of NF-κB activation and malignancy in the Sézary Syndrome. It will be interesting to investigate whether Sézary cells display mutations and/or aberrant expression of other known regulators of NF-κB (*e.g.* Carma1, A20) or distinct oncogenic pathways (*e.g.* the Ras pathway), and whether some of these aberrations cooperate with PP4R1 deficiency to promote constitutive NF-κB signaling and lymphoma survival.

6.3.3 PP4R1 deficiency in Sézary cells: implications for diagnosis and therapy

In general, the pharmacological exploitation of mutations or deficiencies of tumor suppressors or tumor suppressor-like proteins is a challenging strategy because it is difficult – in contrast to drug-mediated targeting of oncogenes – to restore or mimic the function of a specific protein (Luo et al., 2009b). Nonetheless, the finding that PP4R1 is

downregulated in a subset of CTCL cells may have important implications for the molecular diagnosis, classification, and individualized therapy of Sézary tumors. (i) The analysis of PP4R1 expression or functional inactivation might be valuable to categorize CTCL cells in IKK-dependent *vs.* IKK-independent tumors. PP4R1-deficiency was shown to result in constitutive IKK activity. Therefore, PP4R1-deficient CTCL cells are likely to be more sensitive to specific IKK inhibitors, such as the NBP (May et al., 2000) or chemical IKK activation inhibitors (Kiessling et al., 2009) than PP4R1-sufficient cells. In these latter cells constitutive NF-κB signaling may result from aberrations affecting signaling components that are either upstream or downstream (and thus independent) of IKKβ activity. (ii) It is not clear yet, how PP4R1 expression is downregulated. Since loss of PP4R1 seems to occur on a transcriptional level (Fig. 5.15 A-C) possible mechanisms may include promoter mutations or chromosomal aberrations and/or epigenetic alterations such as promoter methylation and histone deacetylation. For instance, loss of A20 expression was shown to be in part due to chromosomal rearrangements and promoter methylations in MALT lymphomas (Chanudet et al., 2010). Treatment of Sézary patients with HDAC or DNA methyl-transferase inhibitors (Heider et al., 2009), in combination with conventional chemotherapeutics or NF-κB inhibitors, such as IAP antagonists (Vucic and Fairbrother, 2007) or proteasome inhibitors (Baud and Karin, 2009; Dunleavy et al., 2009; Richardson et al., 2005) might be a promising approach to restore PP4R1 expression and to sensitize CTCL cells to apoptosis.

6.4 Outlook

The current study has identified the regulatory subunit PP4R1 as a central regulator of NF-κB signaling and T cell activation, and has also provided evidence for PP4R1 as a suppressor of human lymphoma cell survival. These results significantly expanded our understanding of TCR-induced signal transduction and have provided novel insights into the mechanisms governing negative regulation of NF-κB signaling. Further biochemical and functional analyses are required to precisely dissect how the PP4R1/PP4c complex interferes with IKK activation and how this phosphatase module itself is regulated by TCR signaling. Moreover, the analysis of PP4R1 knock-out mice will help to understand the physiological role of PP4R1 in T cell development, activation, and apoptosis as well as its function in other cellular compartments *in vivo*. Furthermore, it is tempting to speculate that PP4R1 controls and limits inflammatory responses, and therefore deregulated PP4R1

activity may be involved in the development of autoimmune disorders or chronic inflammatory diseases. The finding that loss of PP4R1 expression is causative for constitutive IKK/NF-κB signaling and is required for survival of a fraction of CTCL cells implies a role of PP4R1 in the pathogenesis of T cell lymphomas. It will be necessary to investigate whether PP4R1 inactivation is a more general mechanism accompanying or promoting tumorigenesis and may contribute to other NF-κB-driven haematological malignancies. The identification and molecular characterization of PP4R1 as a NF-κB-suppressing regulator might open up new strategies of anti-tumour therapy for a subgroup of NF-κB-dependent lymphomas.

7 Appendix

7.1 List of references

Abraham,R.T. and Weiss,A. (2004). Jurkat T cells and development of the T-cell receptor signalling paradigm. Nat. Rev. Immunol. *4*, 301-308.

Acuto,O., Di Bartolo,V., and Michel,F. (2008). Tailoring T-cell receptor signals by proximal negative feedback mechanisms. Nat. Rev. Immunol. *8*, 699-712.

Aden,D.P., Fogel,A., Plotkin,S., Damjanov,I., and Knowles,B.B. (1979). Controlled synthesis of HBsAg in a differentiated human liver carcinoma-derived cell line. Nature *282*, 615-616.

Agou,F., Traincard,F., Vinolo,E., Courtois,G., Yamaoka,S., Israel,A., and Veron,M. (2004). The trimerization domain of NEMO is composed of the interacting C-terminal CC2 and LZ coiled-coil subdomains. J. Biol. Chem. *279*, 27861-27869.

Ahmed,R. and Gray,D. (1996). Immunological memory and protective immunity: understanding their relation. Science *272*, 54-60.

Akagi,T., Motegi,M., Tamura,A., Suzuki,R., Hosokawa,Y., Suzuki,H., Ota,H., Nakamura,S., Morishima,Y., Taniwaki,M., and Seto,M. (1999). A novel gene, MALT1 at 18q21, is involved in t(11;18) (q21;q21) found in low-grade B-cell lymphoma of mucosa-associated lymphoid tissue. Oncogene *18*, 5785-5794.

Alizadeh,A.A., Eisen,M.B., Davis,R.E., Ma,C., Lossos,I.S., Rosenwald,A., Boldrick,J.C., Sabet,H., Tran,T., Yu,X., Powell,J.I., Yang,L., Marti,G.E., Moore,T., Hudson,J., Jr., Lu,L., Lewis,D.B., Tibshirani,R., Sherlock,G., Chan,W.C., Greiner,T.C., Weisenburger,D.D., Armitage,J.O., Warnke,R., Levy,R., Wilson,W., Grever,M.R., Byrd,J.C., Botstein,D., Brown,P.O., and Staudt,L.M. (2000). Distinct types of diffuse large B-cell lymphoma identified by gene expression profiling. Nature *403*, 503-511.

Alonso,A., Sasin,J., Bottini,N., Friedberg,I., Friedberg,I., Osterman,A., Godzik,A., Hunter,T., Dixon,J., and Mustelin,T. (2004). Protein tyrosine phosphatases in the human genome. Cell *117*, 699-711.

Amir,R.E., Haecker,H., Karin,M., and Ciechanover,A. (2004). Mechanism of processing of the NF-kappa B2 p100 precursor: identification of the specific polyubiquitin chain-anchoring lysine residue and analysis of the role of NEDD8-modification on the SCF(beta-TrCP) ubiquitin ligase. Oncogene *23*, 2540-2547.

Ammirante,M., Luo,J.L., Grivennikov,S., Nedospasov,S., and Karin,M. (2010). B-cell-derived lymphotoxin promotes castration-resistant prostate cancer. Nature *464*, 302-305.

Andrade,M.A. and Bork,P. (1995). HEAT repeats in the Huntington's disease protein. Nat. Genet. *11*, 115-116.

Annunziata,C.M., Davis,R.E., Demchenko,Y., Bellamy,W., Gabrea,A., Zhan,F., Lenz,G., Hanamura,I., Wright,G., Xiao,W., Dave,S., Hurt,E.M., Tan,B., Zhao,H., Stephens,O., Santra,M., Williams,D.R., Dang,L., Barlogie,B., Shaughnessy,J.D., Jr., Kuehl,W.M., and Staudt,L.M. (2007). Frequent engagement of the classical and alternative NF-kappaB pathways by diverse genetic abnormalities in multiple myeloma. Cancer Cell *12*, 115-130.

Arnold,R., Liou,J., Drexler,H.C.A., Weiss,A., and Kiefer,F. (2001). Caspase-mediated cleavage of hematopoietic progenitor kinase 1 (HPK1) converts an activator of NF kappa B into an inhibitor of NF kappa B. J. Biol. Chem. *276*, 14675-14684.

Ashwell,J.D. (2006). The many paths to p38 mitogen-activated protein kinase activation in the immune system. Nat. Rev. Immunol. *6*, 532-540.

Astier,A.L., Beriou,G., Eisenhaure,T.M., Anderton,S.M., Hafler,D.A., and Hacohen,N. (2010). RNA interference screen in primary human T cells reveals FLT3 as a modulator of IL-10 levels. J. Immunol. *184*, 685-693.

Badr,C.E., Hewett,J.W., Breakefield,X.O., and Tannous,B.A. (2007). A highly sensitive assay for monitoring the secretory pathway and ER stress. PLoS. One. *2*, e571.

Baeuerle,P.A. and Baltimore,D. (1988). Activation of DNA-binding activity in an apparently cytoplasmic precursor of the NF-kappa B transcription factor. Cell *53*, 211-217.

Baier-Bitterlich,G., Uberall,F., Bauer,B., Fresser,F., Wachter,H., Grunicke,H., Utermann,G., Altman,A., and Baier,G. (1996). Protein kinase C-theta isoenzyme selective stimulation of the transcription factor complex AP-1 in T lymphocytes. Mol. Cell Biol. *16*, 1842-1850.

Barbie,D.A., Tamayo,P., Boehm,J.S., Kim,S.Y., Moody,S.E., Dunn,I.F., Schinzel,A.C., Sandy,P., Meylan,E., Scholl,C., Frohling,S., Chan,E.M., Sos,M.L., Michel,K., Mermel,C., Silver,S.J., Weir,B.A., Reiling,J.H., Sheng,Q., Gupta,P.B., Wadlow,R.C., Le,H., Hoersch,S., Wittner,B.S., Ramaswamy,S., Livingston,D.M., Sabatini,D.M., Meyerson,M., Thomas,R.K., Lander,E.S., Mesirov,J.P., Root,D.E., Gilliland,D.G., Jacks,T., and Hahn,W.C. (2009). Systematic RNA interference reveals that oncogenic KRAS-driven cancers require TBK1. Nature *462*, 108-112.

Bargou,R.C., Emmerich,F., Krappmann,D., Bommert,K., Mapara,M.Y., Arnold,W., Royer,H.D., Grinstein,E., Greiner,A., Scheidereit,C., and Dorken,B. (1997). Constitutive nuclear factor-kappaB-RelA activation is required for proliferation and survival of Hodgkin's disease tumor cells. J. Clin. Invest *100*, 2961-2969.

Bargou,R.C., Leng,C., Krappmann,D., Emmerich,F., Mapara,M.Y., Bommert,K., Royer,H.D., Scheidereit,C., and Dorken,B. (1996). High-level nuclear NF-kappa B and Oct-2 is a common feature of cultured Hodgkin/Reed-Sternberg cells. Blood *87*, 4340-4347.

Barth,T.F., Martin-Subero,J.I., Joos,S., Menz,C.K., Hasel,C., Mechtersheimer,G., Parwaresch,R.M., Lichter,P., Siebert,R., and Mooller,P. (2003). Gains of 2p involving the REL locus correlate with nuclear c-Rel protein accumulation in neoplastic cells of classical Hodgkin lymphoma. Blood *101*, 3681-3686.

Baud,V. and Karin,M. (2001). Signal transduction by tumor necrosis factor and its relatives. Trends Cell Biol. *11*, 372-377.

Baud,V. and Karin,M. (2009). Is NF-kappaB a good target for cancer therapy? Hopes and pitfalls. Nat. Rev. Drug Discov. *8*, 33-40.

Beckwith,M., Longo,D.L., O'Connell,C.D., Moratz,C.M., and Urba,W.J. (1990). Phorbol ester-induced, cell-cycle-specific, growth inhibition of human B-lymphoma cell lines. J. Natl. Cancer Inst. *82*, 501-509.

Bennett,D., Matthews,R.J., and Satish,J.G. (2006). The whys and wherefores of phosphate removal. EMBO Rep. *7*, 263-268.

Benson,L.M., Null,A.P., and Muddiman,D.C. (2003). Advantages of Thermococcus kodakaraenis (KOD) DNA Polymerase for PCR-mass spectrometry based analyses. J. Am. Soc. Mass Spectrom. *14*, 601-604.

Berns,K., Hijmans,E.M., Mullenders,J., Brummelkamp,T.R., Velds,A., Heimerikx,M., Kerkhoven,R.M., Madiredjo,M., Nijkamp,W., Weigelt,B., Agami,R., Ge,W., Cavet,G., Linsley,P.S., Beijersbergen,R.L., and Bernards,R. (2004). A large-scale RNAi screen in human cells identifies new components of the p53 pathway. Nature *428*, 431-437.

Bharti,A.C., Shishodia,S., Reuben,J.M., Weber,D., Alexanian,R., Raj-Vadhan,S., Estrov,Z., Talpaz,M., and Aggarwal,B.B. (2004). Nuclear factor-kappaB and STAT3 are constitutively active in CD138+ cells derived from multiple myeloma patients, and suppression of these transcription factors leads to apoptosis. Blood *103*, 3175-3184.

Bianchi,K. and Meier,P. (2009). A tangled web of ubiquitin chains: breaking news in TNF-R1 signaling. Mol. Cell *36*, 736-742.

Bidere,N., Ngo,VN., Lee,J., Collins,C., Zheng,L., Wan,F., Davis,R., Ienz,G., Anderson,D., Arnoult,D., Vasquez,A., Saki,K., Zhang,J., Meng,Z., Veenstra,D., Staudt,L., and Lenardo,M. (2008). Casein kinase 1alpha governs antigen-receptor-induced NF-kappaB activation and human lymphoma cell survival. Nature.

Bidere,N., Snow,A.L., Sakai,K., Zheng,L., and Lenardo,M.J. (2006). Caspase-8 Regulation by Direct Interaction with TRAF6 in T Cell Receptor-Induced NF-[kappa]B Activation. Current Biology *16*, 1666-1671.

Birmingham,A., Selfors,L.M., Forster,T., Wrobel,D., Kennedy,C.J., Shanks,E., Santoyo-Lopez,J., Dunican,D.J., Long,A., Kelleher,D., Smith,Q., Beijersbergen,R.L., Ghazal,P., and Shamu,C.E. (2009). Statistical methods for analysis of high-throughput RNA interference screens. Nature Methods *6*, 569-575.

Blonska,M., Pappu,B.P., Matsumoto,R., Li,H., Su,B., Wang,D., and Lin,X. (2007). The CARMA1-Bcl10 signaling complex selectively regulates JNK2 kinase in the T cell receptor-signaling pathway. Immunity. *26*, 55-66.

Boehm,J.S., Zhao,J.J., Yao,J., Kim,S.Y., Firestein,R., Dunn,I.F., Sjostrom,S.K., Garraway,L.A., Weremowicz,S., Richardson,A.L., Greulich,H., Stewart,C.J., Mulvey,L.A., Shen,R.R., Ambrogio,L., Hirozane-Kishikawa,T., Hill,D.E., Vidal,M., Meyerson,M., Grenier,J.K., Hinkle,G., Root,D.E., Roberts,T.M., Lander,E.S., Polyak,K., and Hahn,W.C. (2007). Integrative genomic approaches identify IKBKE as a breast cancer oncogene. Cell *129*, 1065-1079.

Bond,M., Fabunmi,R.P., Baker,A.H., and Newby,A.C. (1998). Synergistic upregulation of metalloproteinase-9 by growth factors and inflammatory cytokines: an absolute requirement for transcription factor NF-kappa B. FEBS Lett. *435*, 29-34.

Bonizzi,G. and Karin,M. (2004). The two NF-kappa B activation pathways and their role in innate and adaptive immunity. Trends Immunol. *25*, 280-288.

Booken,N., Gratchev,A., Utikal,J., Weiss,C., Yu,X., Qadoumi,M., Schmuth,M., Sepp,N., Nashan,D., Rass,K., Tuting,T., Assaf,C., Dippel,E., Stadler,R., Klemke,C.D., and Goerdt,S. (2008). Sezary syndrome is a unique cutaneous T-cell lymphoma as identified by an expanded gene signature including diagnostic marker molecules CDO1 and DNM3. Leukemia *22*, 393-399.

Boshart,M., Gissmann,L., Ikenberg,H., Kleinheinz,A., Scheurlen,W., and zur,H.H. (1984). A new type of papillomavirus DNA, its presence in genital cancer biopsies and in cell lines derived from cervical cancer. EMBO J. *3*, 1151-1157.

Boutros,M. and Ahringer,J. (2008). The art and design of genetic screens: RNA interference. Nat. Rev. Genet. *9*, 554-566.

Boutros,M., Bras,L.P., and Huber,W. (2006). Analysis of cell-based RNAi screens. Genome Biol. *7*, R66.

Bouwmeester,T., Bauch,A., Ruffner,H., Angrand,P.O., Bergamini,G., Croughton,K., Cruciat,C., Eberhard,D., Gagneur,J., Ghidelli,S., Hopf,C., Huhse,B., Mangano,R., Michon,A.M., Schirle,M., Schlegl,J., Schwab,M., Stein,M.A., Bauer,A., Casari,G., Drewes,G., Gavin,A.C., Jackson,D.B., Joberty,G., Neubauer,G., Rick,J., Kuster,B., and Superti-Furga,G. (2004). A physical and functional map of the human TNF-alpha/NF-kappa B signal transduction pathway. Nat. Cell Biol. *6*, 97-105.

Braun,T., Carvalho,G., Fabre,C., Grosjean,J., Fenaux,P., and Kroemer,G. (2006). Targeting NF-kappaB in hematologic malignancies. Cell Death. Differ. *13*, 748-758.

Breitkreutz,A., Choi,H., Sharom,J.R., Boucher,L., Neduva,V., Larsen,B., Lin,Z.Y., Breitkreutz,B.J., Stark,C., Liu,G., Ahn,J., war-Darch,D., Reguly,T., Tang,X., Almeida,R., Qin,Z.S., Pawson,T., Gingras,A.C., Nesvizhskii,A.I., and Tyers,M. (2010). A global protein kinase and phosphatase interaction network in yeast. Science *328*, 1043-1046.

Brenner,D., Brechmann,M., Rohling,S., Tapernoux,M., Mock,T., Winter,D., Lehmann,W.D., Kiefer,F., Thome,M.,

Krammer,P.H., and Arnold,R. (2009). Phosphorylation of CARMA1 by HPK1 is critical for NF-kappa B activation in T cells. Proc. Natl. Acad. Sci. U. S. A *106*, 14508-14513.

Brenner,D., Golks,A., Kiefer,F., Krammer,P.H., and Arnold,R. (2005). Activation or suppression of NFkB by HPK1 determines sensitivity to activation-induced cell death. EMBO J. *24*, 4279-4290.

Brewis,N.D. and Cohen,P.T. (1992). Protein phosphatase X has been highly conserved during mammalian evolution. Biochim. Biophys. Acta *1171*, 231-233.

Brewis,N.D., Street,A.J., Prescott,A.R., and Cohen,P.T. (1993). PPX, a novel protein serine/threonine phosphatase localized to centrosomes. EMBO J. *12*, 987-996.

Brideau,C., Gunter,B., Pikounis,B., and Liaw,A. (2003). Improved Statistical Methods for Hit Selection in High-Throughput Screening. J Biomol Screen *8*, 634-647.

Brummelkamp,T.R., Nijman,S.M., Dirac,A.M., and Bernards,R. (2003). Loss of the cylindromatosis tumour suppressor inhibits apoptosis by activating NF-kappaB. Nature *424*, 797-801.

Bryant,J.C., Westphal,R.S., and Wadzinski,B.E. (1999). Methylated C-terminal leucine residue of PP2A catalytic subunit is important for binding of regulatory Balpha subunit. Biochem. J. *339 (Pt 2)*, 241-246.

Bubeck,W.J., Fu,C., Jackman,J.K., Flotow,H., Wilkinson,S.E., Williams,D.H., Johnson,R., Kong,G., Chan,A.C., and Findell,P.R. (1996). Phosphorylation of SLP-76 by the ZAP-70 protein-tyrosine kinase is required for T-cell receptor function. J. Biol. Chem. *271*, 19641-19644.

Burnet,F.M. (1959). The clonal selection theory of aquired immunity. Cambridge University Press.

Cabannes,E., Khan,G., Aillet,F., Jarrett,R.F., and Hay,R.T. (1999). Mutations in the IkBa gene in Hodgkin's disease suggest a tumour suppressor role for IkappaBalpha. Oncogene *18*, 3063-3070.

Cambier,J.C. (1995). New nomenclature for the Reth motif (or ARH1/TAM/ARAM/YXXL). Immunol. Today *16*, 110.

Cann,A.J., Rosenblatt,J.D., Wachsman,W., Shah,N.P., and Chen,I.S. (1985). Identification of the gene responsible for human T-cell leukaemia virus transcriptional regulation. Nature *318*, 571-574.

Cao,Y., Bonizzi,G., Seagroves,T.N., Greten,F.R., Johnson,R., Schmidt,E.V., and Karin,M. (2001). IKKalpha provides an essential link between RANK signaling and cyclin D1 expression during mammary gland development. Cell *107*, 763-775.

Carnegie,G.K., Sleeman,J.E., Morrice,N., Hastie,C.J., Peggie,M.W., Philp,A., Lamond,A.I., and Cohen,P.T.W. (2003). Protein phosphatase 4 interacts with the Survival of Motor Neurons complex and enhances the temporal localisation of snRNPs. J Cell Sci *116*, 1905-1913.

Carpino,N., Turner,S., Mekala,D., Takahashi,Y., Zang,H., Geiger,T.L., Doherty,P., and Ihle,J.N. (2004). Regulation of ZAP-70 activation and TCR signaling by two related proteins, Sts-1 and Sts-2. Immunity. *20*, 37-46.

Carter,R.S., Geyer,B.C., Xie,M., cevedo-Suarez,C.A., and Ballard,D.W. (2001). Persistent activation of NF-kappa B by the tax transforming protein involves chronic phosphorylation of IkappaB kinase subunits IKKbeta and IKKgamma. J. Biol. Chem. *276*, 24445-24448.

Chan,A.C., van Oers,N.S., Tran,A., Turka,L., Law,C.L., Ryan,J.C., Clark,E.A., and Weiss,A. (1994). Differential expression of ZAP-70 and Syk protein tyrosine kinases, and the role of this family of protein tyrosine kinases in TCR signaling. J. Immunol. *152*, 4758-4766.

Chanudet,E., Huang,Y., Ichimura,K., Dong,G., Hamoudi,R.A., Radford,J., Wotherspoon,A.C., Isaacson,P.G., Ferry,J., and Du,M.Q. (2010). A20 is targeted by promoter methylation, deletion and inactivating mutation in MALT lymphoma. Leukemia *24*, 483-487.

Chen,G., Cao,P., and Goeddel,D.V. (2002). TNF-induced recruitment and activation of the IKK complex require Cdc37 and Hsp90. Mol. Cell *9*, 401-410.

Chen,G.I., Tisayakorn,S., Jorgensen,C., D'Ambrosio,L.M., Goudreault,M., and Gingras,A.C. (2008). PP4R4/KIAA1622 Forms a Novel Stable Cytosolic Complex with Phosphoprotein Phosphatase 4. J. Biol. Chem. *283*, 29273-29284.

Chen,J., Parsons,S., and Brautigan,D.L. (1994). Tyrosine phosphorylation of protein phosphatase 2A in response to growth stimulation and v-src transformation of fibroblasts. J. Biol. Chem. *269*, 7957-7962.

Chen,Z.J. (2005). Ubiquitin signalling in the NF-kappaB pathway. Nat. Cell Biol. *7*, 758-765.

Chen,Z.J., Parent,L., and Maniatis,T. (1996). Site-specific phosphorylation of IkappaBalpha by a novel ubiquitination-dependent protein kinase activity. Cell *84*, 853-862.

Chew,J., Biswas,S., Shreeram,S., Humaidi,M., Wong,E.T., Dhillion,M.K., Teo,H., Hazra,A., Fang,C.C., Lopez-Collazo,E., Bulavin,D.V., and Tergaonkar,V. (2009). WIP1 phosphatase is a negative regulator of NF-kappa B signalling. Nat. Cell Biol. *11*, 659-U493.

Choi,J., Nannenga,B., Demidov,O.N., Bulavin,D.V., Cooney,A., Brayton,C., Zhang,Y., Mbawuike,I.N., Bradley,A., Appella,E., and Donehower,L.A. (2002). Mice deficient for the wild-type p53-induced phosphatase gene (Wip1) exhibit defects in reproductive organs, immune function, and cell cycle control. Mol. Cell Biol. *22*, 1094-1105.

Chowdhury,D., Xu,X.Z., Zhong,X.Y., Ahmed,F., Zhong,J.N., Liao,J., Dykxhoorn,D.M., Weinstock,D.M., Pfeifer,G.P., and Lieberman,J. (2008). A PP4-phosphatase complex dephosphorylates gamma-H2AX generated during DNA replication. Mol. Cell *31*, 33-46.

Chun,H.J., Zheng,L., Ahmad,M., Wang,J., Speirs,C.K., Siegel,R.M., Dale,J.K., Puck,J., Davis,J., Hall,C.G., Skoda-Smith,S., Atkinson,T.P., Straus,S.E., and Lenardo,M.J. (2002). Pleiotropic defects in lymphocyte activation caused by caspase-8 mutations lead to human immunodeficiency. Nature *419*, 395-399.

Clements,J.L., Yang,B., Ross-Barta,S.E., Eliason,S.L., Hrstka,R.F., Williamson,R.A., and Koretzky,G.A. (1998). Requirement for the leukocyte-specific adapter protein SLP-76 for normal T cell development. Science *281*, 416-419.

Cohen,P.T.W., Philp,A., and Vβzquez-Martin,C. (2005). Protein phosphatase 4 - from obscurity to vital functions. FEBS Letters *579*, 3278-3286.

Compagno,M., Lim,W.K., Grunn,A., Nandula,S.V., Brahmachary,M., Shen,Q., Bertoni,F., Ponzoni,M., Scandurra,M., Califano,A., Bhagat,G., Chadburn,A., la-Favera,R., and Pasqualucci,L. (2009). Mutations of multiple genes cause deregulation of NF-kappa B in diffuse large B-cell lymphoma. Nature *459*, 717-U124.

Conte,D., Liston,P., Wong,J.W., Wright,K.E., and Korneluk,R.G. (2001). Thymocyte-targeted overexpression of xiap transgene disrupts T lymphoid apoptosis and maturation. Proc. Natl. Acad. Sci. U. S. A *98*, 5049-5054.

Coornaert,B., Carpentier,I., and Beyaert,R. (2009). A20: central gatekeeper in inflammation and immunity. J. Biol. Chem. *284*, 8217-8221.

Cully,M., You,H., Levine,A.J., and Mak,T.W. (2006). Beyond PTEN mutations: the PI3K pathway as an integrator of multiple inputs during tumorigenesis. Nat. Rev. Cancer *6*, 184-192.

da Cruz e Silva OB, da Cruz e Silva EF, and Cohen,P.T. (1988). Identification of a novel protein phosphatase catalytic subunit by cDNA cloning. FEBS Lett. *242*, 106-110.

Davis,M.M. (2002). A new trigger for T cells. Cell *110*, 285-287.

Davis,R.E., Ngo,V.N., Lenz,G., Tolar,P., Young,R.M., Romesser,P.B., Kohlhammer,H., Lamy,L., Zhao,H., Yang,Y., Xu,W.,

Shaffer,A.L., Wright,G., Xiao,W., Powell,J., Jiang,J.K., Thomas,C.J., Rosenwald,A., Ott,G., Muller-Hermelink,H.K., Gascoyne,R.D., Connors,J.M., Johnson,N.A., Rimsza,L.M., Campo,E., Jaffe,E.S., Wilson,W.H., Delabie,J., Smeland,E.B., Fisher,R.I., Braziel,R.M., Tubbs,R.R., Cook,J.R., Weisenburger,D.D., Chan,W.C., Pierce,S.K., and Staudt,L.M. (2010). Chronic active B-cell-receptor signalling in diffuse large B-cell lymphoma. Nature *463*, 88-92.

Davis,R.E., Brown,K.D., Siebenlist,U., and Staudt,L.M. (2001). Constitutive nuclear factor kappaB activity is required for survival of activated B cell–like diffuse large B cell lymphoma cells. J. Exp. Med. *194*, 1861-1874.

Davis,R.J. (2000). Signal transduction by the JNK group of MAP kinases. Cell *103*, 239-252.

Deacon,E.M., Pallesen,G., Niedobitek,G., Crocker,J., Brooks,L., Rickinson,A.B., and Young,L.S. (1993). Epstein-Barr virus and Hodgkin's disease: transcriptional analysis of virus latency in the malignant cells. J. Exp. Med. *177*, 339-349.

Delhase,M., Hayakawa,M., Chen,Y., and Karin,M. (1999). Positive and negative regulation of I kappa B kinase activity through IKK beta subunit phosphorylation. Science *284*, 309-313.

Deveraux,Q.L., Stennicke,H.R., Salvesen,G.S., and Reed,J.C. (1999). Endogenous inhibitors of caspases. J. Clin. Immunol. *19*, 388-398.

Diamandidou,E., Cohen,P.R., and Kurzrock,R. (1996). Mycosis fungoides and Sezary syndrome. Blood *88*, 2385-2409.

DiDonato,J.A., Hayakawa,M., Rothwarf,D.M., Zandi,E., and Karin,M. (1997). A cytokine-responsive I[kappa]B kinase that activates the transcription factor NF-[kappa]B. Nature *388*, 548-554.

Dierlamm,J., Baens,M., Wlodarska,I., Stefanova-Ouzounova,M., Hernandez,J.M., Hossfeld,D.K., De Wolf-Peeters,C., Hagemeijer,A., Van den,B.H., and Marynen,P. (1999). The apoptosis inhibitor gene API2 and a novel 18q gene, MLT, are recurrently rearranged in the t(11;18)(q21;q21) associated with mucosa-associated lymphoid tissue lymphomas. Blood *93*, 3601-3609.

Dimitratos,S.D., Woods,D.F., Stathakis,D.G., and Bryant,P.J. (1999). Signaling pathways are focused at specialized regions of the plasma membrane by scaffolding proteins of the MAGUK family. Bioessays *21*, 912-921.

Dippel,E., Klemke,C.D., and Goerdt,S. (2003). Current status of cutaneous T-cell lymphoma: molecular diagnosis, pathogenesis, therapy and future directions. Onkologie. *26*, 477-483.

Dolmetsch,R.E., Lewis,R.S., Goodnow,C.C., and Healy,J.I. (1997). Differential activation of transcription factors induced by Ca2+ response amplitude and duration. Nature *386*, 855-858.

Dong,C., Davis,R.J., and Flavell,R.A. (2002). MAP kinases in the immune response. Annu. Rev. Immunol. *20*, 55-72.

Dower,N.A., Stang,S.L., Bottorff,D.A., Ebinu,J.O., Dickie,P., Ostergaard,H.L., and Stone,J.C. (2000). RasGRP is essential for mouse thymocyte differentiation and TCR signaling. Nat. Immunol. *1*, 317-321.

Ducut Sigala,J.L., Bottero,V., Young,D.B., Shevchenko,A., Mercurio,F., and Verma,I.M. (2004). Activation of transcription factor NF-kappaB requires ELKS, an IkappaB kinase regulatory subunit. Science *304*, 1963-1967.

Dummer,R., Sigg-Zemann,S., Kalthof,K., Muletta,S., Meyer,J.C., and Burg,G. (1994). Various cytokines modulate ICAM-1 shedding on melanoma- and CTCL-derived cell lines: inverse regulation of ICAM-1 shedding in a Sezary cell line by interferon-gamma. Dermatology *189*, 120-124.

Dunleavy,K., Pittaluga,S., Czuczman,M.S., Dave,S.S., Wright,G., Grant,N., Shovlin,M., Jaffe,E.S., Janik,J.E., Staudt,L.M., and Wilson,W.H. (2009). Differential efficacy of bortezomib plus chemotherapy within molecular subtypes of diffuse large B-cell lymphoma. Blood *113*, 6069-6076.

Duwel,M., Welteke,V., Oeckinghaus,A., Baens,M., Kloo,B., Ferch,U., Darnay,B.G.,

Ruland,J., Marynen,P., and Krappmann,D. (2009). A20 negatively regulates T cell receptor signaling to NF-kappaB by cleaving Malt1 ubiquitin chains. J. Immunol. *182*, 7718-7728.

Duyao,M.P., Kessler,D.J., Spicer,D.B., Bartholomew,C., Cleveland,J.L., Siekevitz,M., and Sonenshein,G.E. (1992). Transactivation of the c-myc promoter by human T cell leukemia virus type 1 tax is mediated by NF kappa B. J. Biol. Chem. *267*, 16288-16291.

Ea,C.K., Deng,L., Xia,Z.P., Pineda,G., and Chen,Z.J. (2006). Activation of IKK by TNFalpha requires site-specific ubiquitination of RIP1 and polyubiquitin binding by NEMO. Mol. Cell *22*, 245-257.

Ebinu,J.O., Bottorff,D.A., Chan,E.Y., Stang,S.L., Dunn,R.J., and Stone,J.C. (1998). RasGRP, a Ras guanyl nucleotide- releasing protein with calcium- and diacylglycerol-binding motifs. Science *280*, 1082-1086.

Ebinu,J.O., Stang,S.L., Teixeira,C., Bottorff,D.A., Hooton,J., Blumberg,P.M., Barry,M., Bleakley,R.C., Ostergaard,H.L., and Stone,J.C. (2000). RasGRP links T-cell receptor signaling to Ras. Blood *95*, 3199-3203.

Echeverri,C.J., Beachy,P.A., Baum,B., Boutros,M., Buchholz,F., Chanda,S.K., Downward,J., Ellenberg,J., Fraser,A.G., Hacohen,N., Hahn,W.C., Jackson,A.L., Kiger,A., Linsley,P.S., Lum,L., Ma,Y., Mathey-Prevot,B., Root,D.E., Sabatini,D.M., Taipale,J., Perrimon,N., and Bernards,R. (2006). Minimizing the risk of reporting false positives in large-scale RNAi screens. Nat. Methods *3*, 777-779.

Egan,S.E., Giddings,B.W., Brooks,M.W., Buday,L., Sizeland,A.M., and Weinberg,R.A. (1993). Association of Sos Ras exchange protein with Grb2 is implicated in tyrosine kinase signal transduction and transformation. Nature *363*, 45-51.

Eichhorn,P.J., Creyghton,M.P., Wilhelmsen,K., van,D.H., and Bernards,R. (2007). A RNA interference screen identifies the protein phosphatase 2A subunit PR55gamma as a stress-sensitive inhibitor of c-SRC. PLoS. Genet. *3*, e218.

Emmerich,F., Theurich,S., Hummel,M., Haeffker,A., Vry,M.S., Dohner,K., Bommert,K., Stein,H., and Dorken,B. (2003). Inactivating I kappa B epsilon mutations in Hodgkin/Reed-Sternberg cells. J. Pathol. *201*, 413-420.

Epstein,A.L., Henle,W., Henle,G., Hewetson,J.F., and Kaplan,H.S. (1976). Surface marker characteristics and Epstein-Barr virus studies of two established North American Burkitt's lymphoma cell lines. Proc. Natl. Acad. Sci. U. S. A *73*, 228-232.

Epstein,A.L., Levy,R., Kim,H., Henle,W., Henle,G., and Kaplan,H.S. (1978). Biology of the human malignant lymphomas. IV. Functional characterization of ten diffuse histiocytic lymphoma cell lines. Cancer *42*, 2379-2391.

Epstein,M.A., Achong,B.G., Barr,Y.M., Zajac,B., Henle,G., and Henle,W. (1966). Morphological and virological investigations on cultured Burkitt tumor lymphoblasts (strain Raji). J. Natl. Cancer Inst. *37*, 547-559.

Ewing,R.M., Chu,P., Elisma,F., Li,H., Taylor,P., Climie,S., Broom-Cerajewski,L., Robinson,M.D., O'Connor,L., Li,M., Taylor,R., Dharsee,M., Ho,Y., Heilbut,A., Moore,L., Zhang,S., Ornatsky,O., Bukhman,Y.V., Ethier,M., Sheng,Y., Vasilescu,J., bu-Farha,M., Lambert,J.P., Duewel,H.S., Stewart,I.I., Kuehl,B., Hogue,K., Colwill,K., Gladwish,K., Muskat,B., Kinach,R., Adams,S.L., Moran,M.F., Morin,G.B., Topaloglou,T., and Figeys,D. (2007). Large-scale mapping of human protein-protein interactions by mass spectrometry. Mol. Syst. Biol. *3*, 89.

Exley,M., Wileman,T., Mueller,B., and Terhorst,C. (1995). Evidence for multivalent structure of T-cell antigen receptor complex. Mol. Immunol. *32*, 829-839.

Falschlehner,C., Steinbrink,S., Erdmann,G., and Boutros,M. (2010). High-throughput RNAi screening to dissect cellular pathways: A how-to guide. Biotechnology Journal *5*, 368-376.

Fathman,C.G. and Lineberry,N.B. (2007). Molecular mechanisms of CD4+ T-cell anergy. Nat. Rev. Immunol. *7*, 599-609.

Fearon,D.T. and Locksley,R.M. (1996). The Instructive Role of Innate Immunity in the Acquired Immune Response. Science *272*, 50-54.

Fernandez-Miguel,G., Alarcon,B., Iglesias,A., Bluethmann,H., varez-Mon,M., Sanz,E., and de la,H.A. (1999). Multivalent structure of an alphabetaT cell receptor. Proc. Natl. Acad. Sci. U. S. A *96*, 1547-1552.

Fiumara,P., Snell,V., Li,Y., Mukhopadhyay,A., Younes,M., Gillenwater,A.M., Cabanillas,F., Aggarwal,B.B., and Younes,A. (2001). Functional expression of receptor activator of nuclear factor kappaB in Hodgkin disease cell lines. Blood *98*, 2784-2790.

Flaswinkel,H. and Reth,M. (1994). Dual role of the tyrosine activation motif of the Ig-alpha protein during signal transduction via the B cell antigen receptor. EMBO J. *13*, 83-89.

Frey,F. (2009). Identification of novel phosphatases involved in TNF-α induced NF-κB signaling. Master Thesis, German Cancer Research Center (DKFZ), Heidelberg.

Fu,D.X., Kuo,Y.L., Liu,B.Y., Jeang,K.T., and Giam,C.Z. (2003). Human T-lymphotropic virus type I tax activates I-kappa B kinase by inhibiting I-kappa B kinase-associated serine/threonine protein phosphatase 2A. J. Biol. Chem. *278*, 1487-1493.

Gaide,O., Favier,B., Legler,D.F., Bonnet,D., Brissoni,B., Valitutti,S., Bron,C., Tschopp,J., and Thome,M. (2002). CARMA1 is a critical lipid raft-associated regulator of TCR-induced NF-kappa B activation. Nat. Immunol. *3*, 836-843.

Gaide,O., Martinon,F., Micheau,O., Bonnet,D., Thome,M., and Tschopp,J. (2001). Carma1, a CARD-containing binding partner of Bcl10, induces Bcl10 phosphorylation and NF-[kappa]B activation. FEBS Letters *496*, 121-127.

Gerondakis,S., Grossmann,M., Nakamura,Y., Pohl,T., and Grumont,R. (1999). Genetic approaches in mice to understand Rel/NF-kappaB and IkappaB function: transgenics and knockouts. Oncogene *18*, 6888-6895.

Ghosh,S. and Hayden,M.S. (2008). New regulators of NF-kappaB in inflammation. Nat. Rev. Immunol. *8*, 837-848.

Ghosh,S. and Karin,M. (2002). Missing pieces in the NF-kappa B puzzle. Cell *109*, S81-S96.

Gillis,S., Scheid,M., and Watson,J. (1980). Biochemical and biologic characterization of lymphocyte regulatory molecules. III. The isolation and phenotypic characterization of Interleukin-2 producing T cell lymphomas. J. Immunol. *125*, 2570-2578.

Gilmore,T.D., Jean-Jacques,J., Richards,R., Cormier,C., Kim,J., and Kalaitzidis,D. (2003). Stable expression of the avian retroviral oncoprotein v-Rel in avian, mouse, and dog cell lines. Virology *316*, 9-16.

Gingras,A.C., Caballero,M., Zarske,M., Sanchez,A., Hazbun,T.R., Fields,S., Sonenberg,N., Hafen,E., Raught,B., and Aebersold,R. (2005). A Novel, Evolutionarily Conserved Protein Phosphatase Complex Involved in Cisplatin Sensitivity. Molecular & Cellular Proteomics *4*, 1725-1740.

Gootenberg,J.E., Ruscetti,F.W., Mier,J.W., Gazdar,A., and Gallo,R.C. (1981). Human cutaneous T cell lymphoma and leukemia cell lines produce and respond to T cell growth factor. J. Exp. Med. *154*, 1403-1418.

Greenwald,R.J., Freeman,G.J., and Sharpe,A.H. (2005). The B7 family revisited. Annu. Rev. Immunol. *23*, 515-548.

Groves,M.R., Hanlon,N., Turowski,P., Hemmings,B.A., and Barford,D. (1999). The structure of the protein phosphatase 2A PR65/A subunit reveals the conformation of its 15 tandemly repeated HEAT motifs. Cell *96*, 99-110.

Grumont,R.J., Rourke,I.J., O'Reilly,L.A., Strasser,A., Miyake,K., Sha,W., and Gerondakis,S. (1998). B lymphocytes differentially use the Rel and nuclear factor kappaB1 (NF-kappaB1) transcription factors to regulate cell cycle progression and apoptosis in quiescent and mitogen-activated cells. J. Exp. Med. *187*, 663-674.

Gulow,K., Kaminski,M., Darvas,K., Suss,D., Li-Weber,M., and Krammer,P.H. (2005). HIV-1 Trans-Activator of Transcription Substitutes for Oxidative Signaling in Activation-Induced T Cell Death. J Immunol *174*, 5249-5260.

Guo,H. and Damuni,Z. (1993). Autophosphorylation-activated protein kinase phosphorylates and inactivates protein phosphatase 2A. Proc. Natl. Acad. Sci. U. S. A *90*, 2500-2504.

Haas,T.L., Emmerich,C.H., Gerlach,B., Schmukle,A.C., Cordier,S.M., Rieser,E., Feltham,R., Vince,J., Warnken,U., Wenger,T., Koschny,R., Komander,D., Silke,J., and Walczak,H. (2009). Recruitment of the linear ubiquitin chain assembly complex stabilizes the TNF-R1 signaling complex and is required for TNF-mediated gene induction. Mol. Cell *36*, 831-844.

Hacker,H. and Karin,M. (2006). Regulation and Function of IKK and IKK-Related Kinases. Sci. STKE *2006*, re13.

Hanahan,D. and Weinberg,R.A. (2000). The hallmarks of cancer. Cell *100*, 57-70.

Hara,H., Bakal,C., Wada,T., Bouchard,D., Rottapel,R., Saito,T., and Penninger,J.M. (2004). The molecular adapter Carma1 controls entry of I kappa B kinase into the central immune synapse. J. Exp. Med. *200*, 1167-1177.

Hara,H., Wada,T., Bakal,C., Kozieradzki,I., Suzuki,S., Suzuki,N., Nghiem,M., Griffiths,E.K., Krawczyk,C., Bauer,B., D'Acquisto,F., Ghosh,S., Yeh,W.C., Baier,G., Rottapel,R., and Penninger,J.M. (2003). The MAGUK family protein CARD11 is essential for lymphocyte activation. Immunity. *18*, 763-775.

Harris,S.J., Parry,R.V., Westwick,J., and Ward,S.G. (2008). Phosphoinositide lipid phosphatases: natural regulators of phosphoinositide 3-kinase signaling in T lymphocytes. J. Biol. Chem. *283*, 2465-2469.

Hasegawa,K., Martin,F., Huang,G., Tumas,D., Diehl,L., and Chan,A.C. (2004). PEST domain-enriched tyrosine phosphatase (PEP) regulation of effector/memory T cells. Science *303*, 685-689.

Hastie,C.J., Carnegie,G.K., Morrice,N., and Cohen,P.T. (2000). A novel 50 kDa protein forms complexes with protein phosphatase 4 and is located at centrosomal microtubule organizing centres. Biochem. J. *347 Pt 3*, 845-855.

Hayden,M.S. and Ghosh,S. (2004). Signaling to NF-kappa B. Genes & Development *18*, 2195-2224.

Hayden,M.S. and Ghosh,S. (2008). Shared Principles in NF-[kappa]B Signaling. Cell *132*, 344-362.

Heider,U., Rademacher,J., Lamottke,B., Mieth,M., Moebs,M., Metzler,I., Assaf,C., and Sezer,O. (2009). Synergistic interaction of the histone deacetylase inhibitor SAHA with the proteasome inhibitor bortezomib in cutaneous T cell lymphoma. European Journal of Haematology *82*, 440-449.

Helgason,C.D., Damen,J.E., Rosten,P., Grewal,R., Sorensen,P., Chappel,S.M., Borowski,A., Jirik,F., Krystal,G., and Humphries,R.K. (1998). Targeted disruption of SHIP leads to hemopoietic perturbations, lung pathology, and a shortened life span. Genes Dev. *12*, 1610-1620.

Hengartner,M.O. (2000). The biochemistry of apoptosis. Nature *407*, 770-776.

Hennecke,J. and Wiley,D.C. (2001). T cell receptor-MHC interactions up close. Cell *104*, 1-4.

Hermiston,M.L., Xu,Z., and Weiss,A. (2003). CD45: a critical regulator of signaling thresholds in immune cells. Annu. Rev. Immunol. *21*, 107-137.

Hinz,M., Krappmann,D., Eichten,A., Heder,A., Scheidereit,C., and Strauss,M. (1999). NF-kappaB function in growth control: regulation of cyclin D1 expression and G0/G1-to-S-phase transition. Mol. Cell Biol. *19*, 2690-2698.

Hoffmann,A., Natoli,G., and Ghosh,G. (2006). Transcriptional regulation via the NF-kappaB signaling module. Oncogene *25*, 6706-6716.

Hong,S.Y., Yoon,W.H., Park,J.H., Kang,S.G., Ahn,J.H., and Lee,T.H. (2000). Involvement

of two NF-kappa B binding elements in tumor necrosis factor alpha -, CD40-, and epstein-barr virus latent membrane protein 1-mediated induction of the cellular inhibitor of apoptosis protein 2 gene. J. Biol. Chem. *275*, 18022-18028.

Honma,K., Tsuzuki,S., Nakagawa,M., Tagawa,H., Nakamura,S., Morishima,Y., and Seto,M. (2009). TNFAIP3/A20 functions as a novel tumor suppressor gene in several subtypes of non-Hodgkin lymphomas. Blood *114*, 2467-2475.

Horie,R., Watanabe,T., Morishita,Y., Ito,K., Ishida,T., Kanegae,Y., Saito,I., Higashihara,M., Mori,S., Kadin,M.E., and Watanabe,T. (2002). Ligand-independent signaling by overexpressed CD30 drives NF-kappaB activation in Hodgkin-Reed-Sternberg cells. Oncogene *21*, 2493-2503.

Hu,M.C., Tang-Oxley,Q., Qiu,W.R., Wang,Y.P., Mihindukulasuriya,K.A., Afshar,R., and Tan,T.H. (1998). Protein phosphatase X interacts with c-Rel and stimulates c-Rel/nuclear factor kappaB activity. J. Biol. Chem. *273*, 33561-33565.

Hu,Y., Baud,V., Delhase,M., Zhang,P., Deerinck,T., Ellisman,M., Johnson,R., and Karin,M. (1999). Abnormal morphogenesis but intact IKK activation in mice lacking the IKKalpha subunit of IkappaB kinase. Science *284*, 316-320.

Huynh,H., Bottini,N., Williams,S., Cherepanov,V., Musumeci,L., Saito,K., Bruckner,S., Vachon,E., Wang,X., Kruger,J., Chow,C.W., Pellecchia,M., Monosov,E., Greer,P.A., Trimble,W., Downey,G.P., and Mustelin,T. (2004). Control of vesicle fusion by a tyrosine phosphatase. Nat. Cell Biol. *6*, 831-839.

Huynh,H., Wang,X., Li,W., Bottini,N., Williams,S., Nika,K., Ishihara,H., Godzik,A., and Mustelin,T. (2003). Homotypic secretory vesicle fusion induced by the protein tyrosine phosphatase MEG2 depends on polyphosphoinositides in T cells. J. Immunol. *171*, 6661-6671.

Huynh,Q.K., Boddupalli,H., Rouw,S.A., Koboldt,C.M., Hall,T., Sommers,C., Hauser,S.D., Pierce,J.L., Combs,R.G., Reitz,B.A., az-Collier,J.A., Weinberg,R.A., Hood,B.L., Kilpatrick,B.F., and Tripp,C.S. (2000). Characterization of the recombinant IKK1/IKK2 heterodimer. Mechanisms regulating kinase activity. J. Biol. Chem. *275*, 25883-25891.

Hymowitz,S.G. and Wertz,I.E. (2010). A20: from ubiquitin editing to tumour suppression. Nat. Rev. Cancer *10*, 332-341.

Inaba,K., Metlay,J.P., Crowley,M.T., Witmer-Pack,M., and Steinman,R.M. (1990). Dendritic cells as antigen presenting cells in vivo. Int. Rev. Immunol. *6*, 197-206.

Inohara,N., Koseki,T., Lin,J., del,P.L., Lucas,P.C., Chen,F.F., Ogura,Y., and Nunez,G. (2000). An induced proximity model for NF-kappa B activation in the Nod1/RICK and RIP signaling pathways. J. Biol. Chem. *275*, 27823-27831.

Irving,B.A. and Weiss,A. (1991). The cytoplasmic domain of the T cell receptor zeta chain is sufficient to couple to receptor-associated signal transduction pathways. Cell *64*, 891-901.

Isakov,N. and Altman,A. (2002). Protein kinase C(theta) in T cell activation. Annu. Rev. Immunol. *20*, 761-794.

Ishitani,T., Takaesu,G., Ninomiya-Tsuji,J., Shibuya,H., Gaynor,R.B., and Matsumoto,K. (2003). Role of the TAB2-related protein TAB3 in IL-1 and TNF signaling. EMBO J. *22*, 6277-6288.

Israel,A. (2010). The IKK complex, a central regulator of NF-kappaB activation. Cold Spring Harb. Perspect. Biol. *2*, a000158.

Iwasaki,A. and Medzhitov,R. (2010). Regulation of Adaptive Immunity by the Innate Immune System. Science *327*, 291-295.

Izban,K.F., Ergin,M., Qin,J.Z., Martinez,R.L., Pooley,R.J., Jr., Saeed,S., and Alkan,S. (2000). Constitutive expression of NF-kappa B is a characteristic feature of mycosis fungoides: implications for apoptosis resistance and pathogenesis. Hum. Pathol. *31*, 1482-1490.

Janes,P.W., Ley,S.C., and Magee,A.I. (1999). Aggregation of lipid rafts accompanies signaling via the T cell antigen receptor. J. Cell Biol. *147*, 447-461.

Janeway,C.A., Jr. (1989). The priming of helper T cells. Semin. Immunol. *1*, 13-20.

Janeway,C.A., Jr. (1992). The immune system evolved to discriminate infectious nonself from noninfectious self. Immunol. Today *13*, 11-16.

Janssens,V. and Goris,J. (2001). Protein phosphatase 2A: a highly regulated family of serine/threonine phosphatases implicated in cell growth and signalling. Biochem. J. *353*, 417-439.

Janssens,V., Goris,J., and Van,H.C. (2005). PP2A: the expected tumor suppressor. Curr. Opin. Genet. Dev. *15*, 34-41.

Joos,S., Menz,C.K., Wrobel,G., Siebert,R., Gesk,S., Ohl,S., Mechtersheimer,G., Trumper,L., Moller,P., Lichter,P., and Barth,T.F. (2002). Classical Hodgkin lymphoma is characterized by recurrent copy number gains of the short arm of chromosome 2. Blood *99*, 1381-1387.

Jost,P.J. and Ruland,J. (2007). Aberrant NF-{kappa}B signaling in lymphoma: mechanisms, consequences, and therapeutic implications. Blood *109*, 2700-2707.

Jung,D. and Alt,F.W. (2004). Unraveling V(D)J recombination; insights into gene regulation. Cell *116*, 299-311.

Kaltoft,K., Thestrup-Pedersen,K., Jensen,J.R., Bisballe,S., and Zachariae,H. (1984). Establishment of T and B cell lines from patients with mycosis fungoides. Br. J. Dermatol. *111*, 303-308.

Kanayama,A., Seth,R.B., Sun,L., Ea,C.K., Hong,M., Shaito,A., Chiu,Y.H., Deng,L., and Chen,Z.J. (2004). TAB2 and TAB3 activate the NF-kappaB pathway through binding to polyubiquitin chains. Mol. Cell *15*, 535-548.

Kane,L.P., Lin,J., and Weiss,A. (2002). It's all Rel-ative: NF-kappaB and CD28 costimulation of T-cell activation. Trends Immunol. *23*, 413-420.

Kantrow,S.P., Gierman,J.L., Jaligam,V.R., Zhang,P., Piantadosi,C.A., Summer,W.R., and Lancaster,J.R., Jr. (2000). Regulation of tumor necrosis factor cytotoxicity by calcineurin. FEBS Lett. *483*, 119-124.

Kapoor,R., Slade,D.L., Fujimori,A., Pommier,Y., and Harker,W.G. (1995). Altered topoisomerase I expression in two subclones of human CEM leukemia selected for resistance to camptothecin. Oncol. Res. *7*, 83-95.

Karin,M. (2006). Nuclear factor-kappaB in cancer development and progression. Nature *441*, 431-436.

Karin,M. (2009). NF-kappaB as a critical link between inflammation and cancer. Cold Spring Harb. Perspect. Biol. *1*, a000141.

Karin,M. and Ben-Neriah,Y. (2000). Phosphorylation meets ubiquitination: the control of NF-[kappa]B activity. Annu. Rev. Immunol. *18*, 621-663.

Karin,M. and Lin,A. (2002). NF-kappa B at the crossroads of life and death. Nature Immunology *3*, 221-227.

Karin,M., Yamamoto,Y., and Wang,Q.M. (2004). The IKK NF-kappa B system: a treasure trove for drug development. Nat. Rev. Drug Discov. *3*, 17-26.

Kato,M., Sanada,M., Kato,I., Sato,Y., Takita,J., Takeuchi,K., Niwa,A., Chen,Y., Nakazaki,K., Nomoto,J., Asakura,Y., Muto,S., Tamura,A., Iio,M., Akatsuka,Y., Hayashi,Y., Mori,H., Igarashi,T., Kurokawa,M., Chiba,S., Mori,S., Ishikawa,Y., Okamoto,K., Tobinai,K., Nakagama,H., Nakahata,T., Yoshino,T., Kobayashi,Y., and Ogawa,S. (2009). Frequent inactivation of A20 in B-cell lymphomas. Nature *459*, 712-716.

Keats,J.J., Fonseca,R., Chesi,M., Schop,R., Baker,A., Chng,W.J., Van,W.S., Tiedemann,R., Shi,C.X., Sebag,M., Braggio,E., Henry,T., Zhu,Y.X., Fogle,H., Price-Troska,T., Ahmann,G., Mancini,C., Brents,L.A., Kumar,S., Greipp,P., Dispenzieri,A., Bryant,B., Mulligan,G., Bruhn,L., Barrett,M., Valdez,R., Trent,J., Stewart,A.K., Carpten,J., and Bergsagel,P.L. (2007). Promiscuous mutations activate the

noncanonical NF-kappaB pathway in multiple myeloma. Cancer Cell *12*, 131-144.

Khoshnan,A., Bae,D., Tindell,C.A., and Nel,A.E. (2000). The physical association of protein kinase C theta with a lipid raft-associated inhibitor of kappa B factor kinase (IKK) complex plays a role in the activation of the NF-kappa B cascade by TCR and CD28. J. Immunol. *165*, 6933-6940.

Khoshnan,A., Kempiak,S.J., Bennett,B.L., Bae,D., Xu,W., Manning,A.M., June,C.H., and Nel,A.E. (1999). Primary human CD4+ T cells contain heterogeneous I kappa B kinase complexes: role in activation of the IL-2 promoter. J. Immunol. *163*, 5444-5452.

Kiefer,F., Vogel,W.F., and Arnold,R. (2002). Signal transduction and co-stimulatory pathways. Transplant Immunology *9*, 69-82.

Kiessling,M.K., Klemke,C.D., Kaminski,M.M., Galani,I.E., Krammer,P.H., and Gulow,K. (2009). Inhibition of Constitutively Activated Nuclear Factor-{kappa}B Induces Reactive Oxygen Species- and Iron-Dependent Cell Death in Cutaneous T-Cell Lymphoma. Cancer Res *69*, 2365-2374.

Kim,E.J., Hess,S., Richardson,S.K., Newton,S., Showe,L.C., Benoit,B.M., Ubriani,R., Vittorio,C.C., Junkins-Hopkins,J.M., Wysocka,M., and Rook,A.H. (2005). Immunopathogenesis and therapy of cutaneous T cell lymphoma. J. Clin. Invest *115*, 798-812.

Klemke,C.D., Brade,J., Weckesser,S., Sachse,M.M., Booken,N., Neumaier,M., Goerdt,S., and Nebe,T.C. (2008). The diagnosis of Sezary syndrome on peripheral blood by flow cytometry requires the use of multiple markers. Br. J. Dermatol. *159*, 871-880.

Klemke,C.D., Mansmann,U., Poenitz,N., Dippel,E., and Goerdt,S. (2005). Prognostic factors and prediction of prognosis by the CTCL Severity Index in mycosis fungoides and Sezary syndrome. Br. J. Dermatol. *153*, 118-124.

Kloeker,S. and Wadzinski,B.E. (1999). Purification and Identification of a Novel Subunit of Protein Serine/Threonine Phosphatase 4. J. Biol. Chem. *274*, 5339-5347.

Kolfschoten,I.G., van,L.B., Berns,K., Mullenders,J., Beijersbergen,R.L., Bernards,R., Voorhoeve,P.M., and Agami,R. (2005). A genetic screen identifies PITX1 as a suppressor of RAS activity and tumorigenicity. Cell *121*, 849-858.

Kordes,U., Krappmann,D., Heissmeyer,V., Ludwig,W.D., and Scheidereit,C. (2000). Transcription factor NF-kappaB is constitutively activated in acute lymphoblastic leukemia cells. Leukemia *14*, 399-402.

Koretzky,G.A., Abtahian,F., and Silverman,M.A. (2006). SLP76 and SLP65: complex regulation of signalling in lymphocytes and beyond. Nature Reviews Immunology *6*, 67-78.

Kovalenko,A., Chable-Bessia,C., Cantarella,G., Israel,A., Wallach,D., and Courtois,G. (2003). The tumour suppressor CYLD negatively regulates NF-kappaB signalling by deubiquitination. Nature *424*, 801-805.

Krammer,P.H. (2000). CD95's deadly mission in the immune system. Nature *407*, 789-795.

Kray,A.E., Carter,R.S., Pennington,K.N., Gomez,R.J., Sanders,L.E., Llanes,J.M., Khan,W.N., Ballard,D.W., and Wadzinski,B.E. (2005). Positive regulation of IkappaB kinase signaling by protein serine/threonine phosphatase 2A. J. Biol. Chem. *280*, 35974-35982.

Laemmli,U.K., Beguin,F., and Gujer-Kellenberger,G. (1970). A factor preventing the major head protein of bacteriophage T4 from random aggregation. J. Mol. Biol. *47*, 69-85.

Latour,S. and Veillette,A. (2001). Proximal protein tyrosine kinases it immunoreceptor signaling. Current Opinion in Immunology *13*, 299-306.

Lawrence,T., Bebien,M., Liu,G.Y., Nizet,V., and Karin,M. (2005). IKK[alpha] limits macrophage NF-[kappa]B activation and

contributes to the resolution of inflammation. Nature *434*, 1138-1143.

Lee,D.F., Kuo,H.P., Liu,M., Chou,C.K., Xia,W., Du,Y., Shen,J., Chen,C.T., Huo,L., Hsu,M.C., Li,C.W., Ding,Q., Liao,T.L., Lai,C.C., Lin,A.C., Chang,Y.H., Tsai,S.F., Li,L.Y., and Hung,M.C. (2009). KEAP1 E3 ligase-mediated downregulation of NF-kappaB signaling by targeting IKKbeta. Mol. Cell *36*, 131-140.

Lee,E.G., Boone,D.L., Chai,S., Libby,S.L., Chien,M., Lodolce,J.P., and Ma,A. (2000). Failure to regulate TNF-induced NF-kappaB and cell death responses in A20-deficient mice. Science *289*, 2350-2354.

Lee,K., D'Acquisto,F., Hayden,M., Shim,J., and Ghosh S (2005). PDK1 nucleates T cell receptor-induced signaling complex for NF-kappaB activation. Science *308*, 114-118.

Lenz,G., Davis,R.E., Ngo,V.N., Lam,L., George,T.C., Wright,G.W., Dave,S.S., Zhao,H., Xu,W.H., Rosenwald,A., Ott,G., Muller-Hermelink,H.K., Gascoyne,R.D., Connors,J.M., Rimsza,L.M., Campo,E., Jaffe,E.S., Delabie,J., Smeland,E.B., Fisher,R.I., Chan,W.C., and Staudt,L.M. (2008). Oncogenic CARD11 mutations in human diffuse large B cell lymphoma. Science *319*, 1676-1679.

Lenz,G. and Staudt,L.M. (2010). Aggressive lymphomas. N. Engl. J. Med. *362*, 1417-1429.

Leo,A. and Schraven,B. (2001). Adapters in lymphocyte signalling. Current Opinion in Immunology *13*, 307-316.

Letourneur,F. and Klausner,R.D. (1992). Activation of T cells by a tyrosine kinase activation domain in the cytoplasmic tail of CD3 epsilon. Science *255*, 79-82.

Levine,L., Lucci,J.A., III, Pazdrak,B., Cheng,J.Z., Guo,Y.S., Townsend,C.M., Jr., and Hellmich,M.R. (2003). Bombesin stimulates nuclear factor kappa B activation and expression of proangiogenic factors in prostate cancer cells. Cancer Res. *63*, 3495-3502.

Li,H., Kobayashi,M., Blonska,M., You,Y., and Lin,X. (2006a). Ubiquitination of RIP is required for tumor necrosis factor alpha-induced NF-kappaB activation. J. Biol. Chem. *281*, 13636-13643.

Li,H.Y., Liu,H., Wang,C.H., Zhang,J.Y., Man,J.H., Gao,Y.F., Zhang,P.J., Li,W.H., Zhao,J., Pan,X., Zhou,T., Gong,W.L., Li,A.L., and Zhang,X.M. (2008). Deactivation of the kinase IKK by CUEDC2 through recruitment of the phosphatase PP1. Nat. Immunol. *9*, 533-541.

Li,Q., Van,A.D., Mercurio,F., Lee,K.F., and Verma,I.M. (1999). Severe liver degeneration in mice lacking the IkappaB kinase 2 gene. Science *284*, 321-325.

Li,Q. and Verma,I.M. (2002). NF-kappaB regulation in the immune system. Nat. Rev. Immunol. *2*, 725-734.

Li,Q., Lu,Q., Bottero,V., Estepa,G., Morrison,L., Mercurio,F., and Verma,I.M. (2005). Enhanced NF-kappaB activation and cellular function in macrophages lacking IkappaB kinase 1 (IKK1). Proc. Natl. Acad. Sci. U. S. A *102*, 12425-12430.

Li,S., Wang,L., Berman,M.A., Zhang,Y., and Dorf,M.E. (2006b). RNAi Screen in Mouse Astrocytes Identifies Phosphatases that Regulate NF-[kappa]B Signaling. Molecular Cell *24*, 497-509.

Lin,X., Mu,Y., Cunningham,E.T., Jr., Marcu,K.B., Geleziunas,R., and Greene,W.C. (1998). Molecular determinants of NF-kappaB-inducing kinase action. Mol. Cell Biol. *18*, 5899-5907.

Litman,G.W., Rast,J.P., Shamblott,M.J., Haire,R.N., Hulst,M., Roess,W., Litman,R.T., Hinds-Frey,K.R., Zilch,A., and Amemiya,C.T. (1993). Phylogenetic diversification of immunoglobulin genes and the antibody repertoire. Mol. Biol. Evol. *10*, 60-72.

Liu,H., Ye,H., Dogan,A., Ranaldi,R., Hamoudi,R.A., Bearzi,I., Isaacson,P.G., and Du,M.Q. (2001). T(11;18)(q21;q21) is associated with advanced mucosa-associated lymphoid tissue lymphoma that expresses nuclear BCL10. Blood *98*, 1182-1187.

Liu,H.H., Xie,M., Schneider,M.D., and Chen,Z.J. (2006). Essential role of TAK1 in thymocyte development and activation. Proc. Natl. Acad. Sci. U. S. A *103*, 11677-11682.

Liu,K.Q., Bunnell,S.C., Gurniak,C.B., and Berg,L.J. (1998a). T cell receptor-initiated calcium release is uncoupled from capacitative calcium entry in Itk-deficient T cells. J. Exp. Med. *187*, 1721-1727.

Liu,Q., Oliveira-Dos-Santos,A.J., Mariathasan,S., Bouchard,D., Jones,J., Sarao,R., Kozieradzki,I., Ohashi,P.S., Penninger,J.M., and Dumont,D.J. (1998b). The inositol polyphosphate 5-phosphatase ship is a crucial negative regulator of B cell antigen receptor signaling. J. Exp. Med. *188*, 1333-1342.

Liu,S.K., Fang,N., Koretzky,G.A., and McGlade,C.J. (1999). The hematopoietic-specific adaptor protein gads functions in T-cell signaling via interactions with the SLP-76 and LAT adaptors. Curr. Biol. *9*, 67-75.

Liu,Y., Shepherd,E.G., and Nelin,L.D. (2007). MAPK phosphatases--regulating the immune response. Nat. Rev. Immunol. *7*, 202-212.

Lobry,C., Lopez,T., Israel,A., and Weil,R. (2007). Negative feedback loop in T cell activation through IkappaB kinase-induced phosphorylation and degradation of Bcl10. Proc. Natl. Acad. Sci. U. S. A *104*, 908-913.

Locksley,R.M. (2009). Nine lives: plasticity among T helper cell subsets. J Exp. Med *206*, 1643-1646.

Lucas,P.C., Yonezumi,M., Inohara,N., Allister-Lucas,L.M., Abazeed,M.E., Chen,F.F., Yamaoka,S., Seto,M., and Nunez,G. (2001). Bcl10 and MALT1, independent targets of chromosomal translocation in MALT lymphoma, cooperate in a novel NF-kappa B signaling pathway. J. Biol. Chem. *276*, 19012-19019.

Luo,J., Emanuele,M.J., Li,D., Creighton,C.J., Schlabach,M.R., Westbrook,T.F., Wong,K.K., and Elledge,S.J. (2009a). A genome-wide RNAi screen identifies multiple synthetic lethal interactions with the Ras oncogene. Cell *137*, 835-848.

Luo,J., Solimini,N.L., and Elledge,S.J. (2009b). Principles of Cancer Therapy: Oncogene and Non-oncogene Addiction. Cell *136*, 823-837.

MacKeigan,J.P., Murphy,L.O., and Blenis,J. (2005). Sensitized RNAi screen of human kinases and phosphatases identifies new regulators of apoptosis and chemoresistance. Nat. Cell Biol. *7*, 591-600.

Major,M.B., Roberts,B.S., Berndt,J.D., Marine,S., Anastas,J., Chung,N., Ferrer,M., Yi,X., Stoick-Cooper,C.L., von Haller,P.D., Kategaya,L., Chien,A., Angers,S., MacCoss,M., Cleary,M.A., Arthur,W.T., and Moon,R.T. (2008). New regulators of Wnt/beta-catenin signaling revealed by integrative molecular screening. Sci. Signal. *1*, ra12.

Mak,T.W. (2007). The T cell antigen receptor: "The Hunting of the Snark". Eur. J. Immunol. *37 Suppl 1*, S83-S93.

Maksumova,L., Le,H.T., Muratkhodjaev,F., Davidson,D., Veillette,A., and Pallen,C.J. (2005). Protein tyrosine phosphatase alpha regulates Fyn activity and Cbp/PAG phosphorylation in thymocyte lipid rafts. J. Immunol. *175*, 7947-7956.

Maksumova,L., Wang,Y., Wong,N.K., Le,H.T., Pallen,C.J., and Johnson,P. (2007). Differential function of PTPalpha and PTPalpha Y789F in T cells and regulation of PTPalpha phosphorylation at Tyr-789 by CD45. J. Biol. Chem. *282*, 20925-20932.

Malo,N., Hanley,J.A., Cerquozzi,S., Pelletier,J., and Nadon,R. (2006). Statistical practice in high-throughput screening data analysis. Nat. Biotechnol. *24*, 167-175.

Manning,G., Whyte,D.B., Martinez,R., Hunter,T., and Sudarsanam,S. (2002). The protein kinase complement of the human genome. Science *298*, 1912-1934.

Marley,A.E., Sullivan,J.E., Carling,D., Abbott,W.M., Smith,G.J., Taylor,I.W., Carey,F., and Beri,R.K. (1996). Biochemical characterization and deletion analysis of recombinant human protein phosphatase 2C alpha. Biochem. J. *320*, 801-806.

Martin-Subero,J.I., Gesk,S., Harder,L., Sonoki,T., Tucker,P.W., Schlegelberger,B., Grote,W., Novo,F.J., Calasanz,M.J., Hansmann,M.L., Dyer,M.J., and Siebert,R. (2002). Recurrent involvement of the REL and BCL11A loci in classical Hodgkin lymphoma. Blood *99*, 1474-1477.

Matsumoto,R., Wang,D., Blonska,M., Li,H., Kobayashi,M., Pappu,B., Chen,Y., Wang,D., and Lin,X. (2005). Phosphorylation of CARMA1 Plays a Critical Role in T Cell Receptor-Mediated NF-[kappa]B Activation. Immunity *23*, 575-585.

Matzinger,P. (2002). The danger model: a renewed sense of self. Science *296*, 301-305.

May,M.J., D'Acquisto,F., Madge,L.A., Glockner,J., Pober,J.S., and Ghosh,S. (2000). Selective inhibition of NF-kappa B activation by a peptide that blocks the interaction of NEMO with the I kappa B kinase complex. Science *289*, 1550-1554.

May,M.J., Marienfeld,R.B., and Ghosh,S. (2002). Characterization of the Ikappa B-kinase NEMO binding domain. J. Biol. Chem. *277*, 45992-46000.

Mayya,V., Lundgren,D.H., Hwang,S.I., Rezaul,K., Wu,L., Eng,J.K., Rodionov,V., and Han,D.K. (2009). Quantitative phosphoproteomic analysis of T cell receptor signaling reveals system-wide modulation of protein-protein interactions. Sci. Signal. *2*, ra46.

Medzhitov,R. and Janeway,C.A., Jr. (1999). Innate immune induction of the adaptive immune response. Cold Spring Harb. Symp. Quant. Biol. *64*, 429-435.

Medzhitov,R. (2001). Toll-like receptors and innate immunity. Nat Rev Immunol *1*, 135-145.

Medzhitov,R. and Janeway,C. (2000). Innate Immunity. N. Engl. J. Med. *343*, 338-344.

Medzhitov,R. and Janeway,C.A., Jr. (2002). Decoding the Patterns of Self and Nonself by the Innate Immune System. Science *296*, 298-300.

Mercurio,F., Murray,B.W., Shevchenko,A., Bennett,B.L., Young,D.B., Li,J.W., Pascual,G., Motiwala,A., Zhu,H., Mann,M., and Manning,A.M. (1999). IkappaB kinase (IKK)-associated protein 1, a common component of the heterogeneous IKK complex. Mol. Cell Biol. *19*, 1526-1538.

Mercurio,F., Zhu,H.Y., Murray,B.W., Shevchenko,A., Bennett,B.L., Li,J.W., Young,D.B., Barbosa,M., and Mann,M. (1997). IKK-1 and IKK-2: Cytokine-activated I kappa B kinases essential for NF-kappa B activation. Science *278*, 860-866.

Meylan,E., Burns,K., Hofmann,K., Blancheteau,V., Martinon,F., Kelliher,M., and Tschopp,J. (2004). RIP1 is an essential mediator of Toll-like receptor 3-induced NF-kappa B activation. Nat. Immunol. *5*, 503-507.

Meylan,E., Dooley,A.L., Feldser,D.M., Shen,L., Turk,E., Ouyang,C., and Jacks,T. (2009). Requirement for NF-kappaB signalling in a mouse model of lung adenocarcinoma. Nature *462*, 104-107.

Micheau,O. and Tschopp,J. (2003). Induction of TNF receptor I-mediated apoptosis via two sequential signaling complexes. Cell *114*, 181-190.

Mikhailik,A., Ford,B., Keller,J., Chen,Y., Nassar,N., and Carpino,N. (2007). A phosphatase activity of Sts-1 contributes to the suppression of TCR signaling. Mol. Cell *27*, 486-497.

Mittelstadt,P.R., Yamaguchi,H., Appella,E., and Ashwell,J.D. (2009). T cell receptor-mediated activation of p38{alpha} by mono-phosphorylation of the activation loop results in altered substrate specificity. J. Biol. Chem. *284*, 15469-15474.

Mizuguchi,H., Nakatsuji,M., Fujiwara,S., Takagi,M., and Imanaka,T. (1999). Characterization and application to hot start PCR of neutralizing monoclonal antibodies against KOD DNA polymerase. J. Biochem. *126*, 762-768.

Moffat,J. and Sabatini,D.M. (2006). Building mammalian signalling pathways with RNAi screens. Nat. Rev. Mol. Cell Biol. *7*, 177-187.

Moreno-Garcia,M.E., Sommer,K., Haftmann,C., Sontheimer,C., Andrews,S.F., and Rawlings,D.J. (2009). Serine 649 phosphorylation within the protein kinase C-regulated domain down-regulates CARMA1 activity in lymphocytes. J. Immunol. *183*, 7362-7370.

Moreno-Garcia,M.E., Sommer,K., Shinohara,H., Bandaranayake,A.D., Kurosaki,T., and Rawlings,D.J. (2010). MAGUK-Controlled Ubiquitination of CARMA1 Modulates Lymphocyte NF-{kappa}B Activity. Mol. Cell. Biol. *30*, 922-934.

Mullis,K., Faloona,F., Scharf,S., Saiki,R., Horn,G., and Erlich,H. (1986). Specific enzymatic amplification of DNA in vitro: the polymerase chain reaction. Cold Spring Harb. Symp. Quant. Biol. *51 Pt 1*, 263-273.

Mumby,M. (2007). PP2A: unveiling a reluctant tumor suppressor. Cell *130*, 21-24.

Mustelin,T., Alonso,A., Bottini,N., Huynh,H., Rahmouni,S., Nika,K., Louis-dit-Sully,C., Tautz,L., Togo,S.H., Bruckner,S., Mena-Duran,A.V., and al-Khouri,A.M. (2004). Protein tyrosine phosphatases in T cell physiology. Mol. Immunol. *41*, 687-700.

Nakada,S., Chen,G.I., Gingras,A.C., and Durocher,D. (2008). PP4 is a gamma H2AX phosphatase required for recovery from the DNA damage checkpoint. EMBO Rep. *9*, 1019-1026.

Nakahira,M., Tanaka,T., Robson,B.E., Mizgerd,J.P., and Grusby,M.J. (2007). Regulation of signal transducer and activator of transcription signaling by the tyrosine phosphatase PTP-BL. Immunity. *26*, 163-176.

Ngo,V.N., Davis,R.E., Lamy,L., Yu,X., Zhao,H., Lenz,G., Lam,L.T., Dave,S., Yang,L.M., Powell,J., and Staudt,L.M. (2006). A loss-of-function RNA interference screen for molecular targets in cancer. Nature *441*, 106-110.

Ni,H., Ergin,M., Huang,Q., Qin,J.Z., Amin,H.M., Martinez,R.L., Saeed,S., Barton,K., and Alkan,S. (2001). Analysis of expression of nuclear factor kappa B (NF-kappa B) in multiple myeloma: downregulation of NF-kappa B induces apoptosis. Br. J. Haematol. *115*, 279-286.

Oberdoerffer,S., Moita,L.F., Neems,D., Freitas,R.P., Hacohen,N., and Rao,A. (2008). Regulation of CD45 alternative splicing by heterogeneous ribonucleoprotein, hnRNPLL. Science *321*, 686-691.

Oeckinghaus,A. and Ghosh,S. (2009). The NF-kappaB family of transcription factors and its regulation. Cold Spring Harb. Perspect. Biol. *1*, a000034.

Oeckinghaus,A., Wegener,E., Welteke,V., Ferch,U., Arslan,S.C., Ruland,J., Scheidereit,C., and Krappmann,D. (2007). Malt1 ubiquitination triggers NF-kappa B signaling upon T-cell activation. Embo Journal *26*, 4634-4645.

Oh-Hora,M. and Rao,A. (2008). Calcium signaling in lymphocytes. Curr. Opin. Immunol. *20*, 250-258.

Ohashi,P.S. (2002). T-cell signalling and autoimmunity: molecular mechanisms of disease. Nat. Rev. Immunol. *2*, 427-438.

Palkowitsch,L., Leidner,J., Ghosh,S., and Marienfeld,R.B. (2008). Phosphorylation of serine 68 in the IkappaB kinase (IKK)-binding domain of NEMO interferes with the structure of the IKK complex and tumor necrosis factor-alpha-induced NF-kappaB activity. J. Biol. Chem. *283*, 76-86.

Park,S.G., Schulze-Luehrman,J., Hayden,M.S., Hashimoto,N., Ogawa,W., Kasuga,M., and Ghosh,S. (2009). The kinase PDK1 integrates T cell antigen receptor and CD28 coreceptor signaling to induce NF-kappaB and activate T cells. Nat. Immunol. *10*, 158-166.

Pasparakis,M., Luedde,T., and Schmidt-Supprian,M. (2006). Dissection of the NF-kappaB signalling cascade in transgenic and knockout mice. Cell Death. Differ. *13*, 861-872.

Pear,W.S., Nolan,G.P., Scott,M.L., and Baltimore,D. (1993). Production of high-titer helper-free retroviruses by transient transfection. Proc. Natl. Acad. Sci. U. S. A *90*, 8392-8396.

Pelz,O., Gilsdorf,M., and Boutros,M. (2010). web cellHTS2: a web-application for the analysis of high-throughput screening data. BMC. Bioinformatics. *11*, 185.

Perkins,N.D. (2006). Post-translational modifications regulating the activity and function of the nuclear factor kappa B pathway. Oncogene *25*, 6717-6730.

Pfaffl,M.W. (2001). A new mathematical model for relative quantification in real-time RT-PCR. Nucleic Acids Res. *29*, e45.

Pitcher,L.A. and van Oers,N.S. (2003). T-cell receptor signal transmission: who gives an ITAM? Trends Immunol. *24*, 554-560.

Poiesz,B.J., Ruscetti,F.W., Reitz,M.S., Kalyanaraman,V.S., and Gallo,R.C. (1981). Isolation of a new type C retrovirus (HTLV) in primary uncultured cells of a patient with Sezary T-cell leukaemia. Nature *294*, 268-271.

Prajapati,S., Verma,U., Yamamoto,Y., Kwak,Y.T., and Gaynor,R.B. (2004). Protein phosphatase 2Cbeta association with the IkappaB kinase complex is involved in regulating NF-kappaB activity. J. Biol. Chem. *279*, 1739-1746.

Rajewsky,K. (1996). Clonal selection and learning in the antibody system. Nature *381*, 751-758.

Ramadan,N., Flockhart,I., Booker,M., Perrimon,N., and Mathey-Prevot,B. (2007). Design and implementation of high-throughput RNAi screens in cultured Drosophila cells. Nature Protocols *2*, 2245-2264.

Rathmell,J.C. and Thompson,C.B. (2002). Pathways of apoptosis in lymphocyte development, homeostasis, and disease. Cell *109 Suppl*, S97-107.

Rawlings,D.J., Sommer,K., and Moreno-Garcia,M.E. (2006). The CARMA1 signalosome links the signalling machinery of adaptive and innate immunity in lymphocytes. Nat Rev Immunol *6*, 799-812.

Rebeaud,F., Hailfinger,S., and Thome,M. (2007). Dlgh1 and Carma1 MAGUK proteins contribute to signal specificity downstream of TCR activation. Trends Immunol. *28*, 196-200.

Regnier,C.H., Song,H.Y., Gao,X., Goeddel,D.V., Cao,Z., and Rothe,M. (1997). Identification and characterization of an IkappaB kinase. Cell *90*, 373-383.

Reth,M. (1989). Antigen receptor tail clue. Nature *338*, 383-384.

Richardson,P.G., Mitsiades,C., Hideshima,T., and Anderson,K.C. (2005). Proteasome inhibition in the treatment of cancer. Cell Cycle *4*, 290-296.

Rincon,M. (2001). MAP-kinase signaling pathways in T cells. Curr. Opin. Immunol. *13*, 339-345.

Rincon,M. and Davis,R.J. (2009). Regulation of the immune response by stress-activated protein kinases. Immunol. Rev. *228*, 212-224.

Romeo,C., Amiot,M., and Seed,B. (1992). Sequence requirements for induction of cytolysis by the T cell antigen/Fc receptor zeta chain. Cell *68*, 889-897.

Roose,J.P., Mollenauer,M., Gupta,V.A., Stone,J., and Weiss,A. (2005). A diacylglycerol-protein kinase C-RasGRP1 pathway directs Ras activation upon antigen receptor stimulation of T cells. Mol. Cell Biol. *25*, 4426-4441.

Root,D.E., Hacohen,N., Hahn,W.C., Lander,E.S., and Sabatini,D.M. (2006). Genome-scale loss-of-function screening with a lentiviral RNAi library. Nat. Methods *3*, 715-719.

Rosenwald,A., Wright,G., Chan,W.C., Connors,J.M., Campo,E., Fisher,R.I., Gascoyne,R.D., Muller-Hermelink,H.K., Smeland,E.B., Giltnane,J.M., Hurt,E.M., Zhao,H., Averett,L., Yang,L., Wilson,W.H., Jaffe,E.S., Simon,R., Klausner,R.D., Powell,J., Duffey,P.L., Longo,D.L., Greiner,T.C., Weisenburger,D.D., Sanger,W.G., Dave,B.J., Lynch,J.C., Vose,J., Armitage,J.O., Montserrat,E., Lopez-Guillermo,A., Grogan,T.M., Miller,T.P., LeBlanc,M., Ott,G., Kvaloy,S., Delabie,J., Holte,H., Krajci,P., Stokke,T., and Staudt,L.M.

(2002). The use of molecular profiling to predict survival after chemotherapy for diffuse large-B-cell lymphoma. N. Engl. J. Med. *346*, 1937-1947.

Ross,T.M., Pettiford,S.M., and Green,P.L. (1996). The tax gene of human T-cell leukemia virus type 2 is essential for transformation of human T lymphocytes. J. Virol. *70*, 5194-5202.

Rothwarf,D.M., Zandi,E., Natoli,G., and Karin,M. (1998). IKK-gamma is an essential regulatory subunit of the I kappa B kinase complex. Nature *395*, 297-300.

Round,J.L., Humphries,L.A., Tomassian,T., Mittelstadt,P., Zhang,M., and Miceli,M.C. (2007). Scaffold protein Dlgh1 coordinates alternative p38 kinase activation, directing T cell receptor signals toward NFAT but not NF-kappaB transcription factors. Nat. Immunol. *8*, 154-161.

Rudolph,M.G., Stanfield,R.L., and Wilson,I.A. (2006). How TCRs bind MHCs, peptides, and coreceptors. Annu. Rev. Immunol. *24*, 419-466.

Salvador,J.M., Mittelstadt,P.R., Guszczynski,T., Copeland,T.D., Yamaguchi,H., Appella,E., Fornace,A.J., Jr., and Ashwell,J.D. (2005). Alternative p38 activation pathway mediated by T cell receptor-proximal tyrosine kinases. Nat. Immunol. *6*, 390-395.

Samelson,L.E. (2002). Signal transduction mediated by the T cell antigen receptor: the role of adapter proteins. Annu. Rev. Immunol. *20*, 371-394.

Sanger,F., Nicklen,S., and Coulson,A.R. (1977). DNA sequencing with chain-terminating inhibitors. Proc. Natl. Acad. Sci. U. S. A *74*, 5463-5467.

Sasaki,Y., Derudder,E., Hobeika,E., Pelanda,R., Reth,M., Rajewsky,K., and Schmidt-Supprian,M. (2006). Canonical NF-kappaB activity, dispensable for B cell development, replaces BAFF-receptor signals and promotes B cell proliferation upon activation. Immunity. *24*, 729-739.

Sato,S., Sanjo,H., Takeda,K., Ninomiya-Tsuji,J., Yamamoto,M., Kawai,T., Matsumoto,K., Takeuchi,O., and Akira,S. (2005). Essential function for the kinase TAK1 in innate and adaptive immune responses. Nat. Immunol. *6*, 1087-1095.

Scaffidi,C., Schmitz,I., Zha,J., Korsmeyer,S.J., Krammer,P.H., and Peter,M.E. (1999). Differential Modulation of Apoptosis Sensitivity in CD95 Type I and Type II Cells. J. Biol. Chem. *274*, 22532-22538.

Scheidereit,C. (2006). I kappa B kinase complexes: gateways to NF-kappa B activation and transcription. Oncogene *25*, 6685-6705.

Schmidt,C., Peng,B., Li,Z., Sclabas,G.M., Fujioka,S., Niu,J., Schmidt-Supprian,M., Evans,D.B., Abbruzzese,J.L., and Chiao,P.J. (2003). Mechanisms of proinflammatory cytokine-induced biphasic NF-kappaB activation. Mol. Cell *12*, 1287-1300.

Schmitz,R., Hansmann,M.L., Bohle,V., Martin-Subero,J.I., Hartmann,S., Mechtersheimer,G., Klapper,W., Vater,I., Giefing,M., Gesk,S., Stanelle,J., Siebert,R., and Kuppers,R. (2009). TNFAIP3 (A20) is a tumor suppressor gene in Hodgkin lymphoma and primary mediastinal B cell lymphoma. J. Exp. Med. *206*, 981-989.

Schneider,U., Schwenk,H.U., and Bornkamm,G. (1977). Characterization of EBV-genome negative "null" and "T" cell lines derived from children with acute lymphoblastic leukemia and leukemic transformed non-Hodgkin lymphoma. Int. J. Cancer *19*, 621-626.

Schomer-Miller,B., Higashimoto,T., Lee,Y.K., and Zandi,E. (2006). Regulation of IkappaB kinase (IKK) complex by IKKgamma-dependent phosphorylation of the T-loop and C terminus of IKKbeta. J. Biol. Chem. *281*, 15268-15276.

Sen,R. and Baltimore,D. (1986). Multiple nuclear factors interact with the immunoglobulin enhancer sequences. Cell *46*, 705-716.

Senftleben,U., Cao,Y.X., Xiao,G.T., Greten,F.R., Krahn,G., Bonizzi,G., Chen,Y., Hu,Y.L., Fong,A., Sun,S.C., and Karin,M. (2001). Activation by IKK alpha of a second, evolutionary conserved, NF-kappa B signaling pathway. Science *293*, 1495-1499.

Serfling,E., Berberich-Siebelt,F., Chuvpilo,S., Jankevics,E., Klein-Hessling,S., Twardzik,T., and Avots,A. (2000). The role of NF-AT transcription factors in T cell activation and differentiation. Biochim. Biophys. Acta *1498*, 1-18.

Sharma,S. and Rao,A. (2009). RNAi screening: tips and techniques. Nat. Immunol. *10*, 799-804.

Shi,Y. (2009). Serine/threonine phosphatases: mechanism through structure. Cell *139*, 468-484.

Shinkura,R., Kitada,K., Matsuda,F., Tashiro,K., Ikuta,K., Suzuki,M., Kogishi,K., Serikawa,T., and Honjo,T. (1999). Alymphoplasia is caused by a point mutation in the mouse gene encoding Nf-kappa b-inducing kinase. Nat. Genet. *22*, 74-77.

Shortman,K., Egerton,M., Spangrude,G.J., and Scollay,R. (1990). The generation and fate of thymocytes. Semin. Immunol. *2*, 3-12.

Shui,J.W., Hu,M.C., and Tan,T.H. (2007). Conditional knockout mice reveal an essential role of protein phosphatase 4 in thymocyte development and pre-T-cell receptor signaling. Mol. Cell Biol. *27*, 79-91.

Smith-Garvin,J.E., Koretzky,G.A., and Jordan,M.S. (2009). T cell activation. Annu. Rev. Immunol. *27*, 591-619.

Solimini,N.L., Luo,J., and Elledge,S.J. (2007). Non-oncogene addiction and the stress phenotype of cancer cells. Cell *130*, 986-988.

Sommer,K., Guo,B., Pomerantz,J.L., Bandaranayake,A.D., Moreno-Garcia,M.E., Ovechkina,Y.L., and Rawlings,D.J. (2005). Phosphorylation of the CARMA1 Linker Controls NF-[kappa]B Activation. Immunity *23*, 561-574.

Song,X.T., Evel-Kabler,K., Shen,L., Rollins,L., Huang,X.F., and Chen,S.Y. (2008). A20 is an antigen presentation attenuator, and its inhibition overcomes regulatory T cell-mediated suppression. Nat. Med. *14*, 258-265.

Sors,A., Jean-Louis,F., Begue,E., Parmentier,L., Dubertret,L., Dreano,M., Courtois,G., Bachelez,H., and Michel,L. (2008). Inhibition of IkappaB kinase subunit 2 in cutaneous T-cell lymphoma down-regulates nuclear factor-kappaB constitutive activation, induces cell death, and potentiates the apoptotic response to antineoplastic chemotherapeutic agents. Clin. Cancer Res. *14*, 901-911.

Sors,A., Jean-Louis,F., Pellet,C., Laroche,L., Dubertret,L., Courtois,G., Bachelez,H., and Michel,L. (2006). Down-regulating constitutive activation of the NF-kappaB canonical pathway overcomes the resistance of cutaneous T-cell lymphoma to apoptosis. Blood *107*, 2354-2363.

Starkebaum,G., Loughran,T.P., Jr., Waters,C.A., and Ruscetti,F.W. (1991). Establishment of an IL-2 independent, human T-cell line possessing only the p70 IL-2 receptor. Int. J. Cancer *49*, 246-253.

Starr,T.K., Jameson,S.C., and Hogquist,K.A. (2003). Positive and negative selection of T cells. Annu. Rev. Immunol. *21*, 139-176.

Staudt,L.M. (2010). Oncogenic activation of NF-kappaB. Cold Spring Harb. Perspect. Biol. *2*, a000109.

Stefanova,I., Hemmer,B., Vergelli,M., Martin,R., Biddison,W.E., and Germain,R.N. (2003). TCR ligand discrimination is enforced by competing ERK positive and SHP-1 negative feedback pathways. Nat. Immunol. *4*, 248-254.

Stefansson,B. and Brautigan,D.L. (2006). Protein phosphatase 6 subunit with conserved Sit4-associated protein domain targets IkappaBepsilon. J. Biol. Chem. *281*, 22624-22634.

Strasser,A. (2005). The role of BH3-only proteins in the immune system. Nat. Rev. Immunol. *5*, 189-200.

Su,H., Bidere,N., Zheng,L.X., Cubre,A., Sakai,K., Dale,J., Salmena,L., Hakem,R., Straus,S., and Lenardo,M. (2005). Requirement for caspase-8 in NF-kappa B activation by antigen receptor. Science *307*, 1465-1468.

Sun,L.J., Deng,L., Ea,C.K., Xia,Z.P., and Chen,Z.J.J. (2004). The TRAF6 ubiquitin ligase and TAK1 kinase mediate IKK activation by BCL10 and MALT1 in T lymphocytes. Mol. Cell *14*, 289-301.

Sun,S.C. (2008). Deubiquitylation and regulation of the immune response. Nat. Rev. Immunol. *8*, 501-511.

Sun,S.C. and Ballard,D.W. (1999). Persistent activation of NF-kappaB by the tax transforming protein of HTLV-1: hijacking cellular IkappaB kinases. Oncogene *18*, 6948-6958.

Sun,S.C., Ganchi,P.A., Ballard,D.W., and Greene,W.C. (1993). NF-kappa B controls expression of inhibitor I kappa B alpha: evidence for an inducible autoregulatory pathway. Science *259*, 1912-1915.

Sun,S.C., Maggirwar,S.B., and Harhaj,E. (1995). Activation of NF-kappa B by phosphatase inhibitors involves the phosphorylation of I kappa B alpha at phosphatase 2A-sensitive sites. J. Biol. Chem. *270*, 18347-18351.

Sun,W., Wang,H., Zhao,X., Yu,Y., Fan,Y., Wang,H., Wang,X., Lu,X., Zhang,G., Fu,S., and Yang,J. (2010). Protein phosphatase 2A acts as a mitogen-activated protein kinase kinase kinase 3 (MEKK3) phosphatase to inhibit lysophosphatidic acid-induced IkappaB kinase beta /nuclear factor-kappaB activation. J. Biol. Chem.

Sun,W., Yu,Y., Dotti,G., Shen,T., Tan,X., Savoldo,B., Pass,A.K., Chu,M., Zhang,D., Lu,X., Fu,S., Lin,X., and Yang,J. (2009). PPM1A and PPM1B act as IKKbeta phosphatases to terminate TNFalpha-induced IKKbeta-NF-kappaB activation. Cell Signal. *21*, 95-102.

Sun,Z., Arendt,C.W., Ellmeier,W., Schaeffer,E.M., Sunshine,M.J., Gandhi,L., Annes,J., Petrzilka,D., Kupfer,A., Schwartzberg,P.L., and Littman,D.R. (2000). PKC-theta is required for TCR-induced NF-kappaB activation in mature but not immature T lymphocytes. Nature *404*, 402-407.

Suzuki,A., Yamaguchi,M.T., Ohteki,T., Sasaki,T., Kaisho,T., Kimura,Y., Yoshida,R., Wakeham,A., Higuchi,T., Fukumoto,M., Tsubata,T., Ohashi,P.S., Koyasu,S., Penninger,J.M., Nakano,T., and Mak,T.W. (2001). T cell-specific loss of Pten leads to defects in central and peripheral tolerance. Immunity. *14*, 523-534.

Swift,S., Lorens J, Achacosus P, and Nolan GP (2001). Rapid production of retroviruses for efficient gene delivery to mammalian cells using 293T cell-based systems. In Curr Protoc Immunol., p. Unit 10.17C.

Tan,C.S., Pasculescu,A., Lim,W.A., Pawson,T., Bader,G.D., and Linding,R. (2009). Positive selection of tyrosine loss in metazoan evolution. Science *325*, 1686-1688.

Tannous,B.A. (2009). Gaussia luciferase reporter assay for monitoring biological processes in culture and in vivo. Nat. Protoc. *4*, 582-591.

Tannous,B.A., Kim,D.E., Fernandez,J.L., Weissleder,R., and Breakefield,X.O. (2005). Codon-optimized Gaussia luciferase cDNA for mammalian gene expression in culture and in vivo. Mol. Ther. *11*, 435-443.

Tegethoff,S., Behlke,J., and Scheidereit,C. (2003). Tetrameric oligomerization of IkappaB kinase gamma (IKKgamma) is obligatory for IKK complex activity and NF-kappaB activation. Mol. Cell Biol. *23*, 2029-2041.

Thome,M. (2004). CARMA1, BCL-10 and MALT1 in lymphocyte development and activation. Nat. Rev. Immunol. *4*, 348-359.

Tibbles,L.A. and Woodgett,J.R. (1999). The stress-activated protein kinase pathways. Cell Mol. Life Sci. *55*, 1230-1254.

Ting,A.T., Pimentel-Muinos,F.X., and Seed,B. (1996). RIP mediates tumor necrosis factor receptor 1 activation of NF-kappaB but not Fas/APO-1-initiated apoptosis. EMBO J. *15*, 6189-6196.

Tokunaga,F., Sakata,S., Saeki,Y., Satomi,Y., Kirisako,T., Kamei,K., Nakagawa,T., Kato,M., Murata,S., Yamaoka,S., Yamamoto,M., Akira,S., Takao,T., Tanaka,K., and Iwai,K. (2009). Involvement of linear polyubiquitylation of NEMO in NF-kappaB activation. Nat. Cell Biol. *11*, 123-132.

Tolstykh,T., Lee,J., Vafai,S., and Stock,J.B. (2000). Carboxyl methylation regulates phosphoprotein phosphatase 2A by controlling the association of regulatory B subunits. EMBO J. *19*, 5682-5691.

Tonegawa,S. (1993). The Nobel Lectures in Immunology. The Nobel Prize for Physiology or Medicine, 1987. Somatic generation of immune diversity. Scand. J Immunol. *38*, 303-319.

Toth,C.R., Hostutler,R.F., Baldwin,A.S., Jr., and Bender,T.P. (1995). Members of the nuclear factor kappa B family transactivate the murine c-myb gene. J. Biol. Chem. *270*, 7661-7671.

Toyo-oka,K., Mori,D., Yano,Y., Shiota,M., Iwao,H., Goto,H., Inagaki,M., Hiraiwa,N., Muramatsu,M., Wynshaw-Boris,A., Yoshiki,A., and Hirotsune,S. (2008). Protein phosphatase 4 catalytic subunit regulates Cdk1 activity and microtubule organization via NDEL1 dephosphorylation. J. Cell Biol. *180*, 1133-1147.

Trombetta,E.S. and Mellman,I. (2005). Cell biology of antigen processing in vitro and in vivo. Annu. Rev. Immunol. *23*, 975-1028.

Trompouki,E., Hatzivassiliou,E., Tsichritzis,T., Farmer,H., Ashworth,A., and Mosialos,G. (2003). CYLD is a deubiquitinating enzyme that negatively regulates NF-kappaB activation by TNFR family members. Nature *424*, 793-796.

Tsui,H.W., Siminovitch,K.A., de,S.L., and Tsui,F.W. (1993). Motheaten and viable motheaten mice have mutations in the haematopoietic cell phosphatase gene. Nat. Genet. *4*, 124-129.

Tweeddale,M.E., Lim,B., Jamal,N., Robinson,J., Zalcberg,J., Lockwood,G., Minden,M.D., and Messner,H.A. (1987). The presence of clonogenic cells in high-grade malignant lymphoma: a prognostic factor. Blood *69*, 1307-1314.

Uren,A.G., O'Rourke,K., Aravind,L., Pisabarro,M.T., Seshagiri,S., Koonin,E.V., and Dixit,V.M. (2000). Identification of paracaspases and metacaspases: Two ancient families of caspase-like proteins, one of which plays a key role in MALT lymphoma. Molecular Cell *6*, 961-967.

Vallabhapurapu,S. and Karin,M. (2009). Regulation and function of NF-kappaB transcription factors in the immune system. Annu. Rev. Immunol. *27*, 693-733.

Vang,T., Congia,M., Macis,M.D., Musumeci,L., Orru,V., Zavattari,P., Nika,K., Tautz,L., Tasken,K., Cucca,F., Mustelin,T., and Bottini,N. (2005). Autoimmune-associated lymphoid tyrosine phosphatase is a gain-of-function variant. Nat. Genet. *37*, 1317-1319.

Varfolomeev,E., Blankenship,J.W., Wayson,S.M., Fedorova,A.V., Kayagaki,N., Garg,P., Zobel,K., Dynek,J.N., Elliott,L.O., Wallweber,H.J., Flygare,J.A., Fairbrother,W.J., Deshayes,K., Dixit,V.M., and Vucic,D. (2007). IAP antagonists induce autoubiquitination of c-IAPs, NF-kappaB activation, and TNFalpha-dependent apoptosis. Cell *131*, 669-681.

Vaux,D.L. and Korsmeyer,S.J. (1999). Cell death in development. Cell *96*, 245-254.

Viatour,P., Merville,M.P., Bours,V., and Chariot,A. (2005). Phosphorylation of NF-kappa B and I kappa B proteins: implications in cancer and inflammation. Trends Biochem. Sci. *30*, 43-52.

Vilimas,T., Mascarenhas,J., Palomero,T., Mandal,M., Buonamici,S., Meng,F., Thompson,B., Spaulding,C., Macaroun,S., Alegre,M.L., Kee,B.L., Ferrando,A., Miele,L., and Aifantis,I. (2007). Targeting the NF-kappaB signaling pathway in Notch1-induced T-cell leukemia. Nat. Med. *13*, 70-77.

Virshup,D.M. and Shenolikar,S. (2009). From promiscuity to precision: protein phosphatases get a makeover. Mol. Cell *33*, 537-545.

Vonderheid,E.C., Bernengo,M.G., Burg,G., Duvic,M., Heald,P., Laroche,L., Olsen,E., Pittelkow,M., Russell-Jones,R., Takigawa,M., and Willemze,R. (2002). Update on erythrodermic cutaneous T-cell lymphoma: report of the International Society for Cutaneous Lymphomas. J. Am. Acad. Dermatol. *46*, 95-106.

Vucic,D. and Fairbrother,W.J. (2007). The inhibitor of apoptosis proteins as therapeutic targets in cancer. Clin. Cancer Res. *13*, 5995-6000.

Wada,T., Miyata,T., Inagi,R., Nangaku,M., Wagatsuma,M., Suzuki,D., Wadzinski,B.E., Okubo,K., and Kurokawa,K. (2001). Cloning and characterization of a novel subunit of protein serine/threonine phosphatase 4 from mesangial cells. J. Am. Soc. Nephrol. *12*, 2601-2608.

Wan,F., Anderson,D.E., Barnitz,R.A., Snow,A., Bidere,N., Zheng,L., Hegde,V., Lam,L.T., Staudt,L.M., Levens,D., Deutsch,W.A., and Lenardo,M.J. (2007). Ribosomal protein S3: a KH domain subunit in NF-kappaB complexes that mediates selective gene regulation. Cell *131*, 927-939.

Wan,F. and Lenardo,M.J. (2010). The nuclear signaling of NF-kappaB: current knowledge, new insights, and future perspectives. Cell Res. *20*, 24-33.

Wan,Y.Y., Chi,H., Xie,M., Schneider,M.D., and Flavell,R.A. (2006). The kinase TAK1 integrates antigen and cytokine receptor signaling for T cell development, survival and function. Nat. Immunol. *7*, 851-858.

Wang,C., Deng,L., Hong,M., Akkaraju,G.R., Inoue,J., and Chen,Z.J. (2001). TAK1 is a ubiquitin-dependent kinase of MKK and IKK. Nature *412*, 346-351.

Wang,D.H., Matsumoto,R., You,Y., Che,T.J., Lin,X.Y., Gaffen,S.L., and Lin,X. (2004). CD3/CD28 costimulation-induced NF-kappa B activation is mediated by recruitment of protein kinase C-theta, Bcl10, and I kappa B kinase beta to the immunological synapse through CARMA1. Mol. Cell. Biol. *24*, 164-171.

Wang,Y., Vachon,E., Zhang,J., Cherepanov,V., Kruger,J., Li,J., Saito,K., Shannon,P., Bottini,N., Huynh,H., Ni,H., Yang,H., McKerlie,C., Quaggin,S., Zhao,Z.J., Marsden,P.A., Mustelin,T., Siminovitch,K.A., and Downey,G.P. (2005). Tyrosine phosphatase MEG2 modulates murine development and platelet and lymphocyte activation through secretory vesicle function. J. Exp. Med. *202*, 1587-1597.

Wang,Z.H., Ding,M.X., Chew-Cheng,S.B., Yun,J.P., and Chew,E.C. (1999). Bcl-2 and Bax proteins are nuclear matrix associated proteins. Anticancer Res. *19*, 5445-5449.

Wange,R.L. and Samelson,L.E. (1996). Complex complexes: signaling at the TCR. Immunity. *5*, 197-205.

Wegener,E., Oeckinghaus,A., Papadopoulou,N., Lavitas,L., Schmidt-Supprian,M., Ferch,U., Mak,T.W., Ruland,J., Heissmeyer,V., and Krappmann,D. (2006). Essential role for IkappaB kinase beta in remodeling Carma1-Bcl10-Malt1 complexes upon T cell activation. Mol. Cell *23*, 13-23.

Weinstein,I.B. (2002). Cancer. Addiction to oncogenes--the Achilles heal of cancer. Science *297*, 63-64.

Weinstein,I.B. and Joe,A. (2008). Oncogene addiction. Cancer Res. *68*, 3077-3080.

Weiss,A. and Littman,D.R. (1994). Signal transduction by lymphocyte antigen receptors. Cell *76*, 263-274.

Weiss,A. and Stobo,J.D. (1984). Requirement for the coexpression of T3 and the T cell antigen receptor on a malignant human T cell line. J. Exp. Med. *160*, 1284-1299.

Wertz,I.E. and Dixit,V.M. (2010). Signaling to NF-kappaB: regulation by ubiquitination. Cold Spring Harb. Perspect. Biol. *2*, a003350.

Wertz,I.E., O'Rourke,K.M., Zhou,H., Eby,M., Aravind,L., Seshagiri,S., Wu,P., Wiesmann,C., Baker,R., Boone,D.L., Ma,A., Koonin,E.V., and Dixit,V.M. (2004). De-ubiquitination and ubiquitin ligase domains of A20 downregulate NF-kappaB signalling. Nature *430*, 694-699.

Willemze,R., Jaffe,E.S., Burg,G., Cerroni,L., Berti,E., Swerdlow,S.H., Ralfkiaer,E., Chimenti,S., az-Perez,J.L., Duncan,L.M., Grange,F., Harris,N.L., Kempf,W., Kerl,H., Kurrer,M., Knobler,R., Pimpinelli,N., Sander,C., Santucci,M., Sterry,W., Vermeer,M.H., Wechsler,J., Whittaker,S., and Meijer,C.J. (2005). WHO-EORTC classification for cutaneous lymphomas. Blood *105*, 3768-3785.

Willis,T.G., Jadayel,D.M., Du,M.Q., Peng,H., Perry,A.R., bdul-Rauf,M., Price,H., Karran,L., Majekodunmi,O., Wlodarska,I., Pan,L., Crook,T., Hamoudi,R., Isaacson,P.G., and Dyer,M.J. (1999). Bcl10 is involved in t(1;14)(p22;q32) of MALT B cell lymphoma and mutated in multiple tumor types. Cell *96*, 35-45.

Wishart,M.J. and Dixon,J.E. (2002). PTEN and myotubularin phosphatases: from 3-phosphoinositide dephosphorylation to disease. Trends Cell Biol. *12*, 579-585.

Wonerow,P. and Watson,S.P. (2001). The transmembrane adapter LAT plays a central role in immune receptor signalling. Oncogene *20*, 6273-6283.

Woronicz,J.D., Gao,X., Cao,Z., Rothe,M., and Goeddel,D.V. (1997). IkappaB kinase-beta: NF-kappaB activation and complex formation with IkappaB kinase-alpha and NIK. Science *278*, 866-869.

Wright,G., Tan,B., Rosenwald,A., Hurt,E.H., Wiestner,A., and Staudt,L.M. (2003). A gene expression-based method to diagnose clinically distinct subgroups of diffuse large B cell lymphoma. Proc. Natl. Acad. Sci. U. S. A *100*, 9991-9996.

Wu,C.J., Conze,D.B., Li,T., Srinivasula,S.M., and Ashwell,J.D. (2006). Sensing of Lys 63-linked polyubiquitination by NEMO is a key event in NF-kappaB activation [corrected]. Nat. Cell Biol. *8*, 398-406.

Wu,H., Tschopp,J., and Lin,S.C. (2007). Smac mimetics and TNFalpha: a dangerous liaison? Cell *131*, 655-658.

Xavier,R. and Seed,B. (1999). Membrane compartmentation and the response to antigen. Curr. Opin. Immunol. *11*, 265-269.

Xia,Z.P., Sun,L., Chen,X., Pineda,G., Jiang,X., Adhikari,A., Zeng,W., and Chen,Z.J. (2009). Direct activation of protein kinases by unanchored polyubiquitin chains. Nature *461*, 114-119.

Yablonski,D., Kadlecek,T., and Weiss,A. (2001). Identification of a phospholipase C-gamma1 (PLC-gamma1) SH3 domain-binding site in SLP-76 required for T-cell receptor-mediated activation of PLC-gamma1 and NFAT. Mol. Cell Biol. *21*, 4208-4218.

Yablonski,D., Kuhne,M.R., Kadlecek,T., and Weiss,A. (1998). Uncoupling of nonreceptor tyrosine kinases from PLC-gamma1 in an SLP-76-deficient T cell. Science *281*, 413-416.

Yamaoka,S., Courtois,G., Bessia,C., Whiteside,S.T., Weil,R., Agou,F., Kirk,H.E., Kay,R.J., and Israel,A. (1998). Complementation cloning of NEMO, a component of the IkappaB kinase complex essential for NF-kappaB activation. Cell *93*, 1231-1240.

Yang,J., Fan,G.H., Wadzinski,B.E., Sakurai,H., and Richmond,A. (2001b). Protein phosphatase 2A interacts with and directly dephosphorylates RelA. J. Biol. Chem. *276*, 47828-47833.

Yang,J., Lin,Y., Guo,Z., Cheng,J., Huang,J., Deng,L., Liao,W., Chen,Z., Liu,Z., and Su,B. (2001a). The essential role of MEKK3 in TNF-induced NF-kappaB activation. Nat. Immunol. *2*, 620-624.

Yeh,P.Y., Yeh,K.H., Chuang,S.E., Song,Y.C., and Cheng,A.L. (2004). Suppression of MEK/ERK signaling pathway enhances cisplatin-induced NF-kappaB activation by protein phosphatase 4-mediated NF-kappaB p65 Thr dephosphorylation. J. Biol. Chem. *279*, 26143-26148.

Yeh,W.C., Itie,A., Elia,A.J., Ng,M., Shu,H.B., Wakeham,A., Mirtsos,C., Suzuki,N., Bonnard,M., Goeddel,D.V., and Mak,T.W. (2000). Requirement for Casper (c-FLIP) in regulation of death receptor-induced apoptosis and embryonic development. Immunity. *12*, 633-642.

za-Blanc,P., Cooper,C.L., Wagner,K., Batalov,S., Deveraux,Q.L., and Cooke,M.P. (2003). Identification of modulators of TRAIL-induced apoptosis via RNAi-based phenotypic screening. Mol. Cell *12*, 627-637.

Zandi,E., Chen,Y., and Karin,M. (1998). Direct phosphorylation of IkappaB by IKKalpha and IKKbeta: discrimination between free and NF-kappaB-bound substrate. Science *281*, 1360-1363.

Zhang,J., Chang,C.C., Lombardi,L., and la-Favera,R. (1994). Rearranged NFKB2 gene in the HUT78 T-lymphoma cell line codes for a constitutively nuclear factor lacking transcriptional repressor functions. Oncogene *9*, 1931-1937.

Zhang,W., Sloan-Lancaster,J., Kitchen,J., Trible,R.P., and Samelson,L.E. (1998a). LAT: the ZAP-70 tyrosine kinase substrate that links T cell receptor to cellular activation. Cell *92*, 83-92.

Zhang,W., Sommers,C.L., Burshtyn,D.N., Stebbins,C.C., DeJarnette,J.B., Trible,R.P., Grinberg,A., Tsay,H.C., Jacobs,H.M., Kessler,C.M., Long,E.O., Love,P.E., and Samelson,L.E. (1999). Essential role of LAT in T cell development. Immunity. *10*, 323-332.

Zhang,W., Trible,R.P., and Samelson,L.E. (1998b). LAT palmitoylation: its essential role in membrane microdomain targeting and tyrosine phosphorylation during T cell activation. Immunity. *9*, 239-246.

Zhang,W., Trible,R.P., Zhu,M., Liu,S.K., McGlade,C.J., and Samelson,L.E. (2000). Association of Grb2, Gads, and phospholipase C-gamma 1 with phosphorylated LAT tyrosine residues. Effect of LAT tyrosine mutations on T cell angigen receptor-mediated signaling. J. Biol. Chem. *275*, 23355-23361.

Zhang,X.H., Ozawa,Y., Lee,H., Wen,Y.D., Tan,T.H., Wadzinski,B.E., and Seto,E. (2005). Histone deacetylase 3 (HDAC3) activity is regulated by interaction with protein serine/threonine phosphatase 4. Genes & Development *19*, 827-839.

Zhou,G., Boomer,J.S., and Tan,T.H. (2004b). Protein phosphatase 4 is a positive regulator of hematopoietic progenitor kinase 1. J. Biol. Chem. *279*, 49551-49561.

Zhou,G., Mihindukulasuriya,K.A., Corkle-Chosnek,R.A., Van Hooser,A., Hu,M.C.T., Brinkley,B.R., and Tan,T.H. (2002). Protein Phosphatase 4 Is Involved in Tumor Necrosis Factor-+¦-induced Activation of c-Jun N-terminal Kinase. J. Biol. Chem. *277*, 6391-6398.

Zhou,H.L., Wertz,I., O'Rourke,K., Ultsch,M., Seshagiri,S., Eby,M., Xiao,W., and Dixit,V.M. (2004a). Bcl10 activates the NF-kappa B pathway through ubiquitination of NEMO. Nature *427*, 167-171.

Zong,W.X., Edelstein,L.C., Chen,C.L., Bash,J., and Gelinas,C. (1999). The prosurvival Bcl-2 homolog Bfl-1/A1 is a direct transcriptional target of NF-kappa B that blocks TNF alpha-induced apoptosis. Genes & Development *13*, 382-387.

7.2 List of abbreviations

°C	Degree Celsius
Aa	Amino acid
ABC-DLBCL	Activated B cell-like DLBCL
ADAP	Adhesion- and degranulation-promoting adapter protein
Ag	Antigen(s)
ANK	Ankyrin repeat motif
AP-1	Activating protein 1
APC	Antigen presenting cell
APS	Ammonium persulfate
ATL	Adult T cell lymphoma/leukemia
ATP	Adenosine triphosphate
Bcl	B cell lymphoma
BCR	B cell antigen receptor
bp (kb)	Base pair (kilo base pair)
CARD	Caspase recruitment domain
Caspase	Cysteine-aspartate specific protease
CBM complex	Carma1-Bcl10-MALT1 complex
Cbp	Csk-binding protein
CD	Cluster of differentiation
CD95L	CD95 ligand
cDNA	Complementary DNA
CED	Caspase-8 deficiency
c-FLIP	Cellular FLICE inhibitory protein
c-IAP	Cellular inhibitor of apoptosis
CRAC	Calcium release activated calcium channel
Csk	Cellular src kinase
CTLC	Cutaneous T cell lymphoma
CYLD	Cylindromatosis tumor suppressor
d	Day
DAG	Diacylglycerol
DC	Dendritic cell
DD	Death domain
DLBCL	Diffuse large B cell lymphoma
Dlgh1	Discs large homolog 1
DMEM	Dulbecco’s Modified Eagle Medium
DMSO	Dimethyl sulfoxide
DNA	Desoxyribonucleic acid
DTT	Dithiothreitol
DUB	Deubiquitinating enzyme
ECL	Enhanced chemiluminescence
EDTA	Ethylenediaminetetraacetic acid
EGFP	Enhanced GFP
ELISA	Enzyme-linked immunosorbent assay
ER	Endoplasmic reticulum
ERK	Extracellular signal-regulated kinase
EtOH	Ethanol
FACS	Fluorescence activated cell sorter
FCS	Fetal calf serum

FHC	Ferritin heavy chain
Fig.	Figure
g	Gramm
Gads	Grb2-related adaptor downstream of Shc
GAP	GTPase-activating protein
GAPDH	Glyceraldehyde-3-phosphate dehydrogenase
GCB-DLBCL	Germinal center B cell-like DLBCL
GEF	Guanine-nucleotide-exchange factor
GFP	Green fluorescent protein
Grb2	Growth factor receptor-bound protein 2
GRP	GDP release protein
GRR	Glycine rich region
GUK	Guanylat-Kinase-Domäne
GUK	Guanylate kinase
h	Hour
HLH	Helix-loop-helix
HPK1	Haematopoietic progenitor kinase 1
HPRT1	Hypoxanthine phosphoribosyl-transferase 1
HRP	Horseradish peroxidase
HTLV-1	Human T-lymphotropic virus type I
HTS	High throughput screening
IB	Immunoblot(ting)
IFNγ	Interferon γ
IgG	Immunoglobulin
IgG_H	Immunoglobulin heavy chain
IgG_L	Immunoglobulin light chain
IKK	IκB kinase
IL	Interleukin
IMDM	Iscove's modified Eagles medium
Iono	Ionomycin
IP	Immunoprecipitation
IP_3	Inositol 3,4,5-trisphosphate
IRES	Internal ribosomal entry site
ITAM	Immunoreceptor tyrosine-based activation motif
Itk	IL-2 inducible Tec kinase
IκB	Inhibitor of κB proteins
JNK/SAPK	c-Jun N-terminal kinase/stress-activated protein kinase
KBD	Kinase binding domain
KD	Kinase domain
kDa	Kilo Dalton
l	Liter
LAT	Linker of activated T cells
LZ	Leucine zipper
mAb	Monoclonal antibody
MACS	Magnetic activated cell sorter
MAGUK	Membrane-associated guanylate kinase
MALT1	Mucosa-associated lymphoid tissue lymphoma translocation protein 1
MAPK	Mitogen-activated protein kinase
MEF	Murine embryonic fibroblast
MEKK	MAPK/ERK Kinase Kinase
MeOH	Methanol

MF	Mycosis fungoides
MFI	Mean fluorescence intensity
MHC	Major histocompatibility complex
min	Minute(s)
MLK	Mixed-lineage protein kinase
MM	Multiple myeloma
mRNA	Messenger ribonucleic acid
NBD	Nemo-Binde-Domäne
NBP	NBD peptide
Nck	Non-catalytic region of tyrosine kinase
NEMO	NF-κB essential modulator
NES	Nuclear export sequence
NFAT	Nuclear factor of activated T cells
NF-κB	Nuclear factor-kappaB
NIK	NF-κB-inducing kinase
NK cells	Natural killer cells
NLS	Nuclear translocation sequence
p	Peptide
PAGE	Polyacrylamide gel electrophoresis
PAMP	Pathogen-associated molecular pattern
PBL	Peripheral blood leukocyte
PBS	Phosphate buffered saline
PCR	Polymerase chain reaction
PDK1	3-Phosphoinositid-abhängige Kinase 1
PHA	Phytohemagglutinin
PI3K	Phosphoinositide-3 kinase
PKC	Protein kinase C
PLCγ1	Phospholipase Cγ1
PMA	Phorbol 12-myristate-13-acetate
PP1c	Protein phosphatase 1 catalytic subunit
PP2A	Protein phosphatase 2A
PP2Ac	Protein phosphatase 2A catalytic subunit
PP4c	Protein phosphatase 4 catalyticsubunit
PP4R	Protein phosphatase 4 regulatory subunit
PPP	Phosphoprotein phosphatase
PRD	PKC-regulated domain
PRR	Pattern recognition receptor
PSK	Protein serine/threonine kinase
PSP	Protein serine/threonine phosphatase
PSP	Protein serine/threonine phosphatases
PTEN	Phosphatase and tensin homolog
PTK	Protein tyrosine kinase
PTP	Protein tyrosine phosphatase
PTPN	Protein tyrosine phosphatase, non-receptor type
PTPR	Protein tyrosine phosphatase, receptor type
pUb	Poly-ubiquitin
RHD	Rel homology domain
RIP1	Receptor-interacting protein 1
RLU	Relative light unit
RNA	Ribonucleic acid
RNAi	RNA interference

ROS	Reactive oxygen species
rpm	Rotations per minute
RT	Room temperature
RT-PCR	Reverse transcription PCR
SDS	Sodium dodecyl sulfate
Sec	Second
SFK	Src family protein tyrosine kinase
SH	Src homology
SHIP1	SH2 domain-containing inositol phosphatase 1
SHP1	SH2 domain-containing phosphatase 1
shRNA	Short hairpin RNA
siRNA	Small interfering RNA
SLP76	SH2-domain-containing leukocyte protein of 76 kd
SOCE	Store-operated calcium entry
SOS	Son of sevenless
Sts	Suppressor of TCR signaling
Syk	Spleen tyrosine kinase
TAD	Transactivation domain
TAK1	TGF-b-activated kinase 1
T-ALL	T cell acute lymphocytic leukaemia
TCR	T cell antigen receptor
TEMED	N,N,N',N'-Tetramethyl-ethylenediamine
TNFR	TNF receptor
TNF-RSC	TNFR signaling complex
TNFα	Tumor necrosis factor α
TRADD	TNFR1-associated death domain protein
TRAF	TNFR-associated factor
Tris	Tris-[hydroxymethyl]amino-methane
Ub	Ubiquitin
UPL	Universal probe library
vs.	versus
wt	Wild type
ZAP-70	Zeta chain-associated kinase of 70 kDa
ZF	Zinc finger

Amino acid	Three-letter code	Single-letter code
Alanine	Ala	A
Arginine	Arg	R
Asparagine	Asn	N
Aspartic acid	Asp	D
Cysteine	Cys	C
Glutamine	Gln	Q
Glutamic acid	Glu	E
Glycine	Gly	G
Histidine	His	H
Isoleucine	Ile	I
Leucine	Leu	L
Lysine	Lys	K
Methionine	Met	M
Phenylalanine	Phe	F
Proline	Pro	P
Serine	Ser	S
Threonine	Thr	T
Tryptophan	Trp	W
Tyrosine	Tyr	Y
Valine	Val	V
any aa		x

Nucleobase	Symbol
Adenine	A
Cytosine	C
Guanine	G
Thymine	T
Uracil	U

7.3 List of publications

Brechmann,M., Mock,T., Nickles,D., Kiessling,M., Frey,F., Müller,W., Booken,N., Klemke,C.-D., Boutros,M., Krammer,P.H., Arnold,R. (2010). A PP4 phosphatase complex suppresses NF-κB activation and human lymphoma cell survival. (submitted).

Brenner,D., **Brechmann,M.**, Röhling,S., Tapernoux,M., Mock,T., Winter,D., Lehmann,W., Kiefer,F., Thome,M., Krammer,P.H., Arnold,R. (2009). Phosphorylation of CARMA1 by HPK1 is critical for NF-κB activation in T cells. *Proc. Nat. Acad. Sci. USA* **106**, 14508-13.

Abudula,A., Grabbe,A., **Brechmann,M.**, Polaschegg,C., Herrmann,N., Goldbeck,I., Dittmann,K., Wienands,J. (2007). SLP-65 requires SH2-mediated membrane anchoring to receive and transmit signals from the B cell antigen receptor. *J. Biol. Chem.* **282**, 29059-66.

Iwaki,T., Sandoval-Cooper,M.J., **Brechmann,M.**, Ploplis,V.A., Castellino,F.J. (2006). A fibrinogen deficiency accelerates the initiation of LDL cholesterol-driven atherosclerosis via thrombin generation and platelet activation in genetically predisposed mice. *Blood* **107**, 3883-91.

7.4 Declaration

Herewith, I declare that I wrote this thesis independently under supervision, and no other sources and aids than those indicated were used. Furthermore, my submission as a whole is not substantially the same as any that I have previously made or I am currently making, whether in published or unpublished form, for a degree, diploma, or similar qualification at any university or similar institution.

Heidelberg, July 2010

_____

Markus Brechmann